Research Programme of the Research Fund for Coal and Steel

FIre and Seismic performances of Hybrid fire WALLs in case of single-storey industrial and commercial steel buildings (FISHWALL)

Full seismic test report including all detailed experimental data gathered during the seismic tests

Sara Pasquali, Nicola Tondini, Gabriele Zanon

University of Trento

WP4: Seismic behaviour of a hybrid fire wall solution with "fusible" links

Deliverable: D4.1

Grant agreement No: 101034083

Version	Issue	Purpose	Author	Reviewer	Approved
A	D4.1	first version (30/01/2024)	S.Pasquali N Tondini G. Zanon	ALL	C. Renaud

TABLE OF CONTENTS

ABSTRACT

It is well known that the intrinsic fire resistance of single-storey unprotected steel-framed buildings is largely sufficient to guarantee the evacuation of occupants in the event of fire. In consequence, for this type of building, the main concern of national fire regulations in Europe is how to prevent the spread of fire to the whole building. To achieve this objective, two performances shall be usually satisfied, namely, the appropriateness of constructive systems to ensure that there is no progressive collapse between fire compartments, and the efficiency of fire walls to stop the fire inside the initial compartment regardless of the state of structures exposed to fire. In practice, many constructional solutions can be implemented in order to preserve the integrity of the fire walls, while accepting that the fire exposed part of the structure may collapse. One of the most common solutions is to place a non-load bearing wall between two independent steel structures and to connect it to them by means of "fusible" links. In fire situation, these fusible links have to allow the wall to be disconnected from the structure affected by fire without endangering the separating function of the wall, which shall remain fixed to the steel structure on the other side of the wall and therefore not exposed to fire. However, due to the lack of corresponding scientific evidence, questions are being very often raised about the real efficiency of such systems in fire situation, which, in certain cases, have also to provide an adequate seismic resistance, if they are used in seismic areas.

Today, concrete or masonry wall solutions are frequently used for the compartmentation of buildings, predominately for low-rise commercial and industrial steel buildings. However, as an alternative, lightweight sandwich panels (comprising two thin flat metal faces and an insulated core) could become an appropriate steel fire wall solution, offering numerous benefits in comparison to other solutions, including fire resistance, durability, flexibility, fast construction times and easy dismounting. Nonetheless, there is an evident lack of technical information about the adequate fire performance of such type of wall solutions when they are implemented in single-storey buildings with unprotected steel structure, which constitutes a major obstacle for their large use.

In this context, the overall goal of the FISHWALL project is to develop a design guidance and recommendations for an innovative hybrid fire wall solution based on lightweight steel-faced sandwich panels associated with unprotected steel structure under both fire and seismic actions considered individually. This will be achieved through the following specific tasks: i) establishing of a full range of experimental evidence about the fire and seismic behaviour of the investigated hybrid fire wall solution by carrying out a number of tests; ii) investigating intensively the fire and seismic performances of the above hybrid fire wall solution in combination with unprotected single-storey steel structures through a variety of parametric numerical studies by means of validated FE numerical models; iii) developing both cost-effective and innovative “fusible” connection systems for fire walls to be used in combination with unprotected steel structures of single-storey buildings; and iv) developing a design guidance and practical recommendations for the studied hybrid fire wall and fusible links solutions, on the basis of above studies, from which engineers can carry out very efficient design.

The present report aims at summarising the main results of the experimental seismic tests performed on 6 different details based on the “fusible” link solutions defined in task 1.5 of the project. The main objective of these tests was to investigate the seismic behaviour of the of the “fusible” links connecting the fire walls to steel structures of buildings in the earthquake situation.

1 INTRODUCTION

One aim of the project FISHWALL is to provide a hybrid steel-based fire wall solution using sandwich panels for single-storey buildings with unprotected steel structure. This fire wall can be placed between two independent building structures and connect it to them by means of "fusible" links. In case of fire event, the fusible links have to be designed to break and to allow the wall to be disconnected from the structure affected by the fire, without endangering the separating function of the wall, which remains fixed to the steel structure on the other side of the wall and therefore not exposed to the fire. Considering that buildings can be located in seismic prone region, it is necessary to verify that the connection with the fusible links can withstand earthquake forces.

This Deliverable is devoted to report the results obtained by the seismic tests performed by UNITN on the fusible link configurations designed in Deliverable D1.4 [1]. As presented in that report, six different details were conceived to test the widest range of configuration. On each detail, specific local instrumentation was applied in terms of strain gauges, displacement transducers and inclinometers. For each detail, 4 different tests were performed for a total of 24 tests. The tests were conducted according to the ECCS [2] protocol. In this respect, two monotonic tests and two cyclic tests were foreseen. Because of the asymmetry of some specimens, the monotonic tests were in tension and in compression. The force - displacement curves were then used to identify the e_y, which is the conventional yield displacement used to define the displacement history for the cyclic tests. All these aspects are presented in greater detail with respect to each specimen.

1.1 Procedure of the experimental program

A set of 24 tests (including both monotonic and cyclic tests) were conducted on 6 different details developed from 3 reference fusible link solutions common to all the project partners. Due to the selected solutions, the investigated fusible links and associated aluminium bolts are mainly subjected to shear forces. Two aluminium bolts sizes (M12 and M16) were tested. The other geometrical and material characteristics of all details are discussed later in the report.

The shear forces used to design each detail according to the selected level of seismicity is reported in Table 1. They have defined from the results of the seismic global analyses presented in deliverable D1.3 [3]. It is worth noting that the actual strength of the specimens in perfect conditions should be higher given the experimental outcomes of the shear tests on the aluminium bolts (see Table 1 and Table 4). However, additional shear forces caused by eccentricities in the details between the force application load and the centre of mass of the bolt groups may influence the response of some details as shown in the description of the results.

Table 1: List of seismic tests

Test specimen	Seismicity level	Design shear (F_{VEd})	Bolts	Shear planes	Design strength (F_{VRd})	Actual expected resistance	Tests
Detail 1	Low	80 kN	M12	6	123.6 kN	219.6 kN	2 monotonic tests 2 cyclic tests
Detail 2	Moderate	180 kN	M16	8	308.0 kN	634.4 kN	2 monotonic tests 2 cyclic tests
Detail 3.1	Moderate	180 kN	M16	6	231.0 kN	475.8 kN	2 monotonic tests 2 cyclic tests
Detail 3.2	Moderate	180 kN	M12	12	247.2 kN	439.2 kN	2 monotonic tests 2 cyclic tests
Detail 4	Moderate	180 kN	M12	12	247.2 kN	439.2 kN	2 monotonic tests 2 cyclic tests
Detail 5	Moderate	180 kN	M12	12	247.2 kN	439.2 kN	2 monotonic tests 2 cyclic tests

1.2 Instrumentation

All the specimens were inserted in a reaction frame, where it is installed a hydraulic actuator of 1000 kN capacity and a stroke of ± 250 mm, as shown in Figure 1.

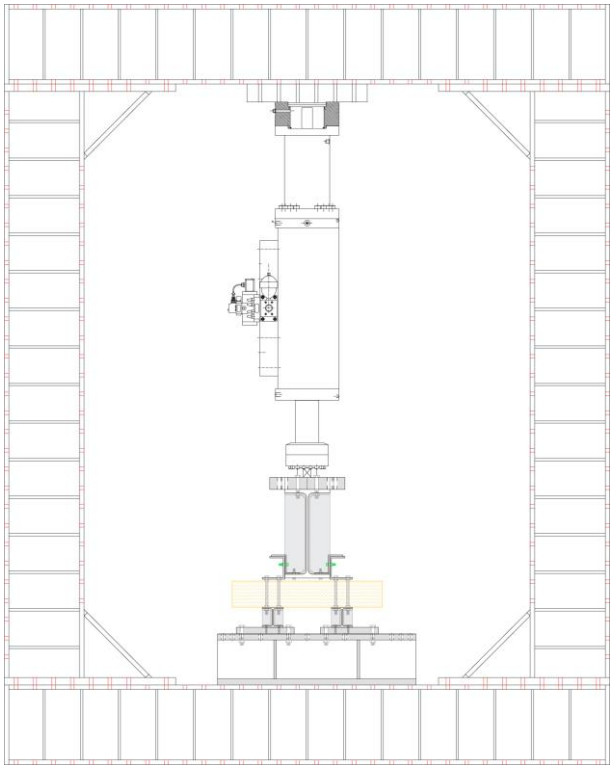

Figure 1. Reaction frame scheme

The actuator has its own load cell and its own displacement transducer. In addition, local instrumentation was applied to each detail. A maximum of 20 channels for strain gauges, 16 channels for displacement transducers and 4 channels for inclinometers were arranged on the specimens to investigate their behaviour. The number of devices was selected based on the detail considered. In general, strain gauges were applied close to the aluminium bolts to detect the steel strains; displacement transducers were installed to check the symmetrical behaviour of the specimens in each direction and, eventually, also some inclinometers were used when large deformations and rotations were expected. Figure 2 shows a typical arrangement of instruments on a specimen.

(a) (b) (c)

Figure 2. Example of local instrumentation used for the tests: a) displacement transducers; b) strain gauges; c) inclinometers.

All the tests were performed in displacement control, with a displacement rate of 0.5mm/min for the monotonic tests and different values for the cyclic tests. The reaction frame flexibility was calculated and removed from the tests data.

1.3 The ECCS procedure

The ECCS procedure [2] is a protocol published in the 80s by a European technical group with the aim to provide a reference to carry out and interpret experimental tests. Indeed, the behaviour of steel structural elements under cyclic loads may differ from the ideal elasto-plastic element, especially in a seismic event. Consequently, testing may be necessary to check the adequacy of the element to the demand by seismic recommendations.

The test procedure may be complete or short. This means that preliminary monotonic displacement increase tests may be necessary in the complete testing procedure, while they could not be performed in the short testing procedure. The complete testing procedure executes three different tests: the first one is a monotonic displacement increase test on the tension range defined as positive. The output is a stress-strain curve (or force-displacement). The second test is a monotonic displacement increase test in a compressive range defined as negative, whose output is again a stress-strain curve. The aim is to define the yield displacement from the curves that are supposed to exhibit some elasto-plastic behaviour. It is worth pointing out that in this experimental campaign the response of the specimens can be brittle, because governed by the bolt failure in shear, and the definition of a yield displacement would not be strictly correct. Nonetheless, to keep the nomenclature consistent with the protocol, in the text, the displacement selected to define the cyclic displacement history will be still called "yield displacement". As shown in Figure 3, the procedure to follow evaluates the tangent at the origin of the curve, then locates a tangent with an E/10 slope, where E is the elastic slope, and eventually defines the displacement corresponding to the intersection of the two tangents. The same procedure is applied to both curves obtained from the monotonic tests. The third test is a cyclic test with increasing displacement, which follows the steps calculated as reported in Figure 3b.

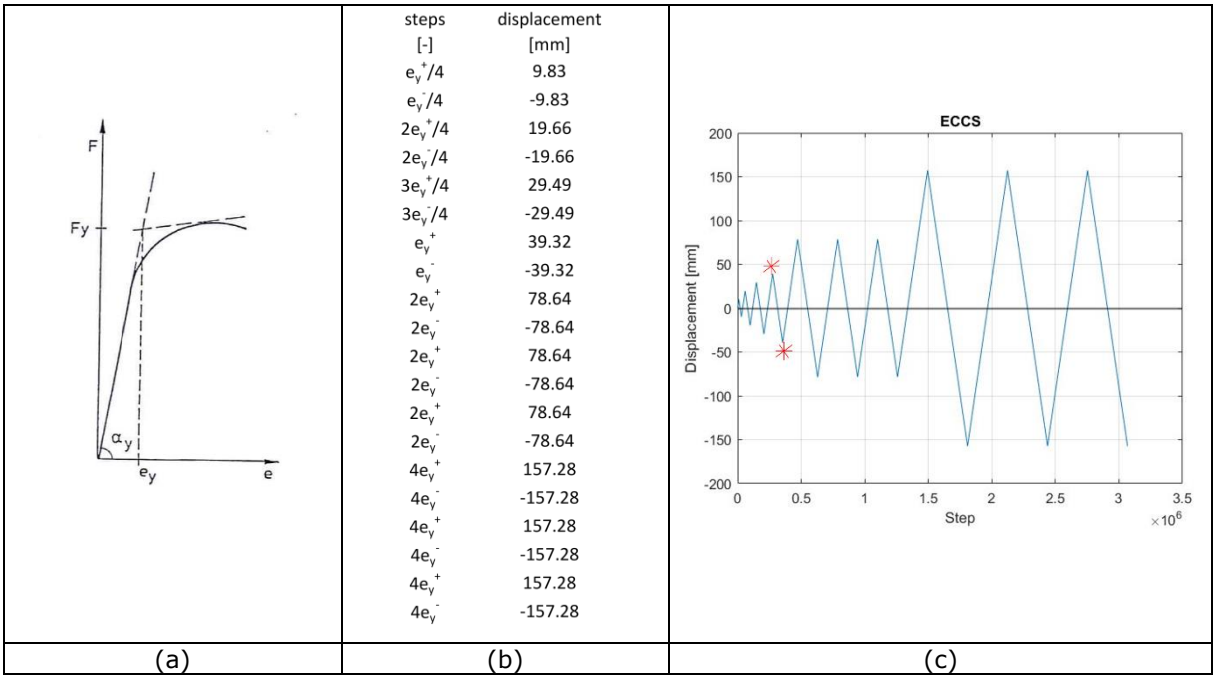

Figure 3. ECCS procedure: a) define of yield displacement, b) example of displacement history steps for cyclic test, c) plot of displacement history.

1.4 Material properties

The following tables reports the mechanical properties of the elements composing the test specimens. In particular, Table 2 reports the actual yield strength of the steel elements used for the details.

Table 2. Mechanical properties of the steel elements

Element	Steel grade	Actual yield strength
HEA140	f_y = 275 MPa	f_y = 353 MPa
HEA180	f_y = 275 MPa	f_y = 311 MPa
HEA600	f_y = 275 MPa	f_y = 314 MPa
HEB140	f_y = 275 MPa	f_y = 298 MPa
HEB180	f_y = 275 MPa	f_y = 328 MPa

UPN160	f_y = 275 MPa	f_y = 342 MPa
T plate th.10 mm	f_y = 235 MPa	f_y = 289 MPa
T plate th.15 mm	f_y = 355 MPa	f_y = 424 MPa

Table 3 and Table 4 illustrate the aluminium bolt characteristics in accordance with the Eurocode 9 [5] and the actual shear resistance obtained through laboratory tests. More details can be found in Deliverable D3.1 [4] and Deliverable D1.4 [1].

Table 3. Aluminium bolt characteristics

Bolt size	**Designation ISO 209-1**	**f_u (MPa)**
M12	AlZn5,5MgCu 7075	490
M16	AlZn5,5MgCu 7075	490

Table 4. Aluminium bolt mechanical properties

Bolt size	**A_{res} (mm^2)**	**Characteristic shear capacity according to EC9 (kN)**	**Experimental shear capacity (kN)**
M12	84.3	20.6	36.6
M16	157	38.5	79.3

2 THE EXPERIMENTAL CAMPAIGN

As already indicated, the experimental campaign involved 4 tests for each detail. The two monotonic tests are presented first, followed by the two cyclic tests.

2.1 Tests on Detail 1

As reported in Deliverable D1.4 [1], all the details were developed from 3 reference fusible link solutions common to all the project partners.

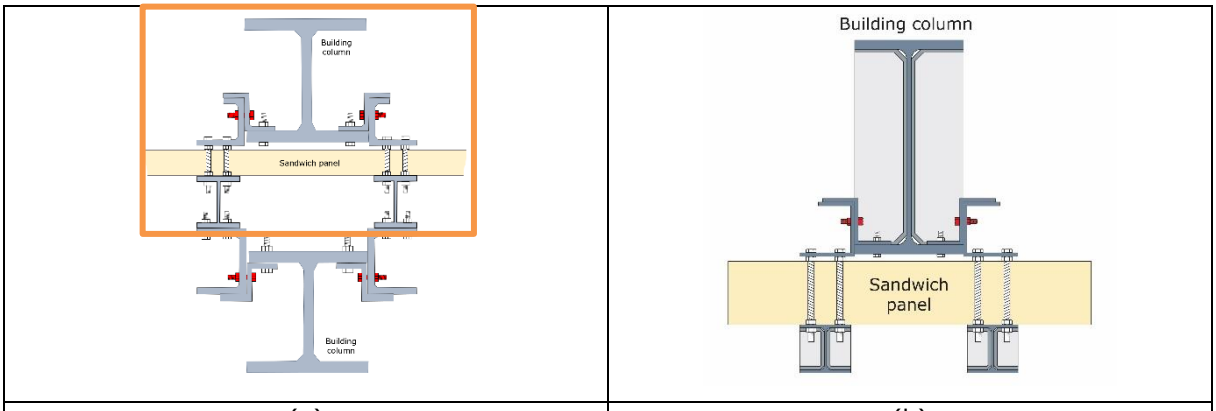

(a) (b)

Figure 4. Detail 1: (a) reference detail; (b) Detail 1 for seismic tests.

Figure 4 reports Detail 1 conceived for the seismic tests and the reference fusible link solution from which it was derived. As can be noticed, some adaptions for the tests, like the addition of some stiffeners to column were necessary to withstand the applied concentrated forces. Moreover, only the upper part of the detail was tested under the seismic forces.

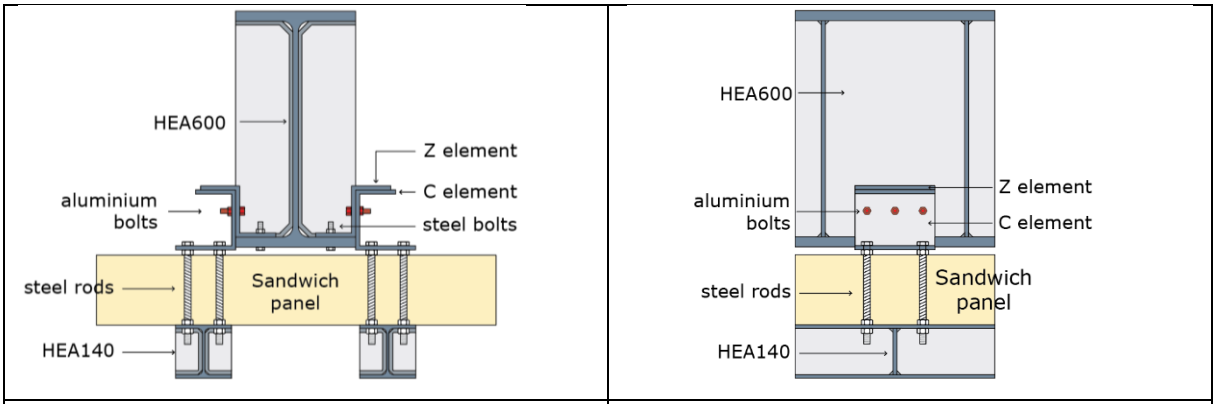

(a) (b)

Figure 5. Detail 1: (a) front view; (b) lateral view.

Table 5: Detail 1 description

Elements	**Main characteristics**
C element	2 100x150x150x10 S275
Z element	2 100x128x100x10 S275
Aluminium bolts	6 M12 AlZn5,5MgCu 7075
Steel rods	8 M16 8.8
Steel bolts	6 M12 8.8

In Figure 5 and in Table 5, the main characteristics of Detail 1 are reported in terms of elements and geometry that compose the specimen. As reported in Table 1, this detail was designed for a shear value of 80 kN, that can be withstood by 6 M12 aluminium bolts.

2.1.1 Monotonic tension test

Figure 6. View of the tension test set-up for detail 1.

In Figure 6, the specimen of Detail 1 inserted in the reaction frame can be observed. Some additional steel tree elements were used as a support for the instrumentation.

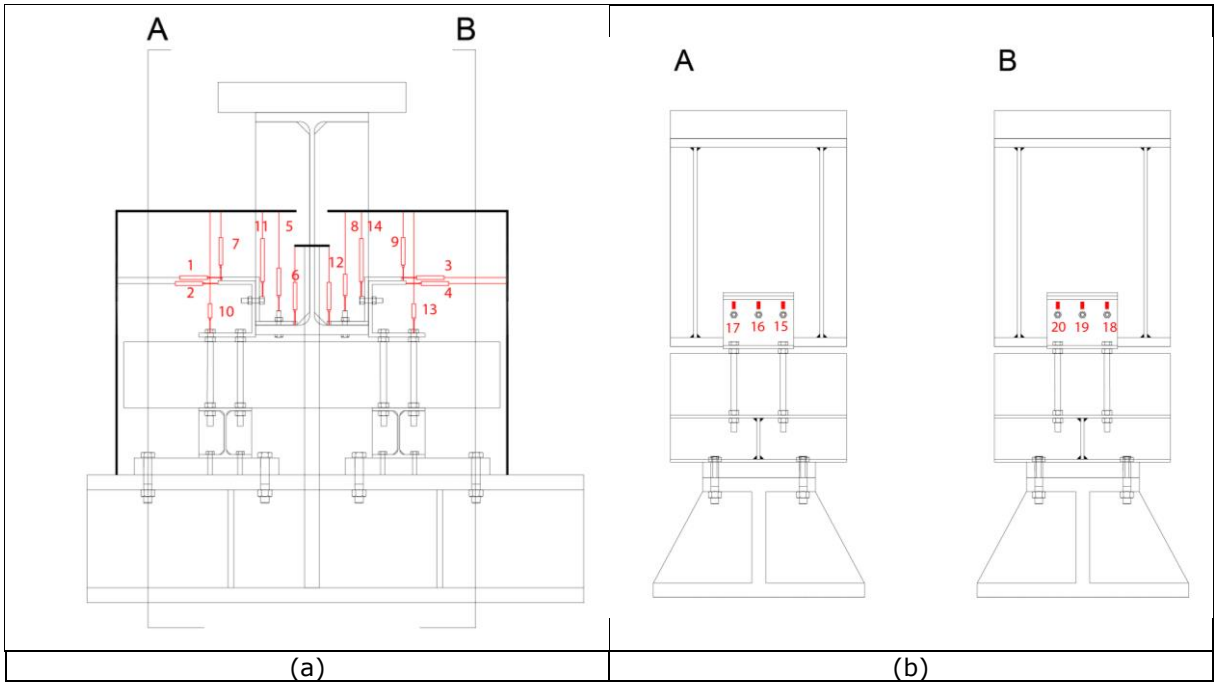

Figure 7. Detail 1: (a) displacement transducers arrangement; (b) strain gauges position.

In Figure 7, the specific instrumentation position and numbering are reported.

The displacement transducers are LVDT (Linear Variable Displacement Transducer) and were located to check specific displacements of the detail:

- LVDT 1, LVDT 2, LVDT 3 and LVDT 4 were installed at the upper part of the Z and C elements to check their possible rotation;
- LVDT 5, and LVDT 8 were installed to check the possible vertical displacement of the steel bolts;
- LVDT 7 and LVDT 9 were installed to record the vertical displacement of the Z elements;
- LVDT 11 and LVDT 14 were installed to check the vertical displacement of the aluminium bolts;
- LVDT 10 and LVDT 13 were installed to check the vertical displacement of the C elements;

- LVDT 6 and LVDT 12 were installed to measure the actual vertical movement of the specimen (HEA600) removing the displacement of the reaction frame caused by its, though small, inherent flexibility.

A total of 6 strain gauges were glued on the steel C elements to measure the vertical strain induced by the aluminium bolts during the test. The instrument acquisitions were recorded at 2 Hz.

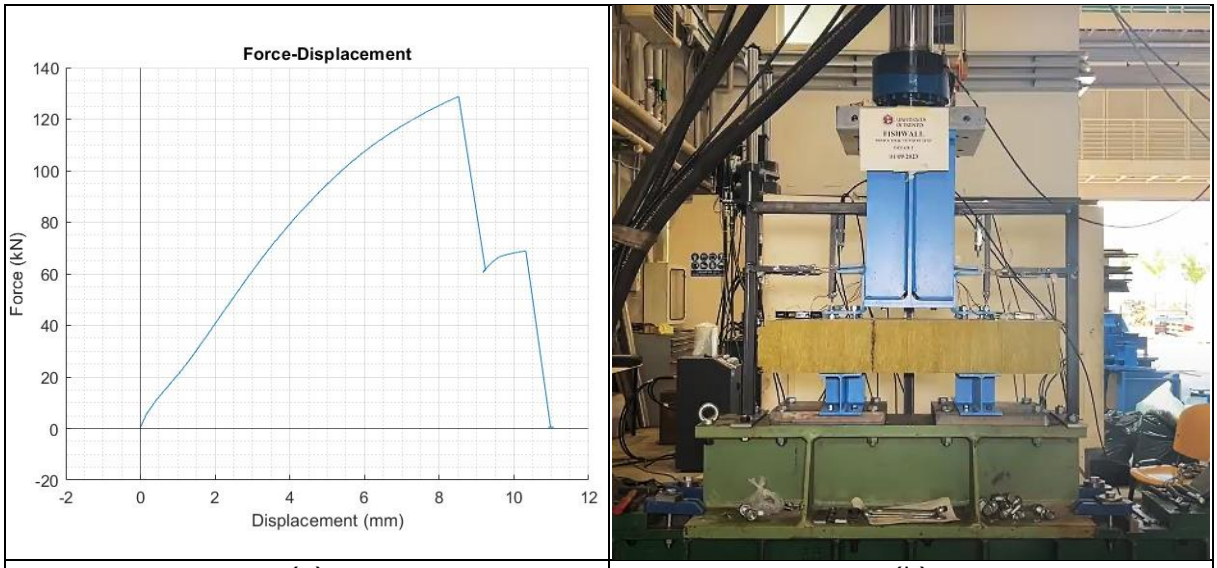

(a) (b)

Figure 8. Detail 1: (a) force-displacement diagram of the monotonic tension test and (b) final specimen deformation

Figure 8 shows the result in terms of the force-displacement curve, where the first peak highlights the failure of the aluminium bolts on the right side of the specimen (considering their position in Figure 6). Then, the load suddenly decreased to increase again up to the failure of the aluminium bolts on the left side. It is worth noting that the design force of 80 kN was reached and the maximum experimental force, i.e. 128.8 kN, is about 60% of the total expected actual resistance, as reported in Table 1. This result is in line with the experimental evidence, because the maximum experimental capacity represents the failure of half of the aluminium bolts. In fact, due to the presence of inherent imperfections in the test specimens, the simultaneous failure of all bolts is highly improbable.

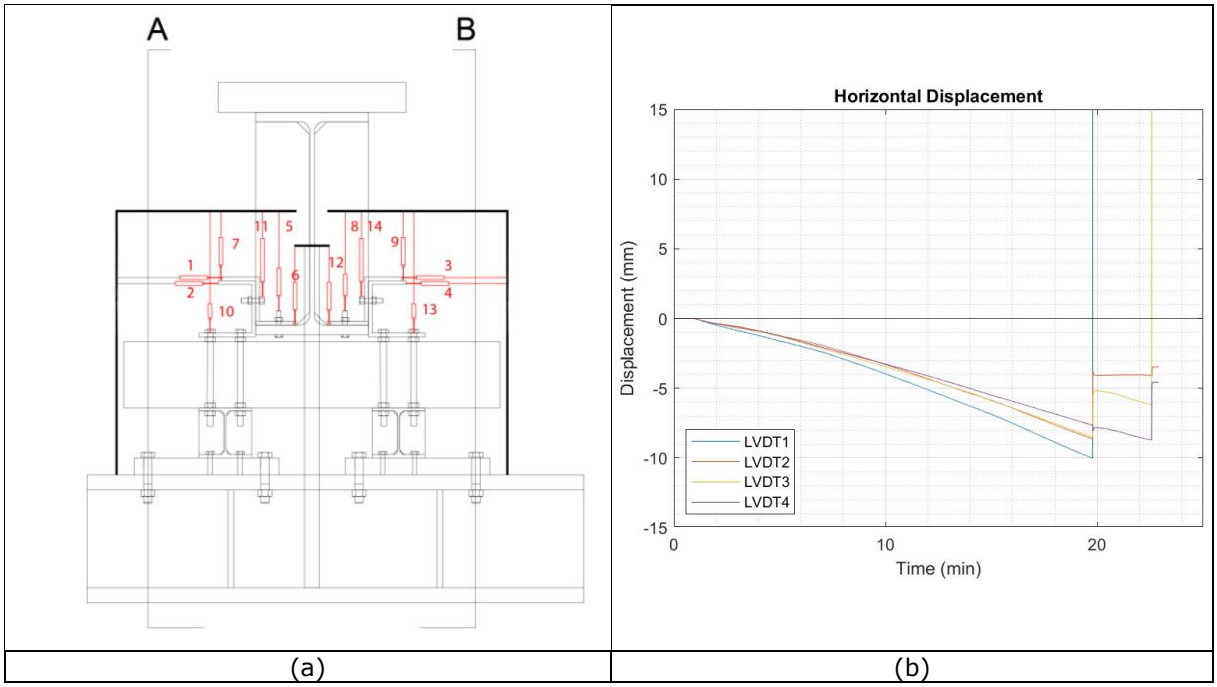

(a) (b)

Figure 9. Detail 1: (a) arrangement of the LVDT, (b) horizontal LVDT results recorded during the tension test.

In Figure 9, the results of the horizontal displacement transducers acquisitions on C and Z elements are reported. As can be noticed, a constant movement of the upper part of the elements was detected, which is in accordance with their final deformation.

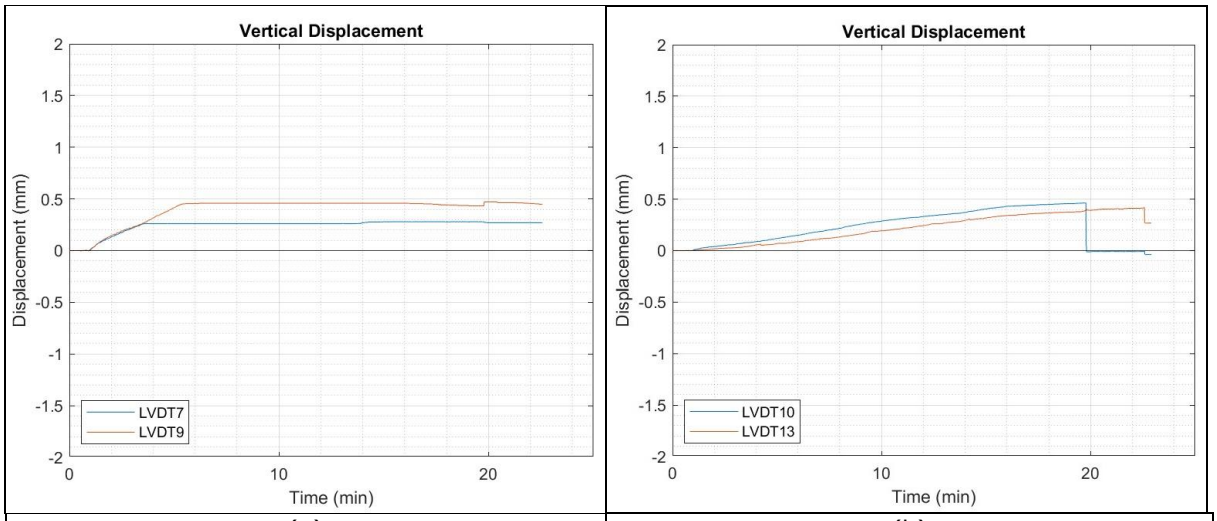

(a) (b)

Figure 10. Detail 1 - LVDT results on of C and Z elements: (a) upper part (b) lower part.

In Figure 10 the vertical displacements are reported. The minimum vertical displacement of the upper part of the Z element, illustrated in Figure 10a, and the displacement of the lower part, depicted in Figure 10b, are in a good agreement with the final deformation of the specimen (Figure 8b).

The other displacement transducers located on the specimen reported a consistent displacement with the global vertical displacement, as reported in Figure 8a.

The results of the strain gauges installed on the steel part close to the aluminium bolts are hereafter analysed. The steel strains depicted by the strain gauges around the aluminium bolts reported a consistent compression with the test, as shown in Figure 11. The local strain levels did not exceed the actual steel yield limit, that is 1376 με, highlighting that significant bearing effects were not detected.

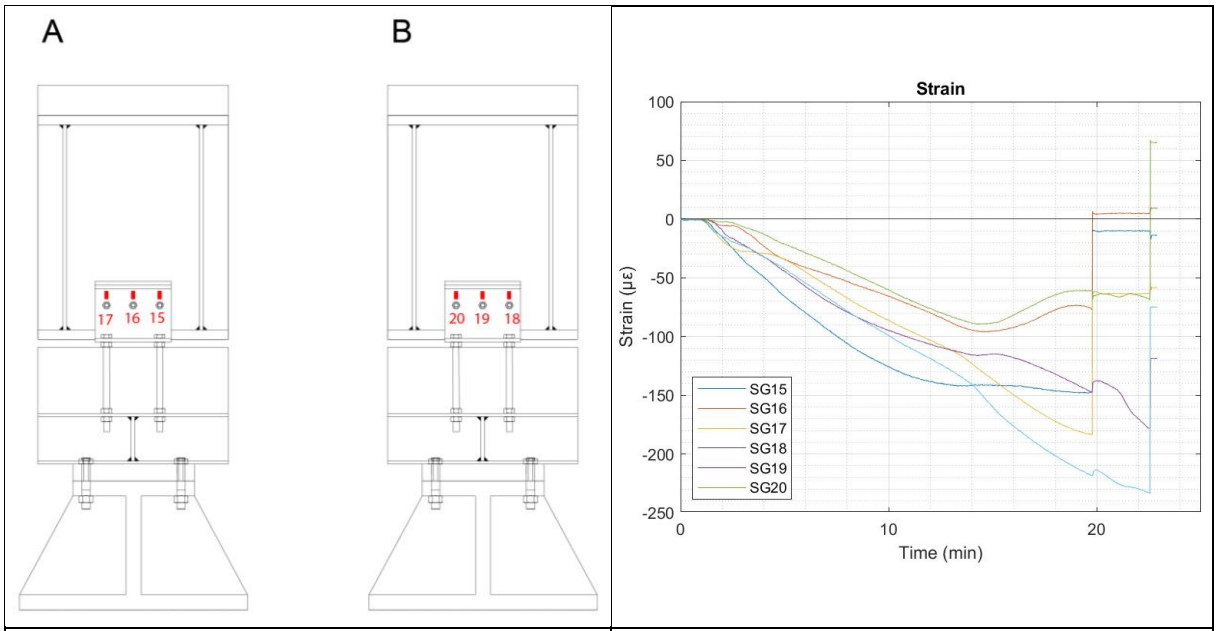

(a) (b)

Figure 11. Detail 1 strain gauges (a) location and (b) results.

2.1.2 Monotonic compression test

In Figure 6 the specimen of Detail 1 inserted in the reaction frame can be observed.

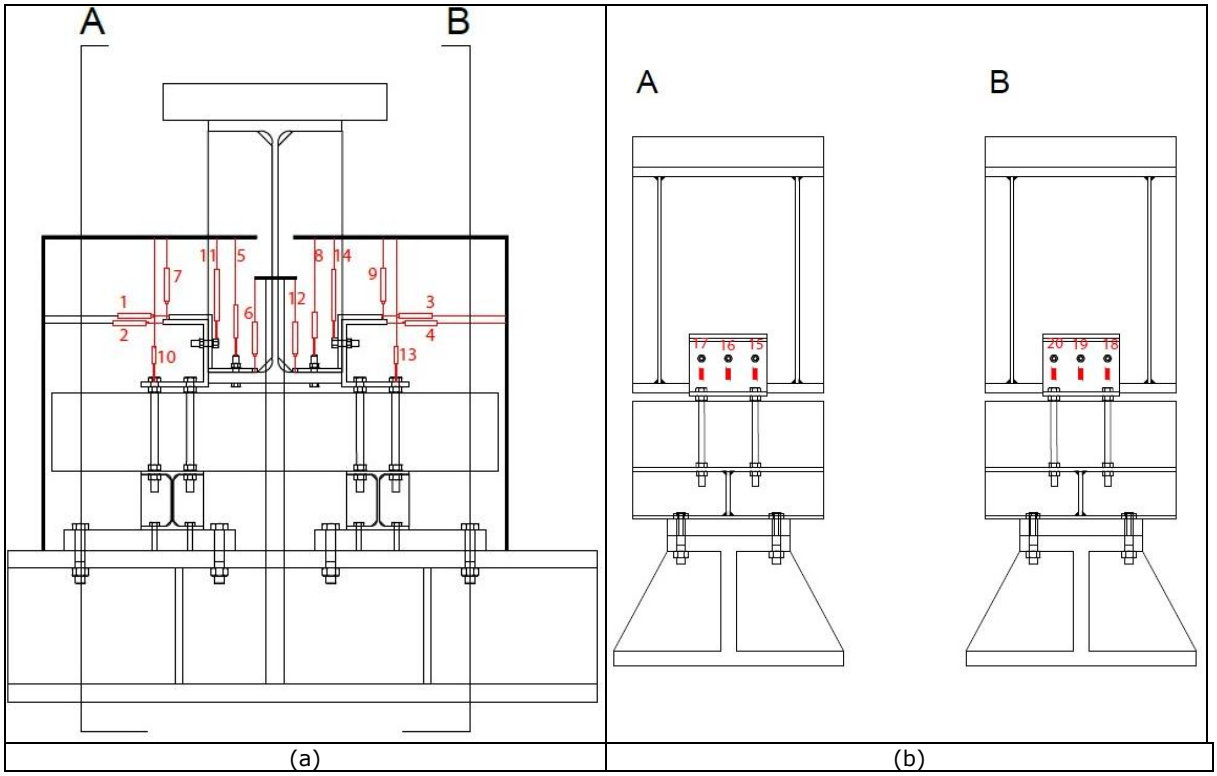

(a) (b)

Figure 12. Detail 1: (a) LVDTs arrangement; (b) strain gauges position on the left side (A) and the right side (B).

In Figure 12, the specific instrumentation position and numbering are reported.

The displacement transducers are LVDTs and were located to check specific detail movements, as reported in Section 2.1.1.

Also in this case, a total of 6 strain gauges were located on the steel C elements to measure the strain induced by the aluminium bolts during the test. The instrument acquisitions were recorded at 2 Hz.

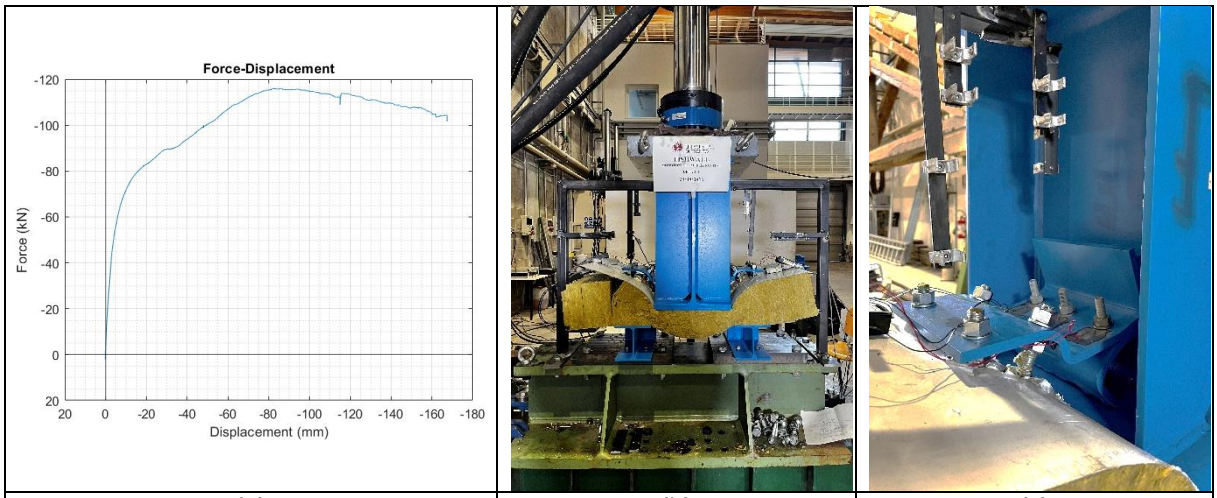

(a) (b) (c)

Figure 13. Detail 1: (a) force-displacement diagram of the monotonic compression test; (b) final specimen deformation and (c) detail deformation.

Figure 13 shows the result of the test in terms of the force-displacement curve, where a ductile behaviour of the specimen can be noticed. Indeed, due to the detail configuration, the compression forces were transmitted through the specimen by contact between the steel elements, which underwent plastic deformation at the end of the test, as can be noticed in Figure 13c. Consequently,

the diagram reported in Figure 13a is representative of the steel elasto-plastic that occurred during the test. Therefore, the aluminium bolts were not affected/damaged.

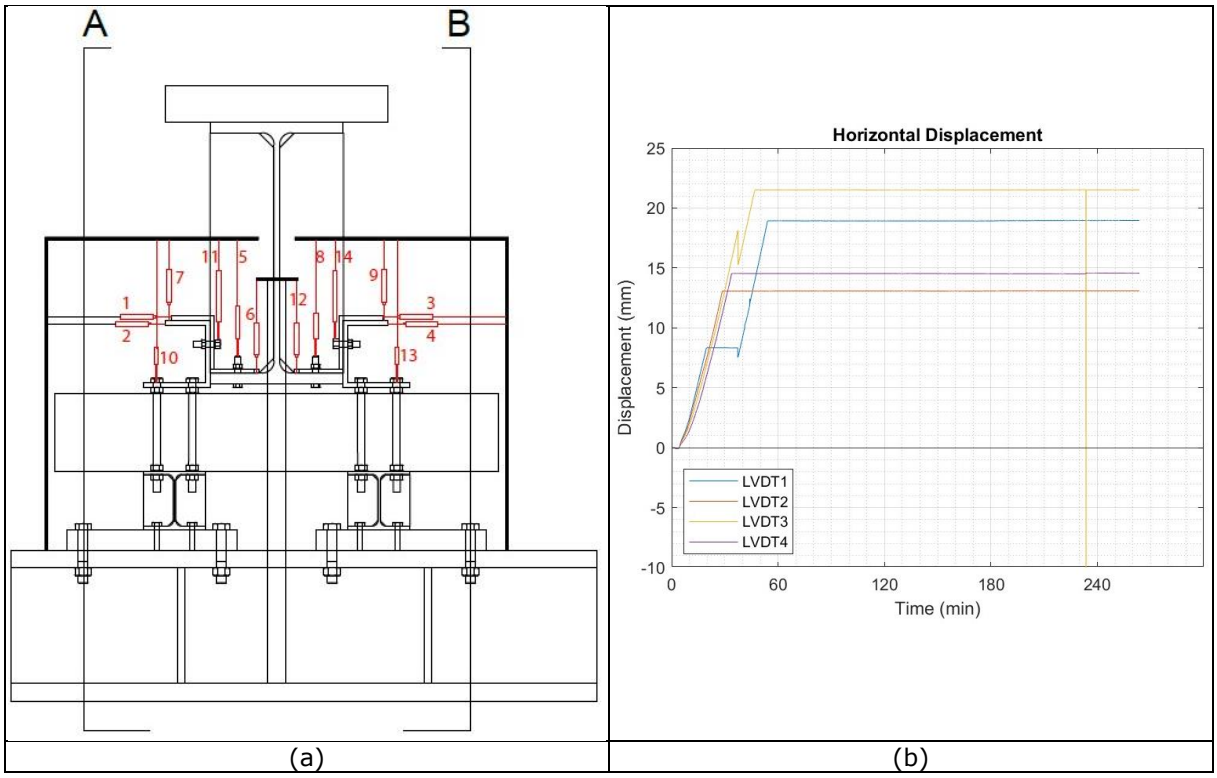

(a) (b)

Figure 14. Detail 1: (a) arrangements of the LVDTs on the specimen; (b) horizontal LVDT results recorded during the compression test.

In Figure 14 the results of the horizontal displacement transducers acquisitions on C and Z elements are reported. As can been noticed, after an initial correct recording, the instruments lost the contact with the steel elements owing to their deformation. Slight differences (about 2 mm) in the readings are related to the specimen inherent imperfections, in particular of the C and Z elements.

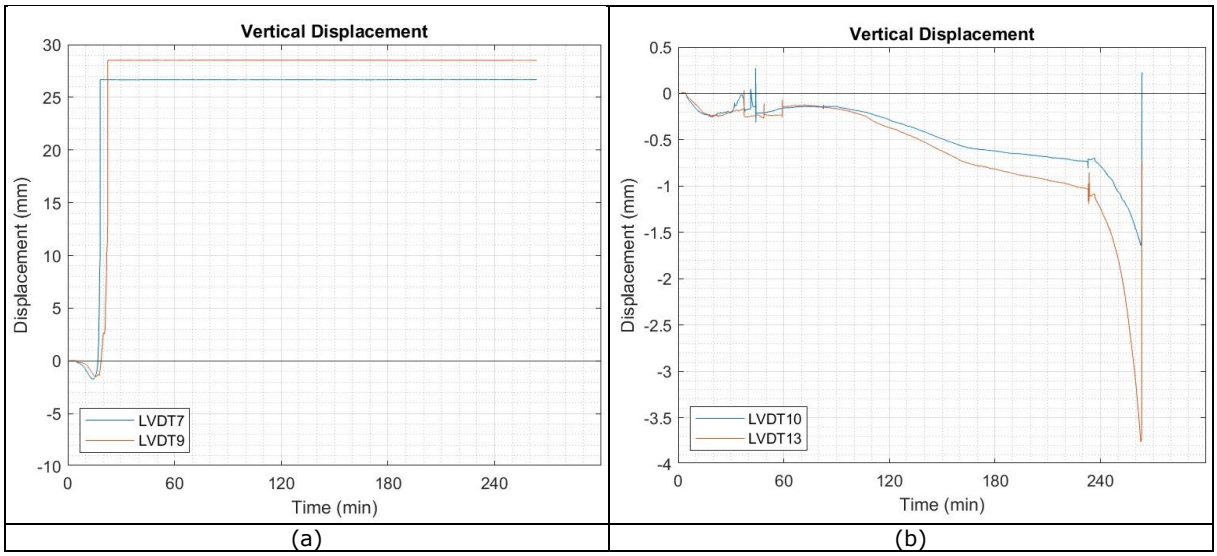

(a) (b)

Figure 15. Detail 1 - LVDT vertical displacements: (a) on upper part of Z elements; (b) on the upper part of C elements.

As mentioned for the vertical displacement, the LVDT on the upper part of the Z element lost contact with the steel part during the test and did not record the displacement after about 20 minutes, as seen in Figure 15a. On the contrary, the displacement transducers on the lower part of the C element acquired a minimum displacement, as reported in Figure 15b.

The other displacement transducers located on the specimen reported a consistent displacement with the global vertical displacement reported in Figure 13a.

The steel strains described by the strain gauges around the aluminium bolts (Figure 16) reported an initial tension phase, due to the large deformation occurred on the steel part, visible in Figure 13c, and a subsequent compression, caused by the contact between the Z element and the HEA600 web. It is possible to observe that the actual steel yield limit was overcome, and an elasto-plastic behaviour of the steel elements connected with the aluminium bolts is confirmed.

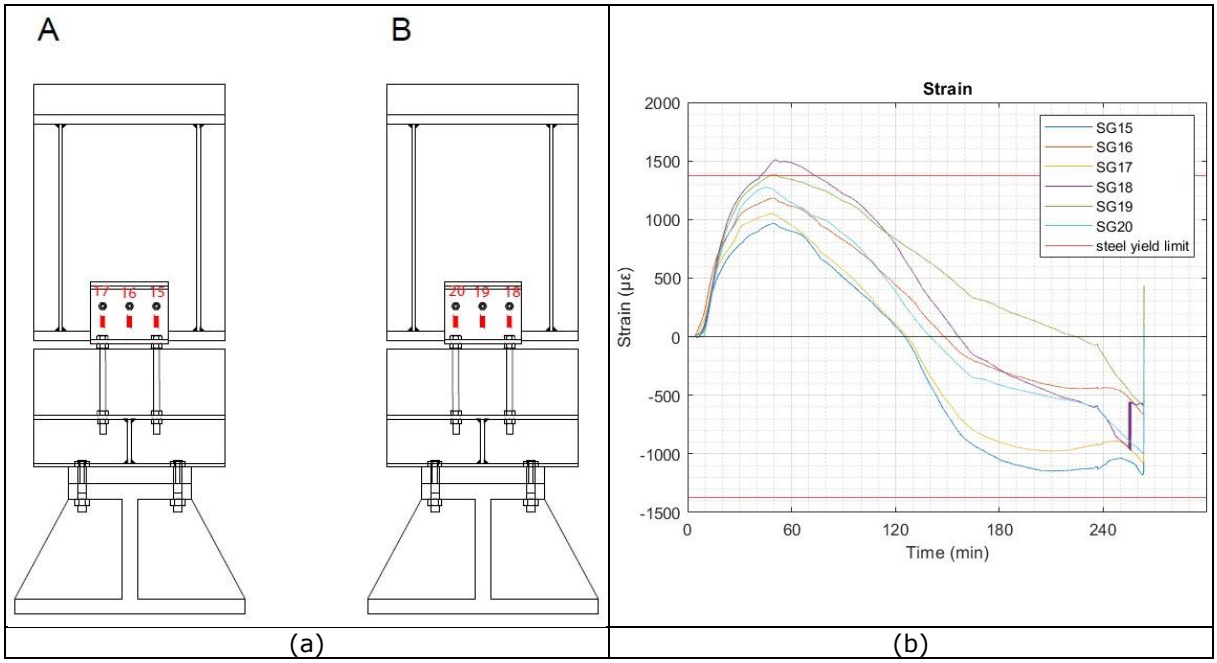

Figure 16. Detail 1: (a) strain gauges position and (b) results

2.1.3 Cyclic tests

In order to follow the ECCS procedure, as reported in Section 1.3, the two monotonic test curves were used to define the yield displacement and the displacement history to carry out the cyclic tests.

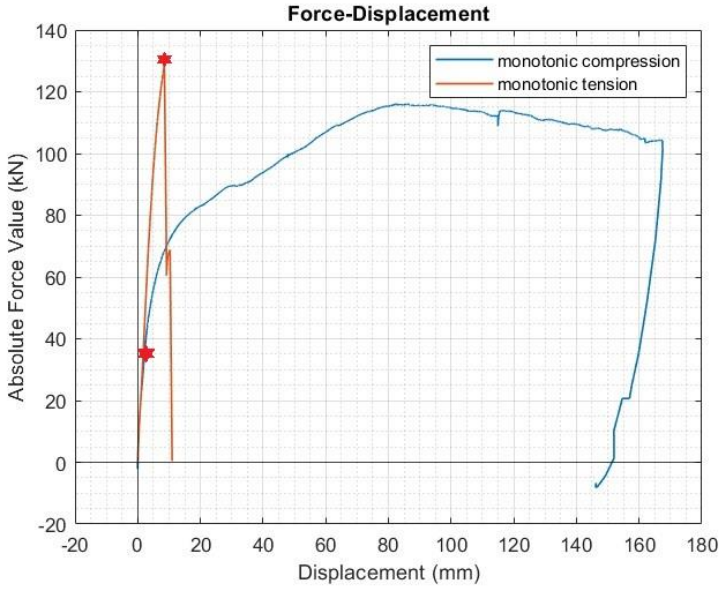

Figure 17. Detail 1 monotonic tests results comparison

Figure 17 reports the comparison, in terms of force-displacement curves, between the monotonic tension and compression tests. The red points represent the selected yield displacements for the cyclic test, that are also reported in Table 6. While the definition of e_y for the compression curve was clear, because of the ductile behaviour of the specimen, the definition of e_y chosen for the curve obtained from the monotonic tension test was not straightforward due to the brittle of behaviour experienced by the specimen. Finally, it was decided to select an e_y corresponding to the first failure of an aluminium bolt, as highlighted in Figure 17.

Table 6: Yield displacement from monotonic curves

e_y	8.5 mm
$-e_y$	2.0 mm

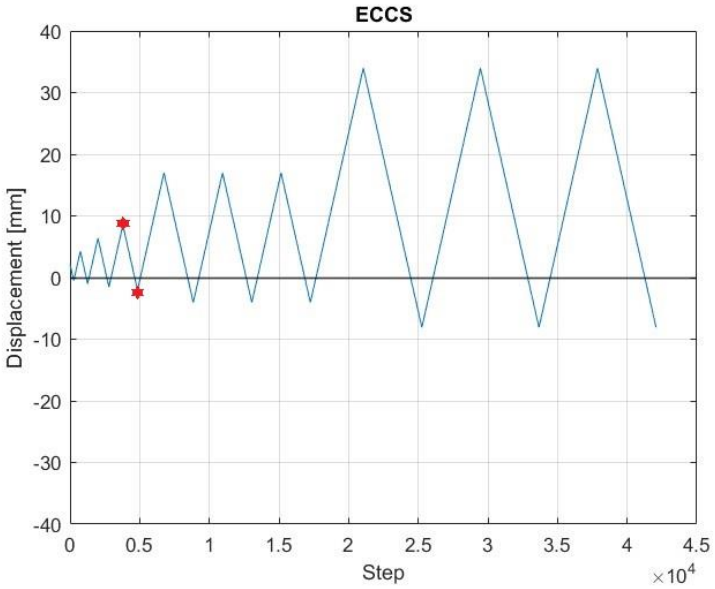

Figure 18. Detail 1 ECCS procedure.

As shown in Figure 18, the displacement history, defined as reported in Section 1.3, is not symmetric. The yield displacements are highlighted in red.

The cyclic tests were conducted in displacement control with different displacement rates. In greater detail, until the e_y, the displacement rate was 0.5 mm/min; for the three cycles at $2e_y$ the displacement rate was 1 mm/min; for the last three cycles at $4e_y$ the displacement rate was set at 2 mm/min.

2.1.3.1 Cyclic test 1

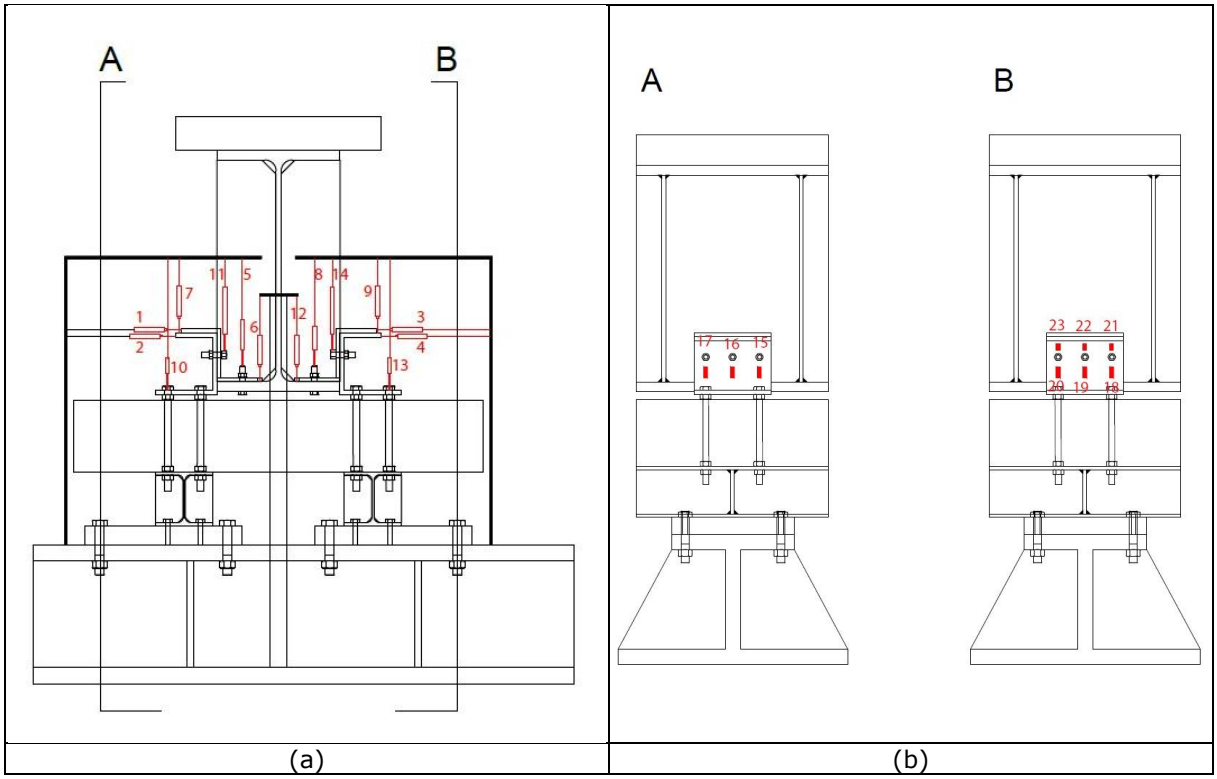

(a) (b)

Figure 19. Detail 1: (a) LVDTs arrangement; (b) strain gauges position on the left side (A) and the right side (B).

Figure 19 reports the instrumentation position and numbering.

The displacement transducers are LVDTs and were located to check specific detail movements as reported in Section 2.1.1.
In this case, 9 strain gauges were located on the steel C elements to measure the strain close to the aluminium bolts during the test. The instruments acquisitions were recorded at 2 Hz.

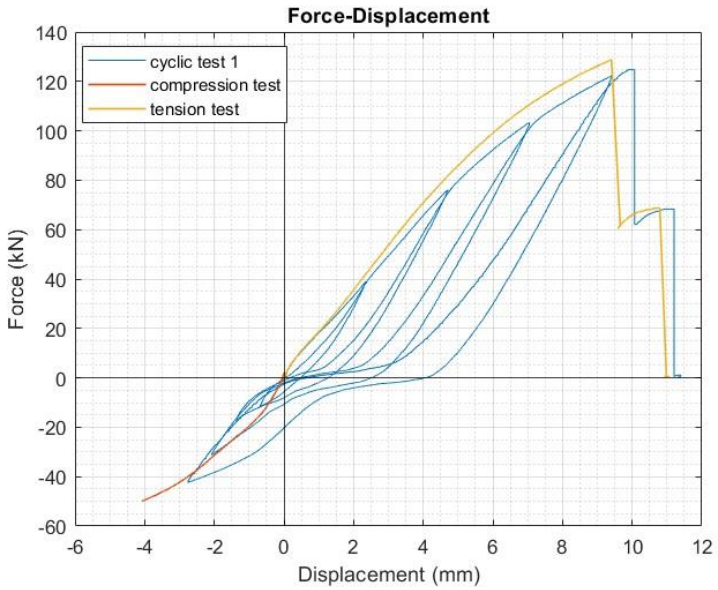

Figure 20. Detail 1 - cyclic test 1 results

The results of the first cyclic test on Detail 1, in terms of force-displacement curve, are shown in Figure 20. The failure of the specimen occurred on the reloading at the first cycle to $2e_y$. Besides the brittle nature of the detail in tension, a small hysteretic behaviour can be observed. It is worth noting that the design force of 80 kN was reached in the tension branch, where the aluminium bolts were effectively working in shear. The comparison between the cyclic and monotonic tests showed good agreement in terms of strength and stiffness degradation.

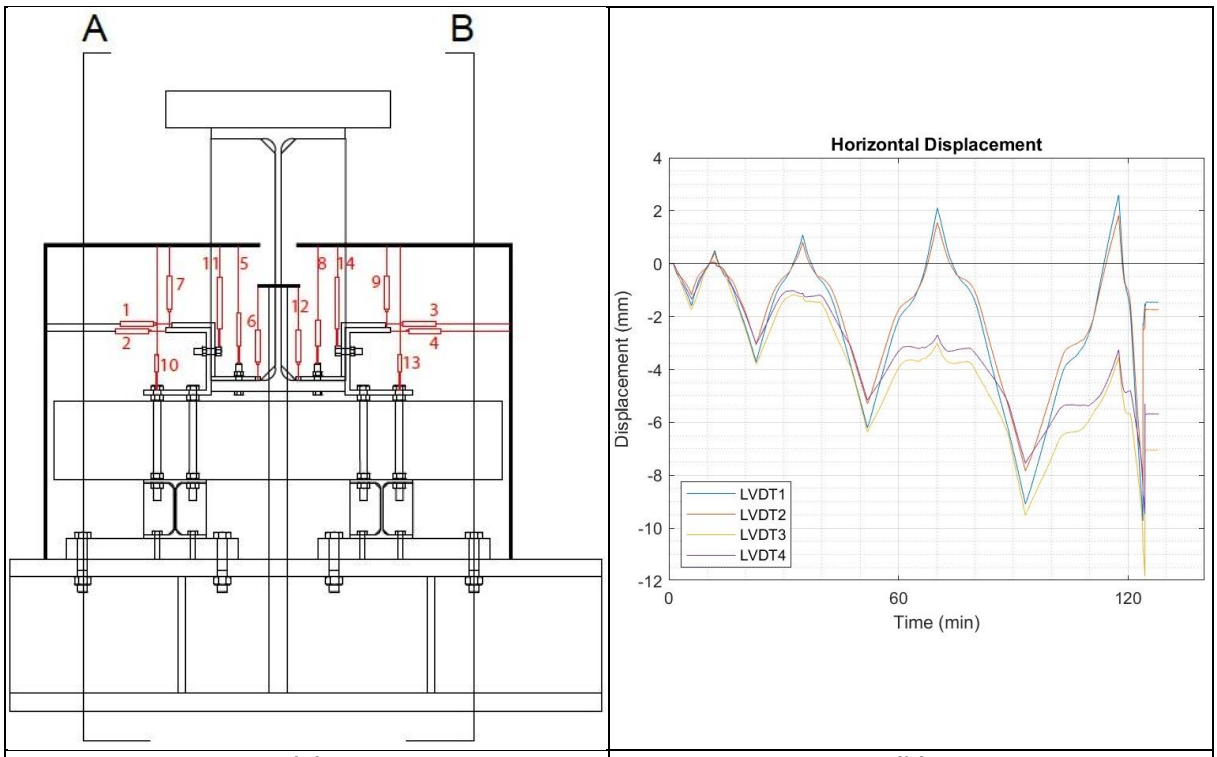

(a) (b)

Figure 21. Detail 1: (a) LVDT on elements C and Z and (b) cyclic test horizontal LVDT results.

The horizontal displacement transducers results are reported in Figure 21. As can be noticed, the trend follows the cyclic path, while a difference in the reloading phase between the left and right parts can be highlighted, with reference to Figure 21a. This difference highlighted a slight asymmetric behaviour of the specimen during the test related to the specimen inherent imperfections, in particular of the C and Z elements.. This is also supported by the vertical LVDTs behaviour on the

lower part of the C elements, as shown in Figure 22a. Indeed, the LVDT 9, located on the specimen right side, recorded larger a displacement than the same instrument on the left side, LVDT 7.

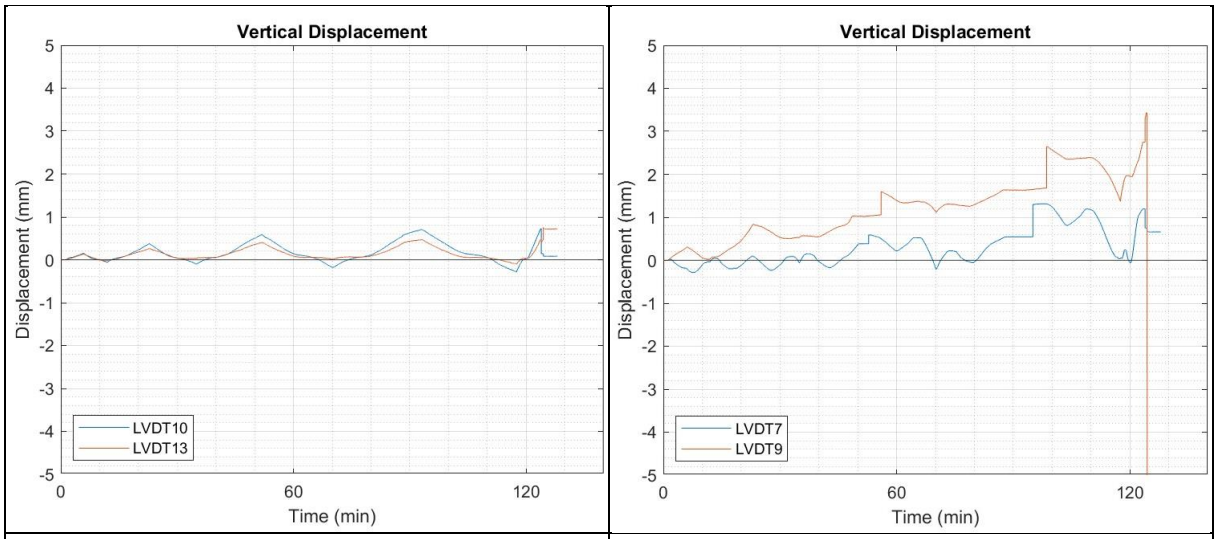

(a) (b)

Figure 22. Detail 1: LVDT vertical displacements observed: (a) on lower part of C elements; (b) on the upper part of Z elements.

All the other displacement transducers, as illustrated in Figure 22, had a consistent behaviour between them and in accordance with the actuator recording.

The strain gauges results installed on the steel parts close to the aluminium bolts are hereafter analysed.

As reported in Figure 23, the strains are consistent with the test trend. In greater detail, the instruments located in the same position on the two sides of the specimen showed the same behaviour, as highlighted in Figure 23a, as well as the instruments installed to detect alternate trends, as depicted in Figure 23b. From Figure 23 it is possible to observe that the strain levels close to the aluminium bolts did not exceed the actual steel yield limit, computed as 1376 με with the actual material properties, both in tension and in compression. In particular, this is due to the fact that in compression the attained force level was not high enough (about 40 kN) to induce inelastic behaviour in the steel elements close to the aluminium bolts.

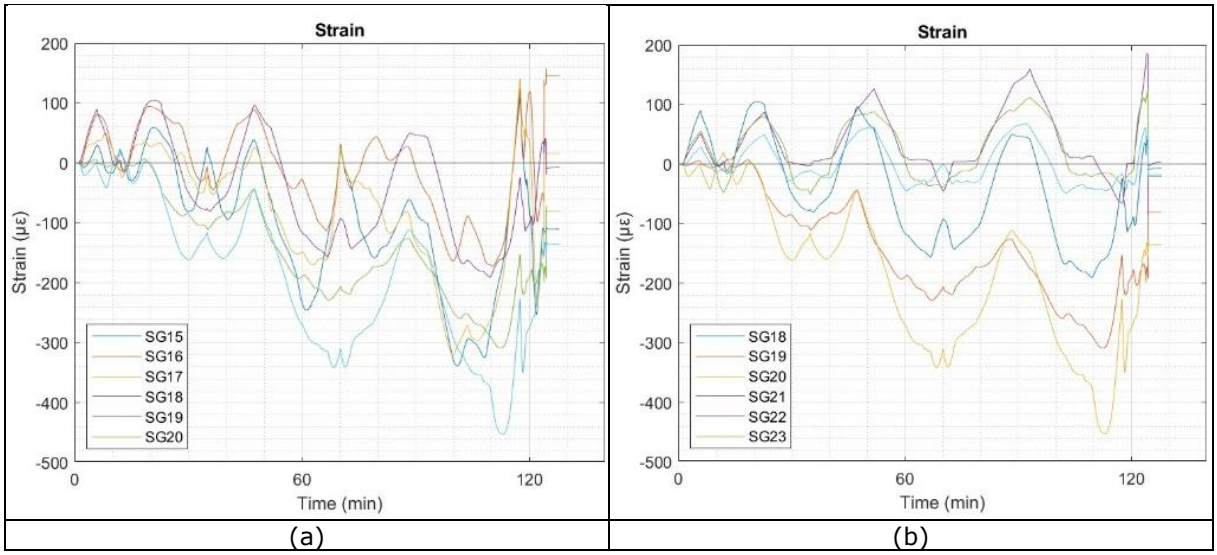

(a) (b)

Figure 23. Detail 1 - strain gauges results: (a) comparison between left and right side; (b) comparison between compression and tension branch.

2.1.3.2 Cyclic test 2

A second cyclic test on Detail 1 was repeated with the same testing protocol and instrumentation. The results of the second cyclic test on Detail 1, in terms of force-displacement curve, are shown in Figure 24. The failure of the specimen occurred on the reloading at the first cycle to $2e_y$, as for the first cyclic test. Besides the brittle nature of the detail, a hysteretic behaviour can be observed. It is

worth noting that, also in this case, the design force of 80 kN was reached in the tension branch, where the aluminium bolts were effectively working in shear. As for the first cyclic test, also in this case, a good agreement between the cyclic test and the monotonic tests can be highlighted. Thus, good repeatability was observed.

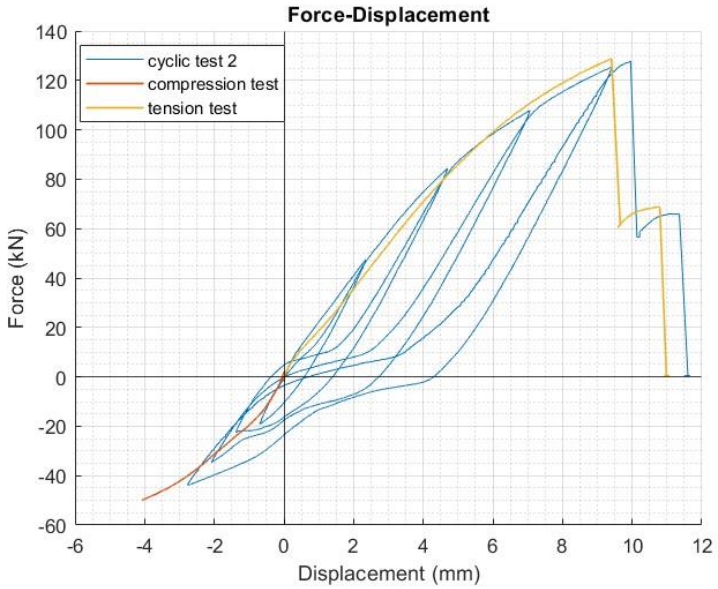

Figure 24. Detail 1 cyclic test 2 results

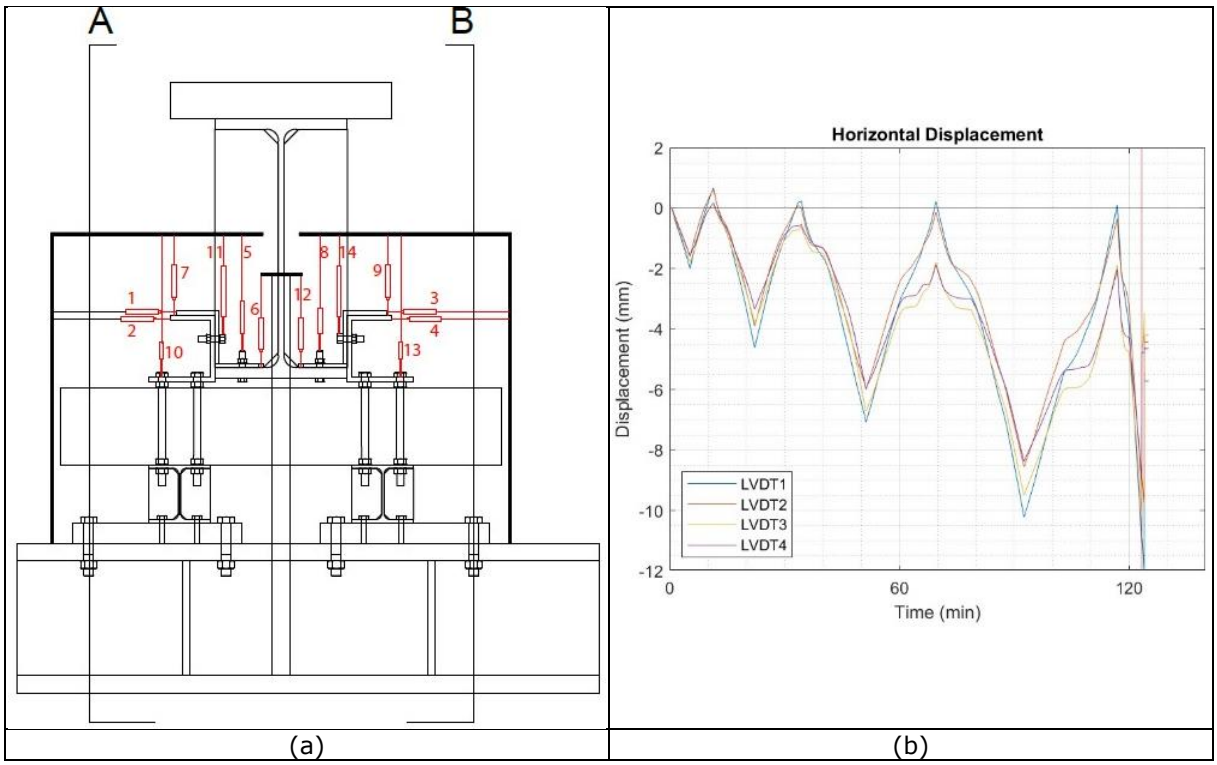

(a) (b)

Figure 25. LVDTs on the Detail 1: (a) arrangements; (b) horizontal LVDT results recorded during the cyclic test on C and Z elements.

The horizontal LVDT results are reported in Figure 25b. As occurred during the first cyclic test, the instruments recorded larger displacements on the specimen left side, caused by a possible asymmetry of the specimen. This was also confirmed by the vertical LVDT on the lower part of the C element, as reported in Figure 26a. In fact, the different displacements recorded by the instruments showed larger movements on the left side of the specimen.

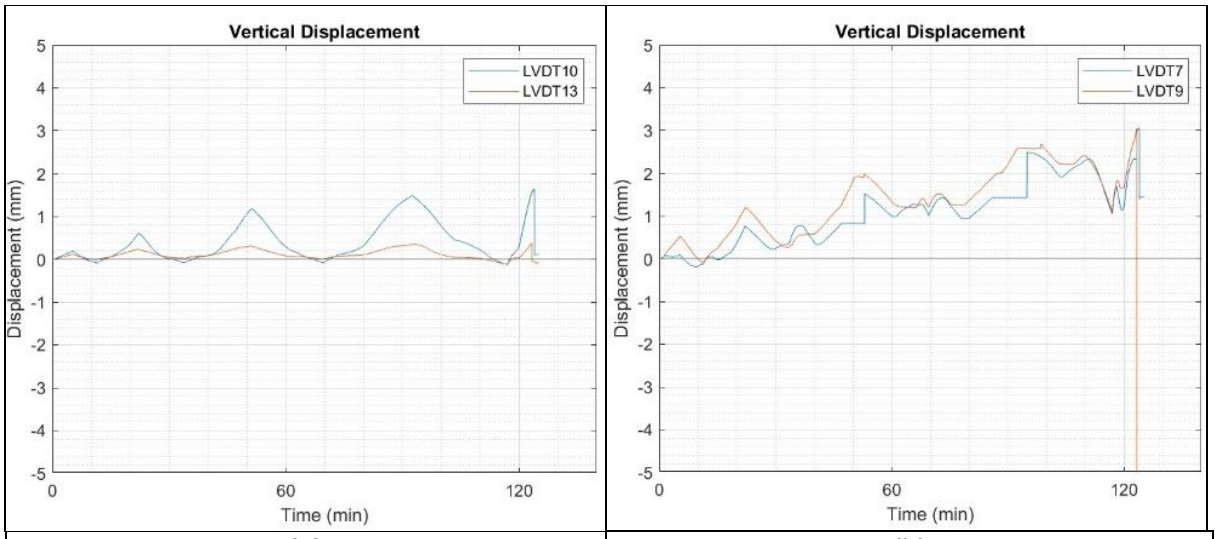

(a) (b)

Figure 26. Detail 1 - LVDT vertical displacements observed: (a) on lower part of C elements; (b) on the upper part of Z elements.

Considering the strain gauges installed on the steel parts close to the aluminium bolts, the results are hereafter reported.

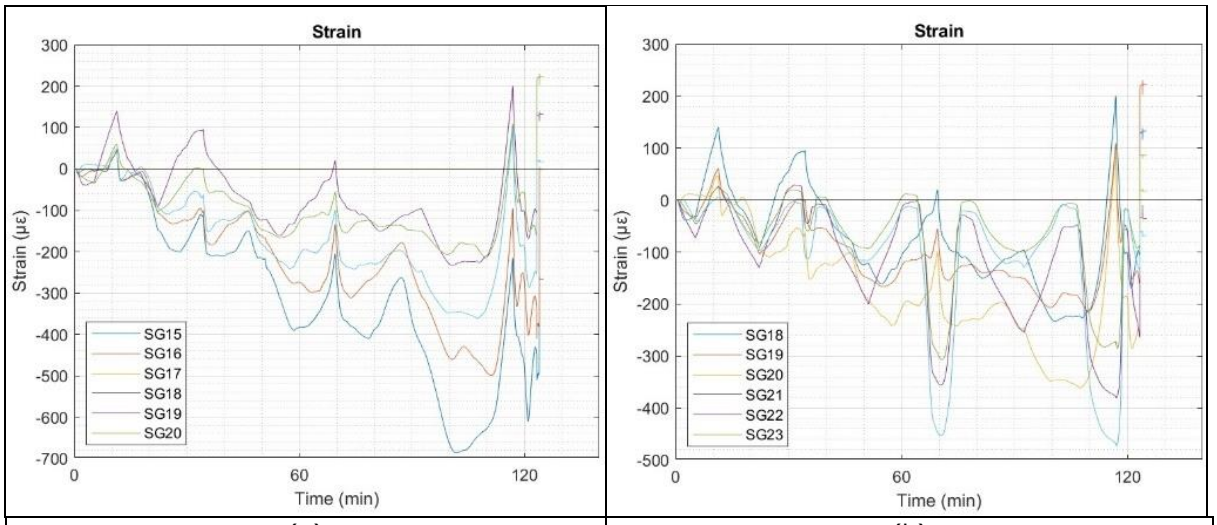

(a) (b)

Figure 27. Detail 1 - strain gauges results: (a) comparison between left and right side; (b) comparison between compression and tension branch.

Figure 27 depicts the strains acquired close to aluminium bolts. The two figures show a good agreement between the two sides of the specimen in terms of a consistent trend (see Figure 27a) and an alternate coherent graph between tension and compression (see Figure 27b). From Figure 27 it is possible to observe that strain levels close to the aluminium bolts did not exceed the actual steel yield limit, i.e. 1376 με, both in tension and in compression. In particular, this is due to the fact that in compression the attained force level was not high enough (about 40 kN) to induce inelastic behaviour in the steel elements close to the aluminium bolts.

2.1.4 Summary

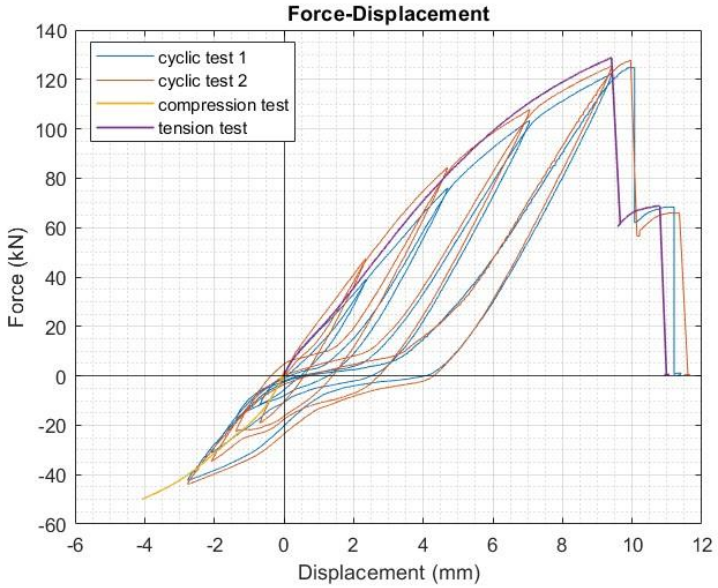

Figure 28. Detail 1 test result comparison.

The test results in terms of force-displacement curves are shown in Figure 28. The graph highlights a good agreement between the tension test and the relative branch of the cyclic tests. The compression part of the cyclic test agrees well in stiffness and strength degradation until the yield displacement. The design force of 80 kN in all the tests was reached. The limited value of the compression branch is due to the behaviour of the studied detail in which the contact between the steel elements removes the forces from the aluminium bolts. Despite the brittle behaviour in tension when the aluminium bolts govern the failure a small hysteretic behaviour was observed. The details failure occurred in all cases in the same way: after the collapse of one side of aluminium bolts, a minimum reloading determined the collapse of the aluminium bolts on the other side. The only exception was observed during the compression test where, the aluminium bolts did not affect the behaviour of the specimen and the curve is representative of the steel elasto-plastic behaviour of the detail elements. Observing the instruments on the samples, the details show a certain asymmetry due to the tolerances in the assembly, but not such as to influence the overall response.

In conclusion, Table 7 summarizes the maximum experimental forces reached by each test at the first failure of an aluminium bolt, in comparison with the design force, in Figure 29 some specimens photos, after the tests, can be observed and in Figure 30 the aluminium bolts after the tests are shown.

Table 7. Failure forces reached during the tests.

Detail 1	**Design force of the aluminium bolts**	**Maximum experimental force**
Monotonic tension test	80 kN	128.8 kN
Monotonic compression test	80 kN	116.0 kN*
Cyclic test 1	80 kN	124.7 kN
Cyclic test 2	80 kN	127.8 kN

*Steel inelastic behaviour and no failure of the aluminium bolts

(a) (b) (c)

Figure 29. Detail 1 at failure: (a) sandwich panel in compression test; (b) plastic deformation of C and Z elements under compression force; (c) movement between C and Z elements subjected to tensile force.

(a) (b)

(c) (d)

Figure 30. Detail 1 aluminium bolts at failure: (a) tension test; (b) compression test; (c) cyclic test 1; (d) cyclic test 2.

2.2 Tests on Detail 2

As reported in Deliverable D1.4 [1], all the details were developed from 3 reference fusible link solutions common to all the project partners.

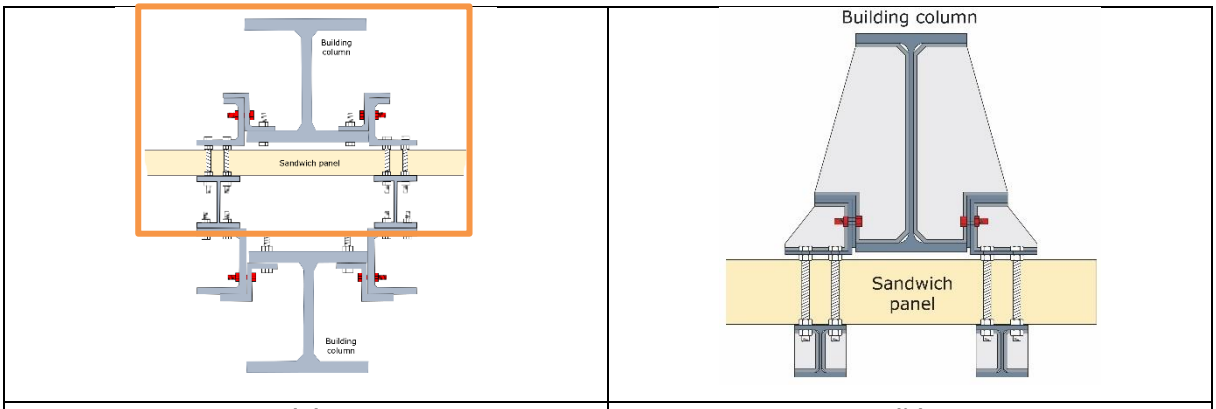

(a) (b)

Figure 31. Detail 2: (a) reference detail, (b) Detail 2 for seismic tests.

Figure 31 reports Detail 2 conceived for the seismic tests and the reference fusible link solution from which it was derived. As can be noticed, on the main column of the building some stiffeners were added in the test specimens to withstand the applied concentrated forces. Only the upper part of the detail was tested under the seismic forces see Figure 31.

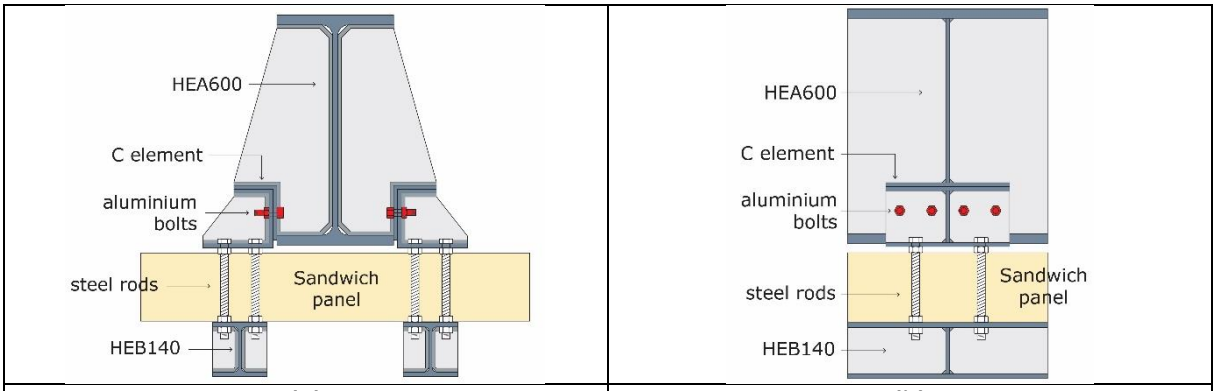

(a) (b)

Figure 32. Detail 2: (a) front view; (b) lateral view

Table 8: Detail 2 description

Elements	**Main characteristics**
C element	2 100x150x180x10 S275
Aluminium bolts	8 M16 AlZn5,5MgCu 7075
Steel rods	8 M20 8.8

In Figure 32 and in Table 8 the main characteristics of Detail 2 are reported in terms of elements and geometry that compose the specimen. As reported in Table 1, this detail was designed for a shear value of 180 kN, that can be withstood by 6 M16 aluminium bolts, but to have a symmetric configuration of the detail as symmetric , 8 M16 were used, 4 on each side, as shown in Figure 32b.

2.2.1 Monotonic tension test

Figure 33. View of the detail 2 test set-up

In Figure 33 the specimen of Detail 2 inserted in the reaction frame can be observed. Some additional steel tree elements were used as support for the instrumentation.

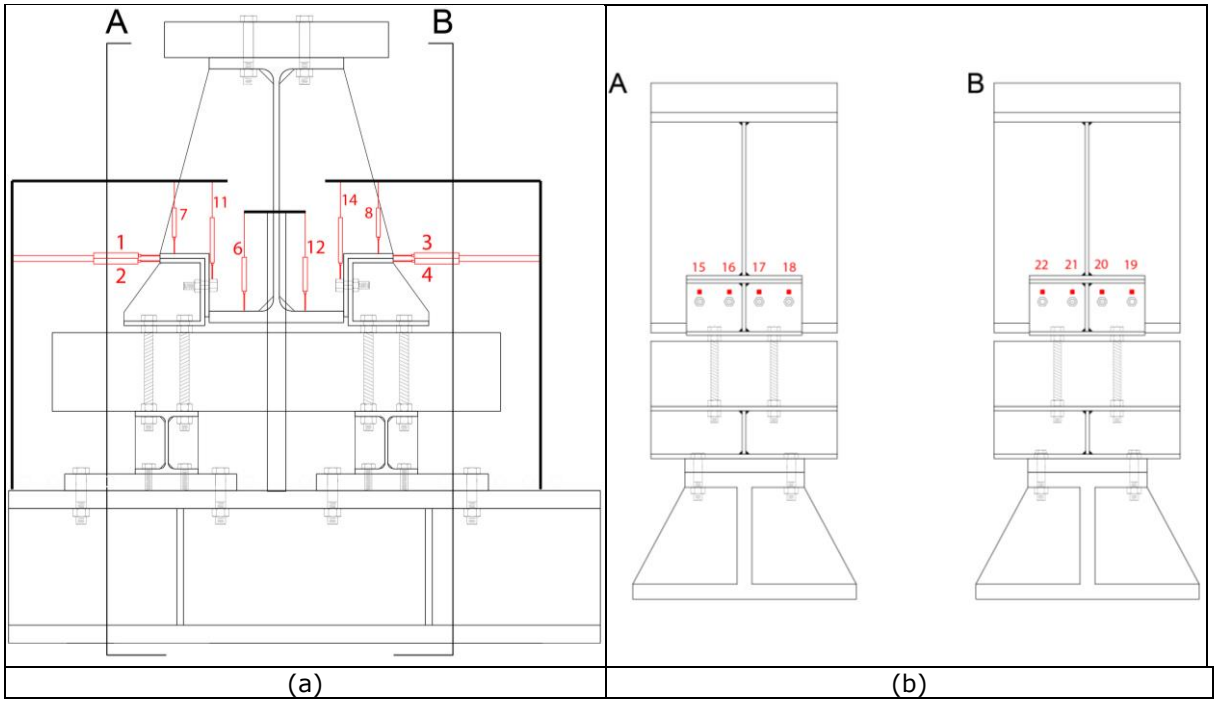

Figure 34. Detail 2: (a) LVDTs arrangement; (b) strain gauges position on the left side (A) and the right side (B).

In Figure 34, the specific instrumentation position and numbering are reported.

The LVDT transducers were located to check specific displacements of the detail:

- LVDT 1, LVDT 2, LVDT 3 and LVDT 4 were installed at the upper part of the C element to check their possible rotation;
- LVDT 7 and LVDT 9 were installed to record the vertical displacement of the C element;
- LVDT 11 and LVDT 14 were installed to check the vertical displacement of the aluminium bolts;
- LVDT 6 and LVDT 12 were installed to measure the actual vertical movement of the specimen (HEA600) removing the displacement of the reaction frame.

A total of 8 strain gauges were glued on the steel C elements to measure the vertical strain close to the aluminium bolts during the test. The instrument acquisitions were recorded at 2 Hz.

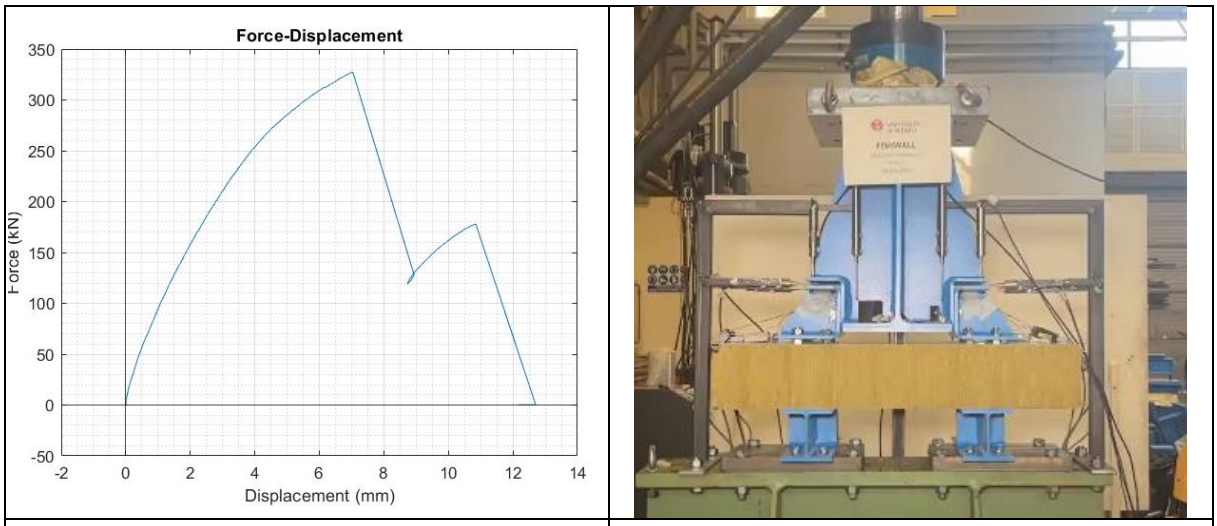

(a) (b)

Figure 35. Detail 2: (a) force-displacement curve of the monotonic tension test; (b) final specimen deformation.

In Figure 35, the result in terms of the force-displacement diagram is shown, where the first peak highlights the failure of the aluminium bolts on the right side (B) of the specimen (considering their position in Figure 33). Then, the load suddenly decreased to increase up again to the failure of the aluminium bolts on the left side (A). It is worth noting that the design force of 180 kN was reached. and the maximum experimental force, i.e. 325.8 kN, is about 52% of the total expected actual resistance, as reported in Table 1. This result is in line with the experimental evidence, because the maximum experimental capacity represents the failure of half of the aluminium bolts. In fact, due to the presence of inherent imperfections in the test specimens, the simultaneous failure of all bolts is highly improbable.

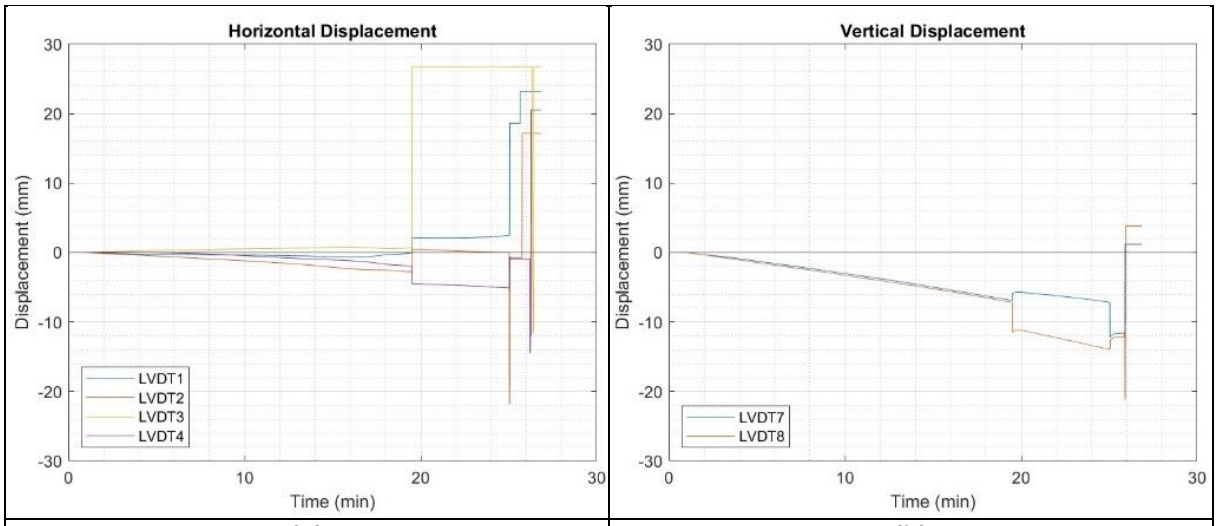

(a) (b)

Figure 36. Detail 2 – LVDT displacements recorded during the test: (a) horizontal displacement on C and L elements (b) vertical displacement L elements.

Figure 36 shows the test results, in terms of horizontal and vertical displacement detected by LVDTs positioned on the specimen. They show a general symmetrical behaviour until the first failure where each instrument is subjected to a different sudden movement. The results on Figure 36 exemplify the behaviour of all the LVDTs.

Considering the strain gauges glued on the steel parts close to the aluminium bolts, the results are hereafter reported. The strain gauges acquisitions are reported in Figure 37. The 8 instruments had the same consistent compressive strain with the test and a coherent behaviour between them. The local strain levels did not exceed the actual steel yield limit, which is 1376 με, highlighting that significant bearing effects were not detected.

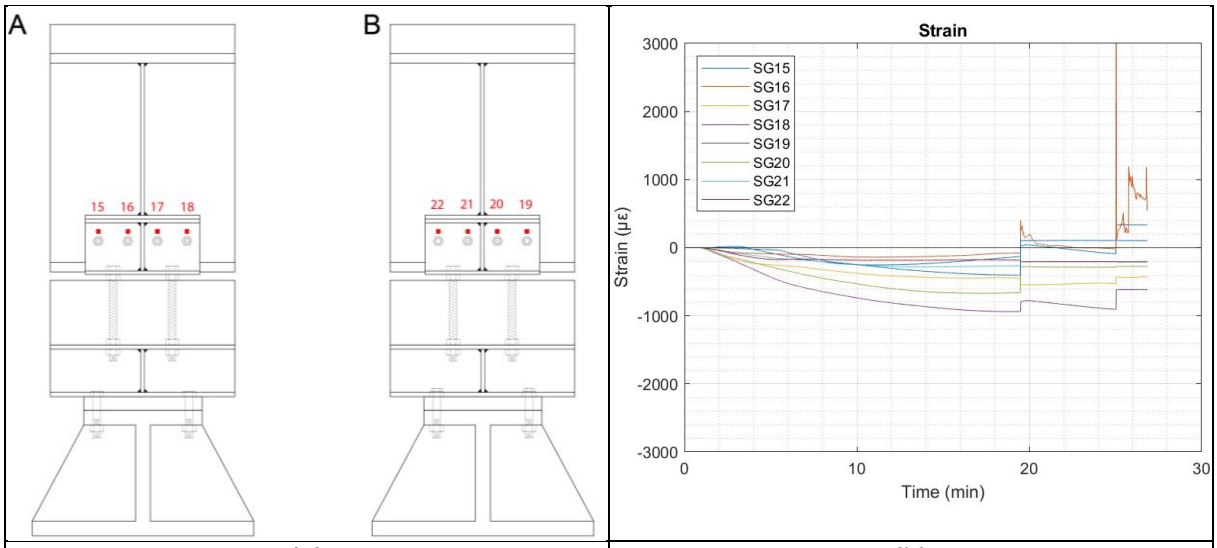

(a) (b)

Figure 37. Detail 2: (a) strain gauges position; (b) strain gauges results.

2.2.2 Monotonic compression test

In Figure 33 the specimen of Detail 2 inserted in the reaction frame can be observed.

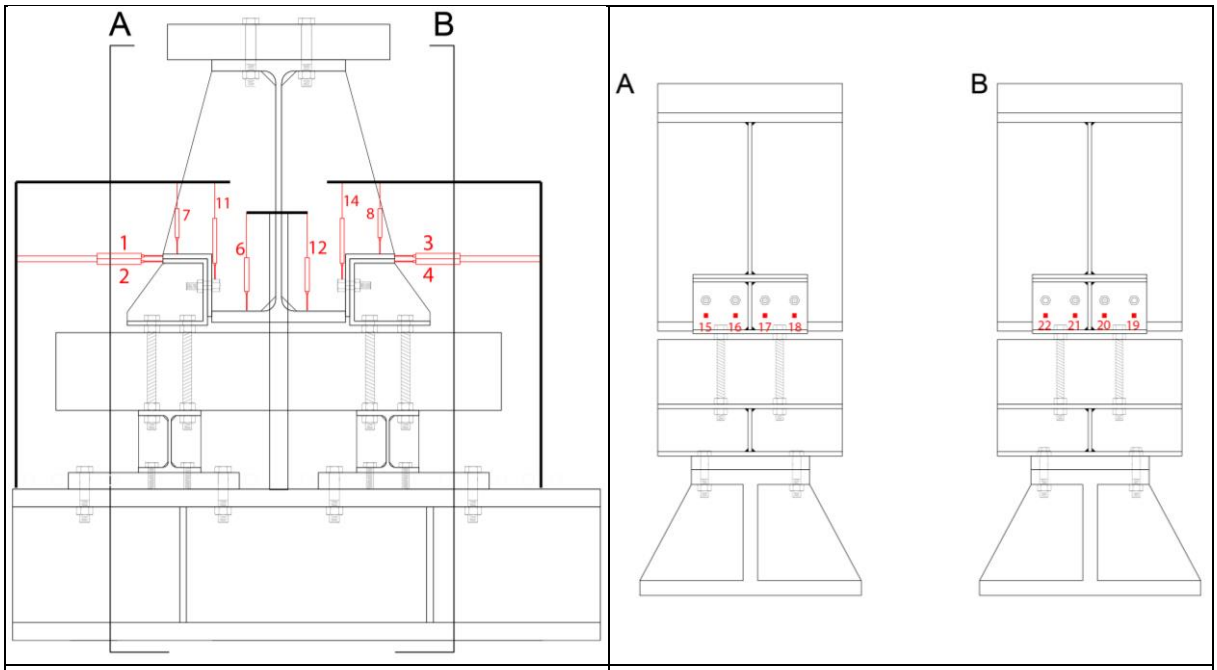

(a) (b)

Figure 38. Detail 2: (a) LVDTs arrangement; (b) strain gauges position on the left side (A) and the right side (B).

In Figure 38, the specific instrumentation position and its numbering are reported.

The displacement transducers are LVDTs and were located as reported in Section 2.2.1.
Also in this case, a total of 8 strain gauges were located on the steel C elements to measure the strain close to the aluminium bolts during the test. The instruments acquisitions were recorded at 2 Hz.

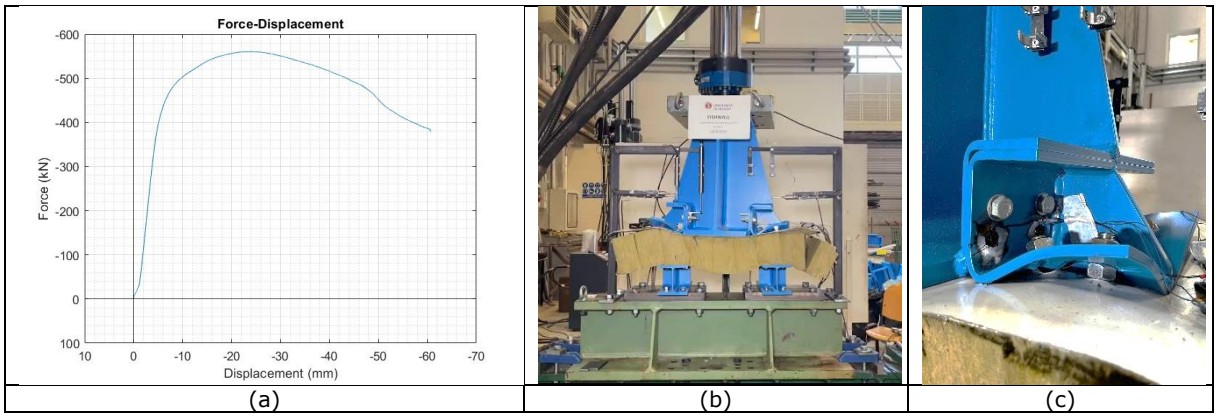

Figure 39. Detail 2: (a) force-displacement curve of the monotonic compression test; (b) final specimen deformation and (c) detail deformation.

Figure 39 shows the result of the test in terms of the force-displacement curve where a ductile behaviour of the specimen can be noticed. Indeed, due to the detail configuration, the compression forces were transmitted through the specimen by contact between the steel elements, which underwent a plastic deformation at the end of the test, as can be noticed in Figure 39c. Consequently, the diagram reported in Figure 39a is representative of the steel elasto-plastic deformation that occurred during the test. Therefore, the aluminium bolts were not affected.

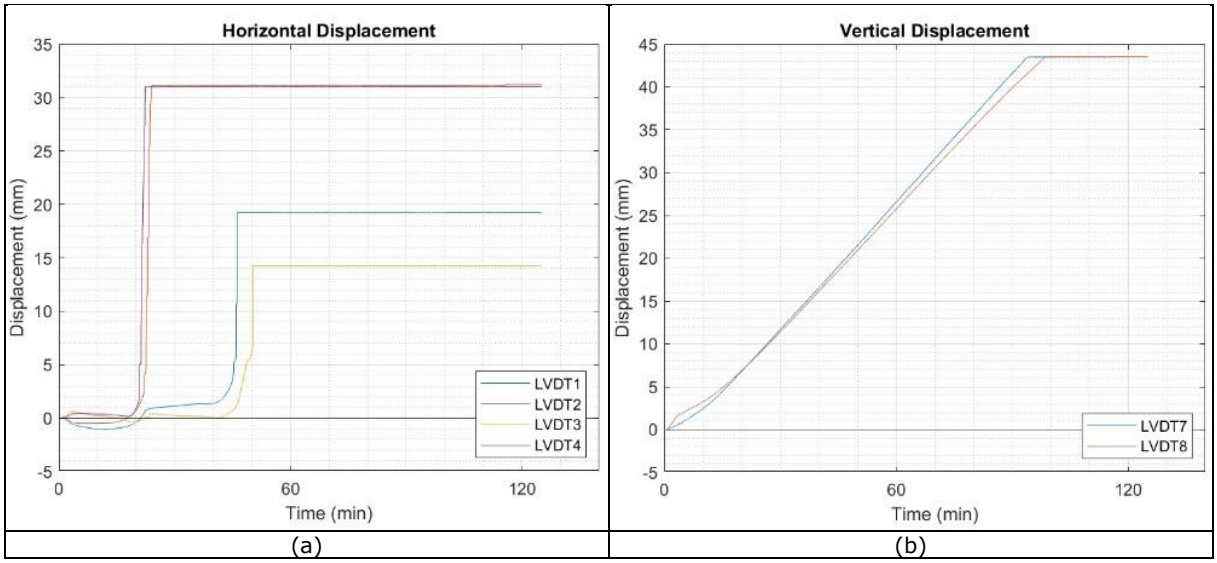

Figure 40. Detail 2 - LVDT results: (a) horizontal displacements on C and L elements; (b) vertical displacements on L elements.

Figure 40 depicts the test results, in terms of horizontal and vertical displacement detected by LVDTs positioned on the specimen. The horizontal instruments recorded only part of test, as can be seen in Figure 40a, because they lost the contact with the steel elements owing to their deformation. Conversely, the vertical LVDTs show a general symmetrical behaviour until the first failure where each instrument is subjected to a sudden movement. The results on Figure 40b exemplify the behaviour of all the LVDTs.

Considering the strain gauges installed on the steel part close to the aluminium bolts, the results are hereafter reported.

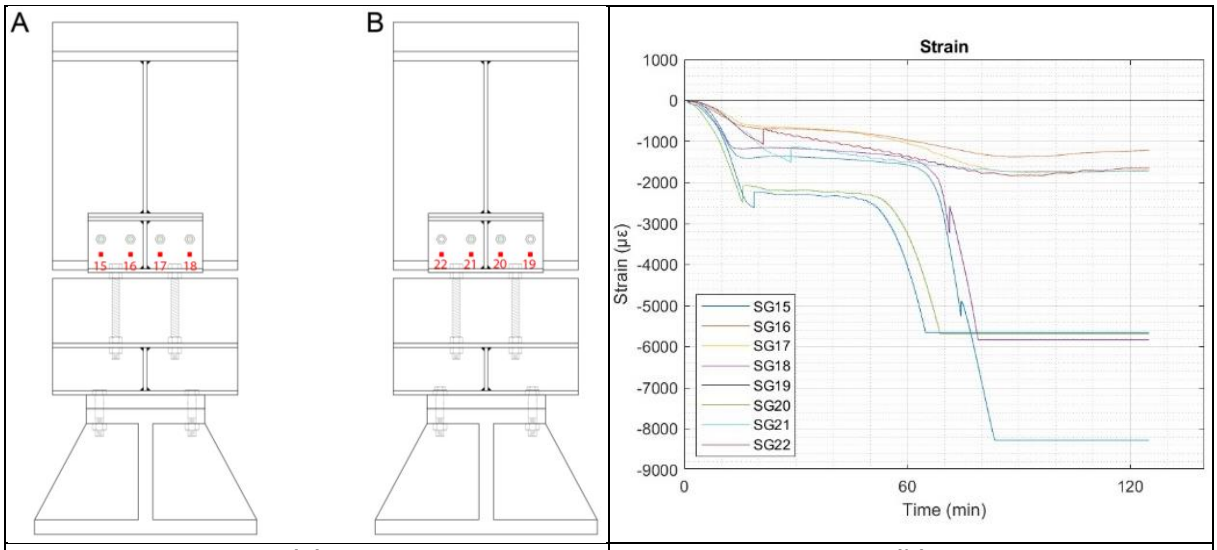

(a) (b)

Figure 41. Detail 2: (a) strain gauges position; (b) strain gauges results.

The strain gauges results are reported in Figure 41b. While for the first part of the test all the instruments have the same trend in compression, the four strain gauges located at the border of the C element, reported in Figure 41a, underwent an increase in strain due to the wide deformation of the elements as can be noticed in Figure 39c. It is possible to observe that the steel elements experienced large inelastic behaviour.

2.2.3 Cyclic tests

In order to follow the ECCS procedure, as reported in Section 1.3, the two monotonic test curves were used to define the yield displacement and the displacement history to perform the cyclic tests.

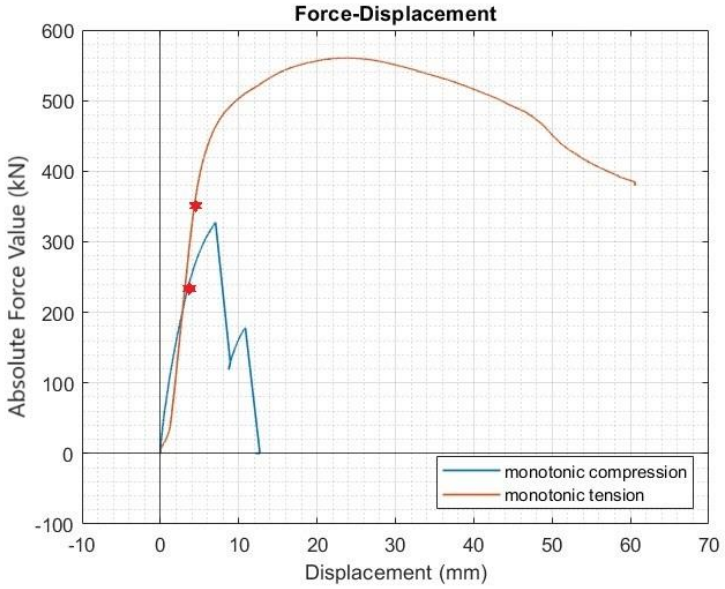

Figure 42. Detail 2 monotonic tests results

Figure 42 reports the comparison, in terms of force-displacement curves, between the monotonic tension and compression tests. The red points represent the selected yield displacements for the cyclic test, that are also reported in Table 9. In order to obtain a more symmetric displacement history, the e_y was calculated by identifying the tangents, for both curves, as reported in Section 1.3. Indeed, for the monotonic tension test a more pronounced stiffness change with respect to Detail 1 was observed before the brittle failure of the aluminium bolts, as highlighted in Figure 42.

Table 9: Yield displacement from monotonic curves

e_y	3.1 mm
$-e_y$	4.3 mm

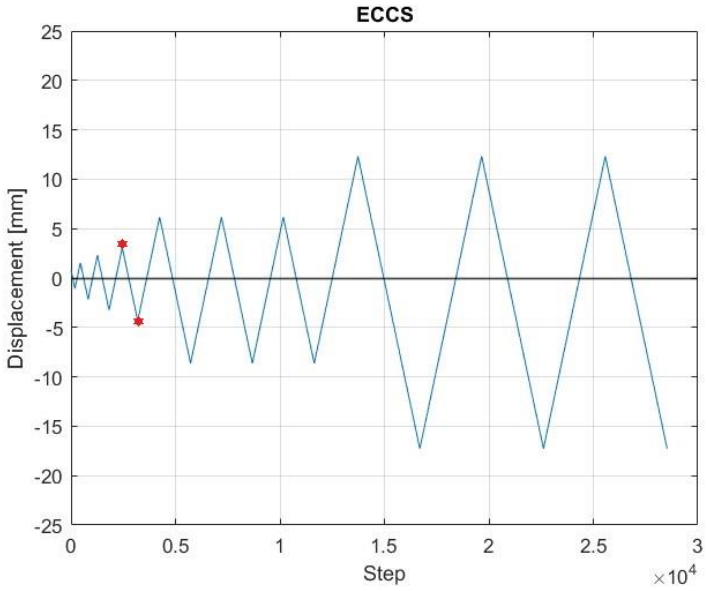

Figure 43. Detail 2 ECCS procedure.

As shown in Figure 43, the displacement history, defined as reported in Section 1.3, is almost symmetric. The yield displacements are highlighted in red.
The cyclic tests were conducted in displacement control with different displacement rates. In greater detail, until attaining e_y the displacement rate was 0.5 mm/min; for the three cycles at $2e_y$ the displacement rate was 1 mm/min; for the last three cycles at $4e_y$ the displacement rate was set at 2 mm/min.

2.2.3.1 Cyclic test 1

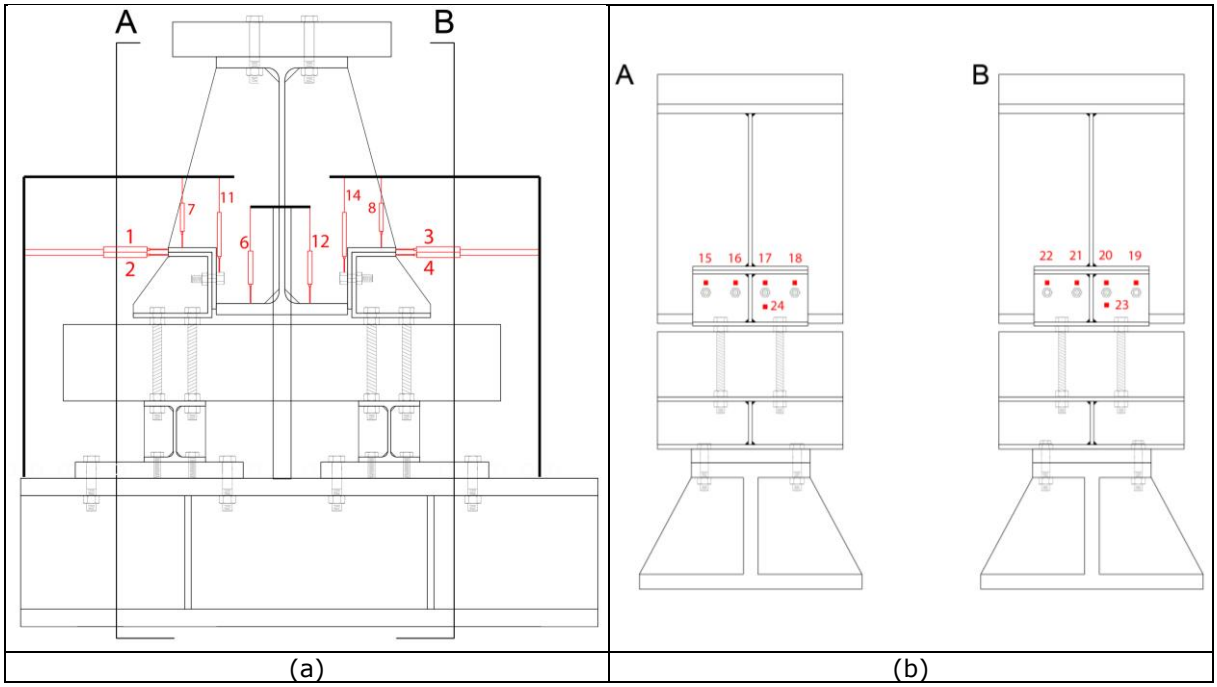

(a) (b)

Figure 44. Detail 2: (a) LVDTs arrangement; (b) strain gauges position on left side (A) and right sibe (B)

Figure 44 reports the instrumentation position and numbering.
The displacement transducers are LVDTs and were located to check specific details movements as well as reported in Section 2.2.1.
In this case, 10 strain gauges were located on the steel C elements to measure the strain induced by the aluminium bolts during the test. The instruments acquisitions were recorded at 2 Hz.

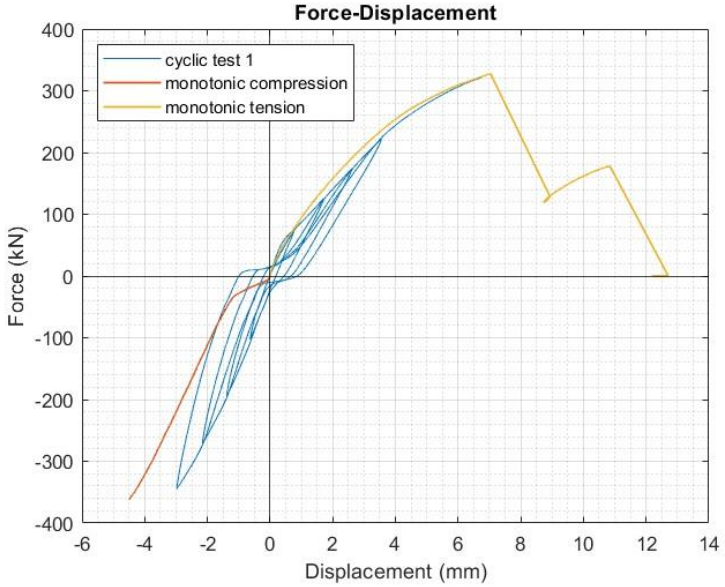

Figure 45. Detail 2 cyclic test 1 results

The results of the first cyclic test on Detail 2, in terms of force-displacement curve, are shown in Figure 45. The failure of the specimen occurred on the reloading at the first cycle to $2e_y$. The brittle nature of the detail in tension, highlights a very small hysteretic behaviour of the detail. It is worth noting that the design force of 180 kN was reached in both the tension and the compression branch. The comparison between the cyclic test and the monotonic tests showed a good agreement in terms of strength and stiffness degradation, especially on the tension part.

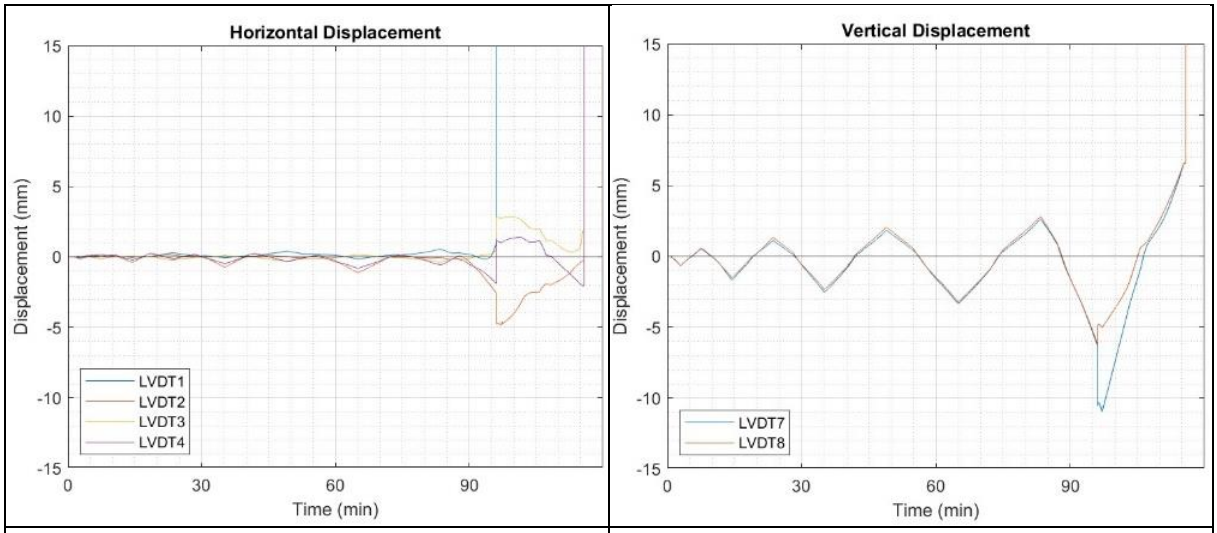

(a) (b)

Figure 46. Detail 2 – LVDT displacements recorded during the test: (a) horizontal displacement on C and L elements (b) vertical displacement L elements.

The horizontal and vertical displacement acquisitions are reported in Figure 46. The two graphs show a consistent symmetry of displacements during the tests, until the first failure occurred.

Considering the strain gauges installed on the steel part close to the aluminium bolts, the results are hereafter reported.

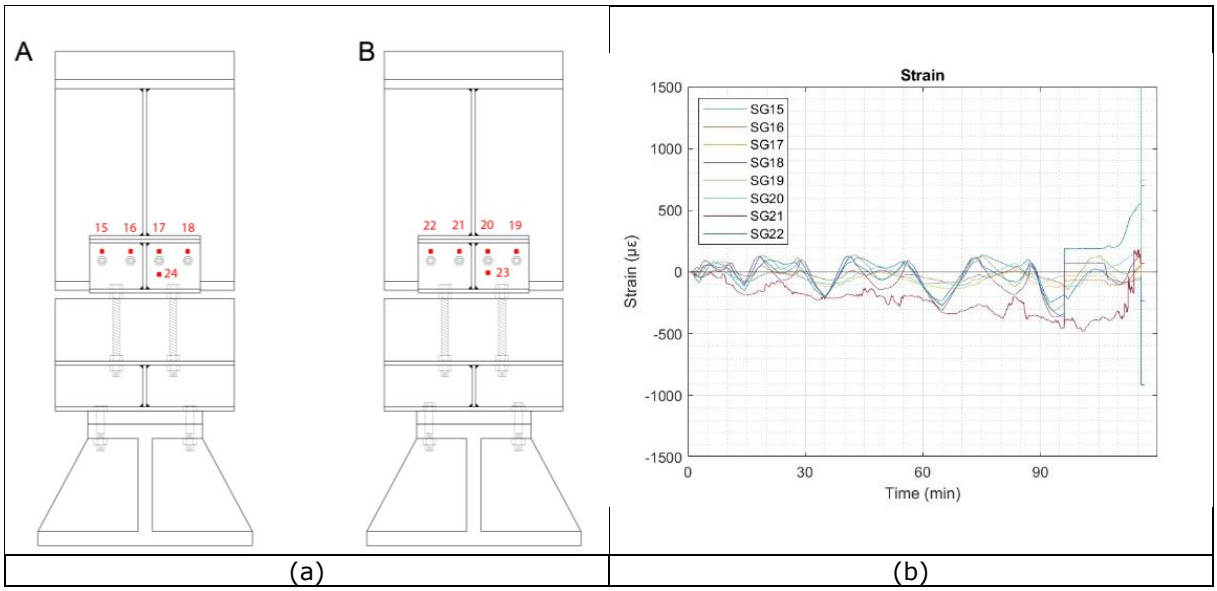

Figure 47. Strain gauges on the Detail 2: (a) arrangement (b) strain comparison between left (A) and right (B) side.

The strain gauges results are reported in Figure 47. The strains observed from the instruments in the external parts of the C element better followed the cyclic trend than the strain gauges on the central part. This behaviour is consistent with the final shape of the specimen, where, indeed, the C element lateral part was more deformed, as reported in Figure 39c.

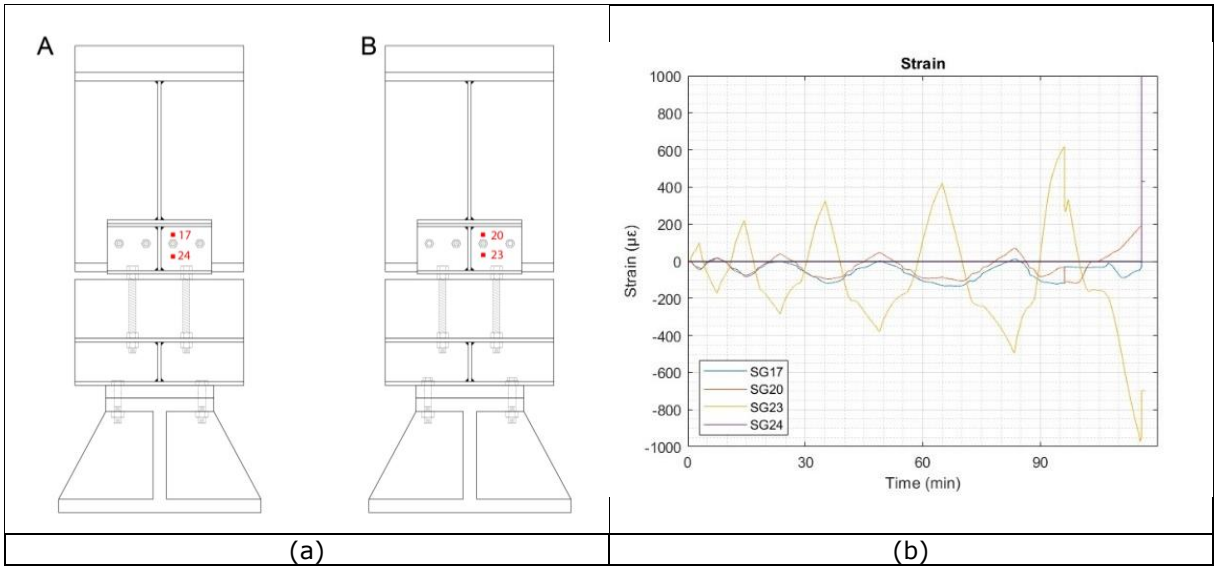

Figure 48. Detail 2: (a) strain gauges result position; (b) strain comparison between tension and Compression.

Figure 48 reports the results in terms of strain between the instruments located on the central part of the C element to detect the deformation in tension and compression. As can be noticed, the instrument 24 did not record any signal. Nevertheless, the other three instruments showed a consistent behaviour with the cyclic history and their relative position. From Figure 47 and Figure 48, it is possible to observe that strain levels close to the aluminium bolts did not exceed the steel yield limit of 1376 με. This is due to the fact that in compression the attained force level was not high enough (about 325 kN) to induce inelastic behaviour in the steel elements close to the aluminium bolts.

2.2.3.2 Cyclic test 2

A second cyclic test on Detail 2 was repeated with the same testing protocol and instrumentation. The results of the second cyclic test on Detail 2, in terms of force-displacement curve, are shown in Figure 49. The failure of the specimen occurred on the reloading at the first cycle to $2e_y$, as for the first cyclic test. Besides the brittle nature of the detail, a hysteretic behaviour can be observed. Also in this case, the design force of 180 kN was reached in the tension branch, when the aluminium bolts

are effectively loaded in shear. As for the first cyclic test, a good agreement between the cyclic test and the monotonic tests can be highlighted. Thus, good repeatability was observed.

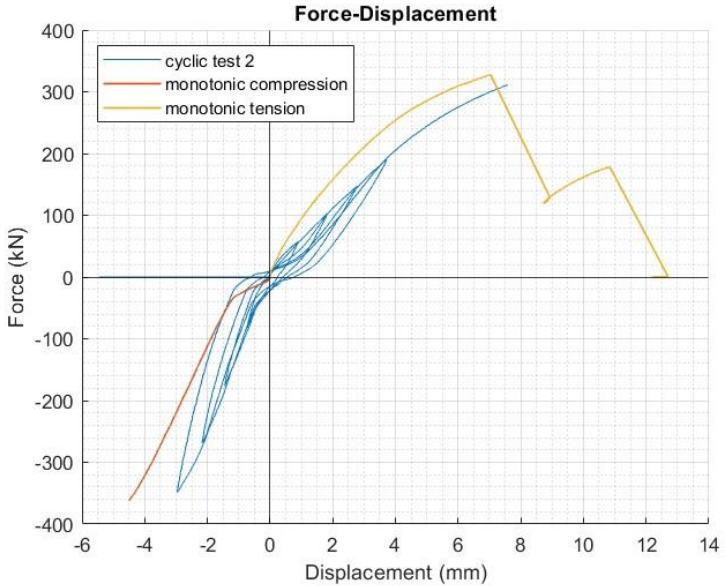

Figure 49. Detail 2 cyclic test 2 results

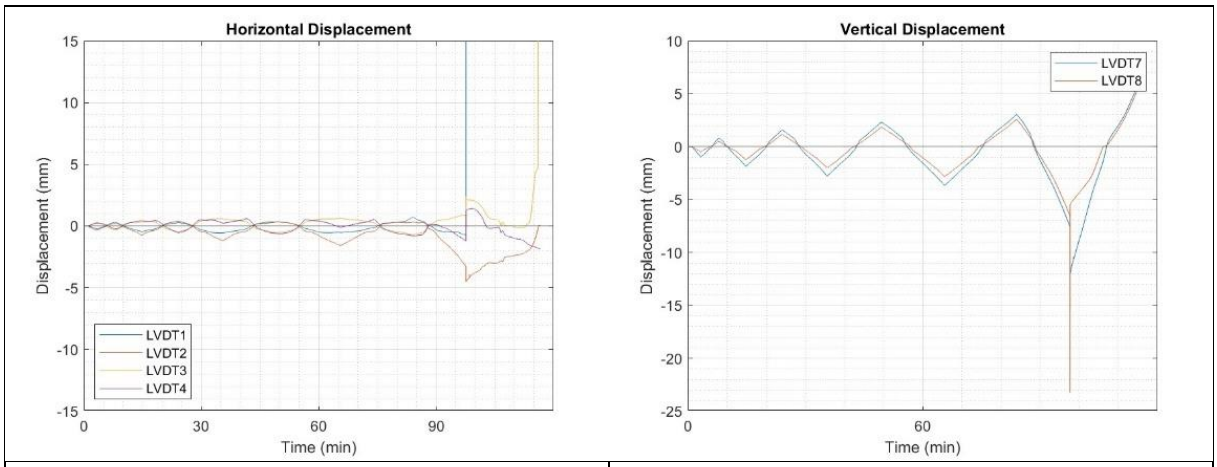

(a) (b)

Figure 50. Detail 2 - LVDT displacements recorded during the test: (a) horizontal displacement on C and L elements (b) vertical displacement L elements.

The horizontal and vertical displacement acquisitions are reported in Figure 50. The two graphs showed a consistent symmetry of displacements during the tests, until the first failure occurred. The same results were obtained by the other displacement transducers installed on the specimen.

Considering the strain gauges installed on the steel part close to the aluminium bolts, the results are hereafter reported.

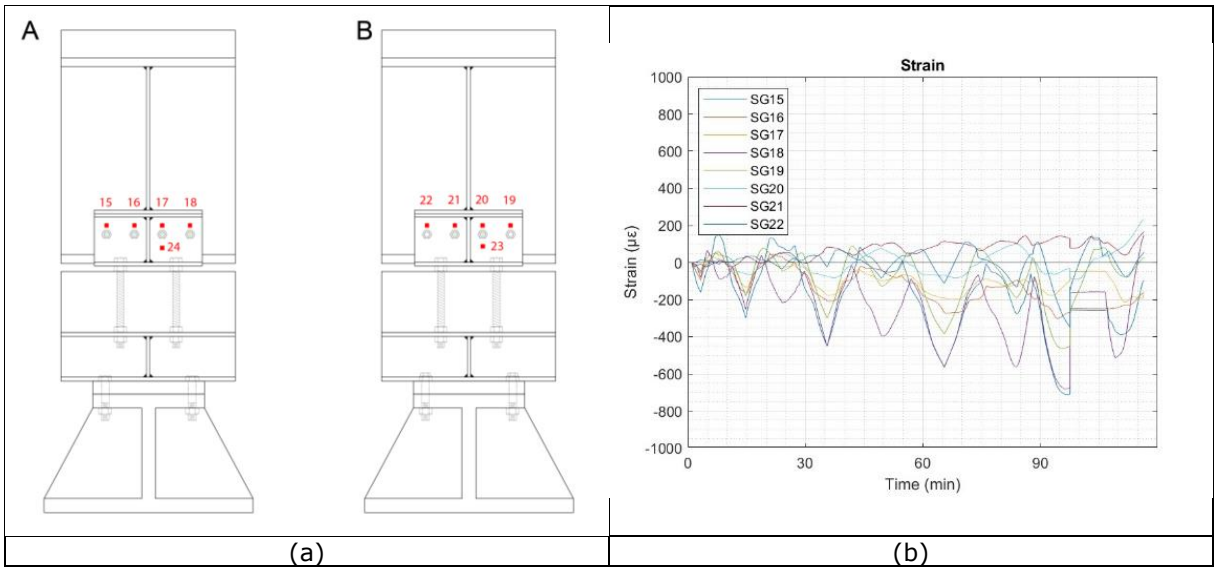

Figure 51. Detail 2 - strain gauges (a) position; (b) strain comparison between left and right side

The strain gauges results are reported in Figure 51. All the instruments recorded the same trend, with a wider deformation in the lateral strain gauges of the C elements that occurred also in the first cyclic test.

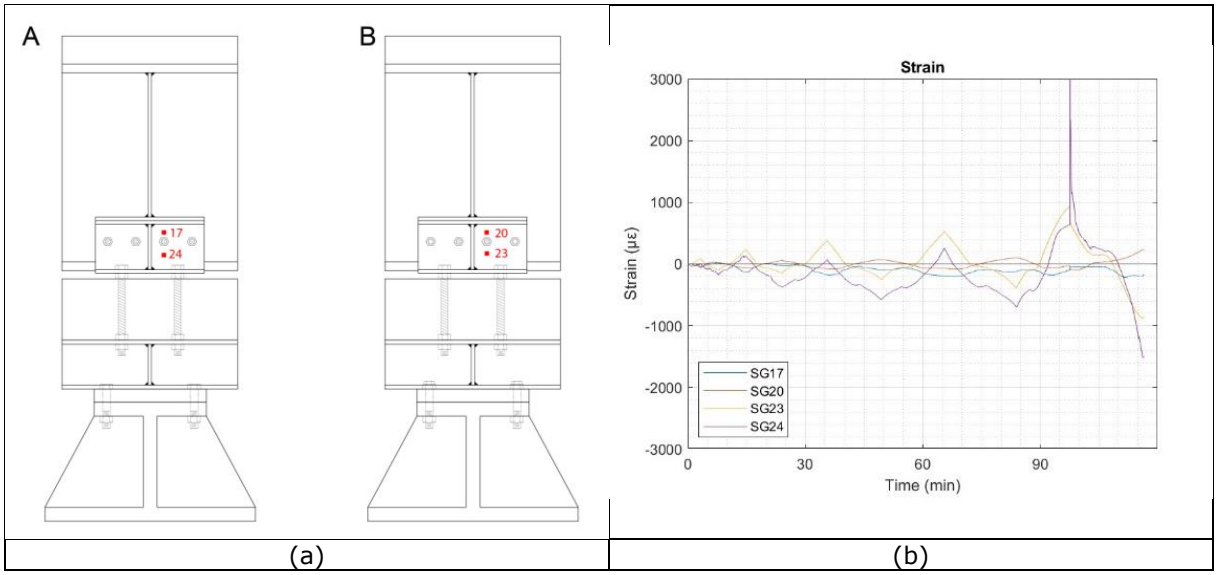

Figure 52. Strain gauges on the Detail 2: (a) arrangement (b) strain comparison between left (A) and right (B) side.

The acquisition of the strain gauges depicted in Figure 52a are compared in Figure 52b. As can be noted, the two couple of strain gauges exhibited a consistent behaviour with the cyclic test. From Figure 51 and Figure 52, it is possible to observe that strain levels close to the aluminium bolts did not exceed the actual steel yield limit of 1376 με. This is due to the fact that in compression the attained force level was not high enough (about 350 kN) to induce inelastic behaviour in the steel elements close to the aluminium bolts.

2.2.4 Summary

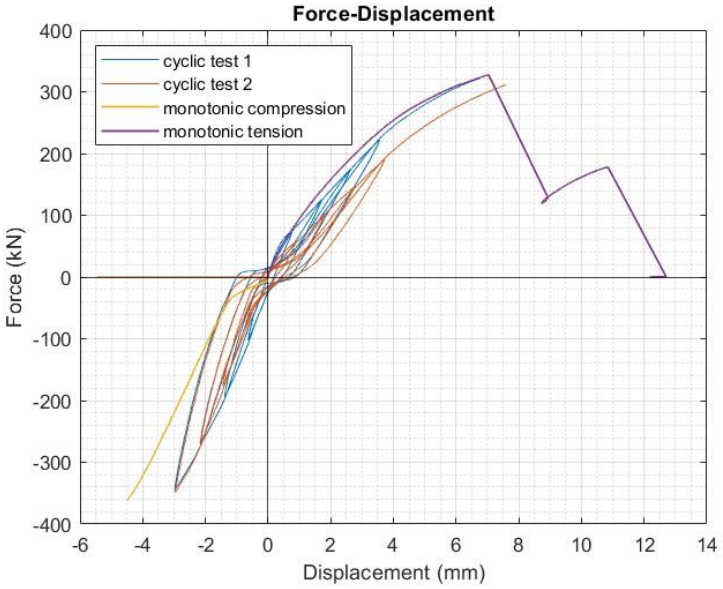

Figure 53. Detail 2 test results comparison

The comparison between the four tests performed on Detail 2 are reported in Figure 53. The two cyclic tests are in a good agreement especially on the compression part, while on the tension part the cycle shape is the same, but the second specimen experienced a lower initial stiffness. The comparison between the monotonic tension test showed a comparable behaviour in terms of stiffness and strength degradation. Considering the compression part of the diagram, a similar behaviour can be noticed between the curves. Due to the geometry of the investigated specimens the behaviour in tension involves the strength of the aluminium bolts, contrary to the compression behaviour. In fact, in compression the contact between the steel elements removes the forces from the aluminium bolts. The brittle nature of the detail in tension, highlights a very small hysteretic behaviour of the detail.

In conclusion, Table 10 summarizes the maximum experimental forces reached by each test at the first failure of an aluminium bolt, in comparison with the design force, in Figure 54. Detail 2 at failure: (a) lateral view of the plastic deformation of C and L elements under compression force; (b) frontal view plastic deformation of C and L elements under compression force; (c) movement between C and L elements subjected to tensile force.

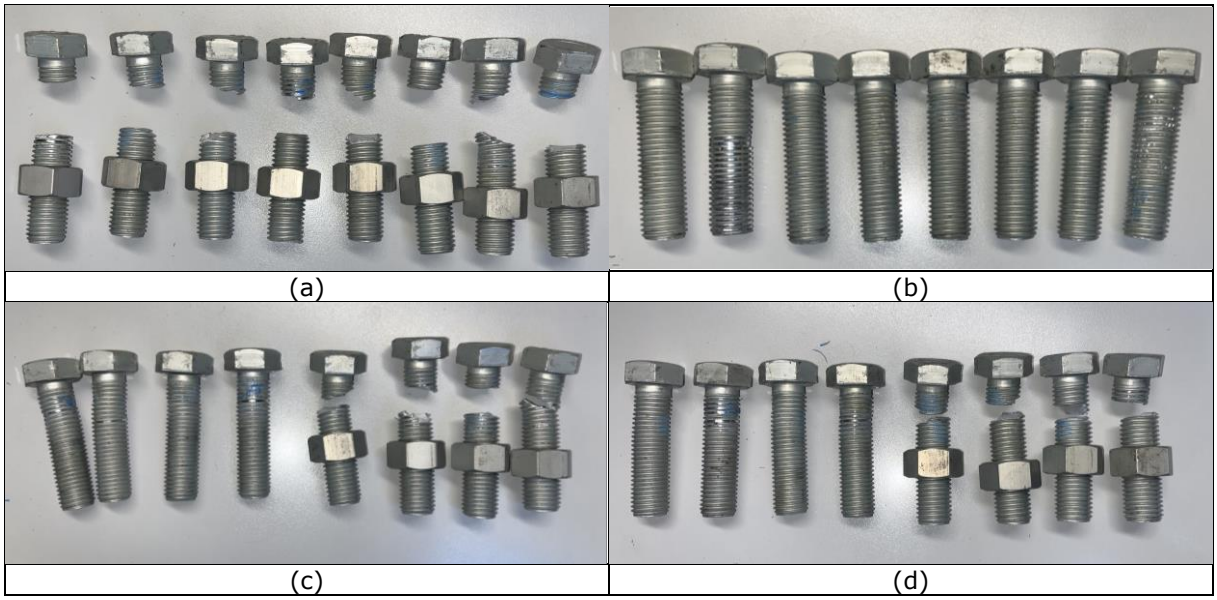

Figure 55. Detail 2 aluminium bolts at failure: (a) tension test; (b) compression test; (c) cyclic test 1; (d) cyclic test 2.

Some specimen photos, after the tests, can be observed Figure 54. The aluminium bolts after the tests are shown in Figure 55.

Table 10. Failure forces reached during the tests.

Detail 2	Design force	Maximum experimental force
Monotonic tension test	180 kN	325.8 kN
Monotonic compression test	180 kN	580.0 kN*
Cyclic test 1	180 kN	321.4 kN
Cyclic test 2	180 kN	310.7 kN

*Steel inelastic behaviour and no failure of the aluminium bolts

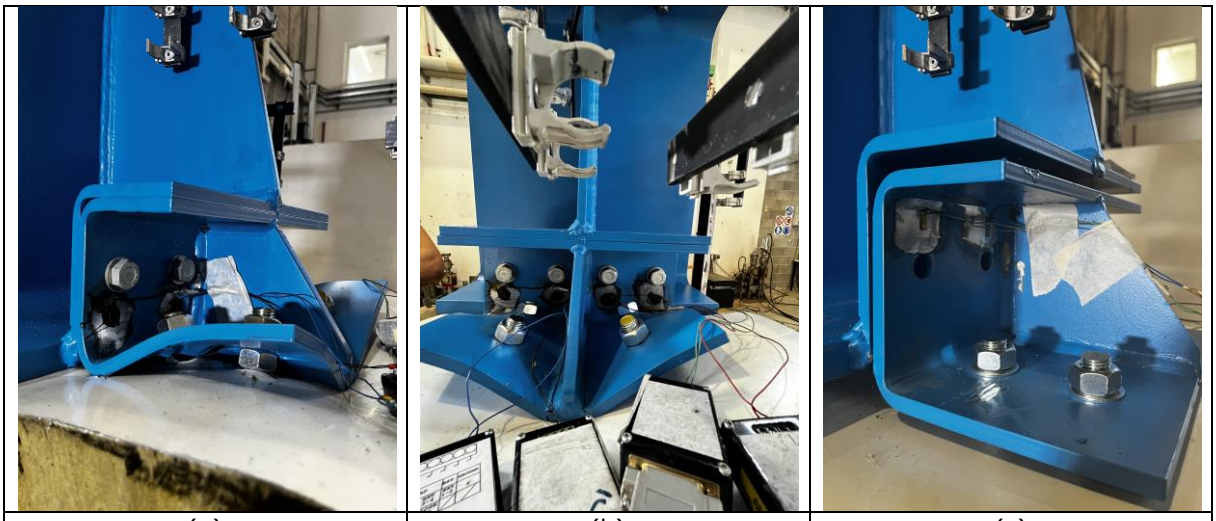

(a) (b) (c)

Figure 54. Detail 2 at failure: (a) lateral view of the plastic deformation of C and L elements under compression force; (b) frontal view plastic deformation of C and L elements under compression force; (c) movement between C and L elements subjected to tensile force.

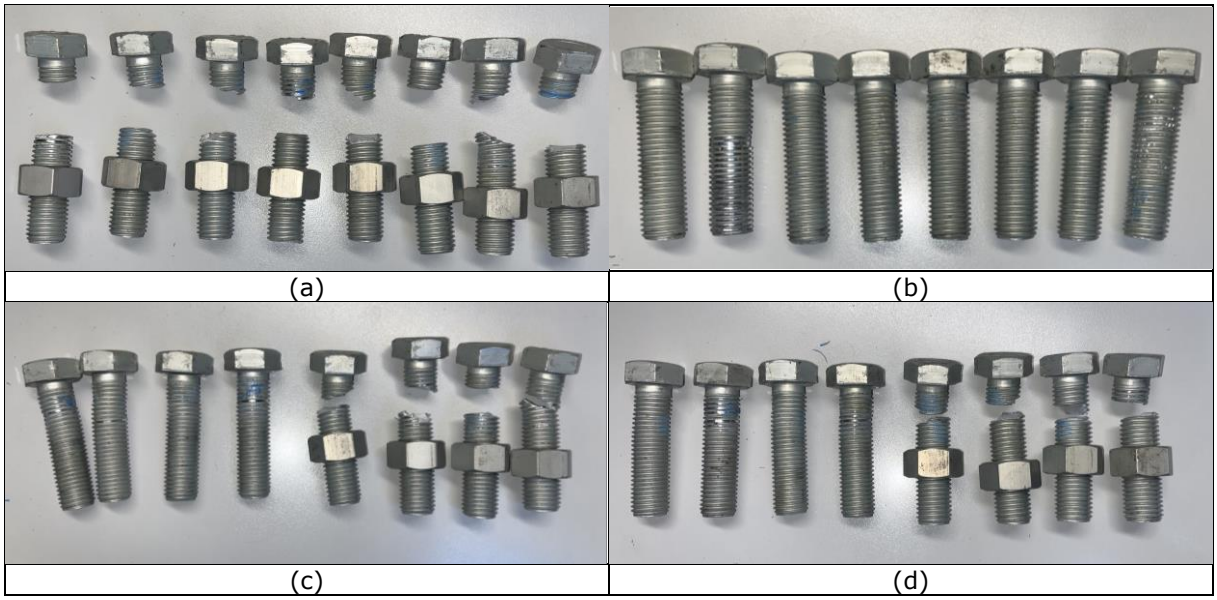

(a) (b) (c) (d)

Figure 55. Detail 2 aluminium bolts at failure: (a) tension test; (b) compression test; (c) cyclic test 1; (d) cyclic test 2.

2.3 Tests on Detail 3.1

As reported in Deliverable D1.4 [1], all the details were developed from 3 reference fusible link solutions common to all the project partners.

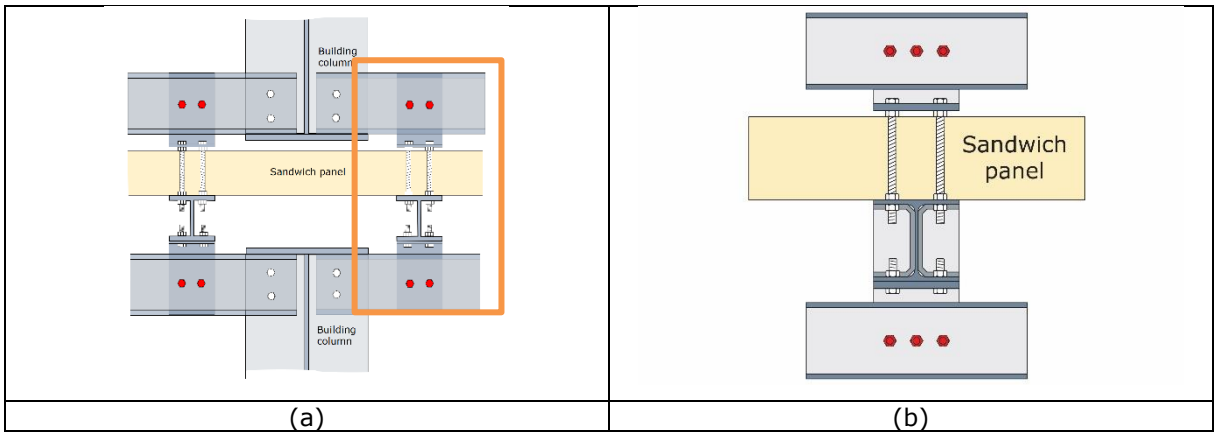

(a) (b)

Figure 56. Detail 3.1: (a) reference detail, (b) Detail 3.1 for seismic tests.

Figure 56 reports Detail 3.1 and the reference fusible link solution from which it was derived. As can be noticed, only one side of the detail was considered.

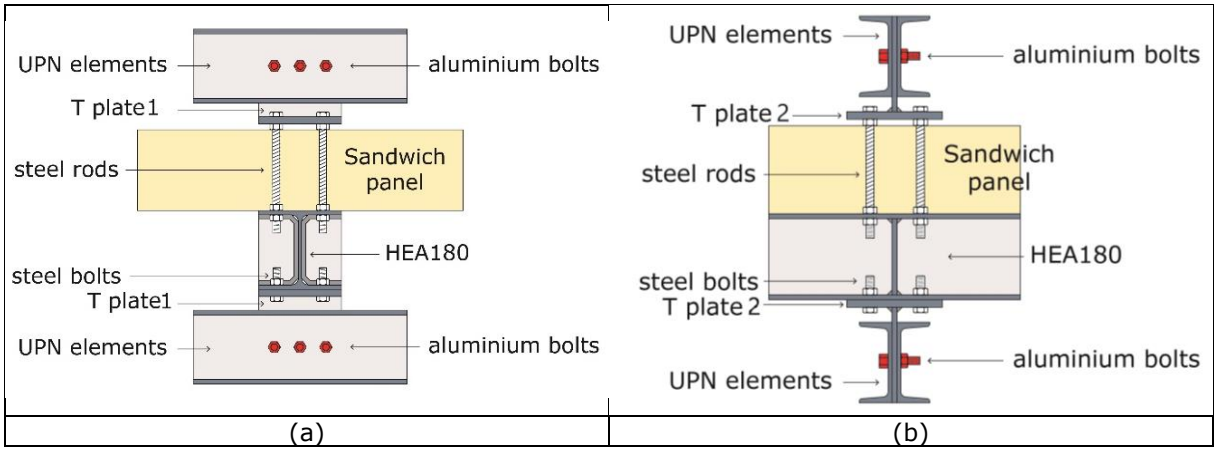

(a) (b)

Figure 57. Detail 3.1: (a) front view and (b) lateral view

Table 11: Detail 3.1 description

Elements	**Main characteristics**
UPN elements	4 UPN 160
Aluminium bolts	6 M16 AlZn5,5MgCu 7075
Steel rods	4 M16 8.8
Steel bolts	4 M16 8.8
T Plate 1- web	2 190x180x10
T plate 2- flange	2 190x180x15

In Figure 57 and in Table 11 the main characteristics of Detail 3.1 are reported in terms of elements and geometry that compose the specimen. As reported in Table 1, this detail was designed for a shear value of 180 kN, that can be withstood by 3 M16 aluminium bolts working on 2 shear planes.

2.3.1 Monotonic tension test

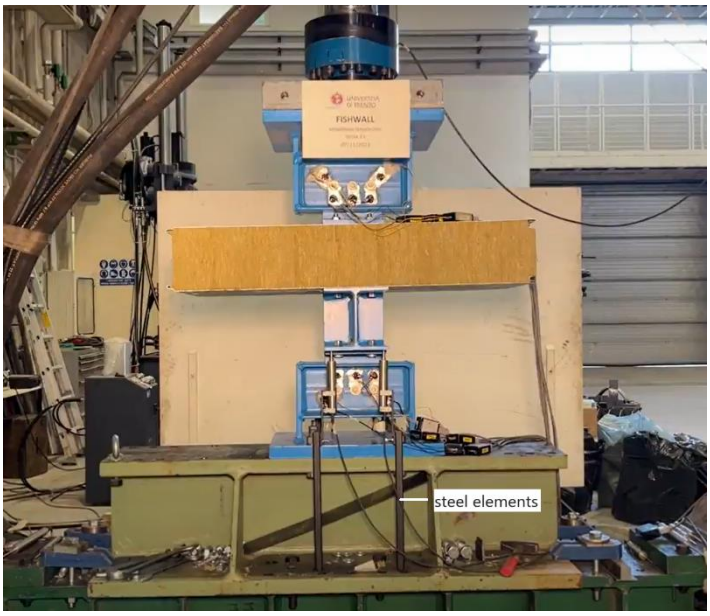

Figure 58. View of the detail 3.1 test setup

In Figure 58 the specimen of Detail 3.1 inserted in the reaction frame can be observed. Some additional steel elements were inserted to support the instrumentation.

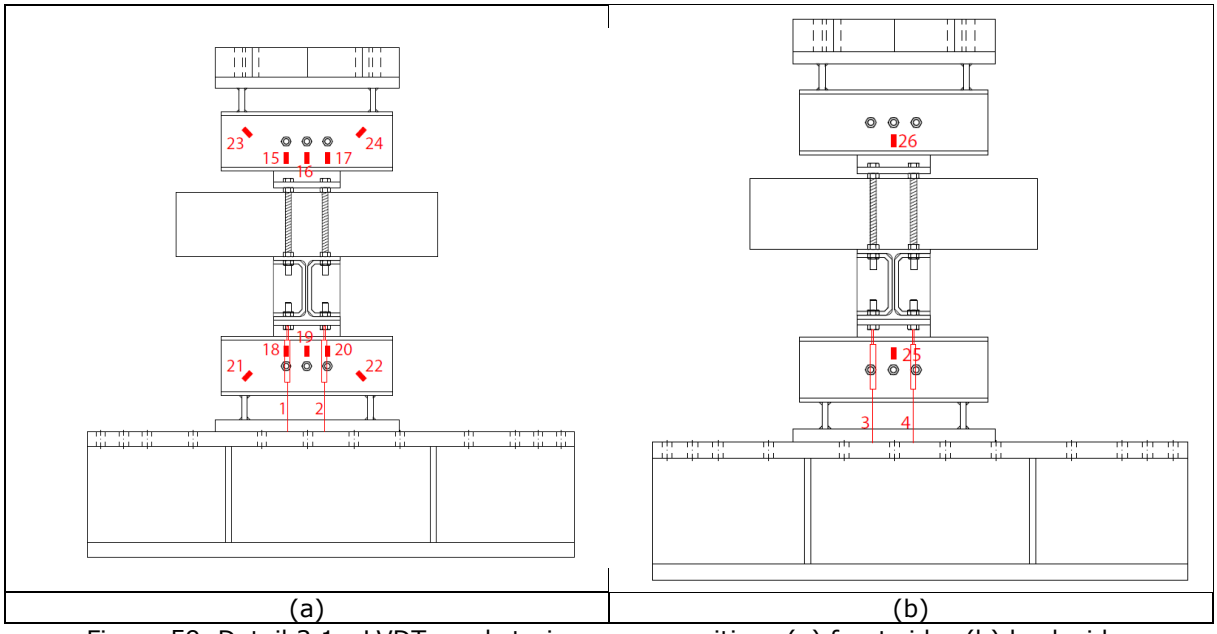

Figure 59. Detail 3.1 - LVDTs and strain gauges position: (a) front side; (b) back side.

In Figure 59, the specific instrumentation position and numbering are reported.

The LVDTs 1,2,3 and 4 were located to check the actual displacement of the specimen. Displacement obtained as difference between that recorded by the actuator transducer removed by the displacement of the frame reaction.

12 strain gauges were glued on the steel UPN elements to measure the strain close to the aluminium bolts during the test and its symmetry. The instruments acquisitions were recorded at 2 Hz.

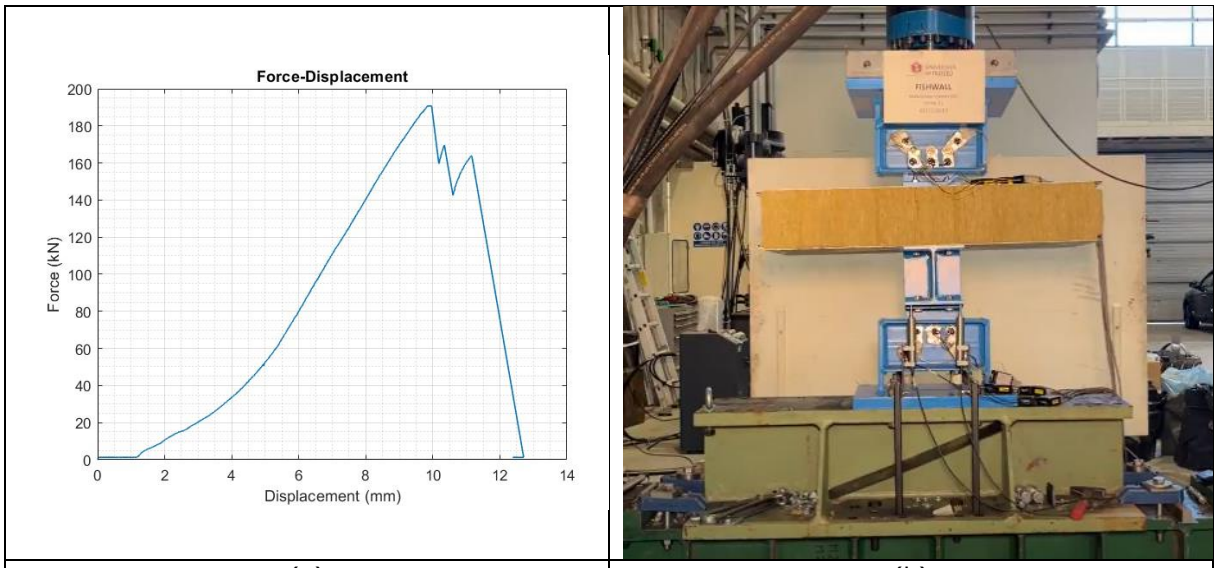

(a) (b)

Figure 60. Detail 3.1: (a) force-displacement diagram of the monotonic tension test and (b) final specimen deformation

Figure 60 reports the result in terms of the force-displacement curve, where the first peak highlights the failure of an aluminium bolt on the lower part of the specimen. Then, the load suddenly decreased to increase up again to the failure of the aluminium bolts located on the upper part till the final collapse of all the other lower aluminium bolts. It is worth noting that the design force of 180 kN was reached.

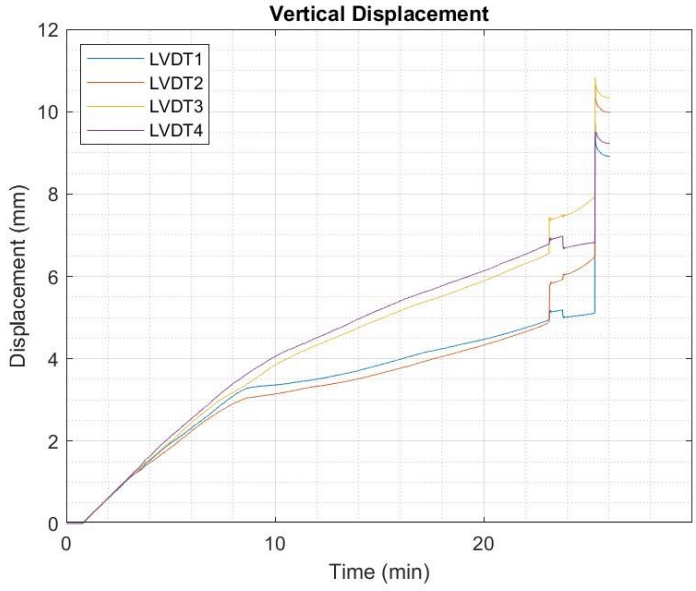

Figure 61. Detail 3.1: vertical displacement results of LVDTs.

Figure 61 illustrates the test results in terms of vertical displacement detected by LVDTs positioned on the specimen. They showed an initial symmetrical behaviour until an increased difference occurred between the instruments on the front and the back side, which could be due to an inherent specimen imperfection, in particular of the T elements that were characterised by noticeable distortions because of the welding process.

A sudden jump in displacement was recorded by LVDTs 2 and 3 when the aluminium bolt close to them failed.

Considering the strain gauges installed on the steel part close to the aluminium bolts, the results are hereafter reported.

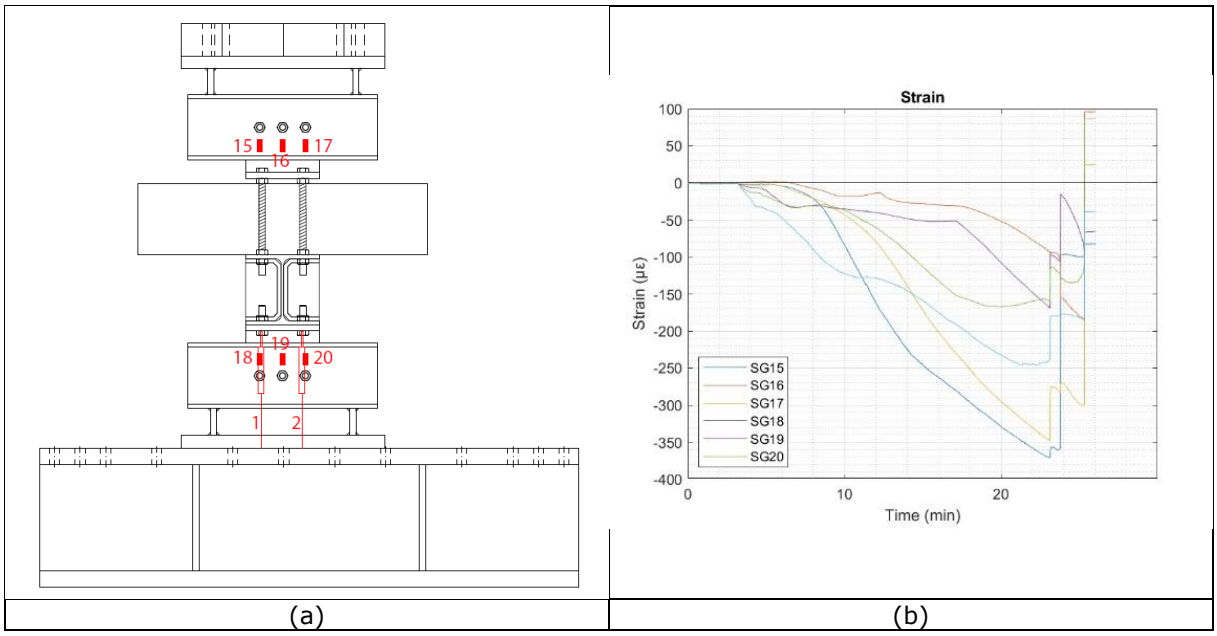

(a) (b)

Figure 62. Detail 3.1: (a) strain gauges position; (b) strain gauges results.

The strain gauge acquisitions are reported in Figure 62. The 6 instruments have the same trend in compression. The local strain levels did not exceed the actual steel yield limit of 1710 με, highlighting that significant bearing effects were not detected. The different values observed by strain gauges are probably due to imperfection of the specimen both in the realization and assembly due to the clearances in the holes.

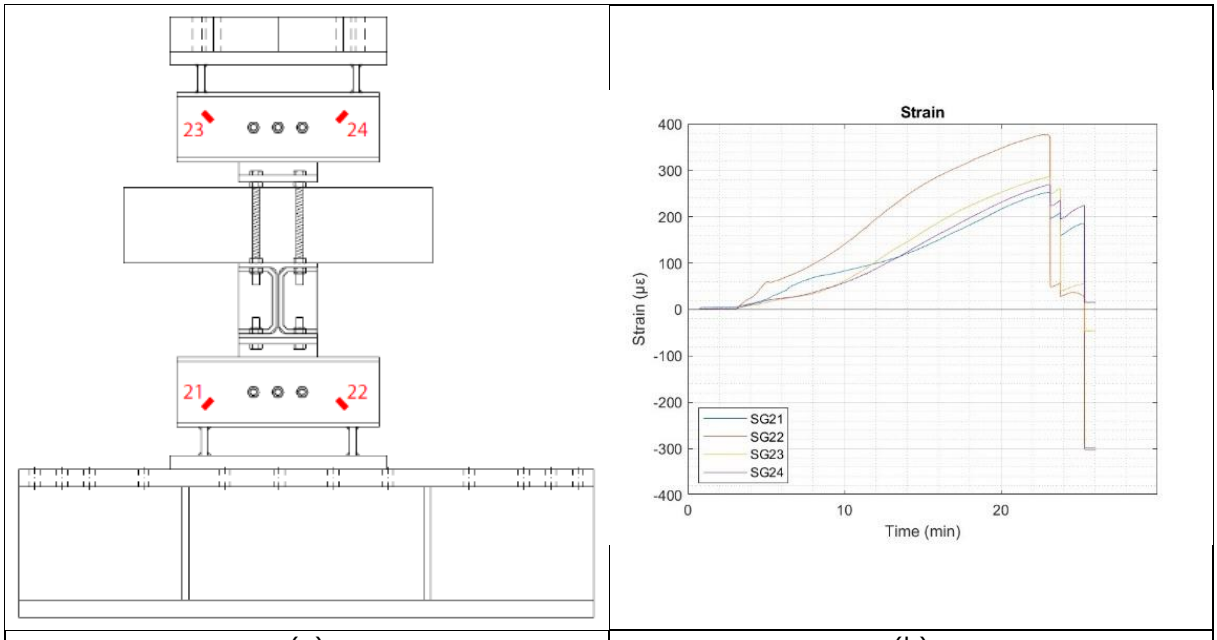

(a) (b)

Figure 63. Detail 3.1: (a) strain gauges position; (b) strain gauges results.

The strain gauges acquisitions are illustrated in Figure 63b. The strain recorded in tension is consistent with the test performed, indeed all the steel parts were subjected to tension.

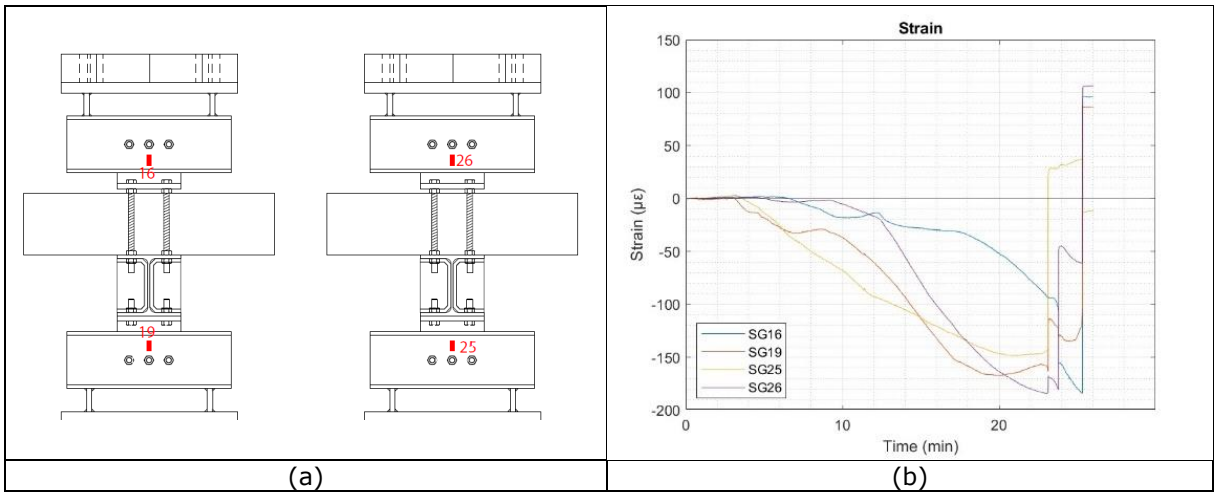

(a) (b)

Figure 64. Detail 3.1 (a) strain gauges position on the front and back side of the specimen; (b) strain gauges results.

The results of the strain gauges depicted in Figure 64a are reported in Figure 64b. The diagram highlights similar strains between the front and back side and therefore the specimen symmetry in terms of local strains. The local strain levels did not exceed the actual steel yield limit, which is 1710 με, highlighting that significant bearing effects were not detected.

2.3.2 Monotonic compression test

In Figure 58 the specimen of Detail 3.1 inserted in the reaction frame can be observed.

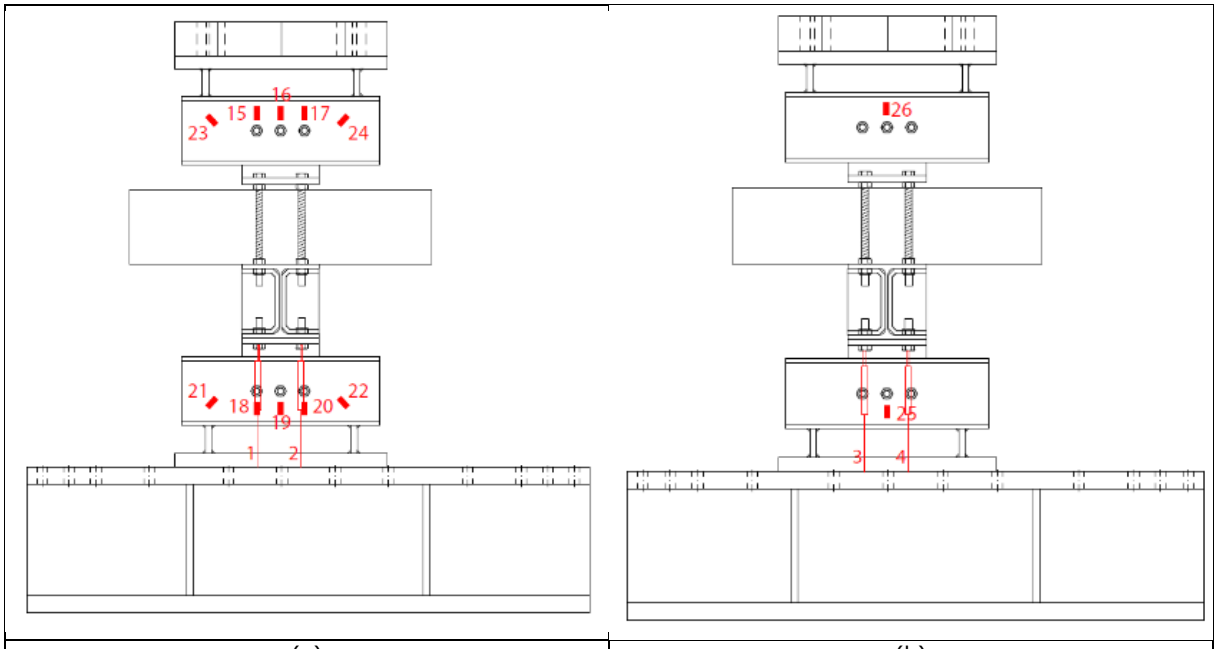

(a) (b)

Figure 65. Detail 3.1 - LVDT and strain gauges position on (a) front side; (b) back side.

In Figure 65, the specific instrumentation position and numbering are reported.
The displacement transducers are LVDTs and were located to check specific details motions as well as reported in Section 2.3.1.
Also in this case, a total of 12 strain gauges were located on both side of the specimen to check the symmetry of the specimen also in terms of deformation. The instruments acquisitions were recorded at 2 Hz.

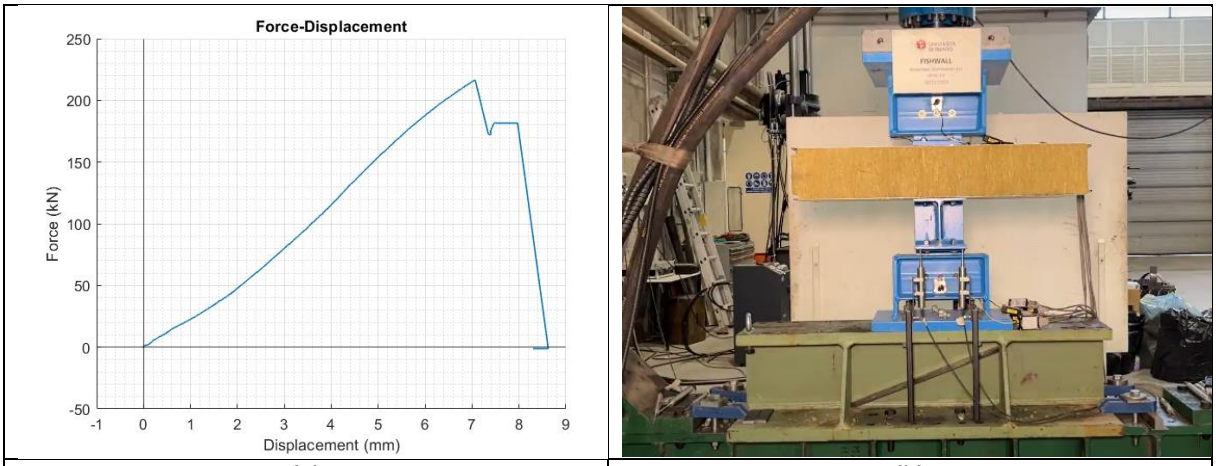

(a) (b)

Figure 66. Detail 3.1 (a) force-displacement diagram of the monotonic compression test and (b) final specimen deformation

In Figure 66, the result in terms of the force-displacement diagram is shown, where the first peak highlights the failure of a shear plane of aluminium bolt on the lower part of the specimen. Then, the load suddenly decreased to increase up again to the failure of all the aluminium bolts on the lower part of the specimen. It is worth noting that the design force of 180 kN was reached.

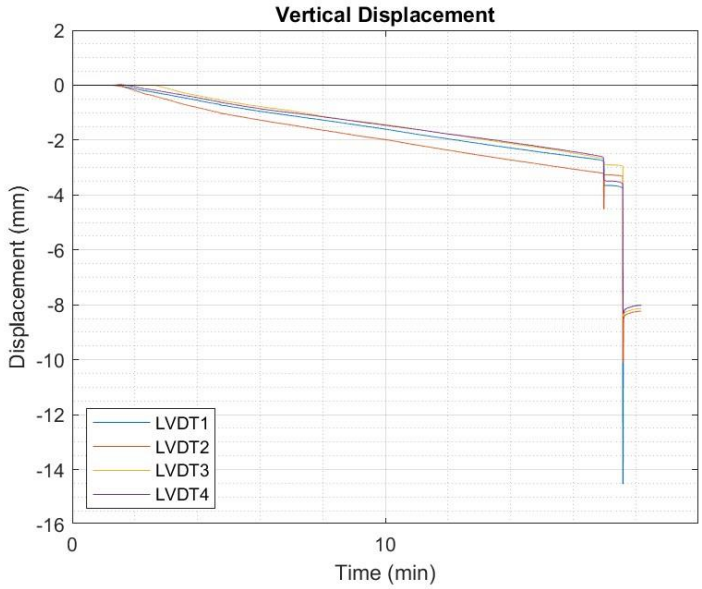

Figure 67. Detail 3.1: vertical displacement results of LVDTs.

The tests results are shown in Figure 67 in terms of vertical displacement detected by LVDTs positioned on the specimen. They showed a symmetrical behaviour until the failure of the aluminium bolts occurred.

Considering the strain gauges installed on the steel part close to the aluminium bolts, the results are hereafter reported.

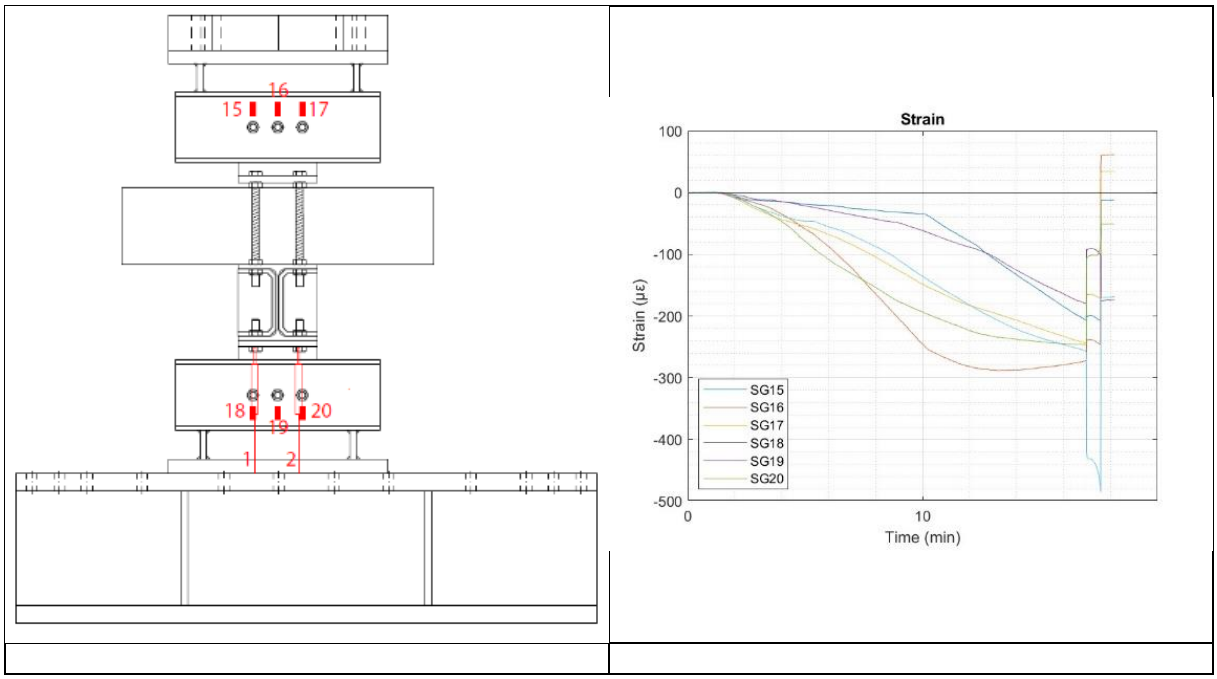

Figure 68. Detail 3.1: (a) Strain gauges position; (b) strain gauges results.

The strain gauges results are reported in Figure 68b. The 6 instruments have the same trend in compression as expected, considering their location and the aluminium bolts movement.

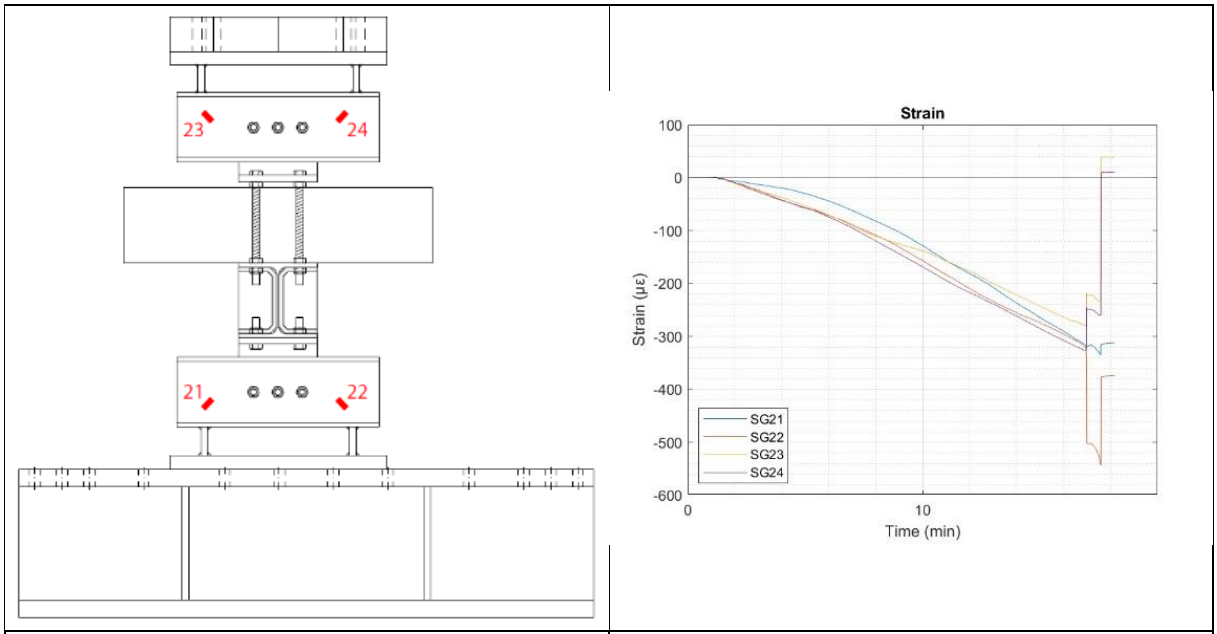

(a) (b)

Figure 69. Detail 3.1: (a) Strain gauges position and (b) results.

The strain gauges results above illustrated, are reported in Figure 69b. The trend recorded is coherent with the test direction in compression and the instruments position.

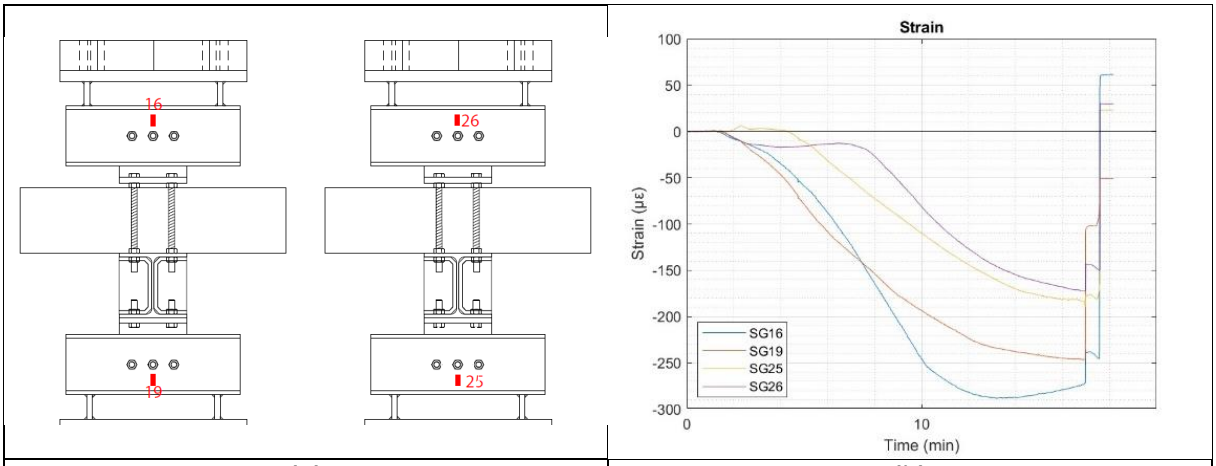

(a) (b)

Figure 70. Detail 3.1: (a) Strain gauges position; (b) strain gauges results.

The results of the strain gauges depicted in Figure 70a, are shown in Figure 70b. The diagram highlights similar strains between the front and back side and therefore the specimen symmetry in terms of local strains. The different values observed by strain gauges are probably due to imperfection of the specimen both in the realization and assembly due to the clearances in the holes. The local strain levels did not exceed the actual steel yield limit, which is 1710 με, highlighting that significant bearing effects were not detected.

2.3.3 Cyclic tests

In order to follow the ECCS procedure, as reported in Section 1.3, the two monotonic test curves were used to define the yield displacement and the displacement history to perform the cyclic tests.

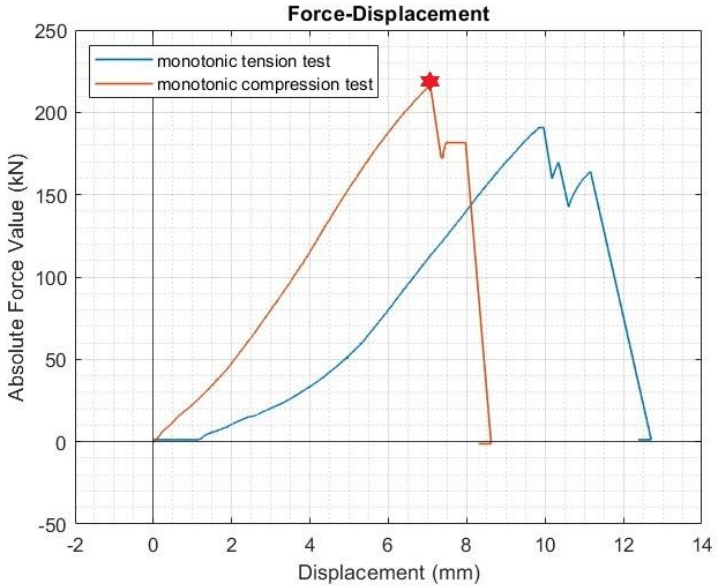

Figure 71. Detail 3.1 monotonic test results

Figure 71 reports the comparison, in terms of force-displacement curves, between the monotonic tension and compression tests. The red point represents the yield displacement for the cyclic test and the value is reported in Table 12. The e_y was chosen considering the monotonic compression curve because the tension curve presents an initial slip. However, besides that, with the exception of a slight difference in stiffness, the two curves are similar. Thus, the yield displacement was selected equal in tension and in compression and its value was chosen corresponding to the first bolt failure in the monotonic compression test.

Table 12: Yield displacement from monotonic curves

e_y	7.1 mm
$-e_y$	7.1 mm

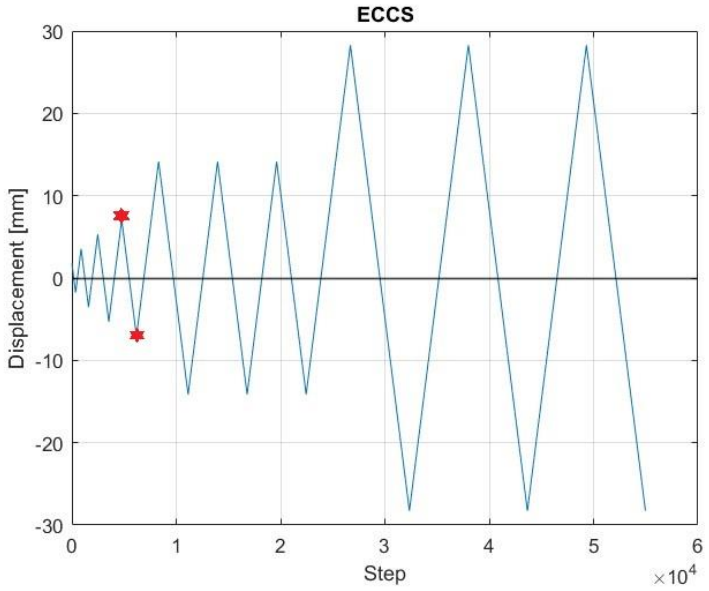

Figure 72. Detail 3.1 ECCS procedure.

Figure 72 depicts the displacement history defined as reported in Section 1.3. The yield displacement previously introduced is highlighted in red. The cyclic tests were conducted in displacement control with different displacement rate: until the e_y the displacement rate was 0.5 mm/min; for the three cycles at $2e_y$ the displacement rate was 1 mm/min; for the last three cycles at $4e_y$ the displacement rate was set at 2 mm/min.

2.3.1.1 Cyclic test 1

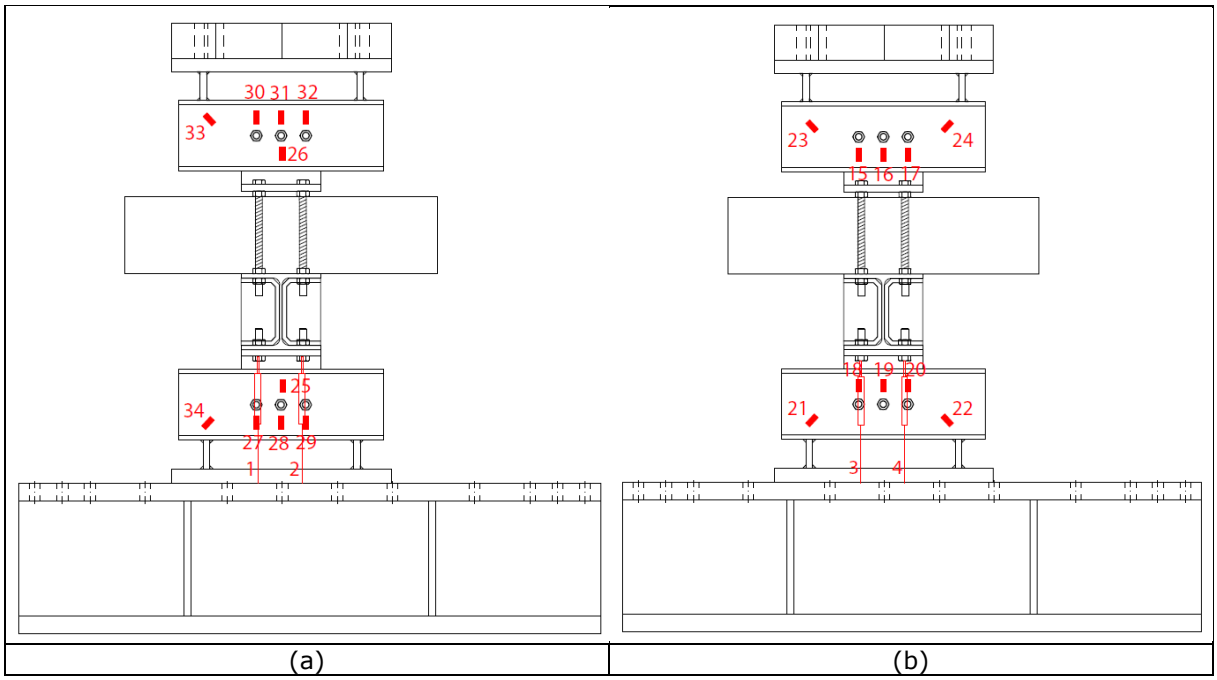

Figure 73. Detail 3.1: LVDTs and strain gauges position (a) on front side; (b) on back side.

The LVDTs were located to check specific detail movements as reported in section 2.3.1.
In this case, 20 strain gauges were located on the steel UPN elements to measure the deformation induced by the aluminium bolts during the test. The instrument acquisitions were recorded at 2 Hz.

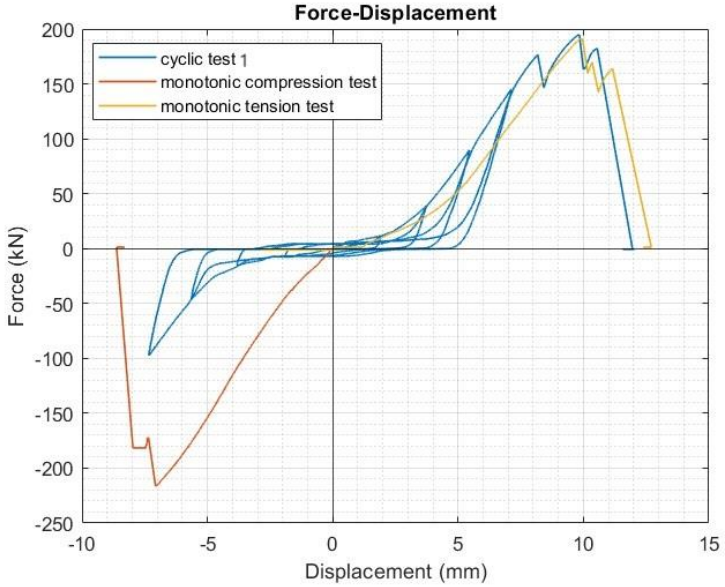

Figure 74. Detail 3.1 cyclic test 1 results.

The results of the first cyclic test on Detail 3.1, in terms of force-displacement curve, are shown in Figure 74. The failure of the specimen occurred on the reloading at the first cycle to $2e_y$. Besides the brittle nature of the detail, a small hysteretic behaviour associated with large slip caused by the bolt-hole clearances can be observed. It is worth noting that the design force of 180 kN was almost reached in the tension branch. The comparison between the cyclic test and the monotonic tests shows a good agreement in terms of strength and stiffness degradation, on the tension part, while on the compression part a significant difference can be noticed. On the compression part of the diagram, a significant pinching phenomenon during the cyclic test was observed. Again, the bolt-hole clearance may have caused it, taking into account that the cyclic test started along the tension branch.

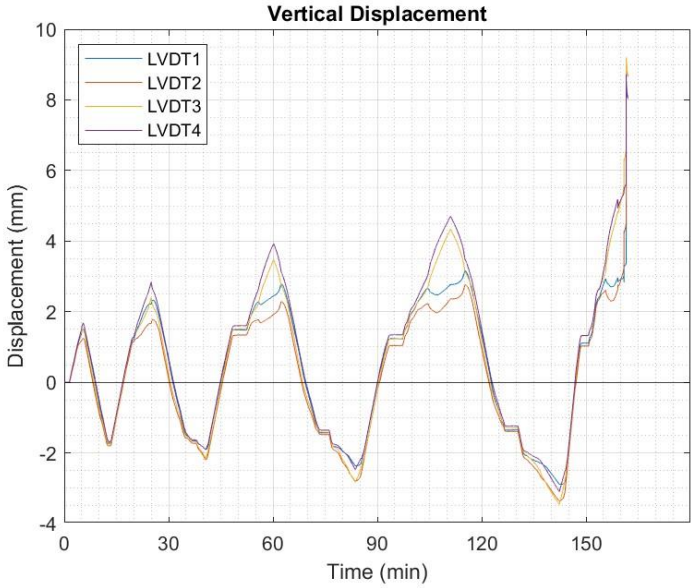

Figure 75. Detail 3.1 LVDTs cyclic test results.

The vertical displacement acquisitions are reported in Figure 75. The graph shows a symmetric behaviour in displacement during the test, with some difference caused by an inherent imperfect specimen.

Considering the strain gauges installed on the steel part close to the aluminium bolts, the results are hereafter reported.

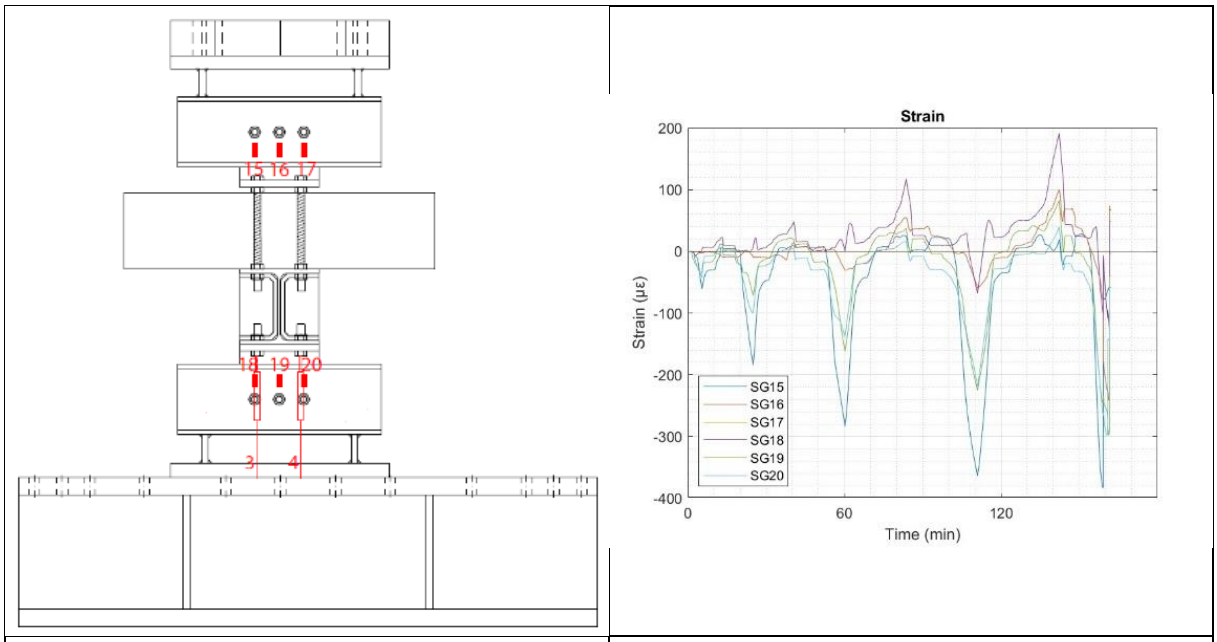

(a) (b)

Figure 76. Detail 3.1: (a) strain gauges results position; (b) strain gauges results.

The strain gauges results are shown in Figure 76b. The upper and the lower instruments recorded the same expected trend.

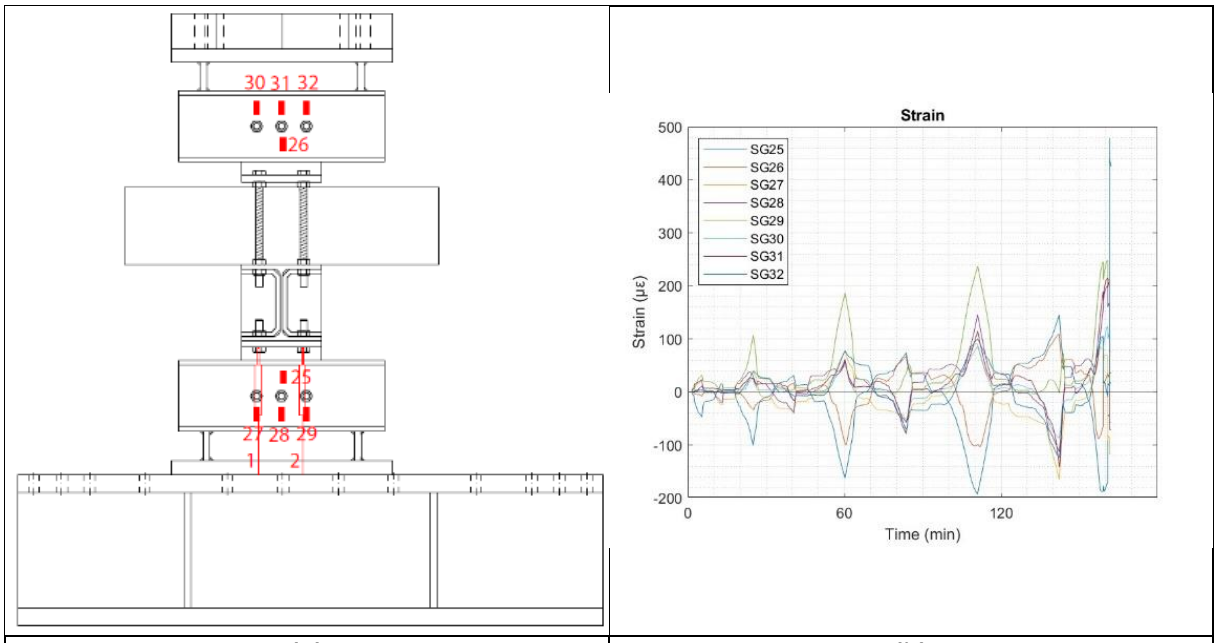

(a) (b)

Figure 77. Detail 3.1: (a) strain gauges results position; (b) strain gauges results.

Figure 77b reports the results of instruments shown in Figure 77a. The acquisitions are coherent with the strain gauges position, indeed the three instruments on the upper and lower part recorded the same trend, that is in opposite directions compared to the two single instruments on the same steel element.

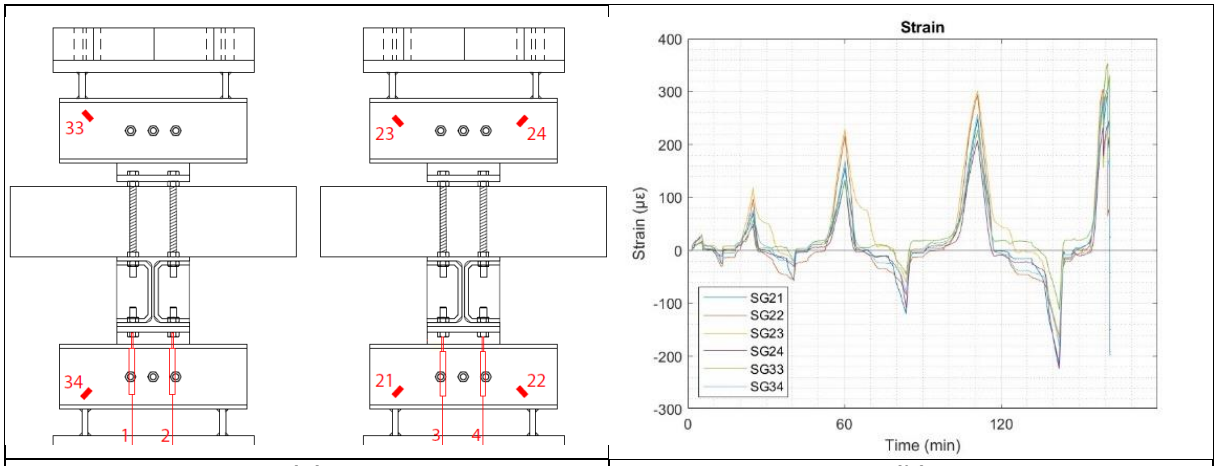

Figure 78. Detail 3.1: (a) strain gauges position; (b) strain gauges results

As illustrated in Figure 78b, the strain gauges illustrated in Figure 78a, had the same trend of acquisition which highlights the symmetry in terms of deformation between the two sides of the specimen. The strain levels did not exceed the yield limit close to the aluminium bolts.

2.3.3.2 Cyclic test 2

The second cyclic test on Detail 3.1 was repeated with the same testing protocol. The instrumentation position on the specimen was slightly modified as is reported in Figure 79.

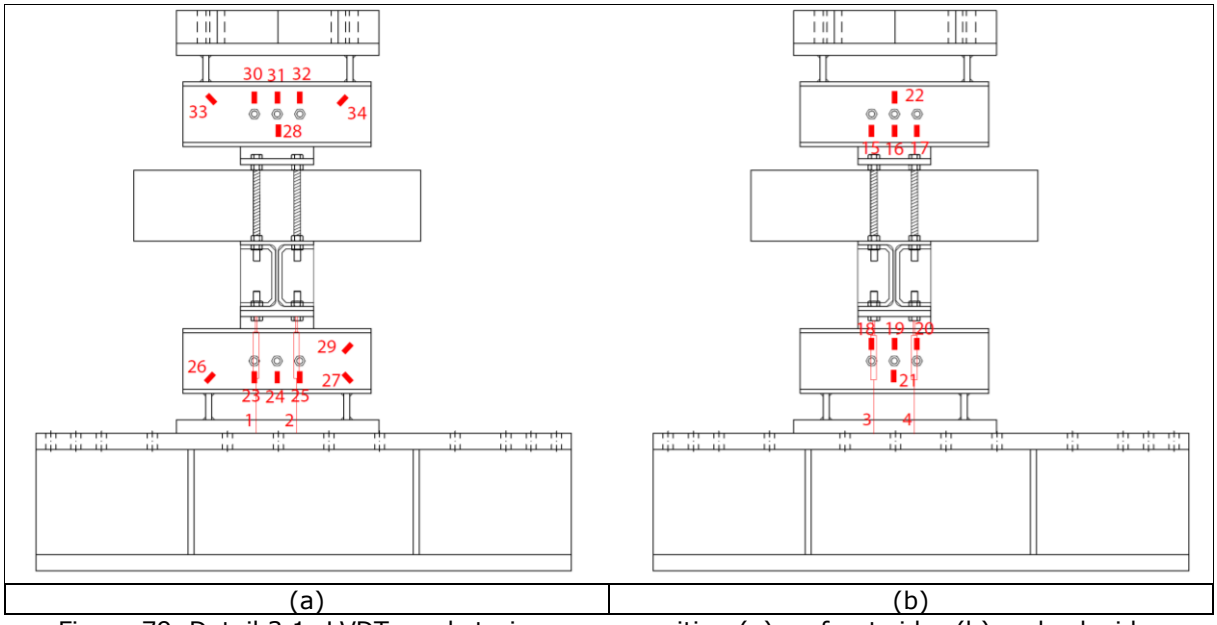

Figure 79. Detail 3.1: LVDTs and strain gauges position (a) on front side; (b) on back side.

The results of the second cyclic test on Detail 3.1, in terms of force-displacement curve, are shown in Figure 78. The failure of the specimen occurred on the reloading at the first cycle to $2e_y$, as for the first cyclic test. Besides the brittle nature of the detail, a small hysteretic behaviour associated with significant pinching due to bolt-hole clearances can be observed. It is worth noting that, also in this case, the design force of 180 kN was reached in the tension branch. As for the first cyclic test, the comparison between the cyclic test and the monotonic tests shows a good agreement in terms of resistances and stiffness degradation for the tension part, while on the compression part a significant difference can be noticed, as also occurred for the first cyclic test. On the compression part of the diagram, a significant pinching phenomenon during the cyclic test was observed. Again, the bolt-hole clearance may have caused it, taking into account that the cyclic test started along tension branch.

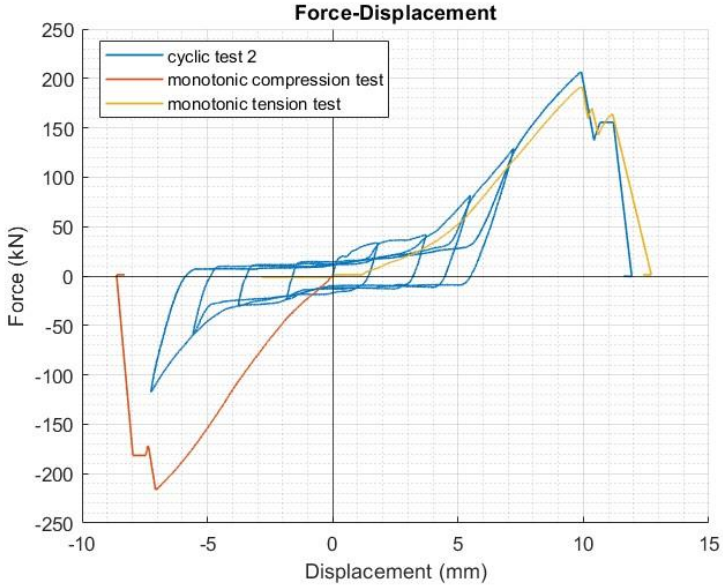

Figure 80. Detail 2 cyclic test 2 results

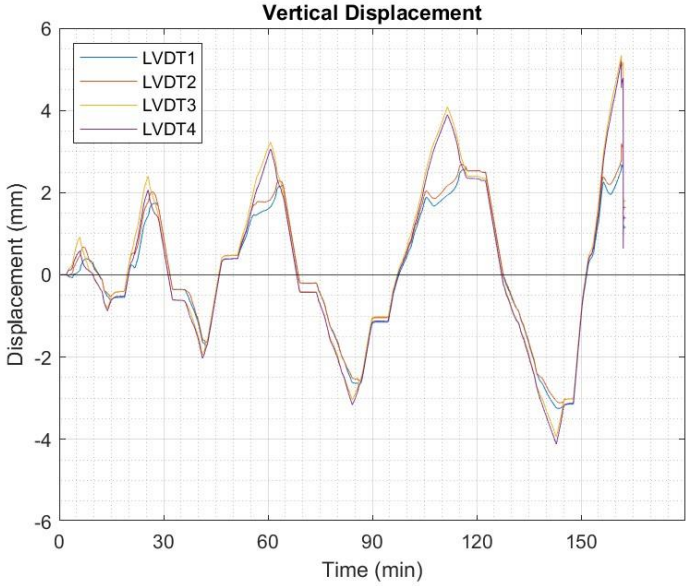

Figure 81. Detail 3.1 cyclic test 2 LVDTs results.

The vertical displacement acquisitions are reported in Figure 81. The graph shows a symmetric behaviour in displacement during the test, with some difference caused by an inherent imperfect specimen.

Considering the strain gauges installed on the steel part close to the aluminium bolts, the results are hereafter reported.

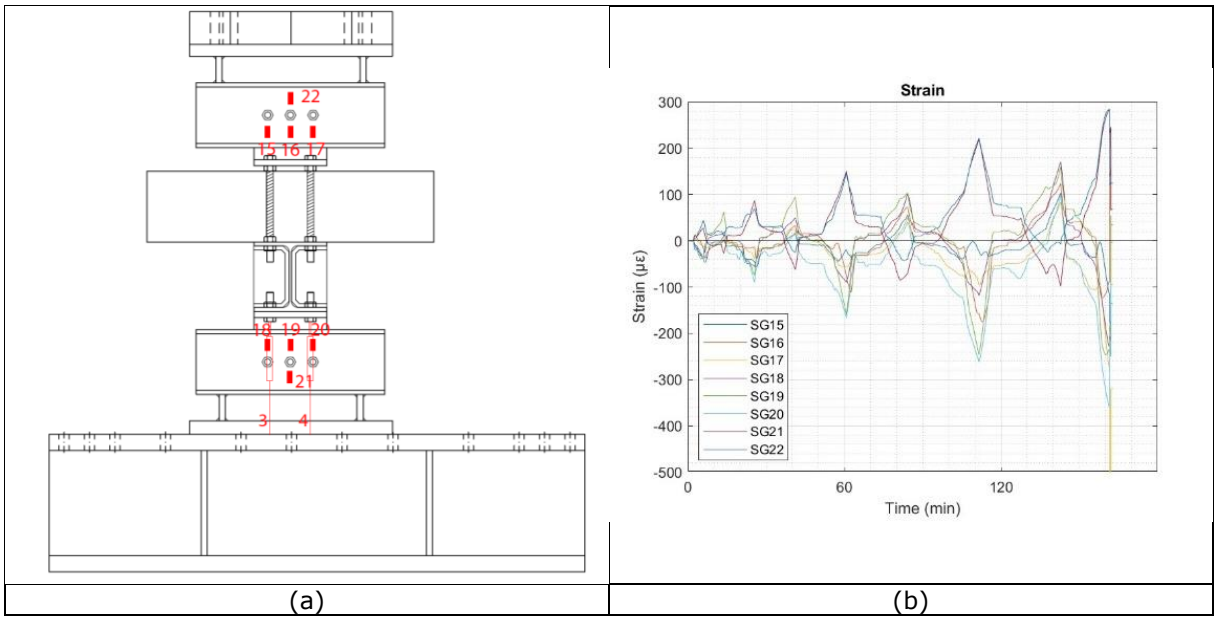

(a) (b)

Figure 82. Detail 3.1: (a) strain gauges position; (b) strain gauges results.

Figure 82b reports the results of the instruments illustrated in Figure 82a. The graph highlights the expected correspondence between the strain gauges 15, 16 and 17 with the 18, 19 and 20, while the 21 and 22 are in a good agreement with each other and are in opposition with the others.

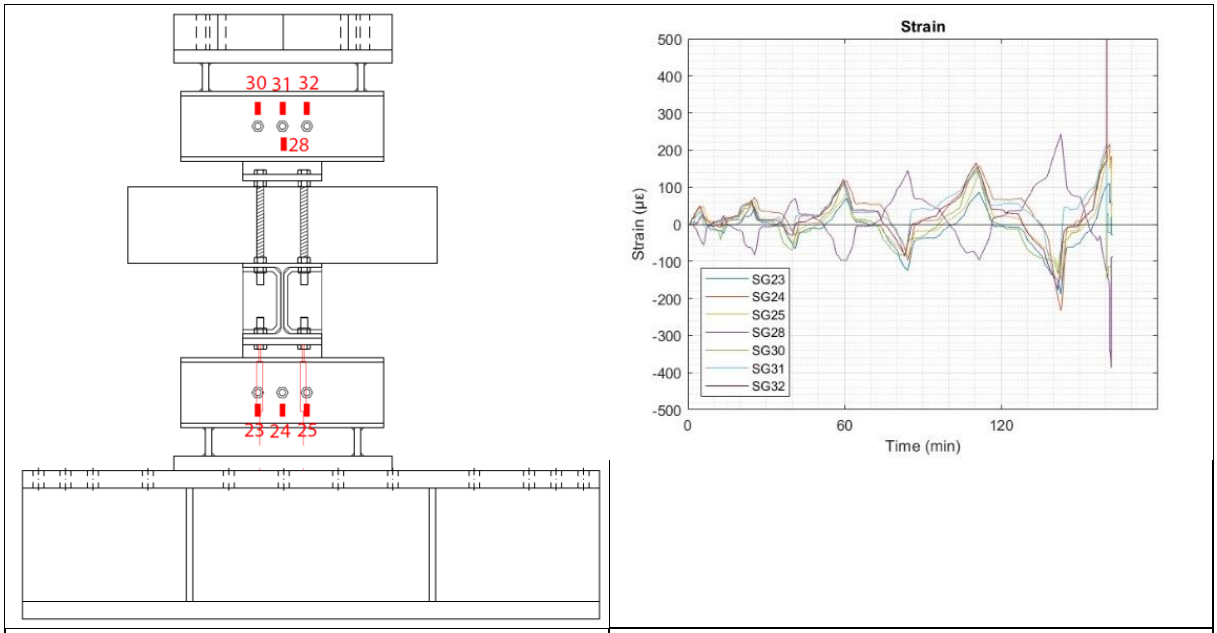

(a) (b)

Figure 83. Detail 3.1: (a) strain gauges position; (b) strain gauges results.

Figure 83b shows the results of the instruments illustrated in Figure 83a. As expected, all the strain gauges have the same trend with the exception of instrument 28 that showed an opposite behaviour due to the position.

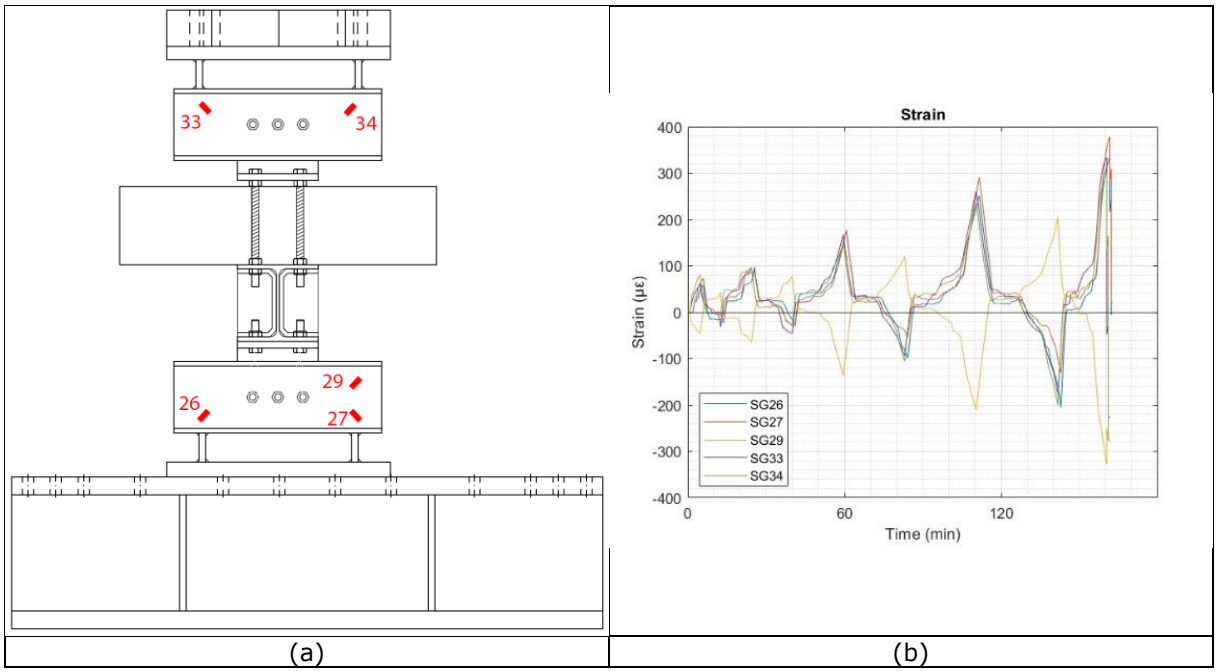

Figure 84. Detail 3.1: (a) strain gauges position; (b) strai gauges results

The strain gauges results are reported in Figure 84b. As for the previous analysis, the instruments acquisition recorded a consistent behaviour between the four strain gauges located at the extremities of the UPN element, while, given its position, the instrument 29 recorded an opposite behaviour. The strain levels did not exceed the yield limit close to the aluminium bolts.
.

2.3.4 Summary

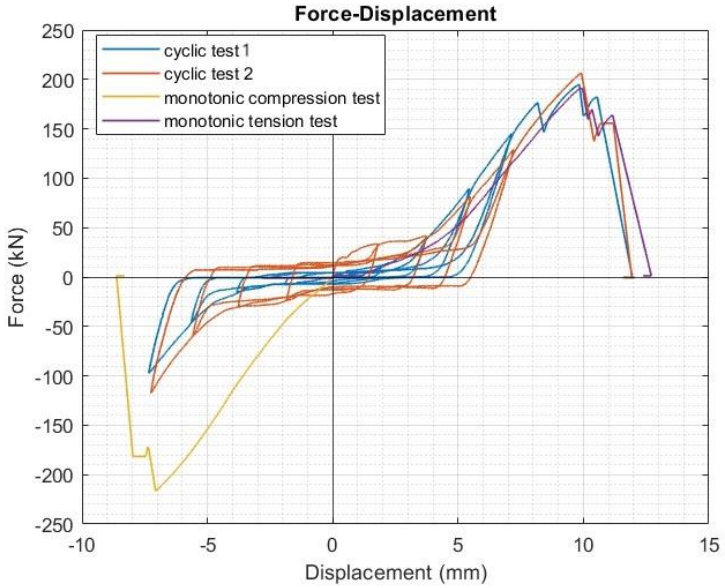

Figure 85. Detail 3.1 test results comparison

The comparison between the four tests performed on Detail 3.1 are reported in Figure 85. The two cyclic tests are in a good agreement: indeed, the second cyclic test exhibited wider cycles due to an initial stiffer cycle than the first cyclic test. The comparison with the monotonic tests highlighted a good agreement with the tension test curve, while in compression the cyclic tests were affected by significant pinching due to bolt-hole clearances, and the agreement with the monotonic test is not as good as with the tension test. However, comparing the slope of the three curves analysed, a similar stiffness was obtained.

In conclusion, Table 13 summarizes the maximum experimental forces reached by each test at the first failure of an aluminium bolt, in comparison with the design force. In Figure 86 some specimens

photos, after the tests, can be observed and in Figure 87 the aluminium bolts after the tests are shown.

Table 13. Failure forces reached during the tests.

Detail 3.1	Design force	Maximum experimental
Monotonic tension test	180 kN	190.7 kN
Monotonic compression test	180 kN	215.4 kN
Cyclic test 1	180 kN	176.6 kN
Cyclic test 2	180 kN	204.9 kN

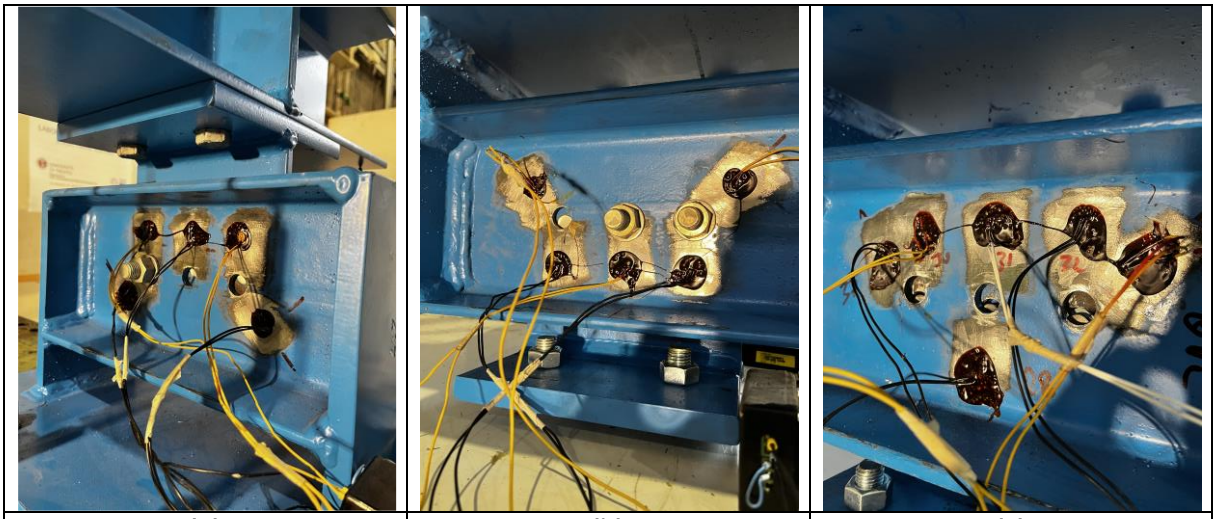

(a) (b) (c)

Figure 86. Detail 3.1 at failure: (a) frontal view of aluminium bolts under tension force; (b) frontal view of aluminium bolts under compression force; (c) movement between UPN160 elements and T plate elements after cyclic test.

(a) (b)

(c) (d)

Figure 87. Detail 3.1 aluminium bolts at failure: (a) tension test; (b) compression test; (c) cyclic test 1; (d) cyclic test 2.

2.4 Tests on Detail 3.2

As reported in D1.4 [1], all the details were developed from 3 reference fusible link solutions common to all the project partners, to obtain the most reliable information.

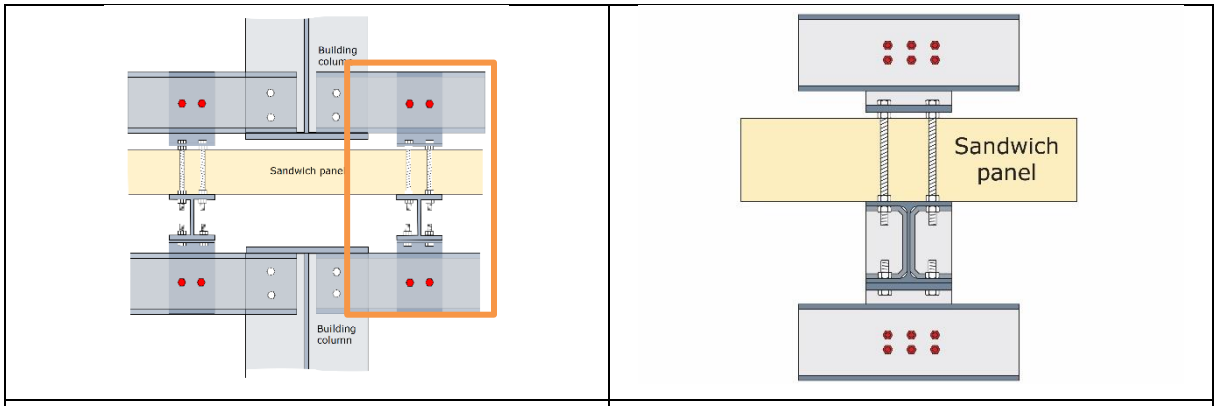

(a) (b)

Figure 88. Detail 3.2: (a) reference detail, (b) Detail 3.2 for seismic tests.

Figure 88 reports Detail 3.2 and the reference fusible link solution from which it was derived. As can be noticed, only one side of the detail was considered and tested with the appropriate number of aluminium bolts to withstand the design force equal to 180 kN. In addition, this detail is similar to Detail 3.1, while increasing the number of aluminium bolts and their diameter, changing from M12 to M16 bolts.

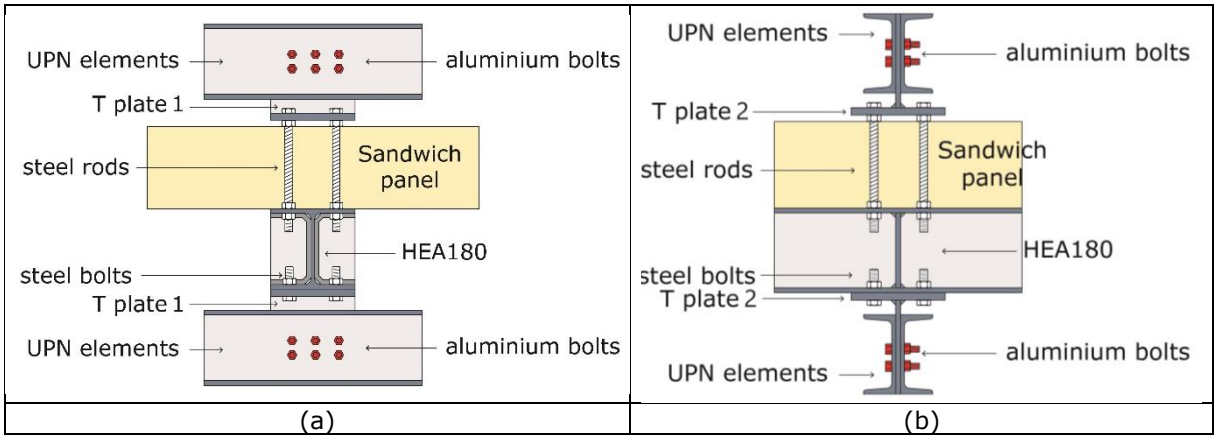

(a) (b)

Figure 89. Detail 3.2: (a) front view; (b) lateral view.

Table 14: Detail 3.2 description

Elements	Main characteristics
UPN elements	4 UPN 160
Aluminium bolts	6 M12 AlZn5,5MgCu 7075
Steel rods	4 M16 8.8
Steel bolts	4 M16 8.8
T Plate 1 -web	2 190x180x10
T plate 2- flange	2 190x180x15

In Figure 89 and in Table 14 the main characteristics of Detail 3.2 in terms of elements and geometry that compose the specimen are reported. As reported in Table 1, this detail was designed for a shear value of 180 kN, that can be withstood by 6M12 aluminium bolts working on two shear planes.

2.4.1 Monotonic tension test

In Figure 90 the specimen of Detail 3.2 inserted in the reaction frame can be observed. In Figure 91, the specific instrumentation position and its numbering are reported.

The 4 LVDTs were located to check the specific movements of the lower part of the specimen to detect possible difference with the upper part, measured by the actuator transducer.

9 strain gauges were glued on the steel UPN elements in order to measure the strain induced by the aluminium bolts during the test as well as its symmetric behaviour. The instrument acquisitions were recorded at 2 Hz.

Figure 90. View of the detail 3.2 test set-up

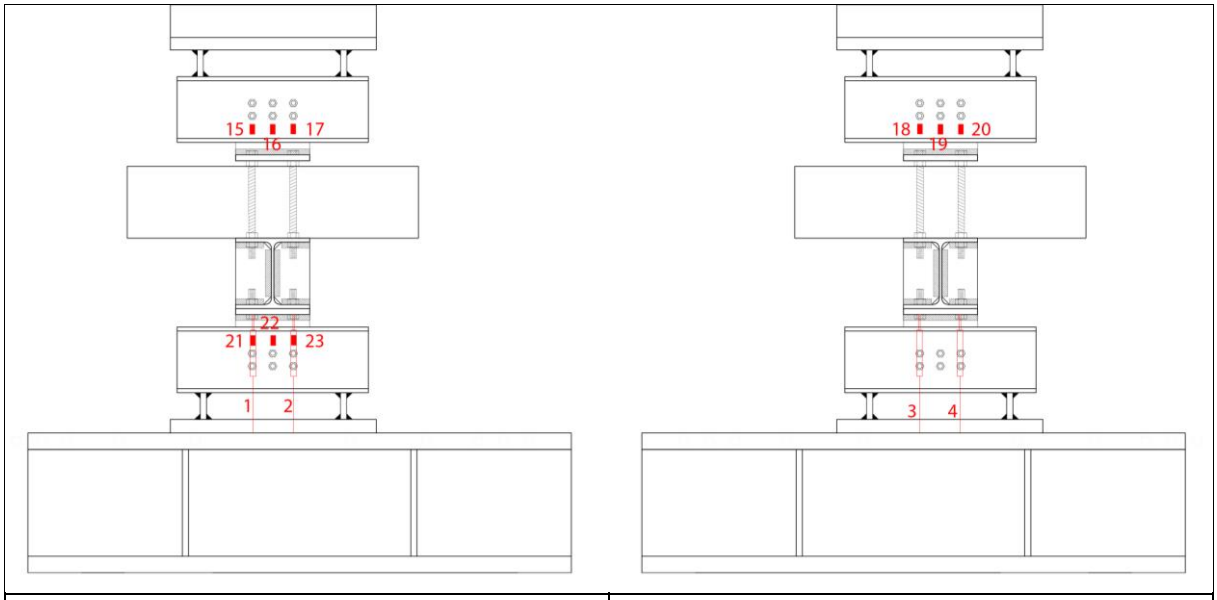

(a) (b)

Figure 91. Detail 3.2: LVDTS and strain gauges position: (a) on front side; (b) on back side.

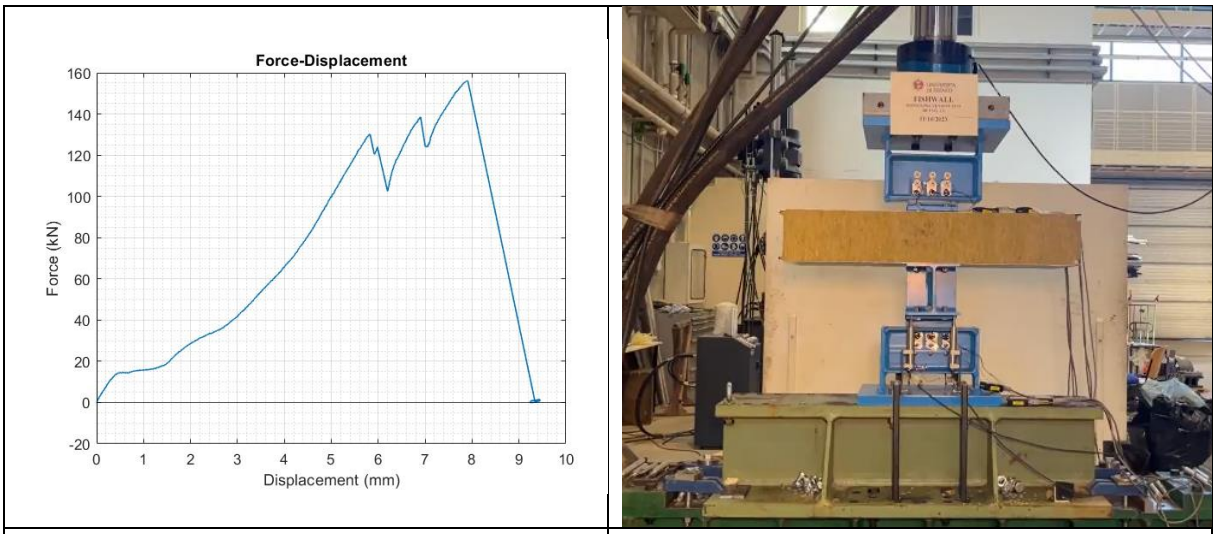

(a) (b)

Figure 92. Detail 3.2: (a) force-displacement diagram of the monotonic tension test and (b) final specimen deformation

In Figure 92, the result in terms of the force-displacement curve is shown, where the peaks highlights the progressive failure of the aluminium bolts of the lower, upper and again lower part of the specimen. It is worth noting that the design force of 180 kN was not reached. The increase of the number of bolts inevitably also increased the imperfections of the specimens: not perfect alignment of the holes, slight different hole dimensions that may have induced higher forces than expected in some aluminium bolts, that collapsed sequentially before reaching the design force.

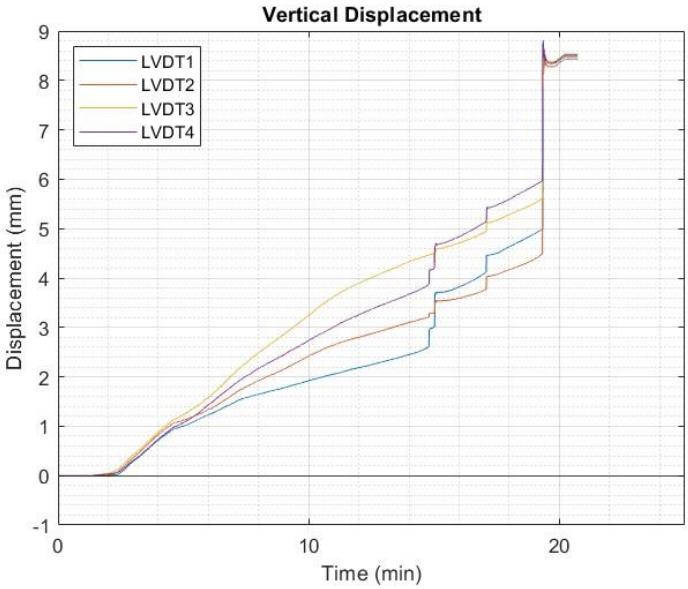

Figure 93. Detail 3.2: vertical displacement results of LVDTs.

The test results, in terms of vertical displacement detected by LVDTs, are depicted in Figure 93. They show an initial symmetrical behaviour until an increased difference occurred between the instruments on the front side and the back side, which could be caused by a specimen imperfection, in particular of the T elements that were characterised by noticeable distortions because of the welding process. The initial slip is related to recover the bolt-hole clearance of the top aluminium bolts.

Considering the strain gauges installed on the steel parts close to the aluminium bolts, the results are hereafter reported.

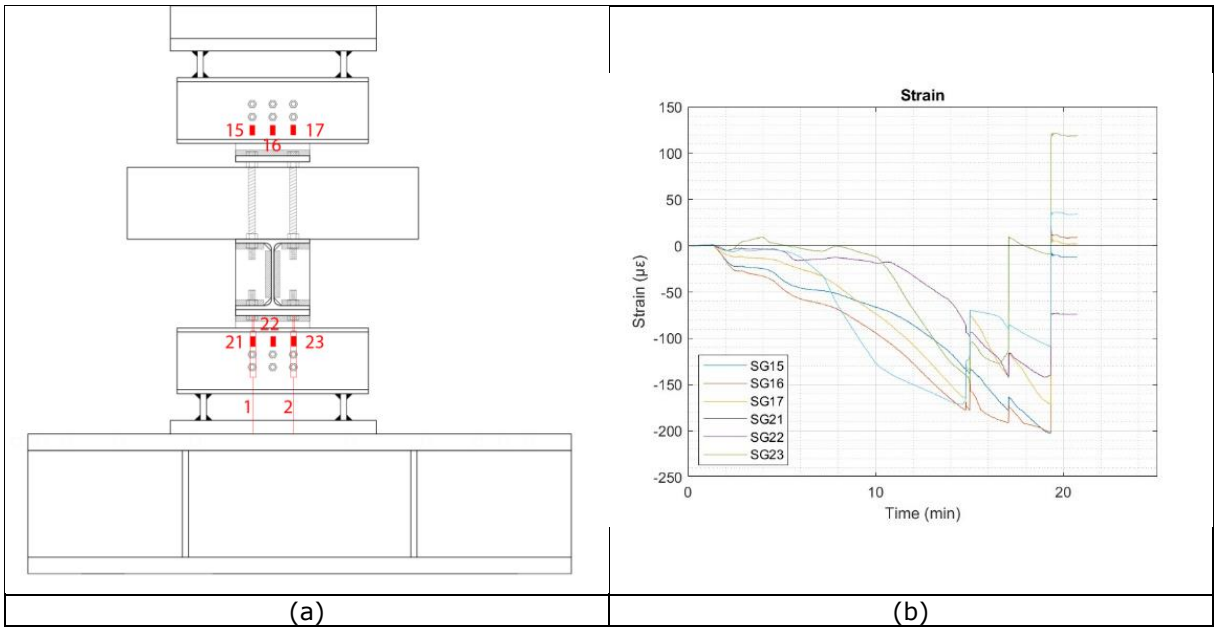

(a) (b)

Figure 94. Detail 3.2: (a) strain gauges position; (b) strain gauges results.

The front side strain gauges acquisitions are reported in Figure 94. As expected, the 6 instruments have the same trend in compression.

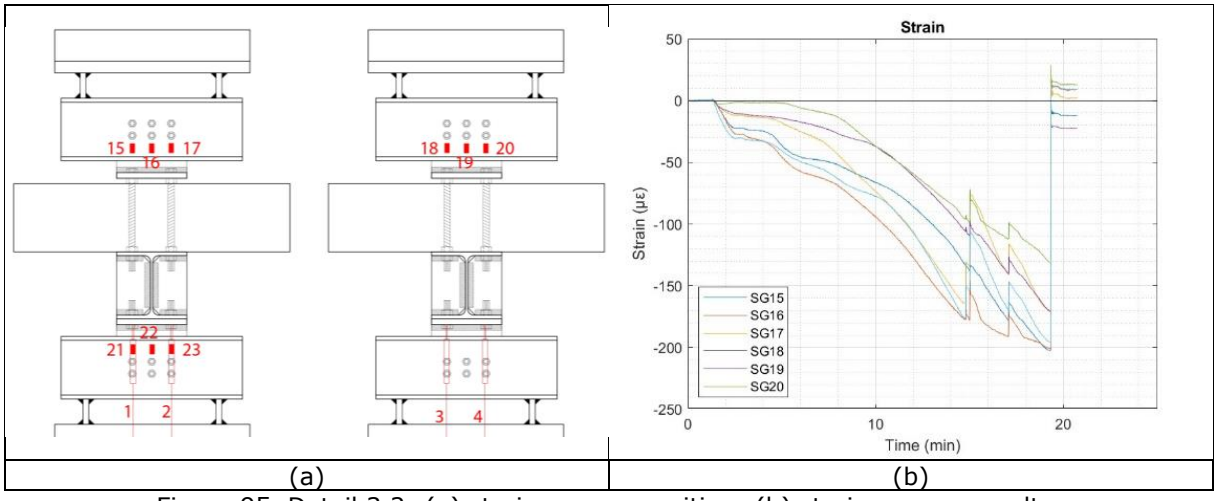

(a) (b)

Figure 95. Detail 3.2: (a) strain gauges position; (b) strain gauges results.

The two sides strain gauge acquisitions are reported in Figure 95. The 6 instruments have the same trend in compression as expected. The local strain levels did not exceed the actual steel yield limit 1710 με, highlighting that significant bearing effects were not detected.

2.4.2 Monotonic compression test

In Figure 90 the specimen of Detail 3.2 inserted in the reaction frame can be observed.

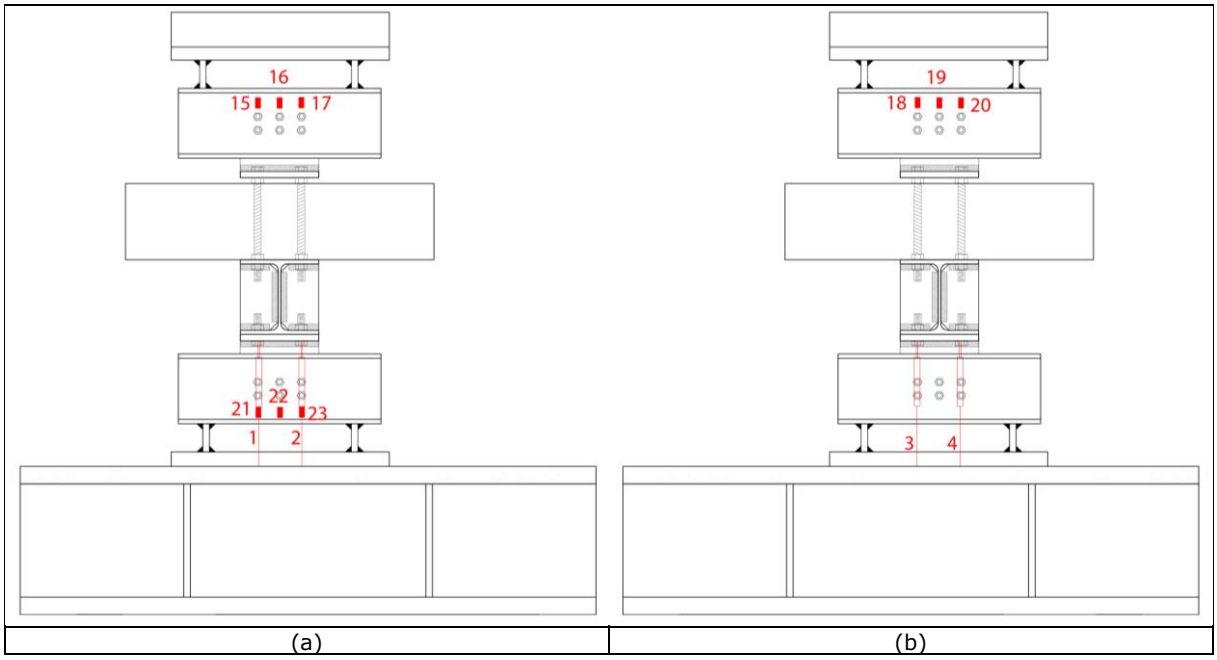

(a) (b)

Figure 96. Detail 3.2: LVTDs and strain gauges position on (a) front side; (b) back side.

In Figure 96, the specific instrumentation position and numbering are reported. The LVDTs were located to check specific detail movements, as reported in Section 2.4.1. Also in this case, 9 strain gauges were located on both side of the specimen to check the symmetry of the specimen. The instruments acquisitions were recorded at 2 Hz.

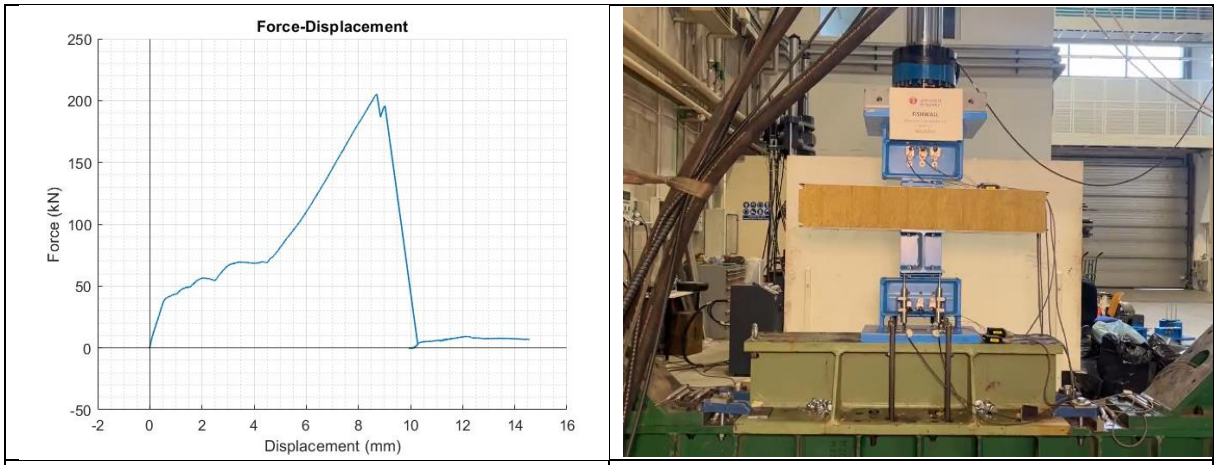

(a) (b)

Figure 97. Detail 3.2 (a) force-displacement curva of the monotonic compression test; (b) final specimen deformation.

Figure 97a reports the result in terms of the force-displacement diagram. After an initial phase marked by the recover of the bolt-hole clearance, the force increased until the failure of all the aluminium bolts of the lower part of the specimen. It is worth noting that, differently from the monotonic tension test, the design force of 180 kN was reached.

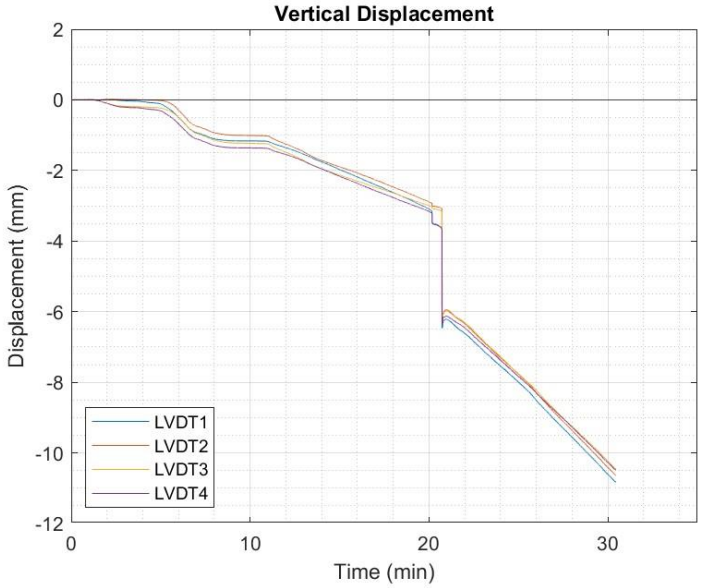

Figure 98. Detail 3.2: vertical displacement results of LVDTs.

The test results, in terms of vertical displacement detected by LVDTs positioned on the specimen, in Figure 98 are shown. They highlighted a symmetrical behaviour during all the test duration, including the failure moment at minute 21.

Considering the strain gauges installed on the steel part close to the aluminium bolts, the results are hereafter reported.

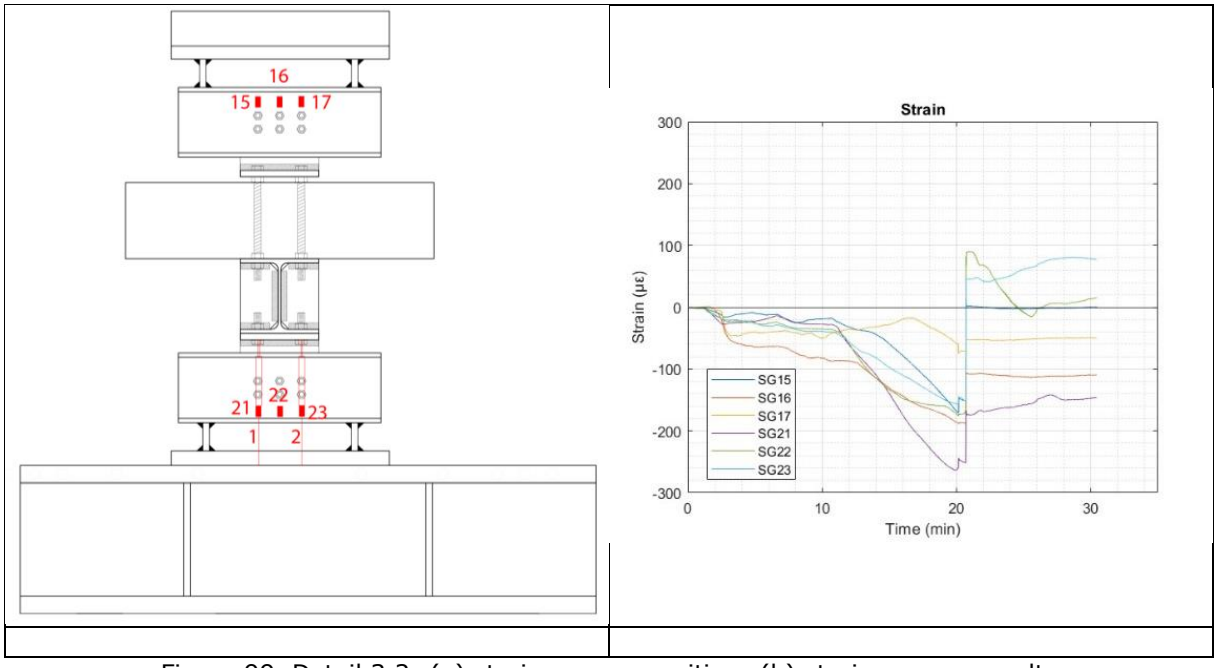

Figure 99. Detail 3.2: (a) strain gauges position; (b) strain gauges results.

The strain gauges results are reported in Figure 99b. The trend recorded is consistent with the test direction in compression and the instruments position. After the first peak, the lower strain gauges experienced a tension phase due to the aluminium bolt failure close to them.

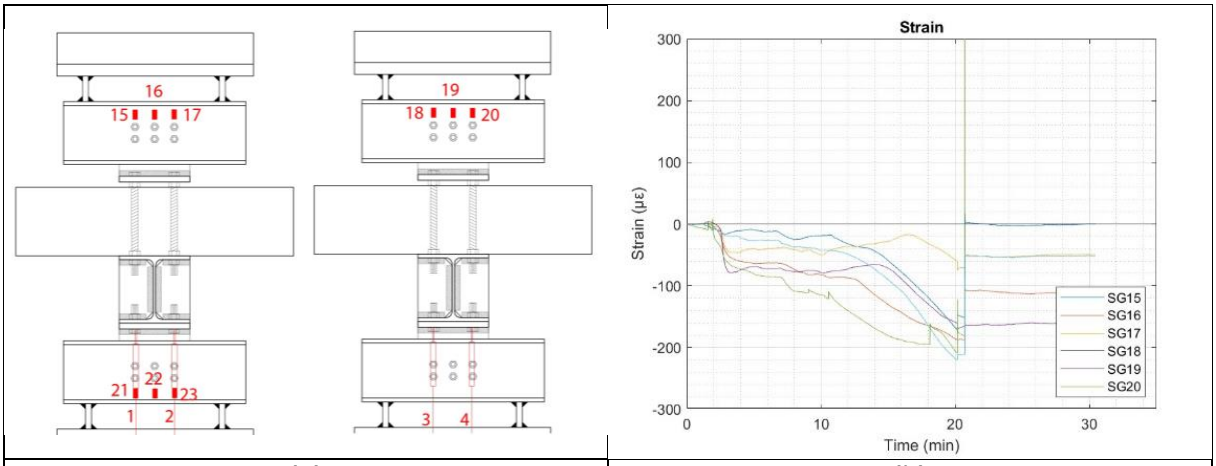

(a) (b)

Figure 100. Detail 3.2: (a) strain gauges position; (b) strain gauges results.

The results of the strain gauges depicted in Figure 100a, are shown in Figure 100b. The diagram highlights similar strains between the front and back side and therefore the specimen symmetry in terms of strain. The local strain levels did not exceed the actual steel yield limit 1710 με, highlighting that significant bearing effects were not detected.

2.4.3 Cyclic tests

In order to follow the ECCS procedure, as reported in Section 1.3, the two monotonic tests curves were used to define the yield displacement and the displacement history to carry out the cyclic tests.

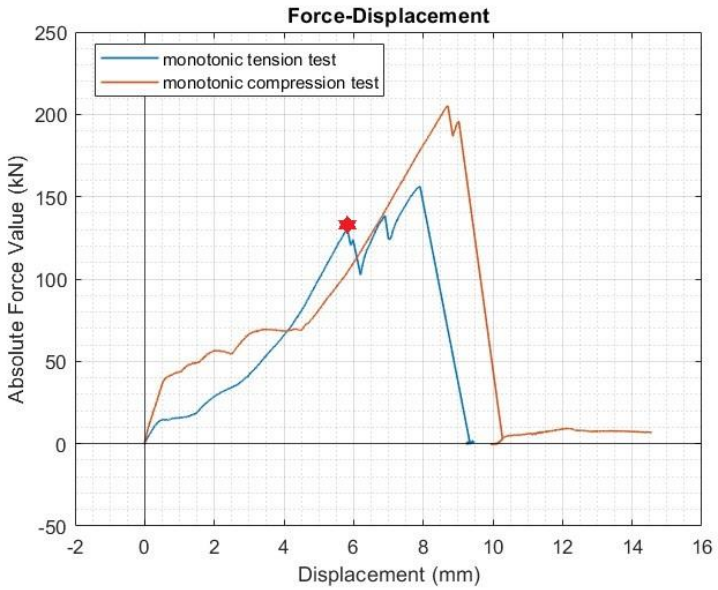

Figure 101. Detail 3.2 monotonic tests results

Figure 101 reports the comparison, in term of force-displacement curves, between the monotonic tension and compression tests. The red point represents the yield displacement selected for the cyclic test, which is also reported in Table 15. The e_y value was selected equal in tension and compression since the two responses were similar but for the maximum force that was more affected by imperfections in the monotonic tension test. Since a higher number of cycles was preferred, the failure point of the monotonic tension curve was chosen.

Table 15: Yield displacement from monotonic curves

e_y	5.8 mm
$-e_y$	5.8 mm

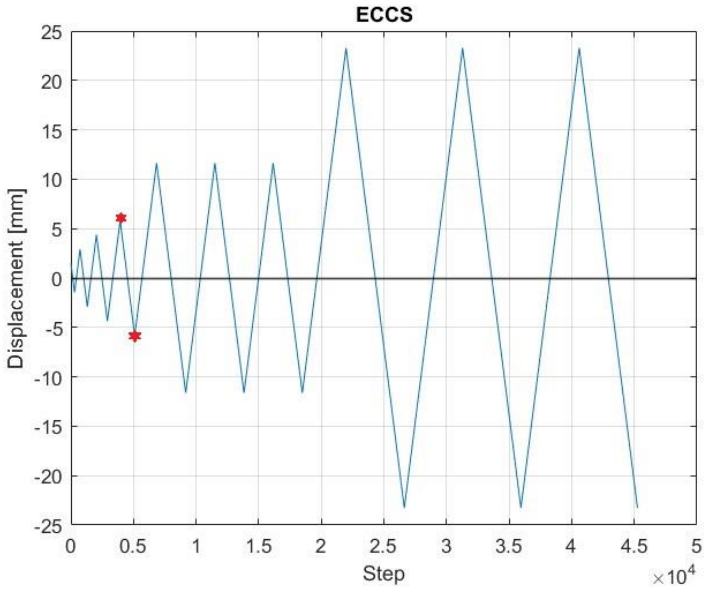

Figure 102. Detail 3.2 ECCS procedure.

Figure 102 shows the cyclic displacement history, where the yield displacement previously introduced is highlighted in red.

The cyclic tests were conducted in displacement control with different displacement rates: until the e_y the displacement rate was 0.5 mm/min; for the three cycles at $2e_y$ the displacement rate was 1 mm/min; for the last three cycles at $4e_y$ the displacement rate was set at 2 mm/min.

2.4.3.1 Cyclic test 1

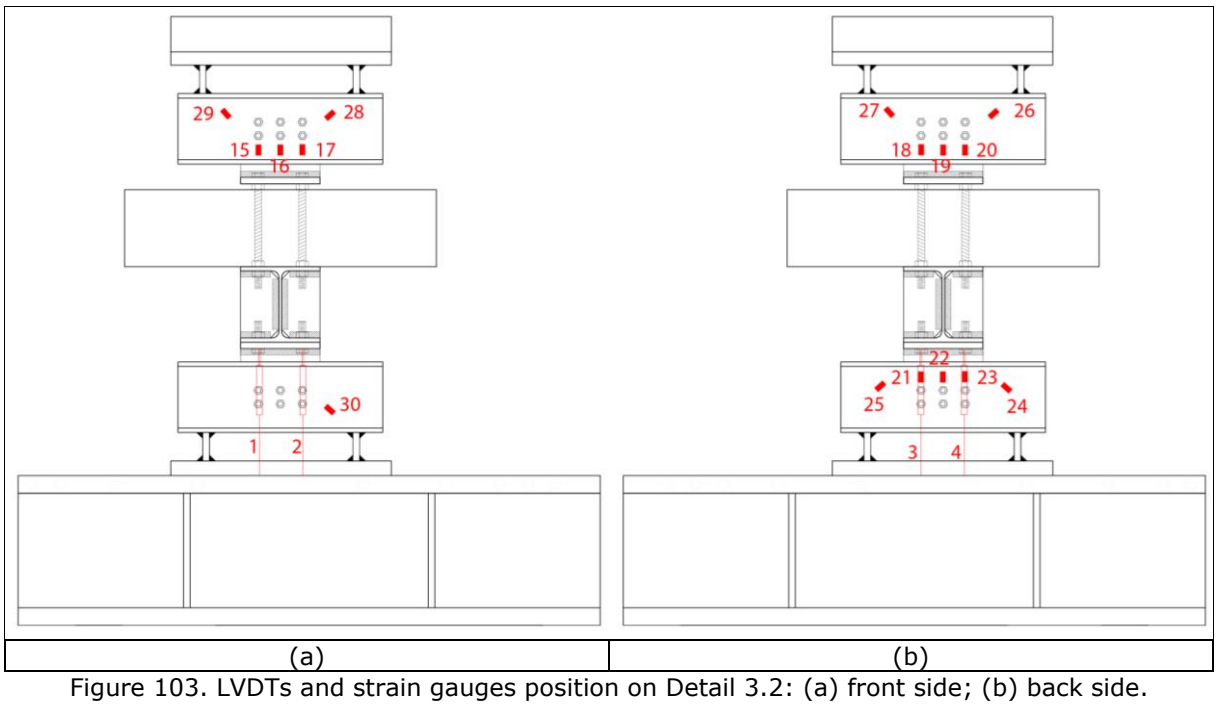

Figure 103. LVDTs and strain gauges position on Detail 3.2: (a) front side; (b) back side.

The location of the displacement LVDT transducers is reported Figure 103. Moreover, 16 strain gauges were located on the steel UPN elements to measure the strain close to the aluminium bolts. The instruments acquisitions were recorded at 2 Hz.

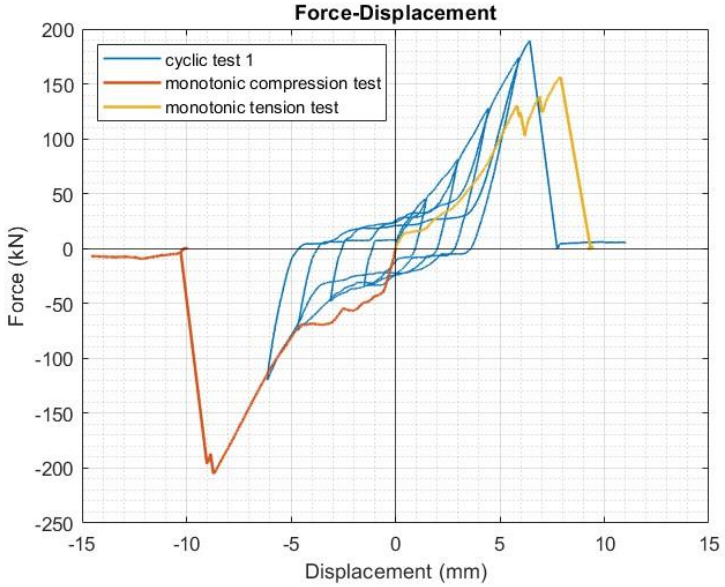

Figure 104. Detail 3.2 cyclic test 1 results

The results of the first cyclic test on Detail 3.2, in terms of force-displacement curve, are shown in Figure 104. The failure of the specimen occurred on the reloading at the first cycle to $2e_y$. Besides the brittle nature of the detail, a small hysteretic behaviour can be observed. Pinching, owing to the bolt-hole clearance, is also clearly visible. It is worth noting that the design force of 180 kN was reached in the tension branch, whilst it was not reach during the monotonic tension test. This was due to the higher imperfections of this detail. In fact, the bolt-hole clearance effect was not high enough to significantly affect the maximum force capacity relative to the cyclic behaviour in tension as for the monotonic tension test. Consequently, the stiffness in the cyclic test was higher. Moreover, the failure involved the collapse of all the six aluminium bolts located on the lower part of the specimen, while the tension test was characterized by a progressive failure of the aluminium bolts. In the compression part, in spite of an initial behaviour influenced by the pinching, stiffness at higher displacement levels fits well with what obtained in the monotonic compression curve.

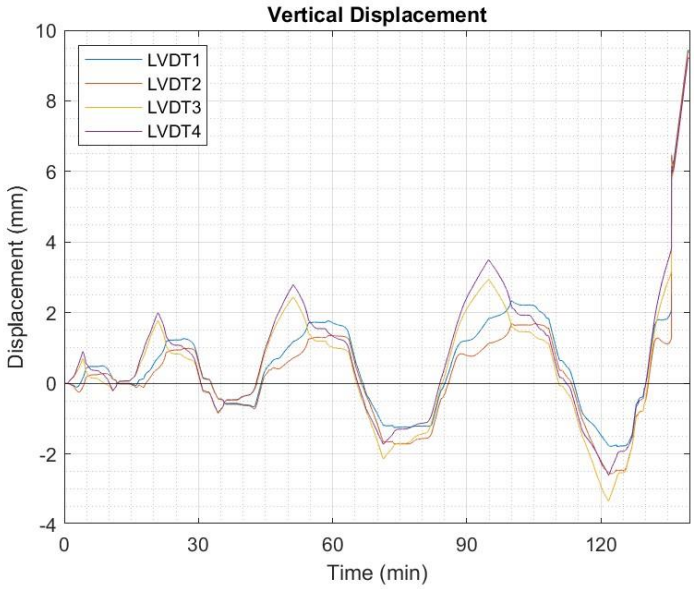

Figure 105. Detail 3.2 LVDTs cyclic test 1 results.

The vertical displacement acquisitions are reported in Figure 105. The graph shows some asymmetric behaviour due to the imperfections of the specimen.

Considering the strain gauges installed on the steel parts close to the aluminium bolts, the results are reported in Figure 106 to Figure 108. All instruments recorded consistent strain values with the cyclic behaviour with strain values below the actual yield limit of the steel elements of 1710 με, given the brittle collapse nature of the detail.

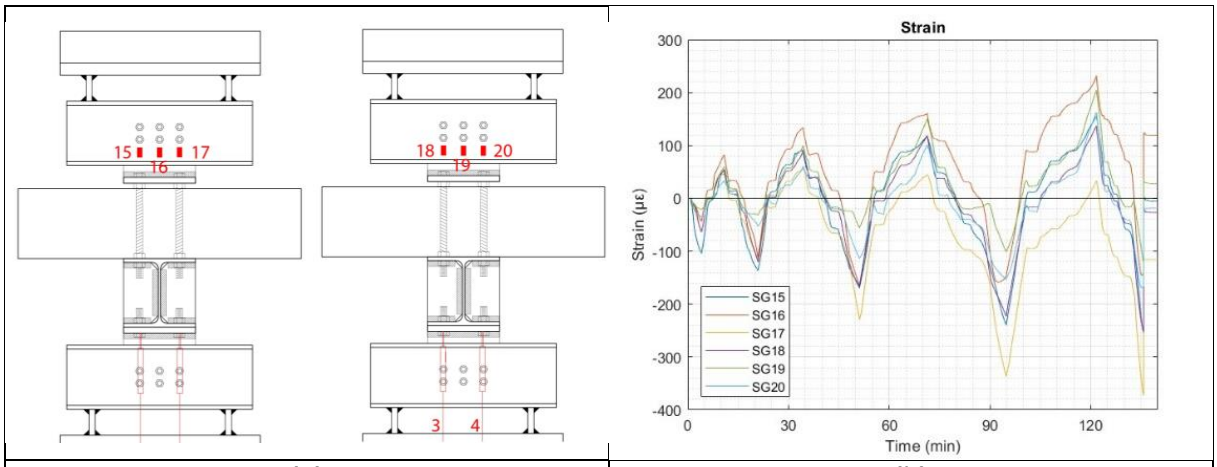

(a) (b)

Figure 106. Detail 3.2: (a) strain gauges results position; (b) strain gauges results.

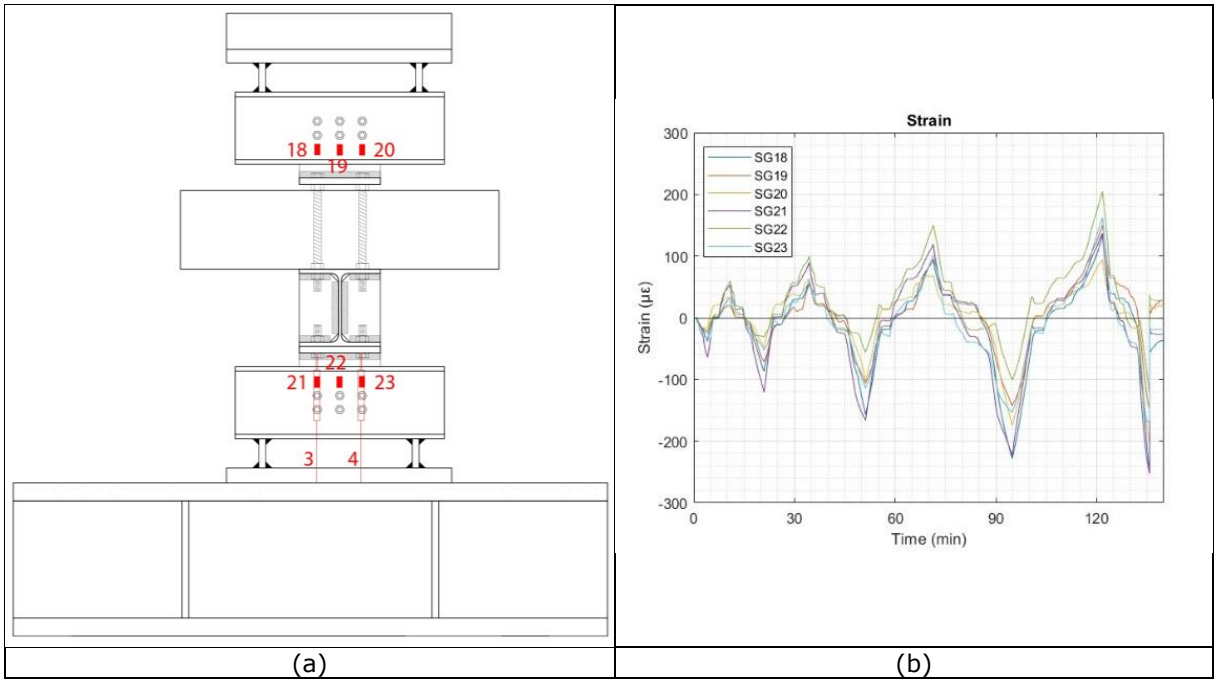

(a) (b)

Figure 107. Strain gauges on Detail 3.2: (a) position; (b) results.

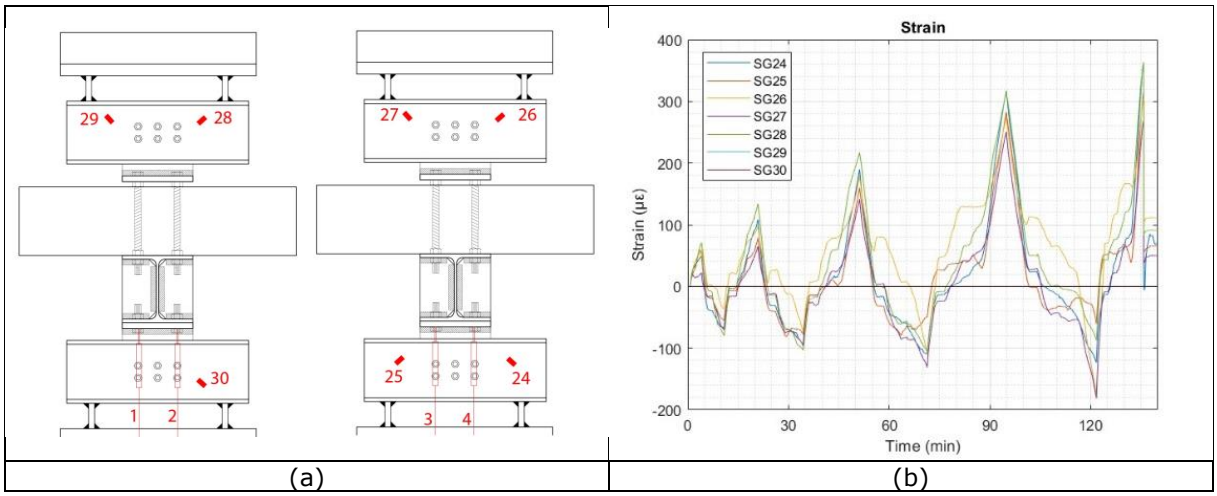

(a) (b)

Figure 108. Strain gauges on Detail 3.2: (a) position; (b) results.

2.4.3.2 Cyclic test 2

The second cyclic test on Detail 3.2 was repeated with the same testing protocol. The instrumentation position on the specimen was slightly modified as reported in Figure 109.

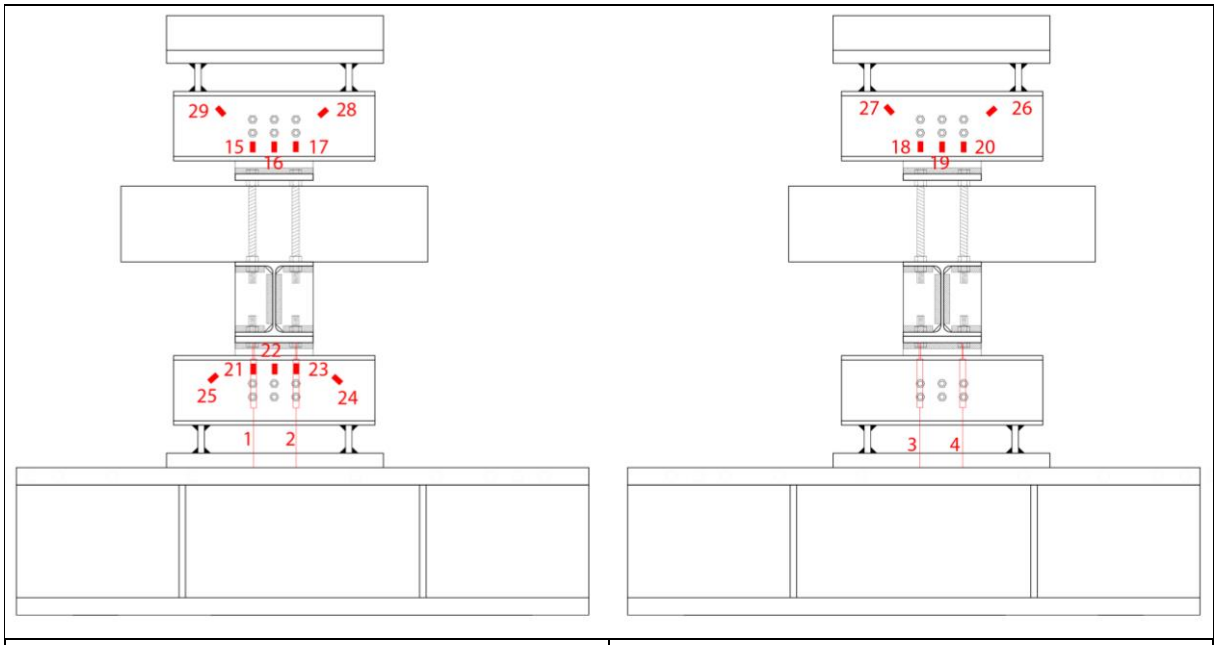

(a) (b)

Figure 109. Detail 3.2: LVDTs and strain gauges position for the cyclic test 2 (a) on front side; (b) on back side.

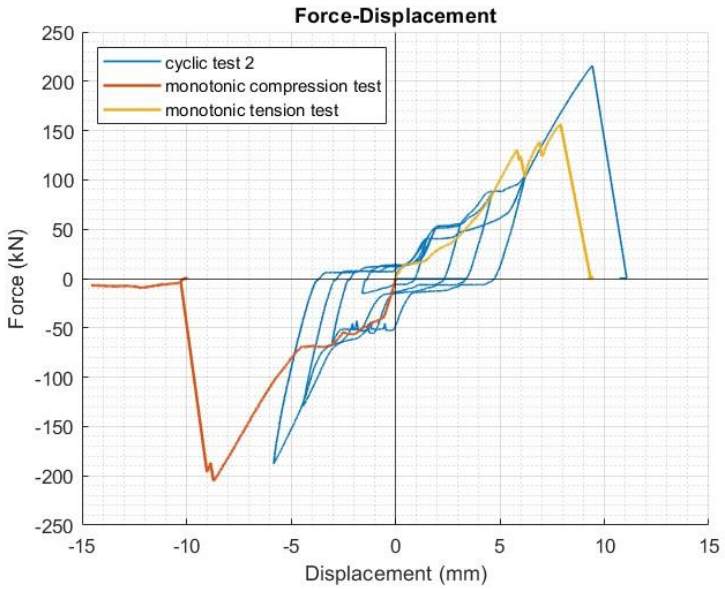

Figure 110. Detail 3.2 cyclic test 2 results

The results of the second cyclic test on Detail 3.2, in terms of force-displacement curve, are shown in Figure 110. The failure of the specimen occurred on the reloading at the first cycle to $2e_y$, as for the first cyclic test. Besides the brittle nature of the detail, a small hysteretic behaviour can be observed. Pinching, owing to the bolt-hole clearance, is also clearly visible from Figure 110. It is worth noting that, also in this case, the design force of 180 kN was reached in the tension, whilst it was not reached in the monotonic tension test. This was due to the higher imperfections of this detail. In fact, the bolt-hole clearance effect was not high enough to significantly affect the maximum force capacity relative to the cyclic behaviour in tension as for the monotonic tension test. The failure involved the collapse of all the six aluminium bolts located on the lower part of the specimen, while the tension test was characterized by a progressive failure of the aluminium bolts. In the compression part, the pinching effect was lower than in the monotonic test and higher force levels were observed for smaller displacements.

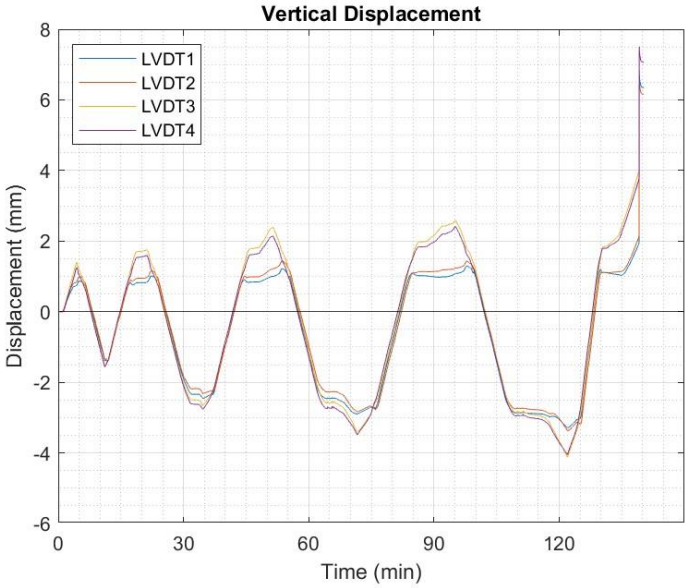

Figure 111. Detail 3.2 cyclic test 2 LVDTs results.

The vertical displacement acquisitions are reported in Figure 111. The graph shows some asymmetric behaviour due to the imperfections of the specimen.

Considering the strain gauges installed on the steel parts close to the aluminium bolts, the results are reported in Figure 112 to Figure 114. The general trend of the instruments agrees with the test with some exceptions that are mainly due to the malfunctioning of the instruments. The local strain levels did not exceed the actual steel yield limit of 1710 με, highlighting that significant bearing effects were not detected.

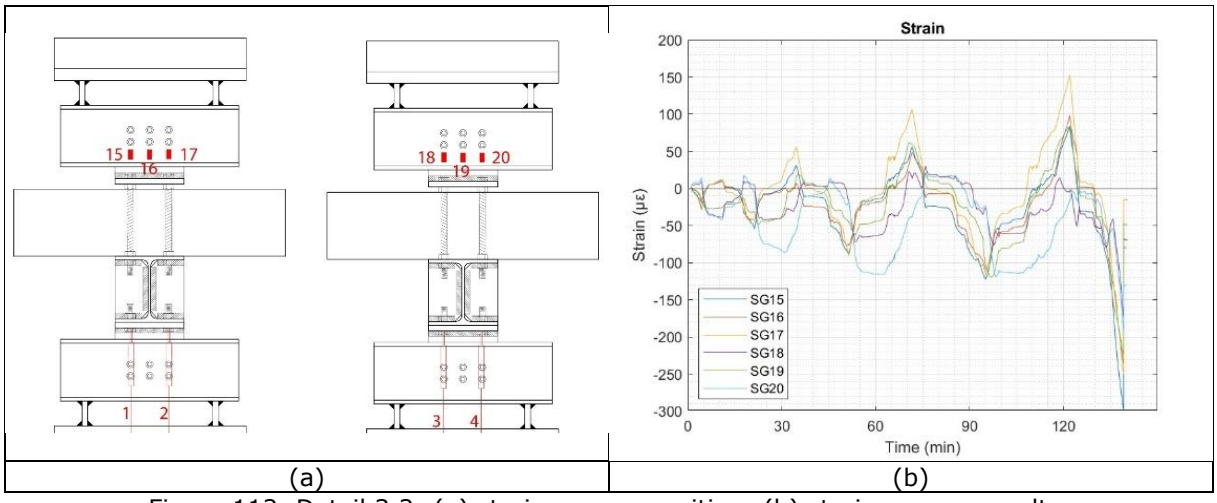

(a) (b)

Figure 112. Detail 3.2: (a) strain gauges position; (b) starin gauges results.

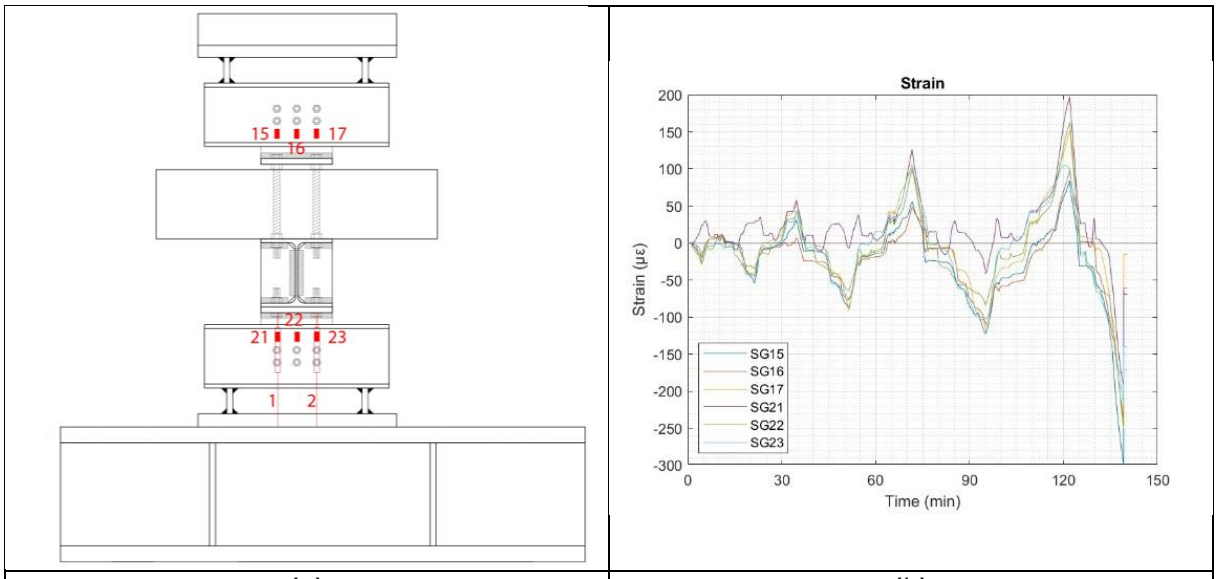

(a) (b)

Figure 113. Detail 3.2: (a) strain gauges position; (b) starin gauges results.

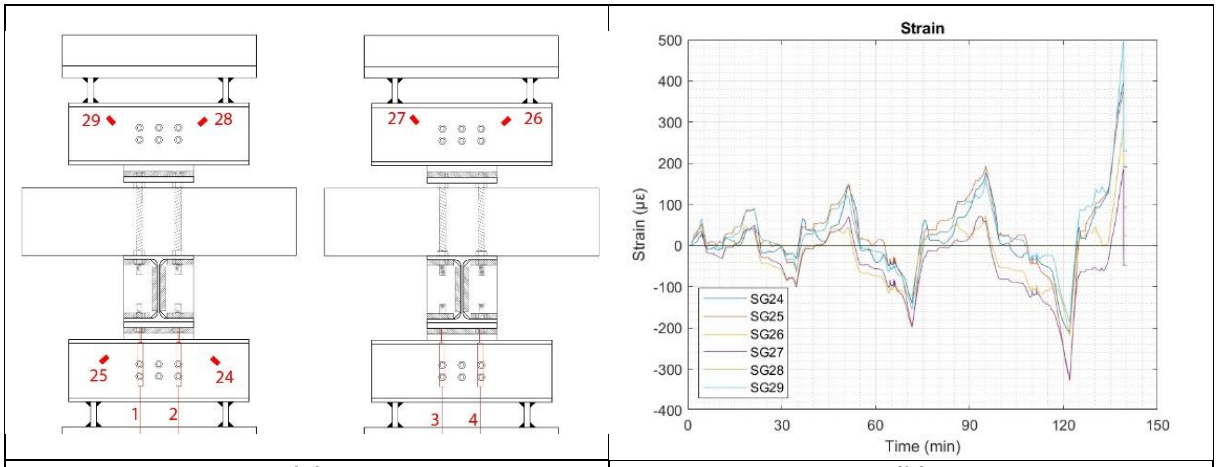

(a) (b)

Figure 114. Detail 3.2: (a) strain gauges position; (b) strain gauges results.

2.4.4 Summary

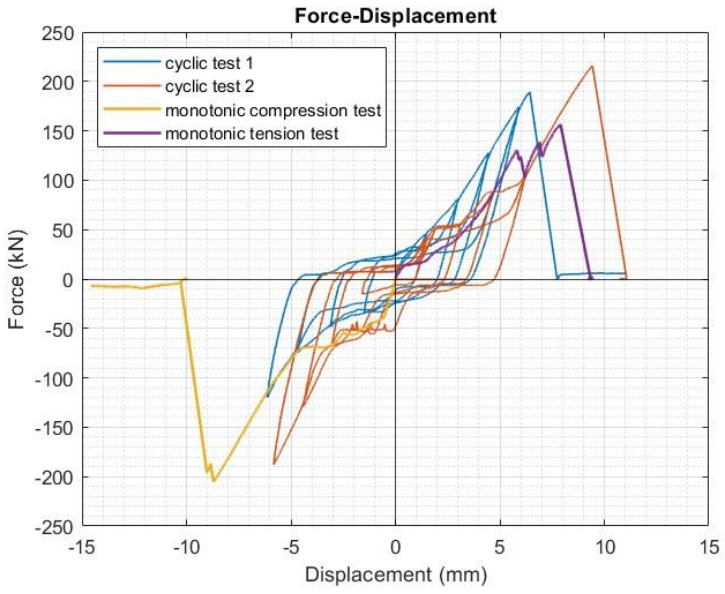

Figure 115. Detail 3.2 test results comparison

The comparison, in terms of force-displacement curve, of the four tests performed on Detail 3.2 is shown in Figure 115. With respect to Detail 3.1, Detail 3.2 exhibited more imperfections caused by a higher number of bolts. This entailed higher variability in terms of the response among the tests. In fact, Figure 115 shows some non-negligible difference between the cyclic tests in terms of both force and displacement. Significant pinching effects related to the bolt-hole clearances were observed. In particular, in the monotonic tension test the collapse was determined by progressive failure of some aluminium bolts, and the ultimate load was less than the design force, i.e. 180 kN. Instead, for the other tests the maximum capacity was higher than the design force as the collapse involved all 6 aluminium bolts. For that reason, it was decided to perform a third cyclic test on Detail 3.2.

2.4.4.1 Cyclic test 3

The third cyclic test on Detail 3.2 was repeated with the same testing protocol and instrumentation position as reported in Figure 109.

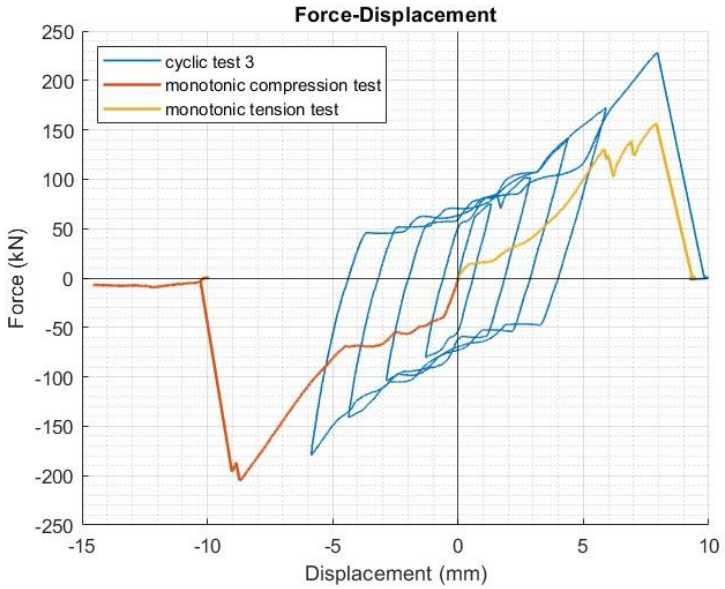

Figure 116. Detail 3.2 cyclic test 3 results

In this case the assembly of the specimen was conducted with the aim to centre the aluminium bolts to reduce the effect of the imperfections on the response. In this regard, a specific procedure was followed. Once the specimen was under the actuator, instead of positioning the aluminium bolts, the components of the detail were aligned using calibrated pins, that fills the hole with clearance of about 0.2 mm. Completed the alignment phase one pin at a time was replaced with the aluminium bolts. In that way, the holes of the six steel elements were aligned.

The results of the third cyclic test on Detail 3.2, in terms of force-displacement curve, are shown in Figure 116 and Figure 117. The failure of the specimen occurred on the reloading at the first cycle to $2e_y$, as for the other cyclic tests. Besides the brittle nature of the detail, larger hysteretic behaviour with respect to the other cyclic tests can be observed. The design force of 180 kN was reached in the tension with the collapse of all the six aluminium bolts located on the lower part of the specimen at the same displacement of the monotonic tension test. Moreover, because of a better bolt alignment, higher values of force and less pinching effects were observed. The procedure used to assembly this specimen is not applicable for structural applications because time consuming.

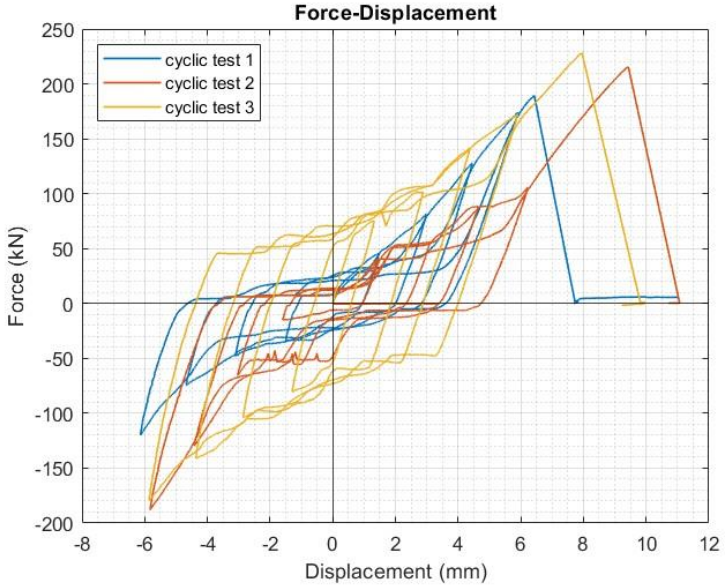

Figure 117. Detail 3.2 cyclic test comparison

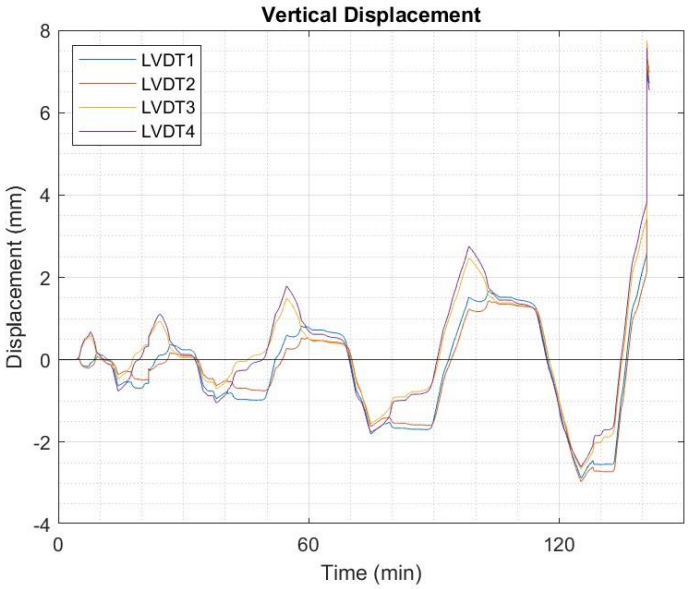

Figure 118. Detail 3.2 cyclic test 3 LVDTs results.

The vertical displacement acquisitions are reported in Figure 118. The graph showed a consistent symmetry of displacement during the tests with some differences owing to the specimen imperfections.

Considering the strain gauges installed on the steel parts close to the aluminium bolts, the results are reported in Figure 119 to Figure 121. The general trend of the instruments agrees with the test with some exceptions that are mainly due to the malfunctioning of the instruments. The local strain levels did not exceed the actual steel yield limit 1710 με, highlighting that significant bearing effects were not detected.

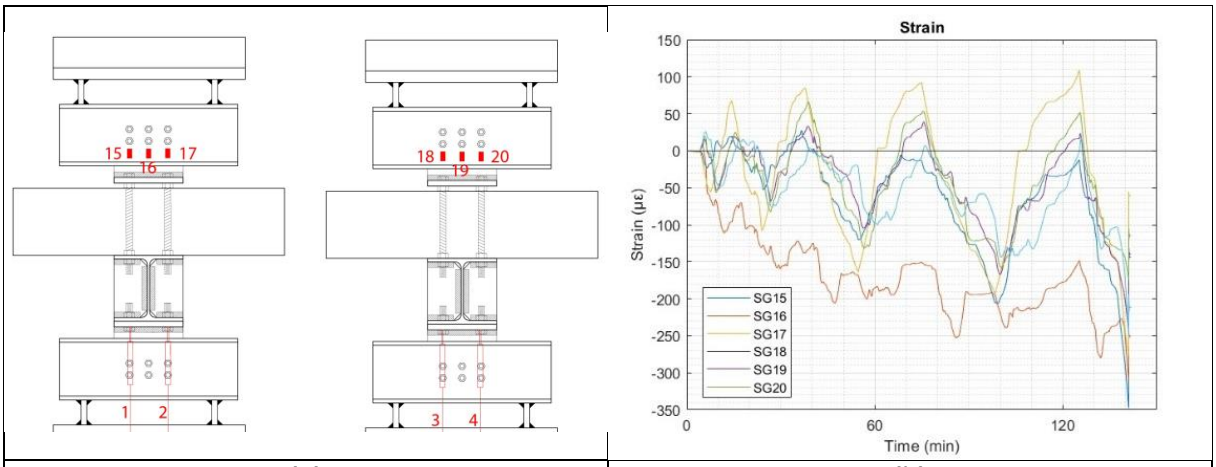

(a) (b)

Figure 119. Detail 3.2: (a) strain gauges position; (b) strain gauges results.

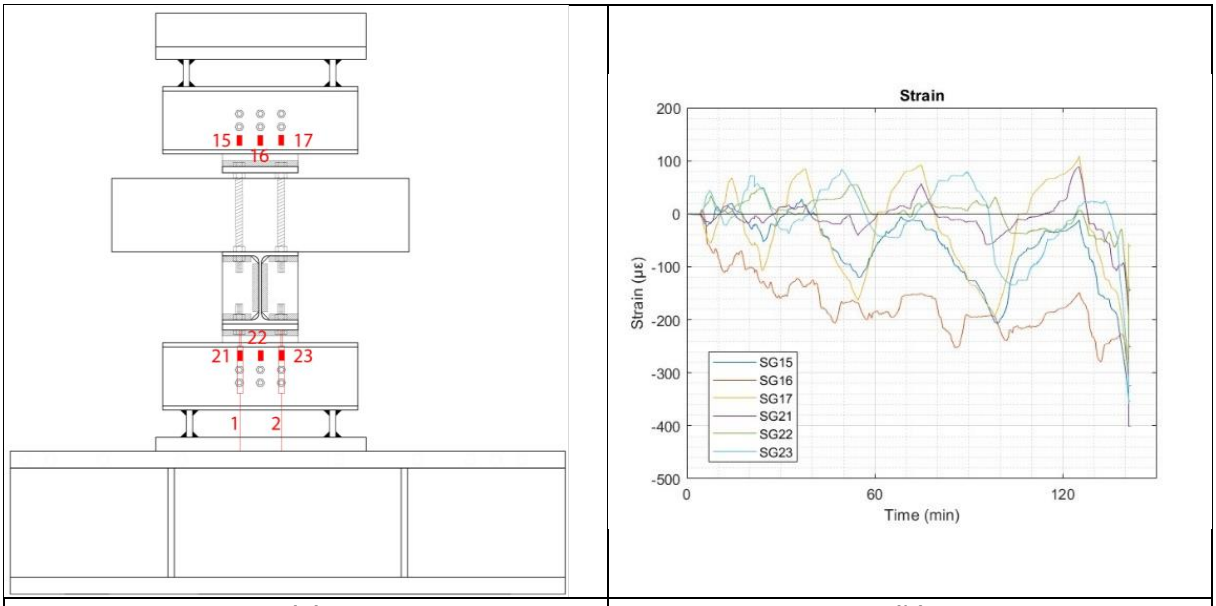

(a) (b)

Figure 120. Detail 3.2: (a) strain gauges position; (b) strain gauges results.

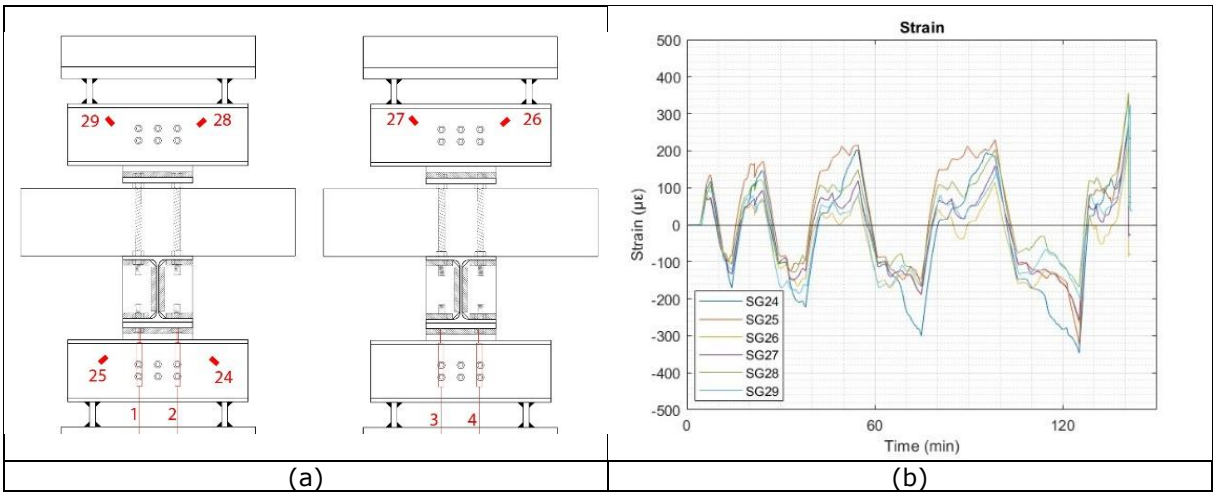

(a) (b)

Figure 121. Detail 3.2: (a) strain gauges position; (b) strain gauges results.

In conclusion, Table 16 summarizes the maximum experimental forces reached by each test at the first failure of an aluminium bolt, in comparison with the design force, in Figure 122 some specimens photos, after the tests, can be observed and in Figure 123 the aluminium bolts after the tests are shown.

Table 16. Failure forces reached during the tests.

Detail 3.2	Design force	Maximum experimental
Monotonic tension test	180 kN	130.2 kN
Monotonic compression test	180 kN	205.2 kN
Cyclic test 1	180 kN	189.3 kN
Cyclic test 2	180 kN	215.4 kN
Cyclic test 3	180 kN	228.2 kN

(a) (b) (c)

Figure 122. Detail 3.2 at failure: (a) frontal view of aluminium bolts under tension force; (b) frontal view of aluminium bolts under compression force; (c) movement between UPN160 elements and T plate elements after cyclic test.

(a) (b)

(c) (d) (e)

Figure 123. Detail 3.2 aluminium bolts at failure: (a) tension test; (b) compression test; (c) cyclic test 1; (d) cyclic test 2; (e) cyclic test 3.

2.5 Tests on Detail 4

As reported in Deliverable D1.4 [1], all the details were developed from 3 reference fusible link solutions common to all the project partners.

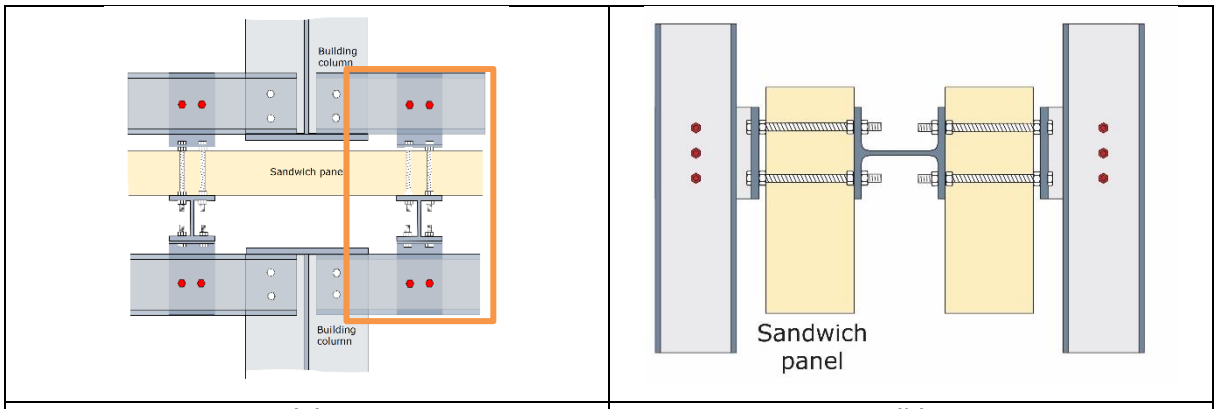

(a) (b)

Figure 124. Detail 4: (a) reference detail, (b) Detail 4 for seismic tests.

Figure 124 reports Detail 4 and the reference fusible link solution from which it was derived. As can be noticed, the original detail was modified. In fact, only one side of it was kept, it was rotated by 90 degrees and two sandwich panels were added to have a symmetric specimen, as shown in Figure 124b. The panel was added to better characterized its influence on the response of the fusible link connection. Six M12 aluminium bolts working on 2 shear planes were involved to withstand the design force equal to 180 kN.

Figure 125 and Table 17 report the main characteristics of Detail 4 in terms of elements and geometry that compose the specimen. As reported in Table 1, it was designed for a shear value of 180 kN, that can be withstood by 6 M12 aluminium bolts working on two shear planes.

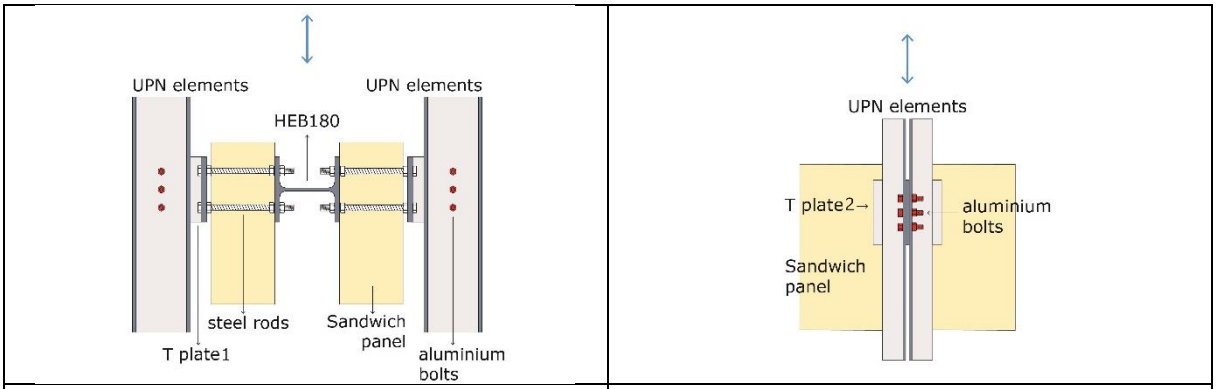

(a) (b)

Figure 125. Detail 4: (a) front view; (b) lateral view.

Table 17: Detail 4 description

Elements	Main characteristics
UPN elements	4 UPN 160
Aluminium bolts	6 M12 AlZn5,5MgCu 7075
Steel rods	8 M20 10.9
T Plate 1 – web	2 190x180x10
T plate 2 -flange	2 190x180x15

2.5.1 Monotonic tension test

Figure 126. View of the detail 4 test set-up

In Figure 126 the specimen of Detail 4 inserted in the reaction frame can be observed. Some additional steel elements were inserted to support the instrumentation.

In Figure 127 and Figure 128, the specific instrumentation position and numbering are reported.

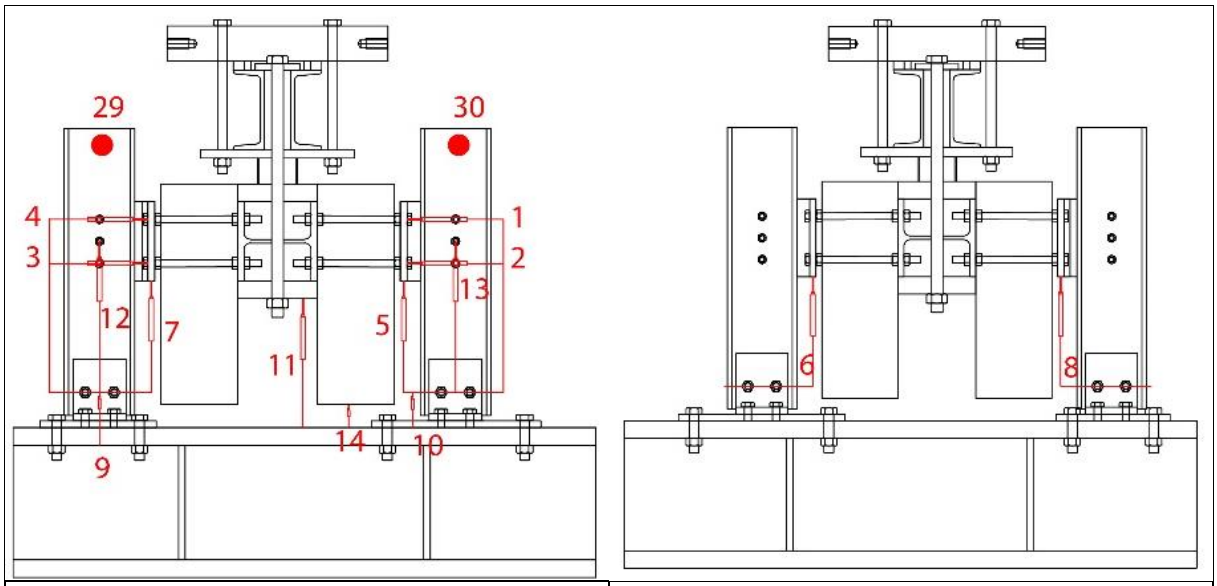

(a) (b)

Figure 127. LVDTs and inclinometers position on Detail 4: (a) front side; (b) back side.

The displacement LVDT transducers were located to check specific detail movements:

- LVDT 1 - LVDT 4 to check the possible rotation of the T plate elements;
- LVDT5, LVDT6, LVDT7 e LVDT8 to check the possible rotation of the T plate elements and to check their vertical displacement;
- LVDT9 e LVDT10 to record a possible displacement of the base beam;
- LVDT11 to check a possible difference between the actuator displacement and the H element;
- LVDT12 e LVDT13 to check the aluminium bolt vertical displacement;
- LVDT14 to check its vertical displacement of the sandwich panel.

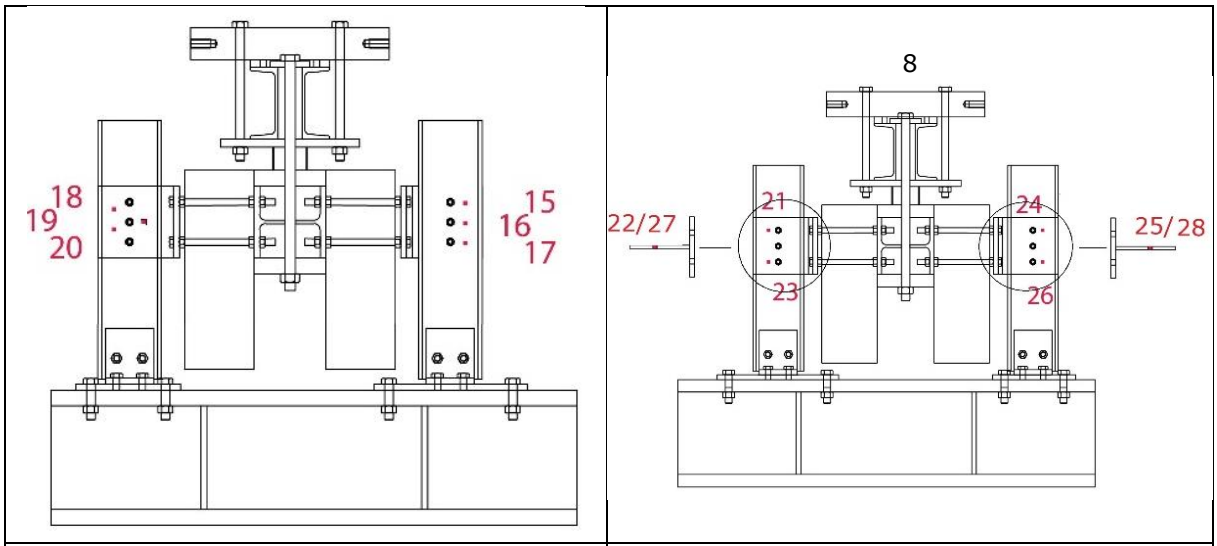

(a) (b)

Figure 128. Detail 4 - strain gauges position: (a) on front side; (b) on back side.

A total of 14 strain gauges were glued on the steel UPN elements:

- From number 15 to 21 plus 23, 24, and 26 were placed to check the horizontal strains;
- Numbers 22, 25, 27 and 28 were located on the T elements to check bending actions on T elements.

The instruments acquisitions were recorded at 2 Hz.

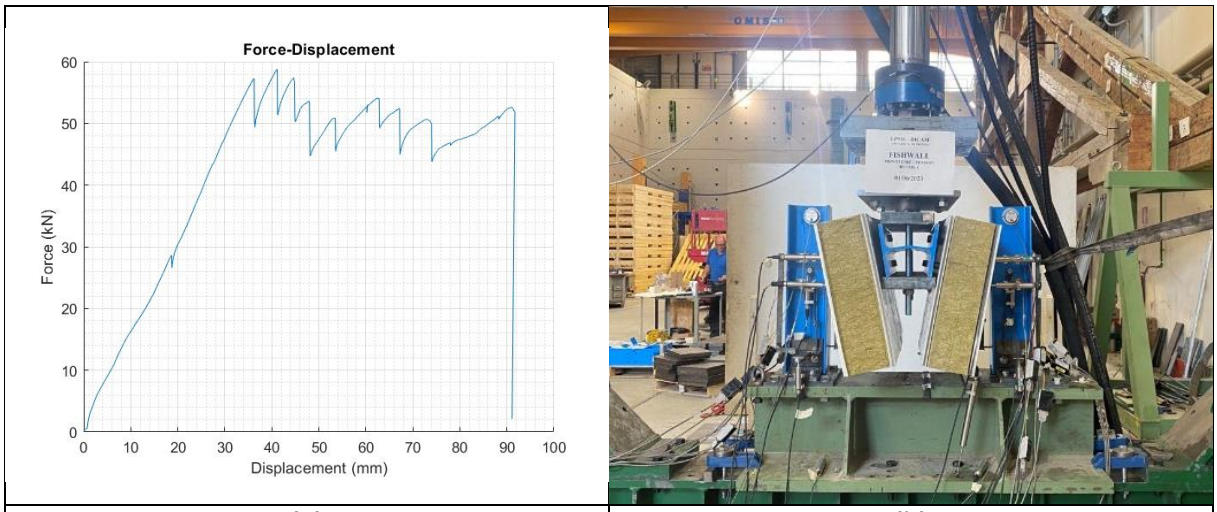

(a) (b)

Figure 129. Detail 4: (a) force-displacement curve of the monotonic tension test and (b) final specimen deformation.

Figure 129 shows the result in terms of the force-displacement curve. As can be noticed, many peaks characterized the curve. In fact, each peak corresponds to the failure of one or more shear planes that occurred during the test. Indeed 9 peaks can be observed of 12 shear planes present on the specimen. As a consequence, the design force of 180 kN was not reached. The main reason was the specimen configuration that induced large rotations of the panels owing to flexural deformation of the steel rods, causing additional moments on the aluminium bolt group that entailed additional horizontal shear forces. As a result, the top and the bottom bolts were more stressed than expected and failed before reaching the design strength of the detail.

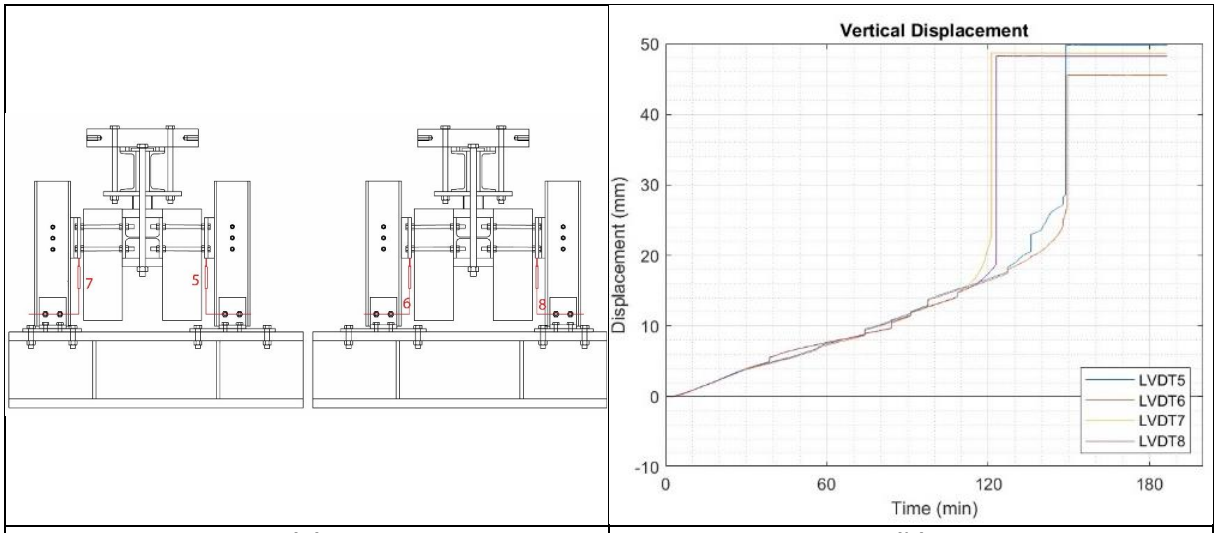

(a) (b)

Figure 130. Detail 4: LVDTs: (a) position;(b) vertical displacement measurements.

The vertical displacement recorded by the instruments in Figure 130a is reported in Figure 130b. The acquisitions highlighted a symmetrical behaviour of the specimen until the instruments lost their contact with the steel elements due to the large deformations occurred during the test.

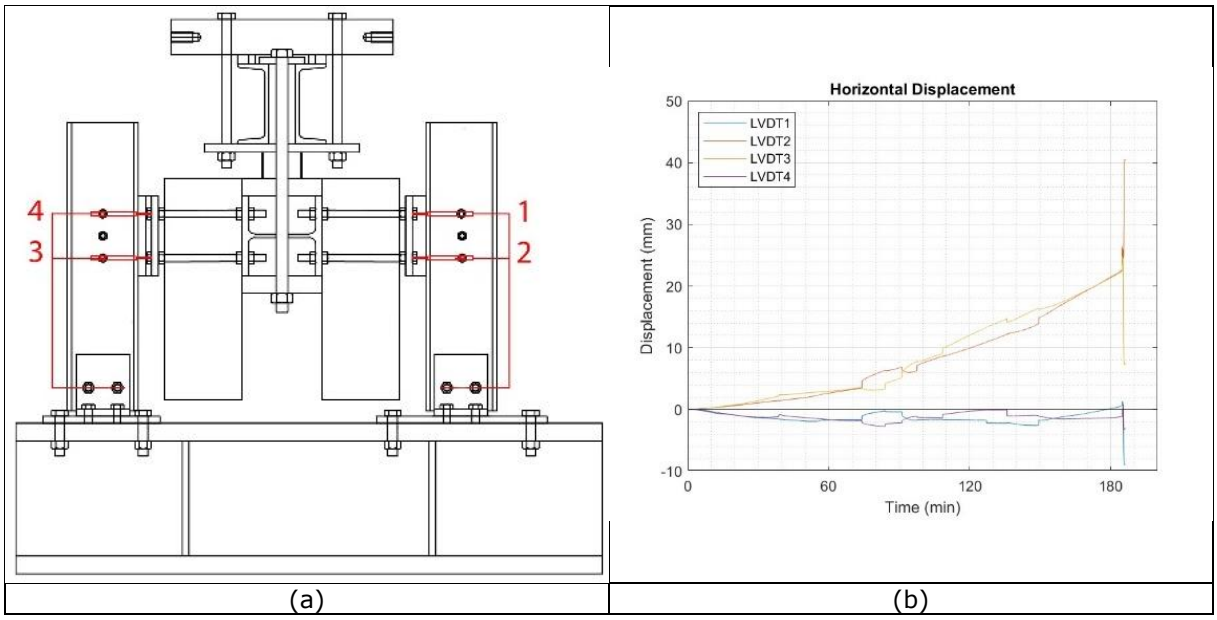

(a) (b)

Figure 131. Detail 4: LVDTs: (a) position;(b) horizontal displacement measurements.

The test results, in terms of horizontal displacement detected by LVDTs positioned on the specimen, are shown in Figure 131. The opposite sign of the acquisitions of the upper and the lower instruments was consistent with the rotation of the T element. They showed an initial symmetrical behaviour until the failure of the first external bolts that caused asymmetric rotations of the specimen.

Considering the strain gauges installed on the steel part close to the aluminium bolts, the results are here after reported. Figure 132 reports the strain gauges acquisition on the T steel elements. The instruments trend is symmetrical between the top and bottom instruments. The opposite sign recorded by the strain gauges is consistent with the global deformation. In fact, due to the rotation of the sandwich panels caused by flexural deformation of the steel rods, the T-elements rotated inducing a compression on the top strain gauges and a tension of the bottom ones. Figure 133 and Figure 134 show strain readings that are consistent with the global specimen deformation. The local strain levels did not exceed the actual steel yield limit of 1710 με, highlighting that significant bearing effects were not detected.

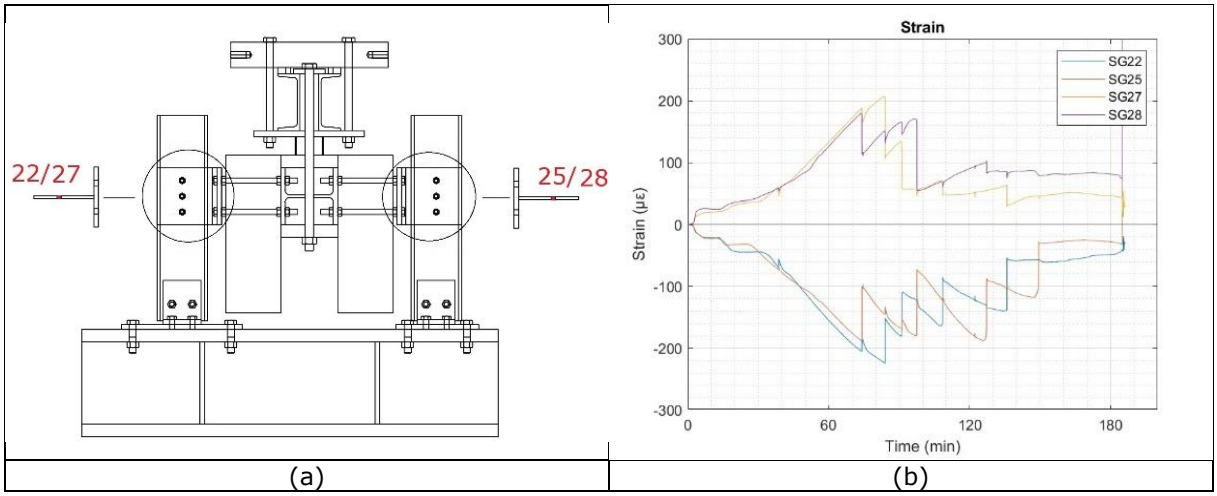

(a) (b)

Figure 132. Detail 4: (a) strain gauges position; (b) stran gauges results.

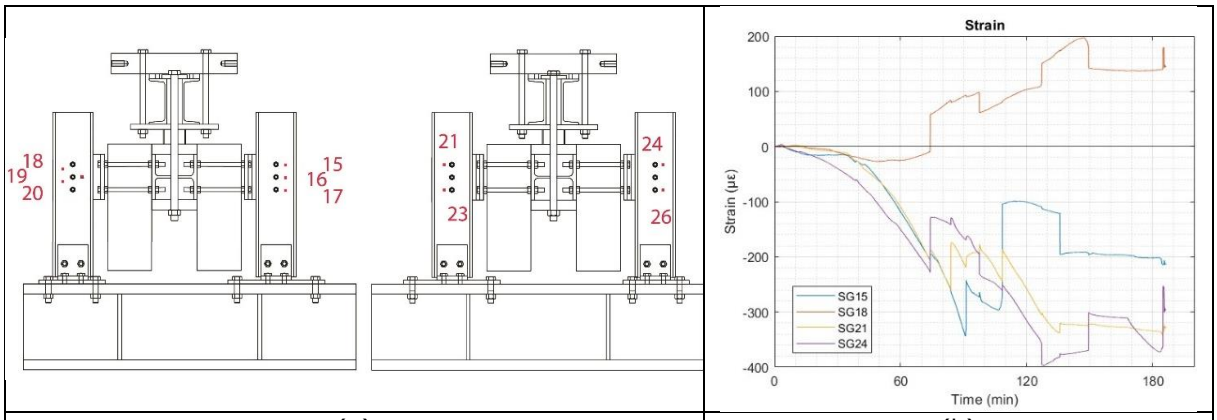

(a) (b)

Figure 133. Detail 4: (a) strain gauges position; (b) strain gauges results.

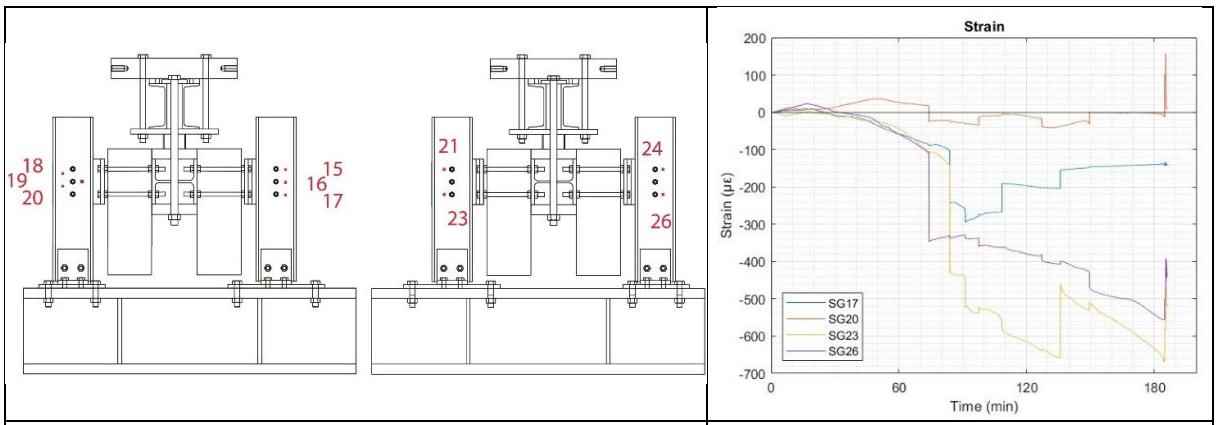

(a) (b)

Figure 134. Detail 4: (a) strain gauges position; (b) strain gauges results.

2.5.2 Monotonic compression test

In Figure 135 and in Figure 136, the specific instrumentation position and numbering are reported. The LVDTs were used to observe the displacements. Also in this case, 14 strain gauges were located on the specimen. The instrument acquisitions were recorded at 2 Hz.

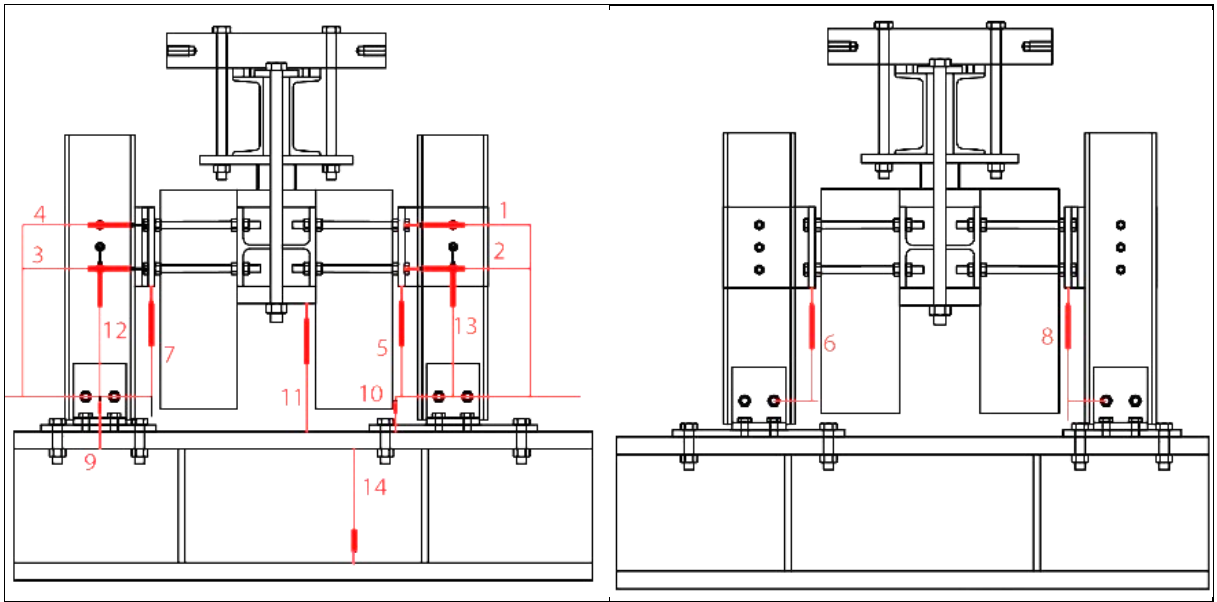

(a) (b)

Figure 135. Detail 4: - LVDTs position: (a) on front side; (b) on back side.

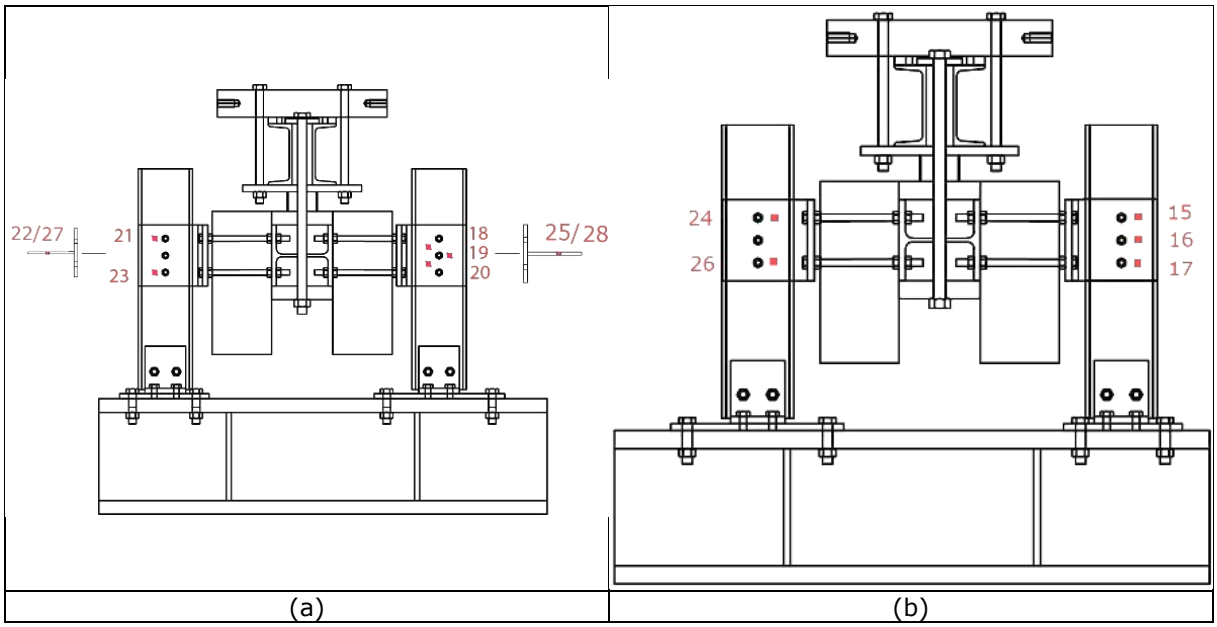

(a) (b)

Figure 136. Detail 4 - strain gauges position: (a) on front side; (b) on back side.

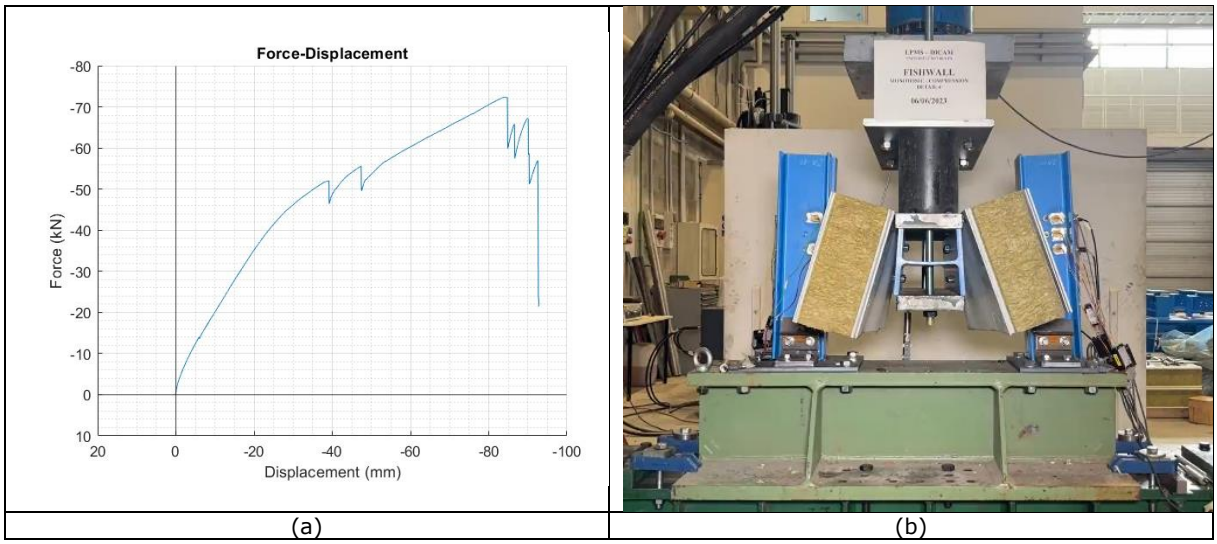

(a) (b)

Figure 137. Detail 4: (a) force-displacement curve of the monotonic compression test; (b) final specimen deformation.

In Figure 137, the result in terms of the force-displacement diagram is shown. As can be noticed, also in this case, many peaks characterized the curve. Each peak corresponds to the failure of one or many shear planes that occurred during the test. Indeed 6 peaks can be observed of 12 shear planes present on the specimen. At the end of the test, 8 shear planes actually failed, while 2 bolts did not fail. The design force of 180 kN was not reached. Again, similarly with the monotonic tension test, the main reason was the specimen configuration that induced large rotations of the panels owing to flexural deformation of the steel rods, causing additional moments on the aluminium bolt group that entailed additional horizontal shear forces. As a result, the top and the bottom bolts were more stressed than expected and failed before reaching the design strength of the detail. This behaviour is also confirmed by the LVTD and strain gauge measurements, as shown in Figure 138 to Figure 142. The local strain levels did not exceed the actual steel yield limit 1710 με, highlighting that significant bearing effects were not detected.

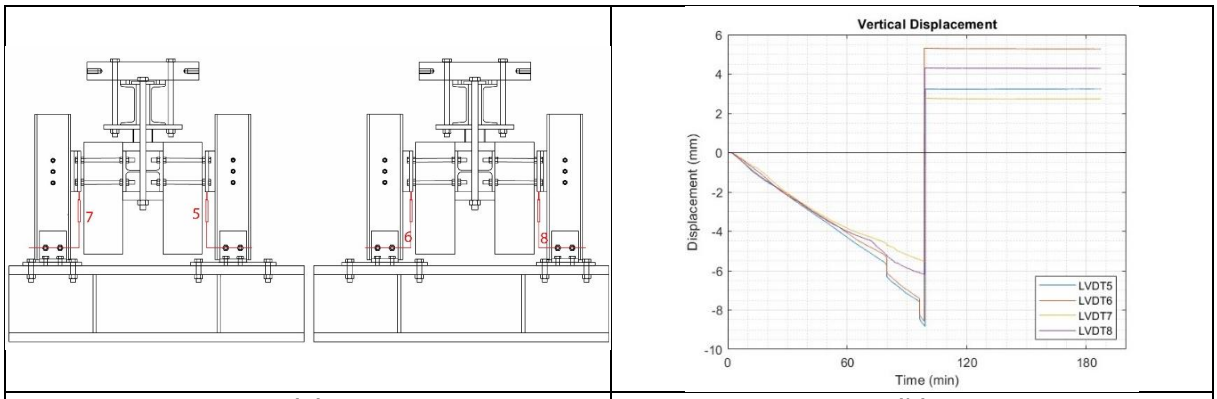

(a) (b)

Figure 138. Detail 4: LVDTs: (a) position;(b) vertical displacement measurements.

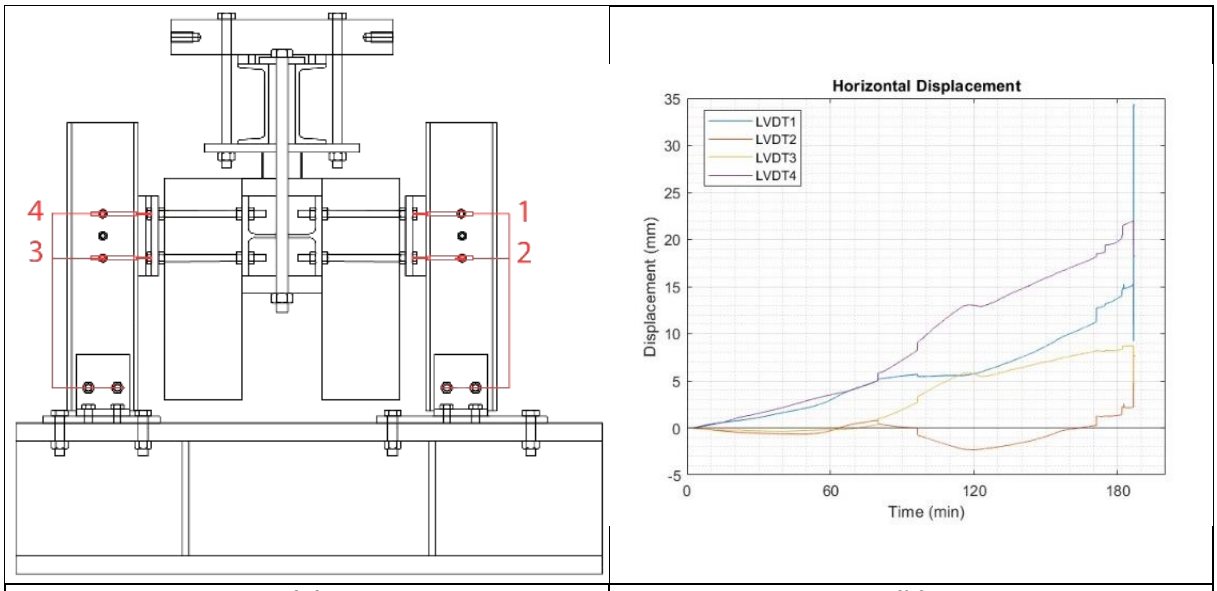

(a) (b)

Figure 139. Detail 4: LVDTs: (a) position;(b) horizontal displacement measurements.

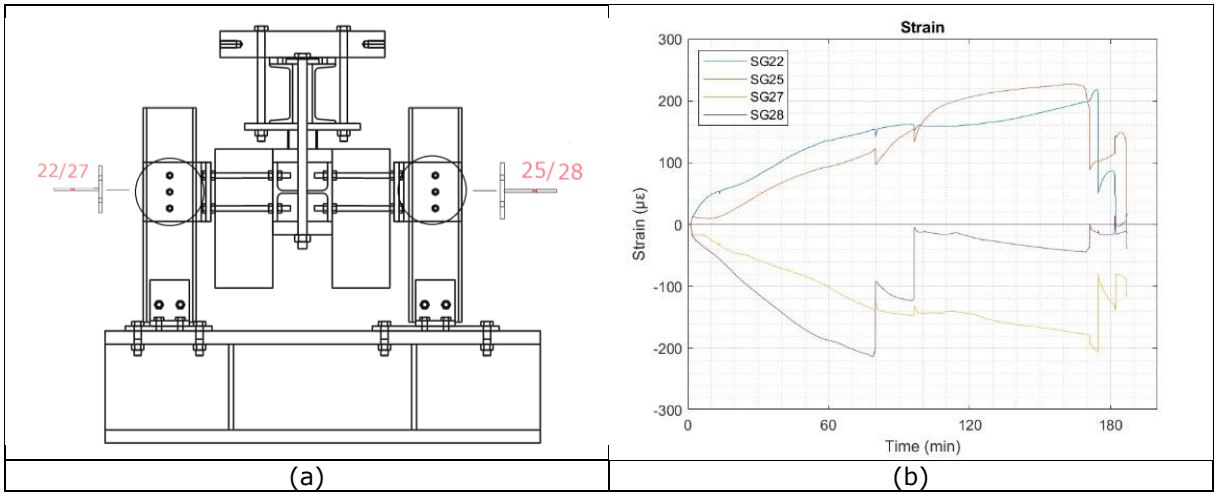

(a) (b)

Figure 140. Detail 4: (a) strain gauges position; (b) strain gauges results.

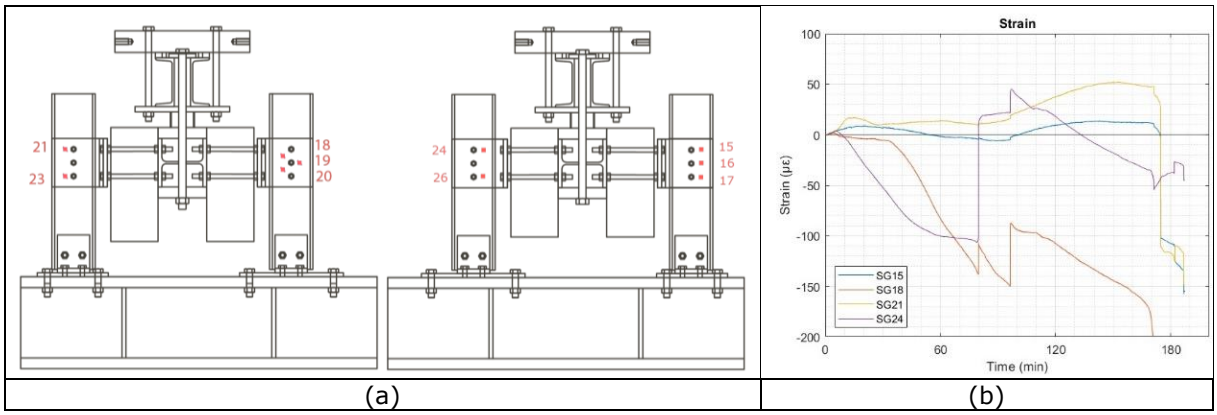

(a) (b)

Figure 141. Detail 4: (a) strain gauges position; (b) strain gauges results results.

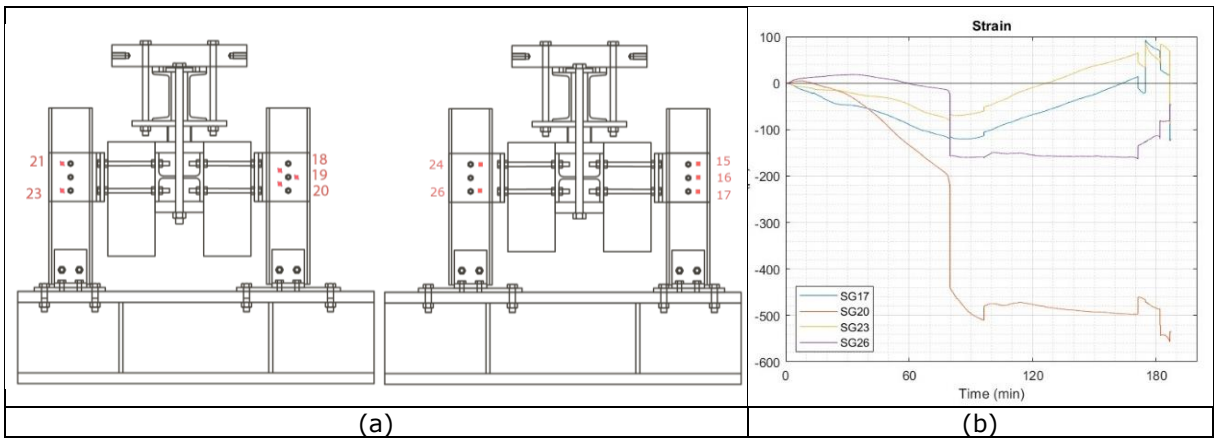

(a) (b)

Figure 142. Detail 4: (a) strain gauges position; (b) strain gauges results results.

2.5.3 Cyclic tests

In order to follow the ECCS procedure, as reported in Section 1.3, the two monotonic tests curves were used to define the yield displacement and the displacement history to carry out the cyclic tests.

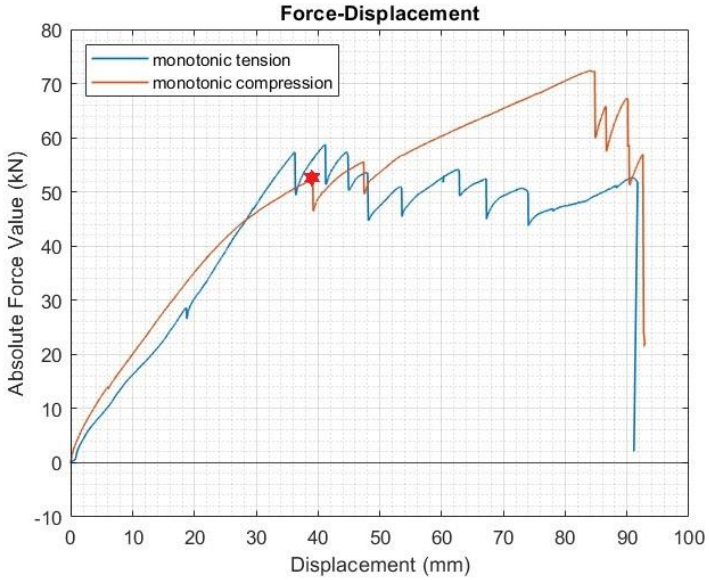

Figure 143. Detail 4 monotonic tests results

Figure 143 reports the comparison, in terms of force-displacement curves, between the monotonic tension and compression tests. The yield displacement for the cyclic test is reported in Table 18. Since the two curves were similar, the e_y was chosen at the first bolt failure in the monotonic compression test.

Table 18: Yield displacement from monotonic curves

e_y	39.3 mm
$-e_y$	39.3 mm

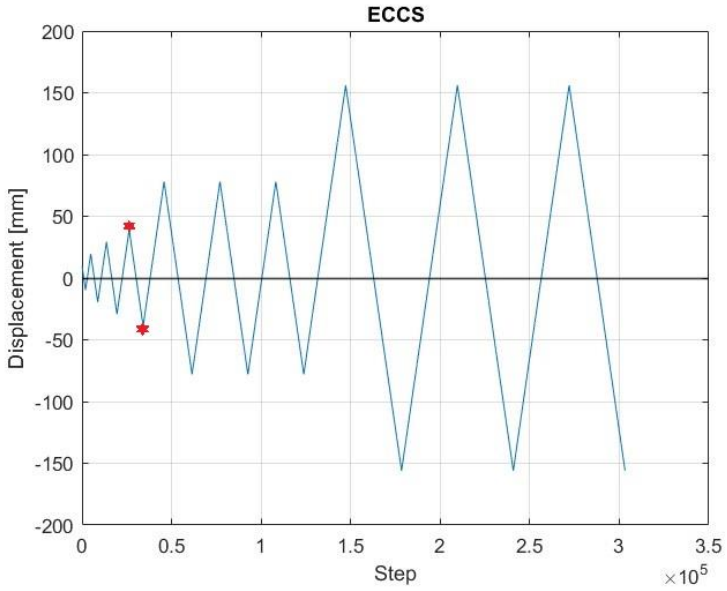

Figure 144. Detail 4 ECCS procedure.

As shown in Figure 144, the displacement history obtained is symmetric. The yield displacement previously introduced is highlighted in red.
The cyclic tests were conducted in displacement control with a displacement rate of 0.5 mm/min.

2.5.3.1 Cyclic test 1

In Figure 145 and in Figure 146, the specific instrumentation position and numbering are reported. In this case, 11 strain gauges were located on the steel UPN elements to measure the strain induced by the aluminium bolts during the test. The instruments acquisitions were recorded at 2 Hz.

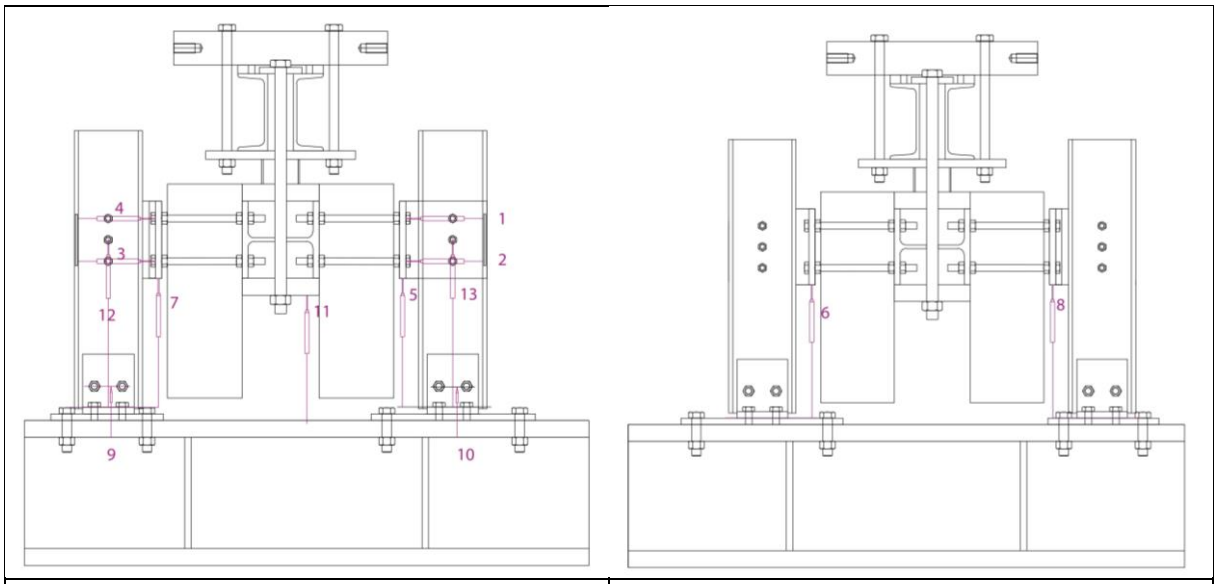

(a) (b)

Figure 145. Detail 4: (a) LVDTs on front side; (b) LVDTs on back side.

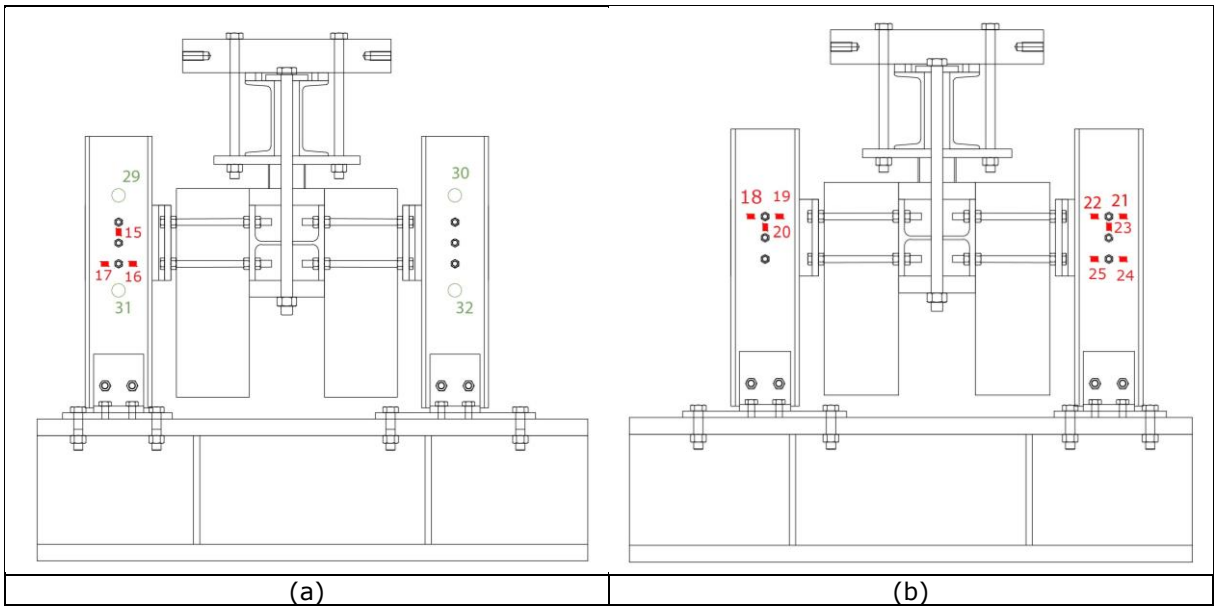

(a) (b)

Figure 146. Detail 4: (a) strain gauges on front side; (b) srain gauges on back side.

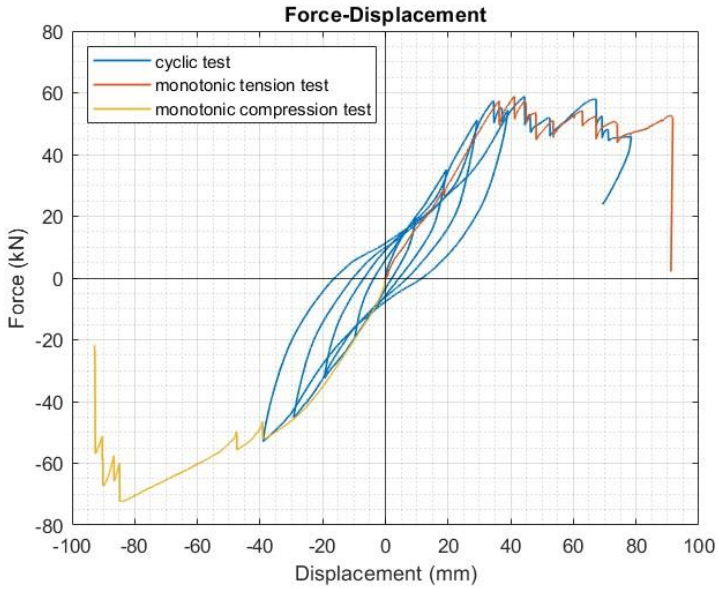

Figure 147. Detail 4 cyclic test 1 results

The results of the first cyclic test on Detail 4, in terms of force-displacement curve, are shown in Figure 147. The failure of the specimen occurred on the reloading at the first cycle to $2e_y$. Besides the brittle nature of the detail, a small hysteretic behaviour can be observed. It is worth noting that also during this test, the design force of 180 kN was not reached; as occurred during the monotonic tests, because of the additional shear forces on the aluminium bolts caused by the large rotations induced by the sandwich panels owing to flexural deformation of the steel rods. The comparison between the cyclic test and the monotonic tests shows a good agreement both in the tension and in the compression branch. The collapse of the specimen was determined by the progressive failure of one or many shear planes.

This behaviour is also confirmed by the LVTD and strain gauge measurements, as shown in Figure 148 to Figure 153. The local strain levels did not exceed the actual steel yield limit of 1710 με, highlighting that significant bearing effects were not detected.

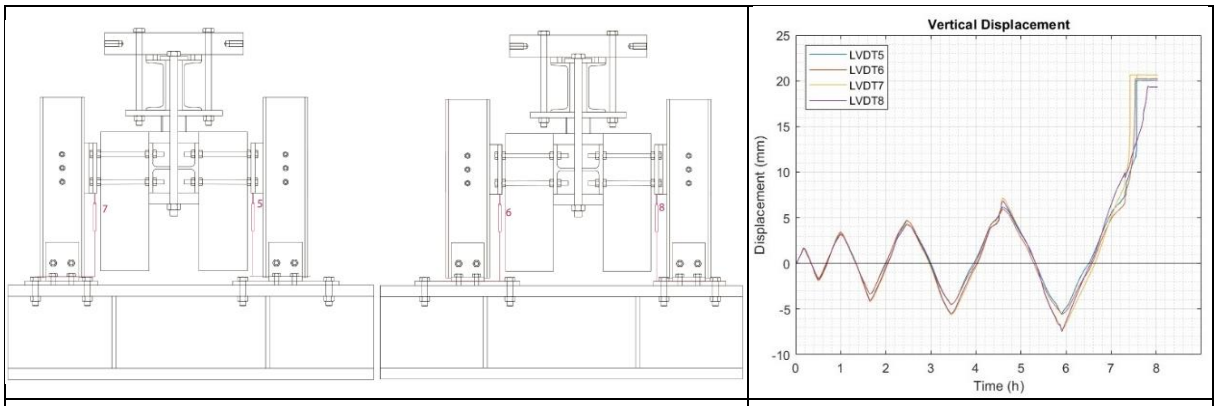

(a) (b)

Figure 148. Detail 4: LVDTs: (a) position;(b) vertical displacement recorded during cyclic test 1.

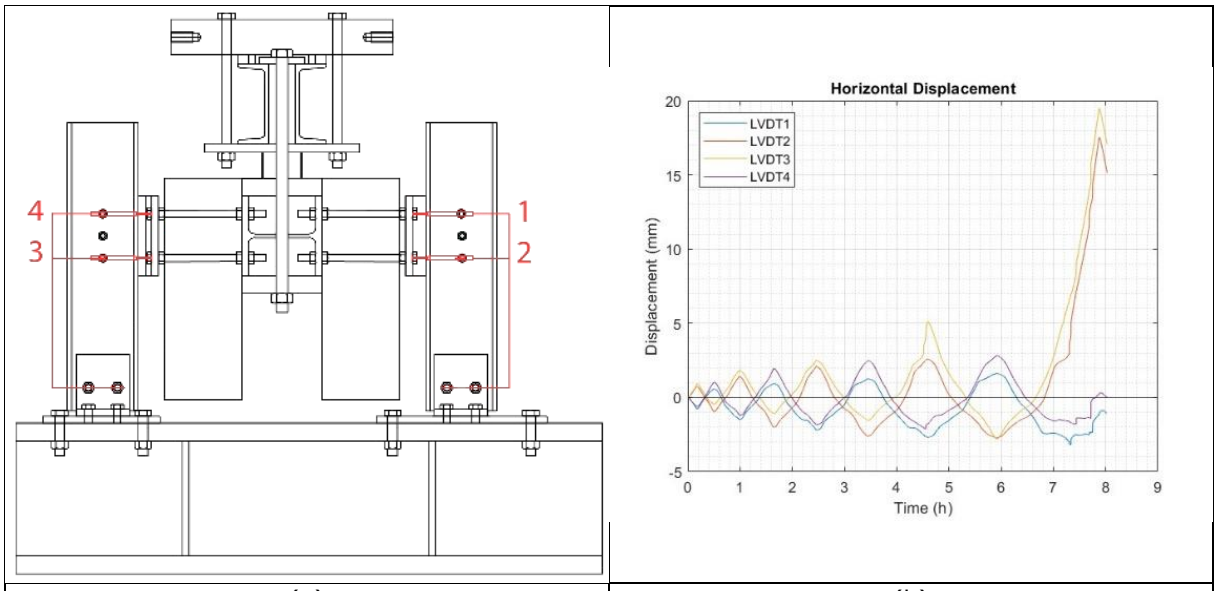

(a) (b)

Figure 149. Detail 4: LVDTs: (a) position;(b) horizontal displacement recorded during cyclic test 1.

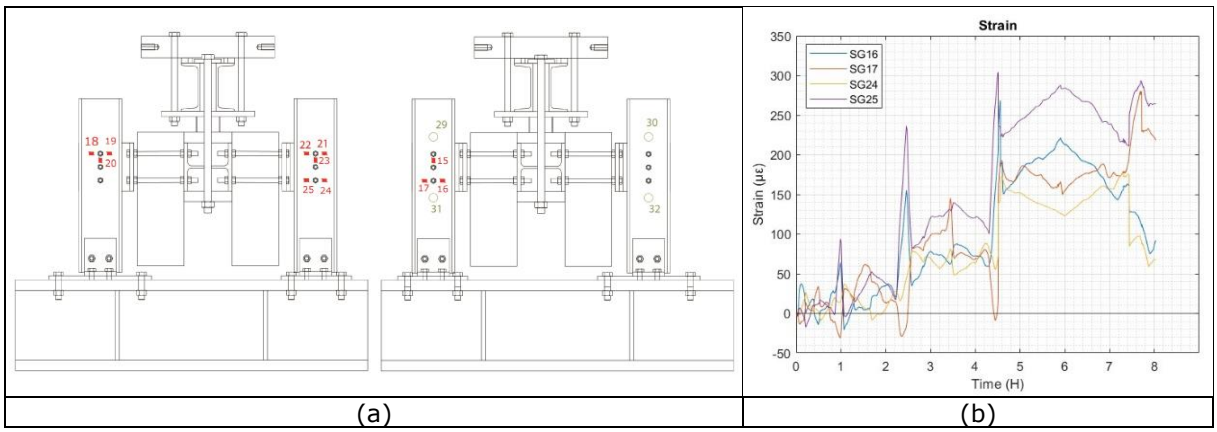

(a) (b)

Figure 150. Detail 4: (a) strain gauges results position; (b) strain gauges results.

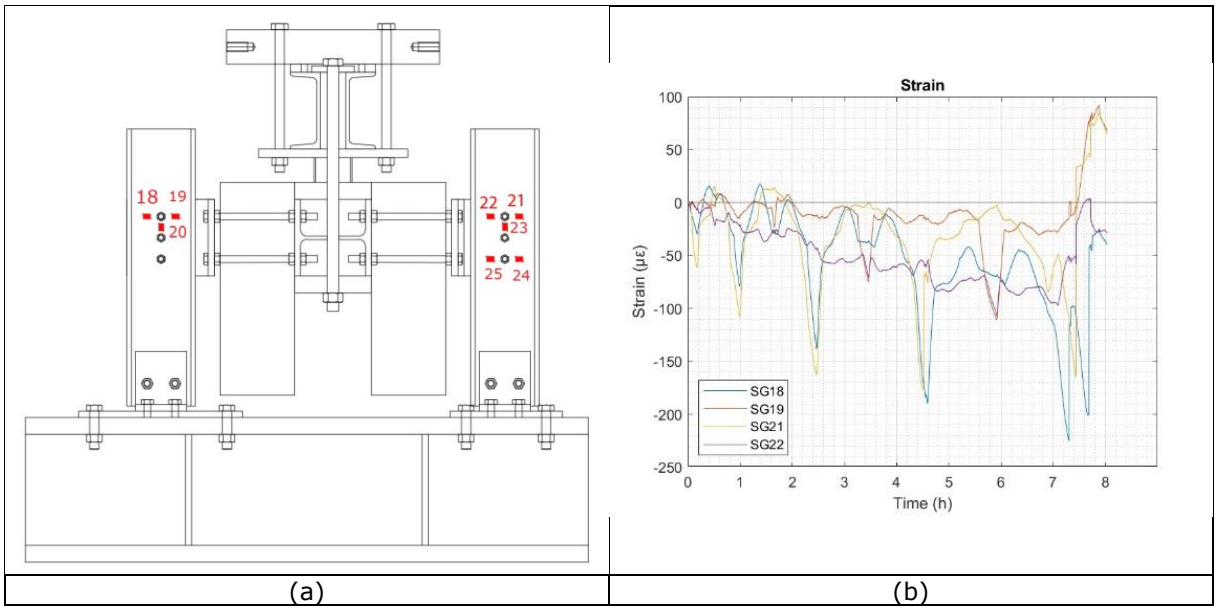

(a) (b)

Figure 151. Detail 4: (a) strain gauges position; (b) strain gauges results.

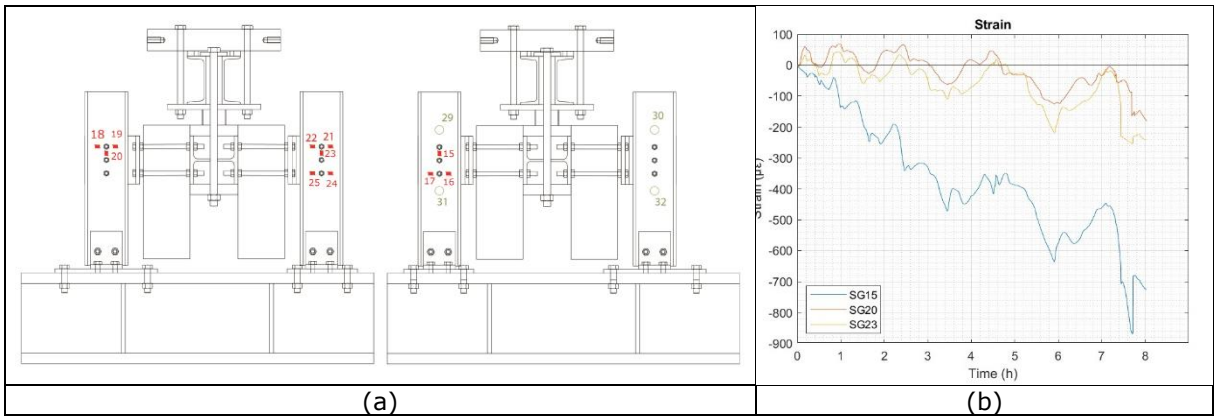

(a) (b)

Figure 152. Detail 4: (a) strain gauges position; (b) strain gauges results.

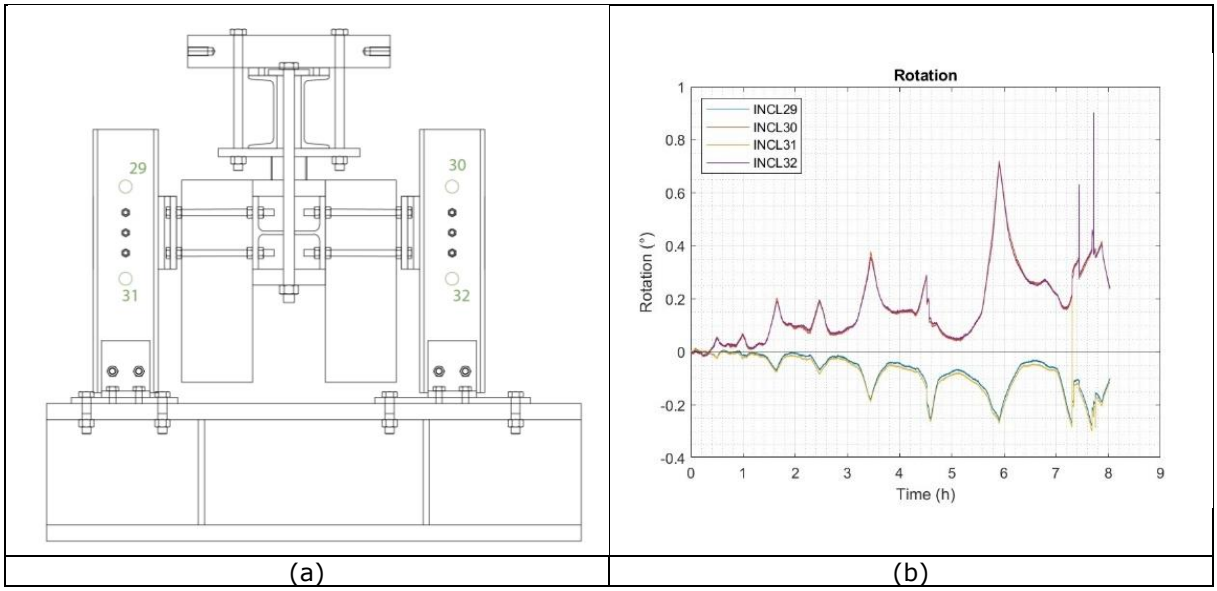

(a) (b)

Figure 153. Detail 4: (a) inclinometers position; (b) inclinometers results.

2.5.3.2 Cyclic test 2

In Figure 154 and in Figure 155 , the specific instrumentation position and numbering are reported. In this case, 14 strain gauges were located on the steel UPN elements to measure the strain induced by the aluminium bolts during the test. The instruments acquisitions were recorded at 2 Hz.

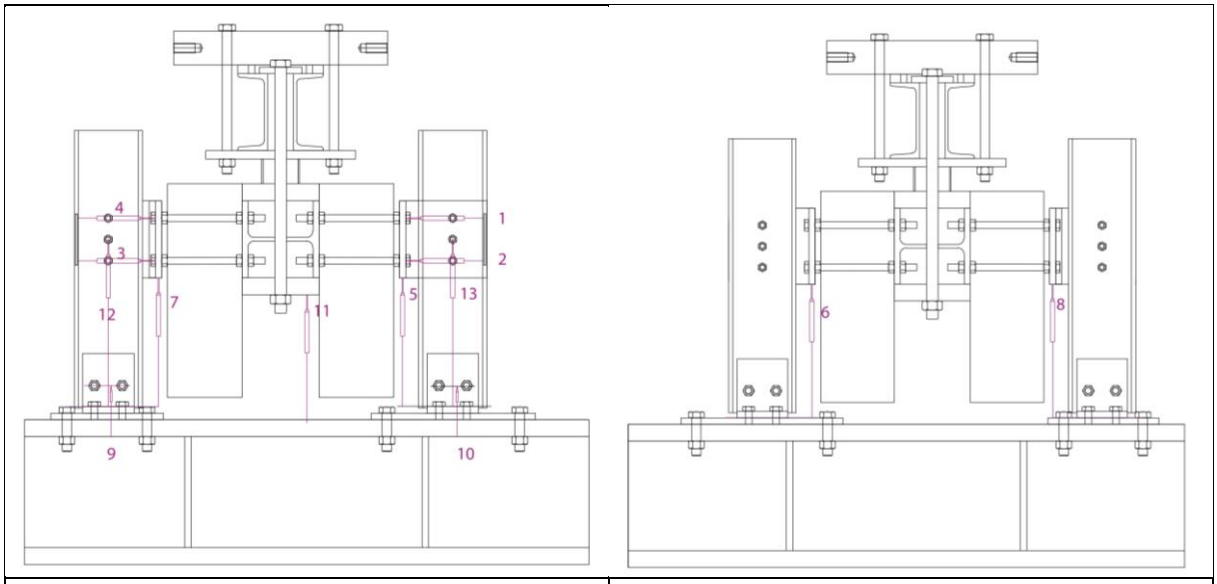

(a) (b)

Figure 154. Detail 4: (a) LVDTs on front side; (b) LVDTs on back side.

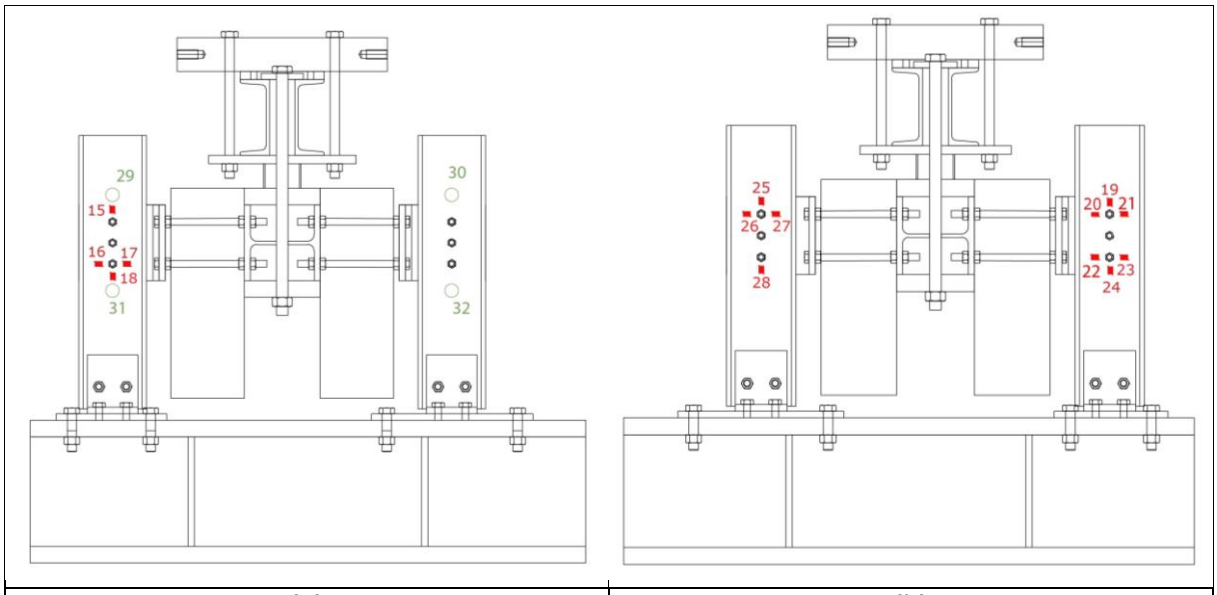

(a) (b)

Figure 155. Detail 4: (a) strain gauges on front side; (b) strain gauges on back side.

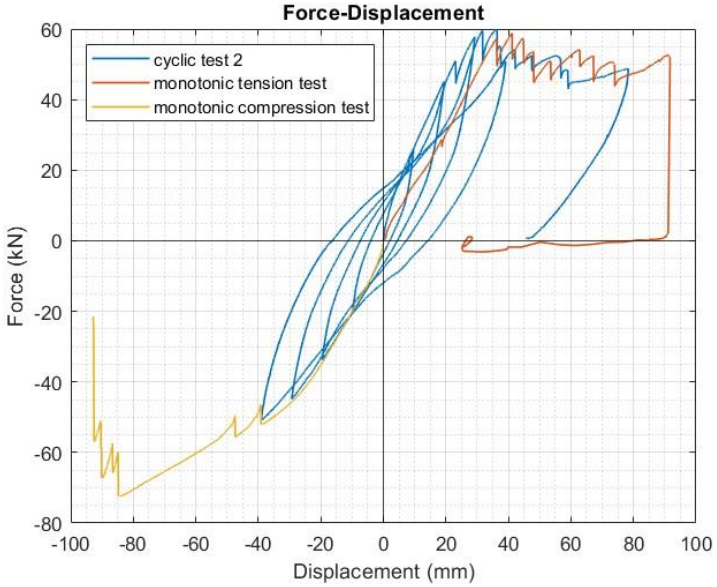

Figure 156. Detail 4 cyclic test 2 results

The results of the second cyclic test on Detail 4, in terms of force-displacement curve, are shown in Figure 156. The failure of the specimen occurred on the reloading at the first cycle to $2e_y$. Besides the brittle nature of the detail, a small hysteretic behaviour can be observed. It is worth noting that also during this test, the design force of 180 kN was not reached. As occurred in the monotonic tests and the first cyclic test, the large deformations induced by the sandwich panels, owing to the flexural behaviour of the steel rods, determined additional horizontal forces on the aluminium bolts that led to their progressive failure. The comparison between the cyclic test and the monotonic tests shows a general good agreement both in the tension and the compression branch. On the tension part the cyclic test was stiffer than the respective monotonic test. The collapse of the specimen was determined by the progressive failure of one or many shear planes.
This behaviour is also confirmed by the LVTD and strain gauge measurements, as shown in Figure 157 to Figure 163. The local strain levels did not exceed the actual steel yield limit of 1710 με, highlighting that significant bearing effects were not detected.

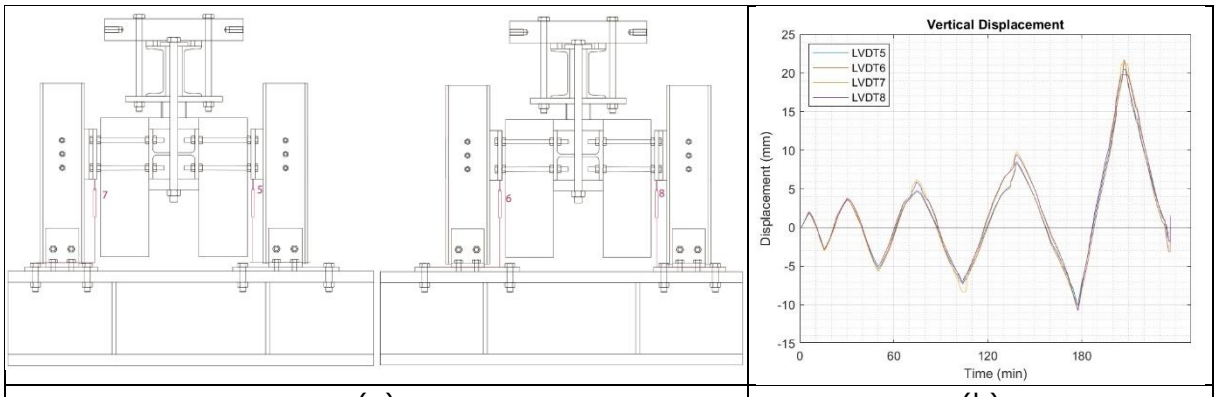

(a) (b)

Figure 157. Detail 4: LVDTs: (a) position;(b) vertical displacement recorded during cyclic test 2.

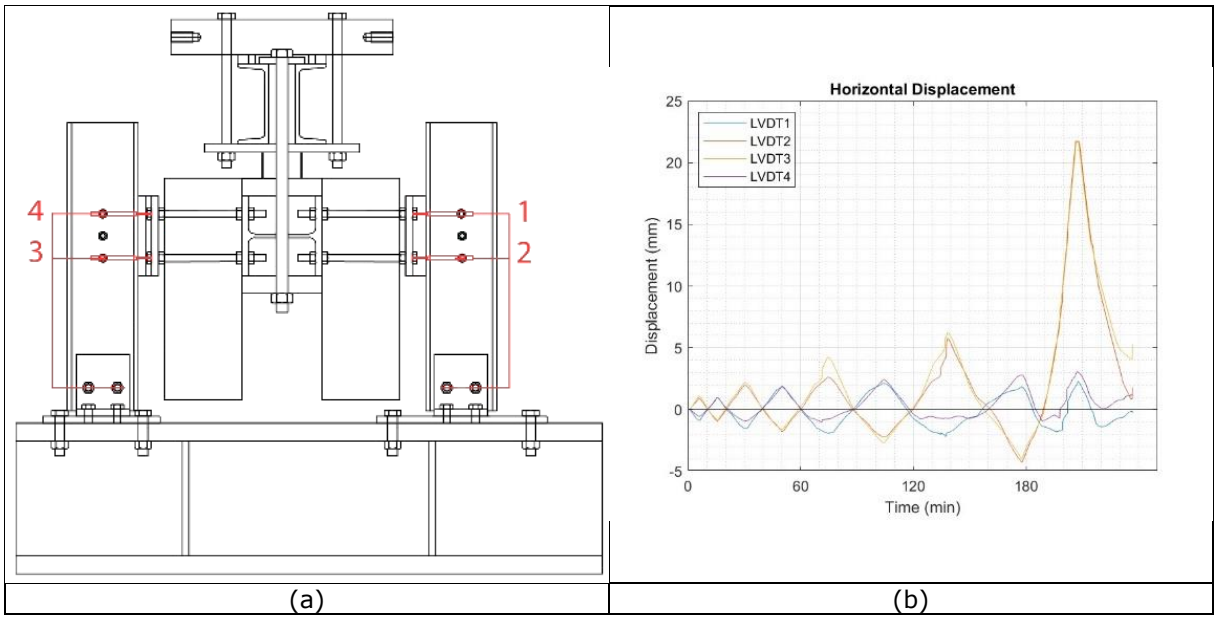

(a) (b)

Figure 158. Detail 4: LVDTs: (a) position;(b) horizontal displacement recorded during cyclic test 2.

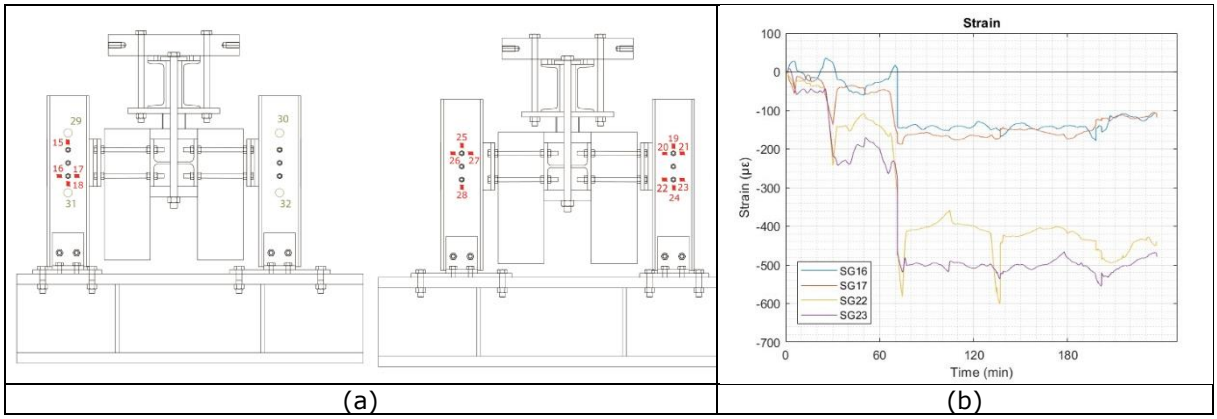

(a) (b)

Figure 159. Detail 4: (a) strain gauges position; (b) strain gauges results.

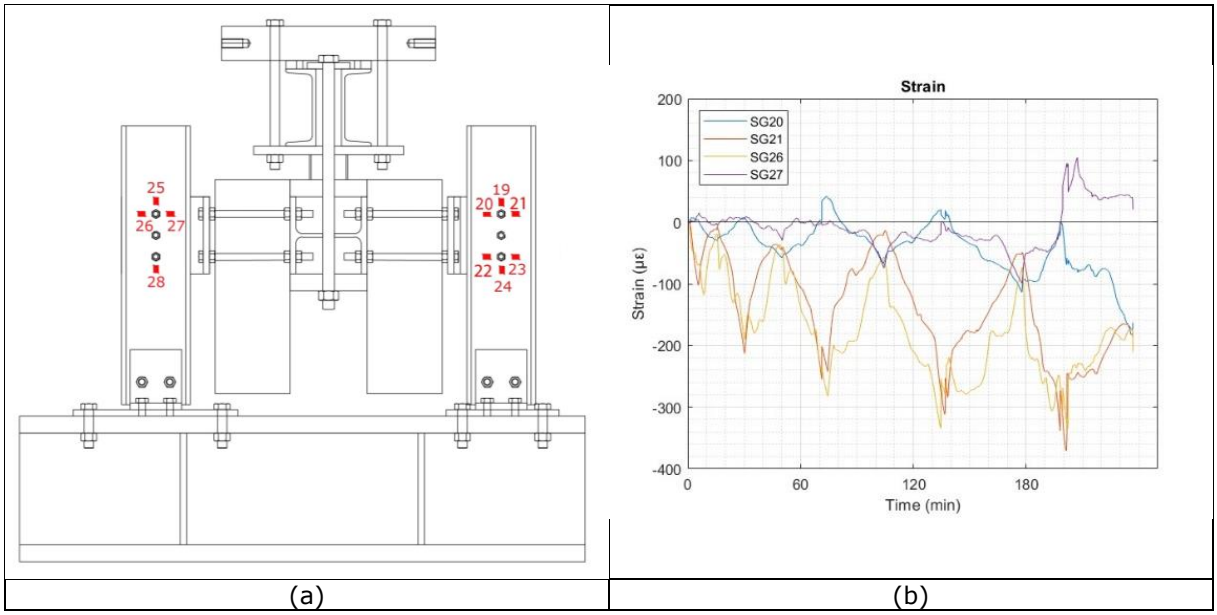

(a) (b)

Figure 160. Detail 4: (a) strain gauges position; (b) strain gauges results.

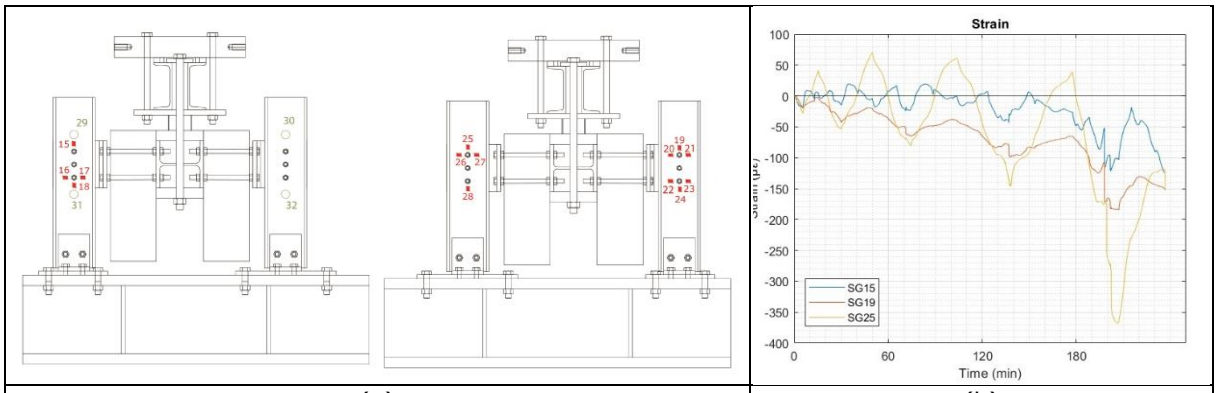

(a) (b)

Figure 161. Detail 4: (a) strain gauges position; (b) strain gauges results.

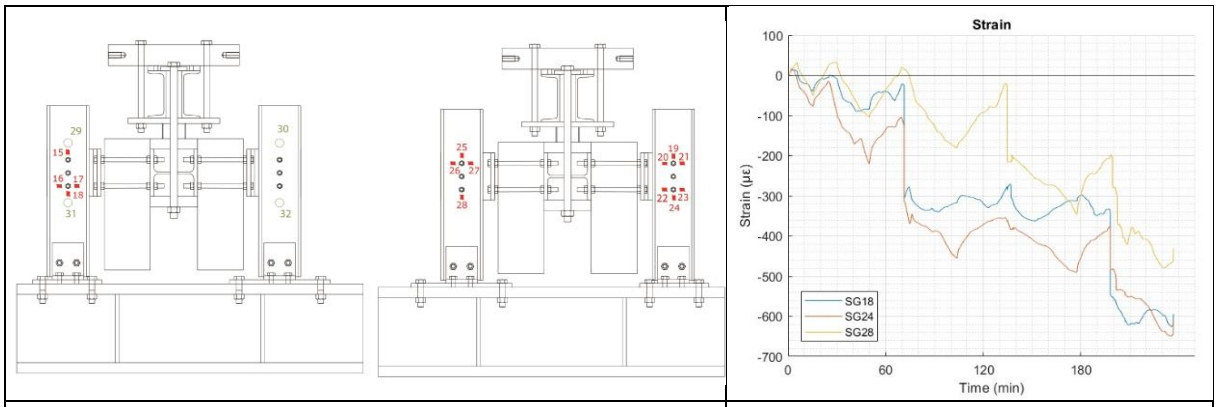

(a) (b)

Figure 162. Detail 4: (a) strain gauges position; (b) strain gauges results.

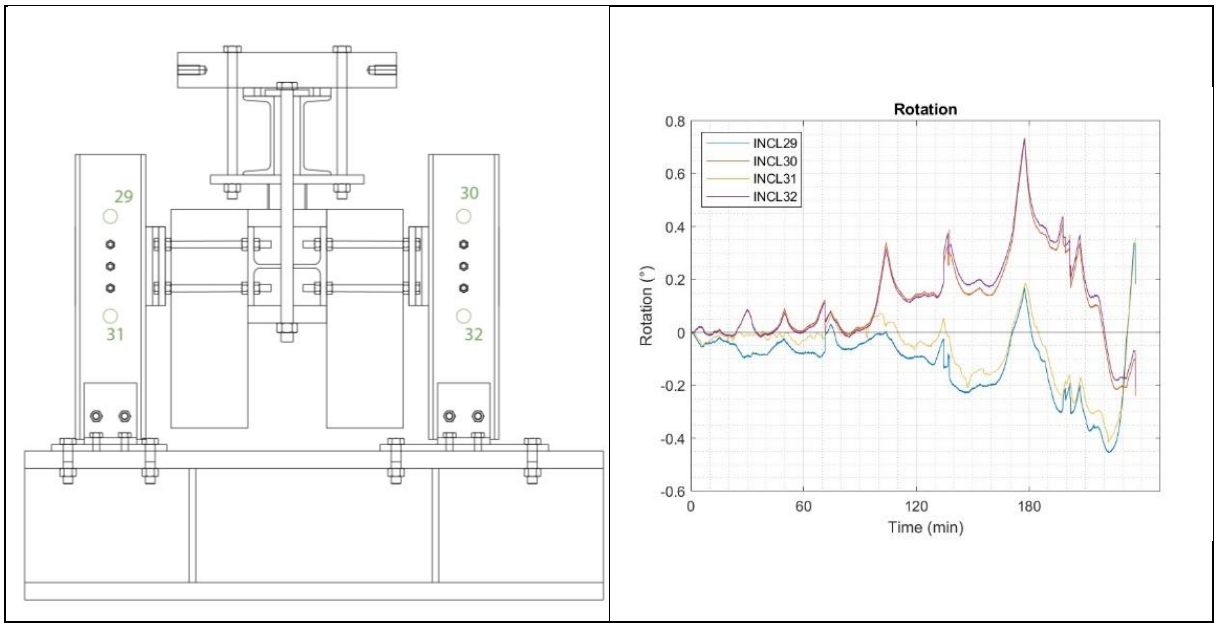

(a) (b)

Figure 163. Detail 4: (a) inclinometers position; (b) inclinometers results.

2.5.4 Summary

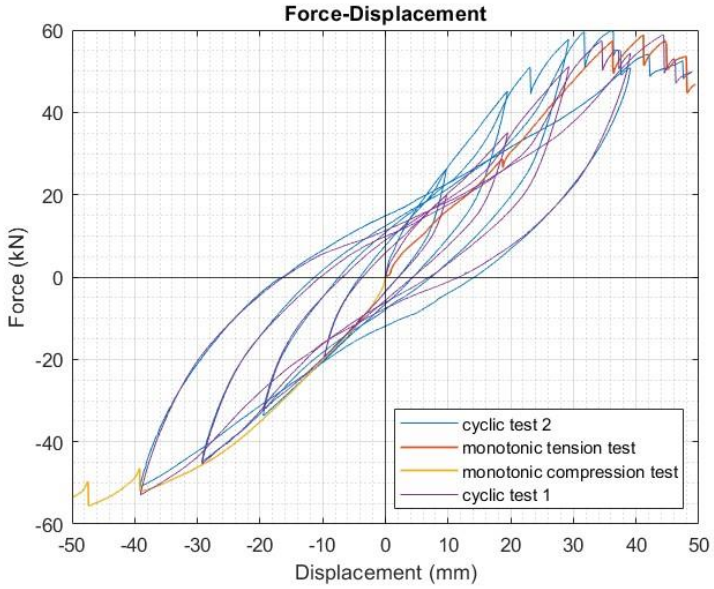

Figure 164. Detail 4 test results comparison

The comparison between the four tests performed on Detail 4 is reported in Figure 164. The four tests are in a good agreement, in particular on the compression side, where a correspondence in terms of stiffness and strength degradation can be observed. On the tension part, the trend of the monotonic test and the two cyclic tests is the same, while a stiffer curve can be observed on the second cyclic test. This difference may be caused by a different procedure in assembling the specimen or by an intrinsic imperfection of the elements. The failure mode is the same for each test, where a progressive failure of one or many shear planes occurred. The design force of 180 kN was not reached in any tests. In fact, the detail configuration and the presence of the sandwich panels with steel rods led to large deformations that induced additional forces on the aluminium bolts, determining their previous collapse. It is worth noting that such large rotations of the sandwich panel are not likely to occur in reality because the wall will be anchored to the ground and its length will be much higher. Nevertheless, the tests provided some useful information on the interaction between the sandwich panel and the steel rods, whose behaviour was not significantly affected by the panels.

In conclusion, Table 19 summarizes the maximum experimental forces reached by each test at the first failure of an aluminium bolt, in comparison with the design force, in

		
(d)	(e)	(e)

Figure 165 some specimens photos, after the tests, can be observed and in Figure 166 the aluminium bolts after the tests are shown.

Table 19. Failure forces reached during the tests.

Detail 4	Design force	Maximum experimental

Monotonic tension test	180 kN	56.9 kN
Monotonic compression test	180 kN	52.0 kN
Cyclic test 1	180 kN	57.1 kN
Cyclic test 2	180 kN	50.9 kN

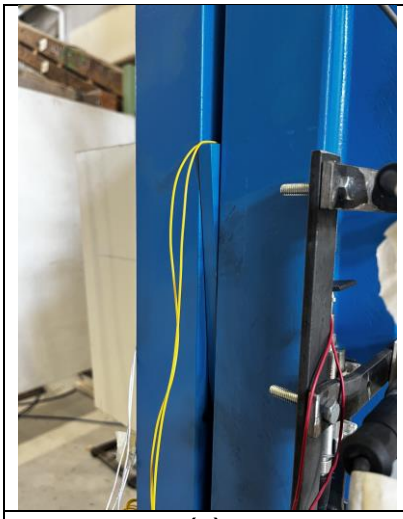
(a)

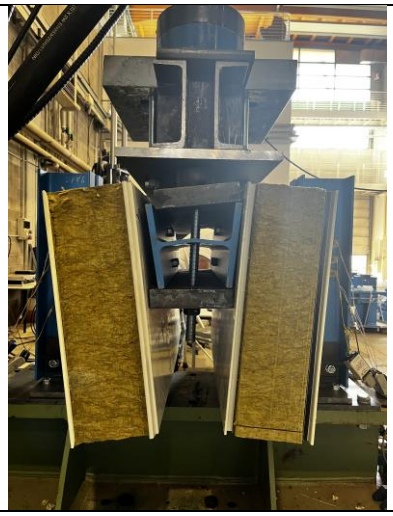
(b)

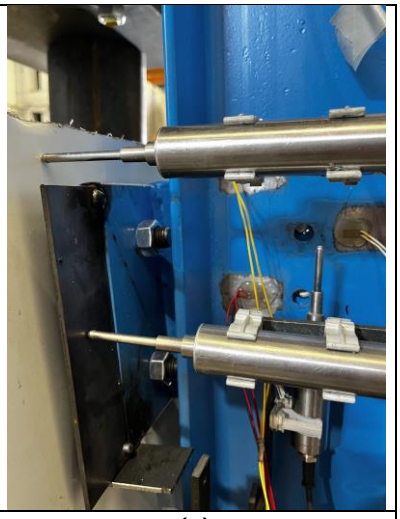
(c)


(d)


(e)


(e)

Figure 165. Detail 4 at failure: (a) lateral view of T plate element rotation under tension force; (b) frontal view of sandwich panels and HEB180 element under compression force; (c) movement of sandwich panel and T plate elements after cyclic test; (d), (e) and (f) details of the rods after the compression test


(a)


(b)

(c) (d)

Figure 166. Detail 4 aluminium bolts at failure: (a) tension test; (b) compression test; (c) cyclic test 1; (d) cyclic test 2.

2.6 Tests on Detail 5

As reported in Deliverable D1.4 [1], all the details were developed from 3 reference fusible link solutions common to all the project partners.

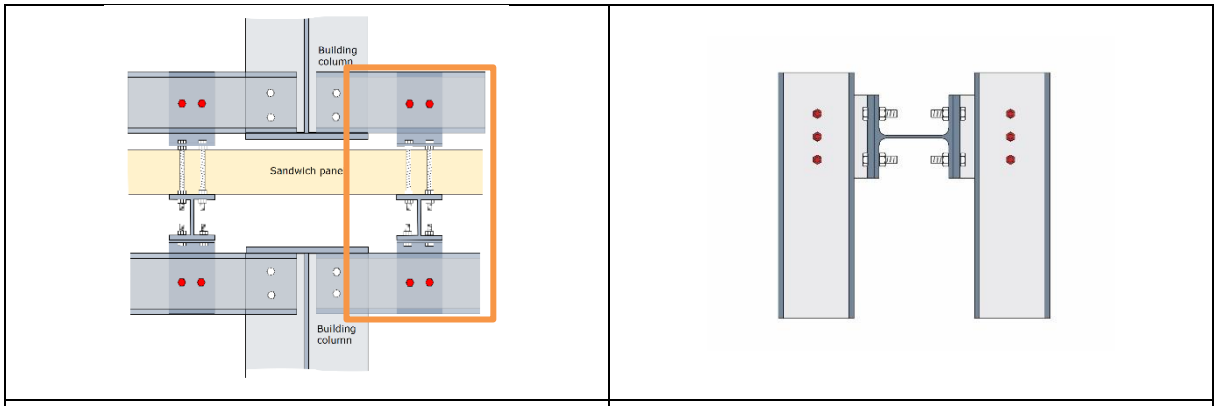

(a) (b)

Figure 167. Detail 5: (a) reference detail, (b) Detail 5 for seismic tests.

Figure 167 reports Detail 5 and the reference fusible link solution from which it was derived. It is the same Detail but for the sandwich panels were omitted so as to analyse the difference. Six M12 aluminium bolts working on 2 shear planes were involved to withstand the design force equal to 180 kN.

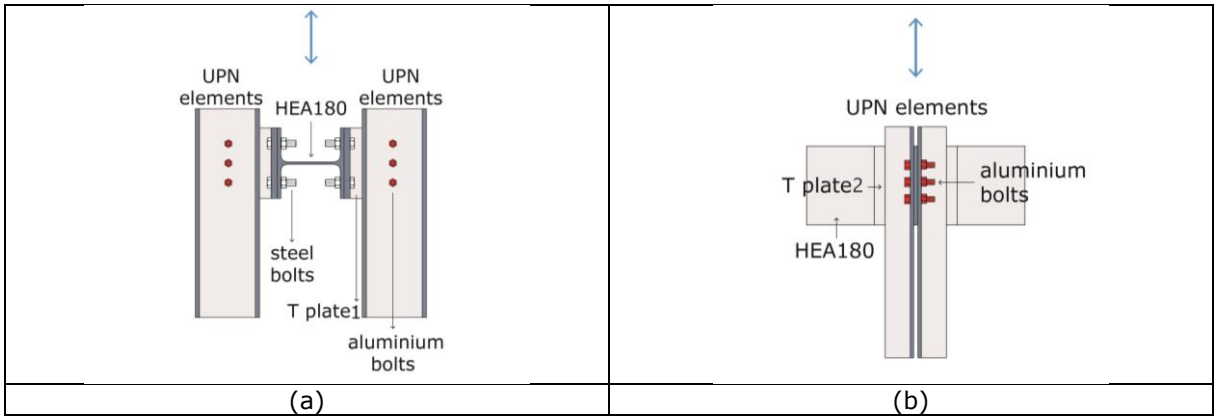

(a) (b)

Figure 168. Detail 5: (a) front view; (b) lateral view.

Table 20: Detail 5 description

Elements	**Main characteristics**
UPN elements	4 UPN 160
Aluminium bolts	6 M12 AlZn5,5MgCu 7075
Steel bolts	8 M16 8.8
T Plate 1 - web	2 190x180x10
T plate 2 - flange	2 190x180x15

In Figure 168 and in Table 20 the main characteristics of Detail 5 in terms of elements and geometry are reported. This detail was designed for a shear value of 180 kN, that can be withstood by 6 M12 aluminium bolts working on two shear planes.

2.6.1 Monotonic tension test

Figure 169. Detail 5 test set-up

In Figure 169 the specimen of Detail 5 inserted in the reaction frame can be observed.

In Figure 170 and in Figure 171, the specific instrumentation position and numbering are reported.

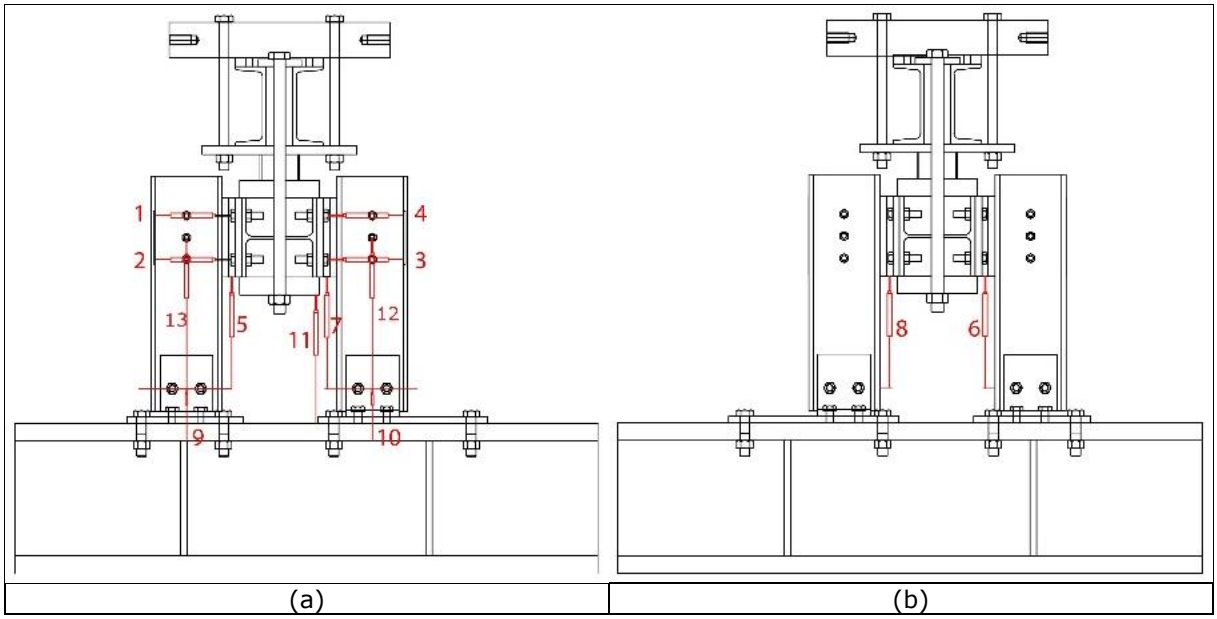

Figure 170. LVDTs and inclinometers position on Detail 5: (a) front side; (b) back side.

The LVDT transducers were located to check specific detail movements:

- LVDT 1, LVDT 2, LVDT 3 and LVDT 4 to check the possible rotation of the T plate elements;
- LVDT5, LVDT6, LVDT7 and LVDT8 to check the possible rotation of the T plate elements and to check their vertical displacement;
- LVDT9 and LVDT10 to record a possible deformation of the base beam;
- LVDT11 to check a possible difference between the actuator displacement and the H element;
- LVDT12 and LVDT13 to check the aluminium bolts vertical displacement.

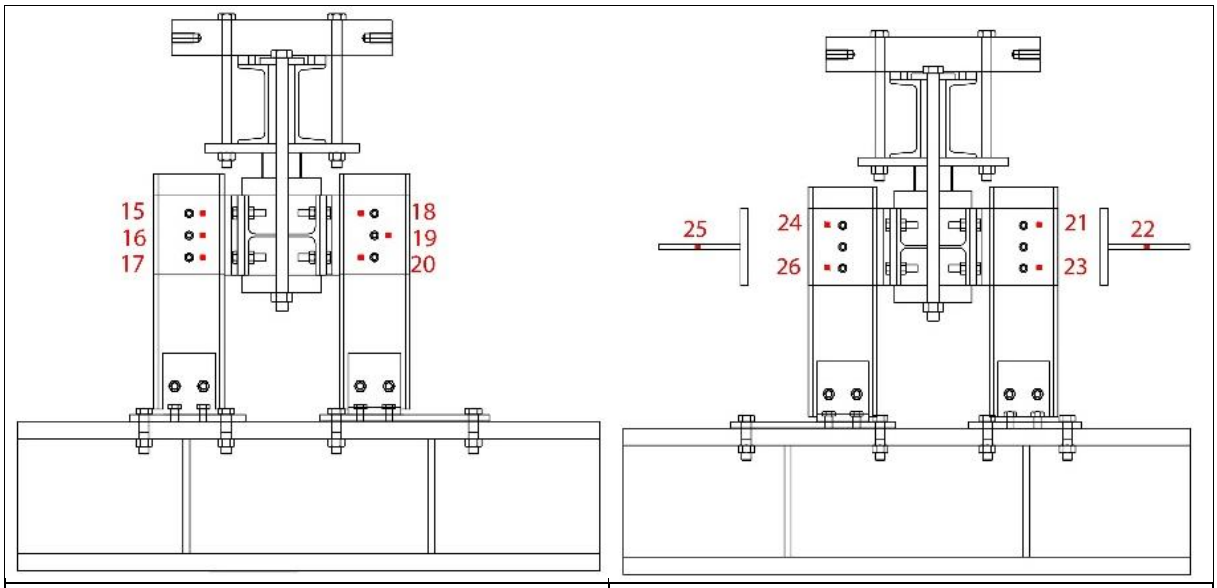

(a) (b)

Figure 171. Detail 5 - strain gauges position; (a) on front side; (b) on back side.

A total of 12 strain gauges were glued on the steel UPN elements:

- From number 15 to 21 plus 23, 24, and 26 were placed to check the horizontal strains caused by possible additional forces;
- Numbers 22 and 25 were located on the T elements to compare the rotation on the opposite sides.

The instruments acquisitions were recorded at 2 Hz.

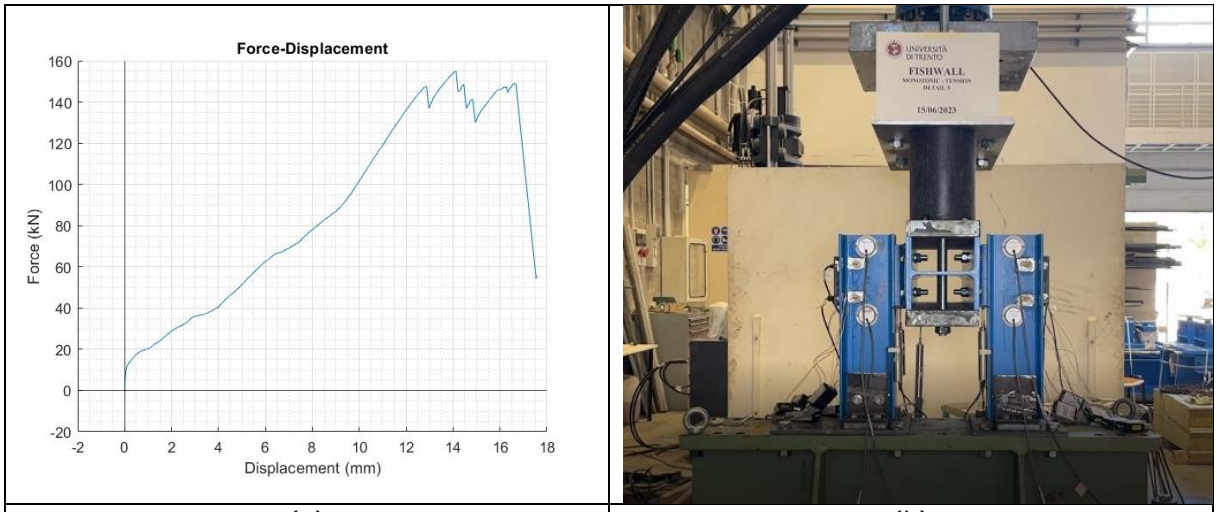

(a) (b)

Figure 172. Detail 5: (a) force-displacement curve of the monotonic tension test and (b) final specimen deformation.

In Figure 172, the result in terms of the force-displacement diagram is shown. As can be noticed, many peaks characterized the curve. Each peak corresponds to the failure of one or many shear planes that occurred during the test. Indeed 8 peaks can be observed of 12 shear planes present on the specimen. In addition, the force design of 180 kN was not reached, due to asymmetries in the specimen that overload certain aluminium bolts than others. The main reason was the specimen rotations, even though much smaller than for Detail 4, causing additional moments on the aluminium bolt group that entailed additional horizontal shear forces. As a result, the top and the bottom bolts were more stressed than expected and failed before to reach the design strength of the detail. Nonetheless, higher force levels were attained with respect to Detail 4, because the eccentricities and the rotations were lower.

These findings are also confirmed by the LVTD and strain gauge measurements, as shown in Figure 173 to Figure 177. The local strain levels did not exceed the actual steel yield limit of 1710 με, highlighting that significant bearing effects were not detected.

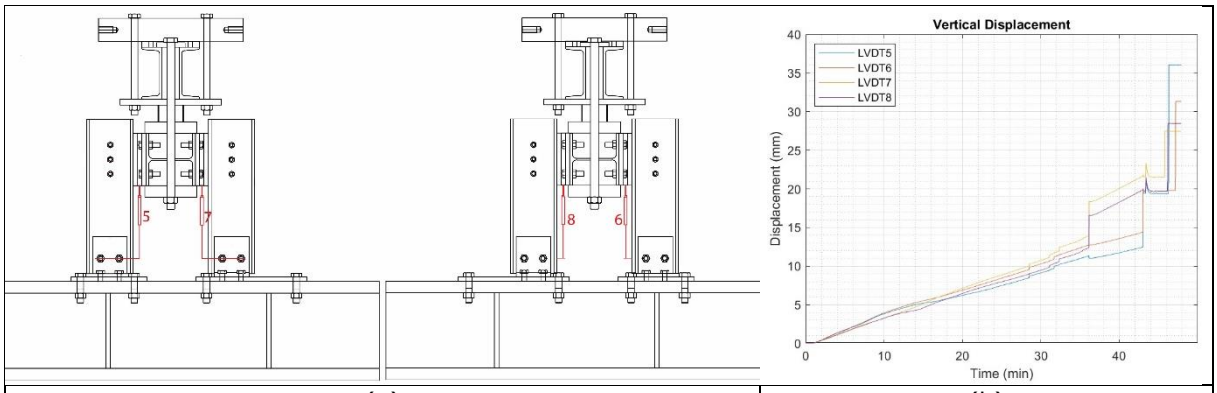

(a) (b)

Figure 173. Detail 5: LVDTs: (a) position;(b) vertical displacement measurements.

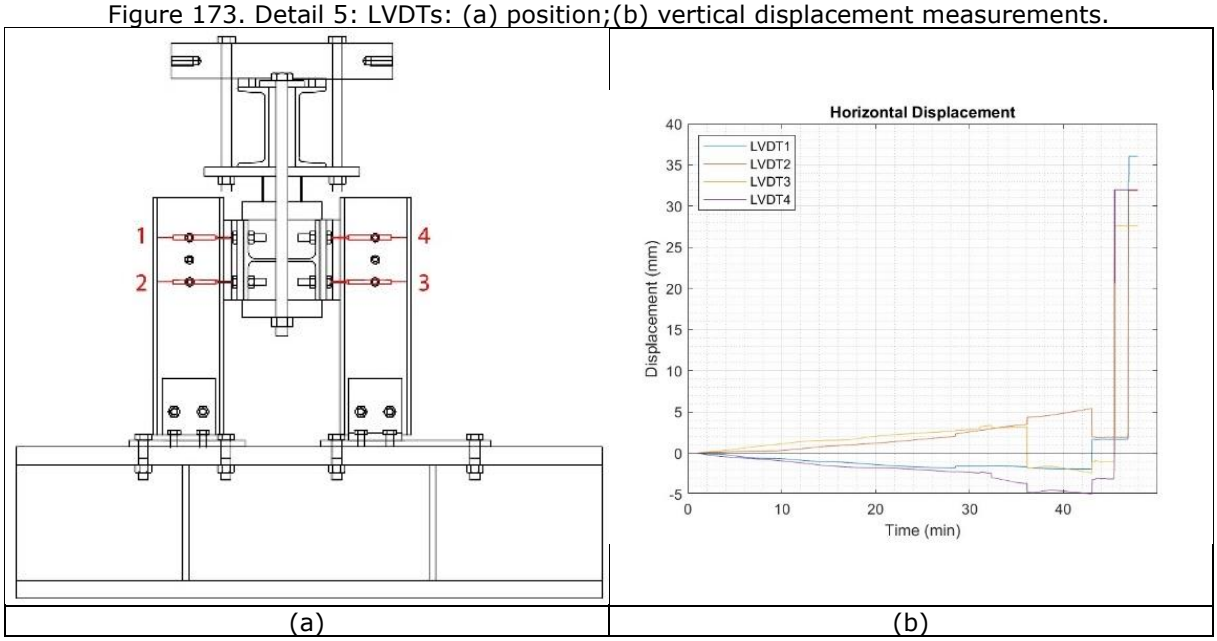

(a) (b)

Figure 174. Detail 5: LVDTs: (a) position;(b) horizontal displacement measurements.

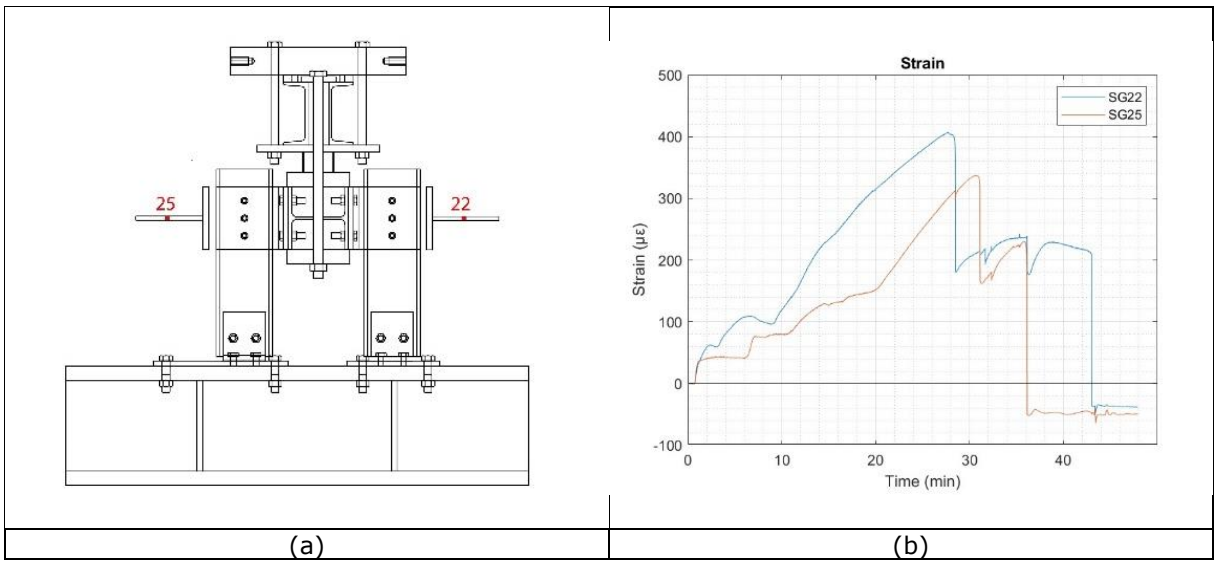

(a) (b)

Figure 175. Detail 5: (a) strain gauges position; (b) strain gauges results.

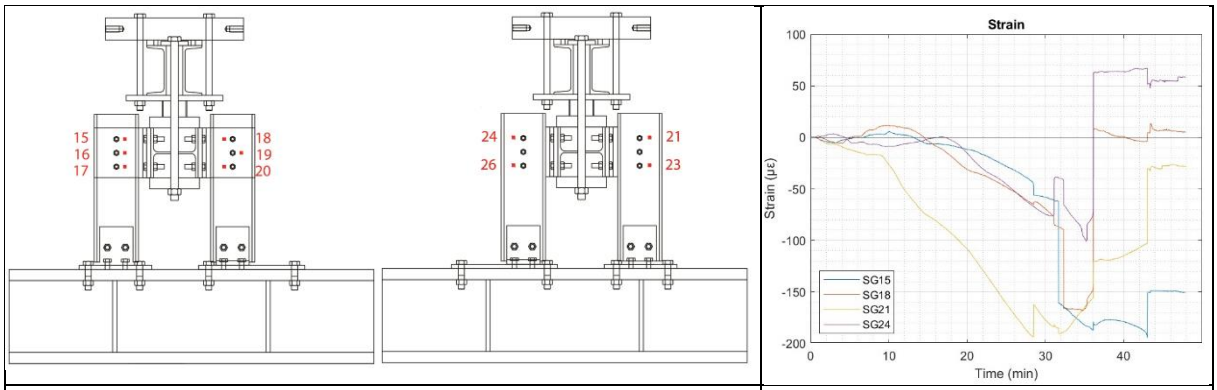

(a) (b)

Figure 176. Detail 5: (a) strain gauges position; (b) strain gauges results.

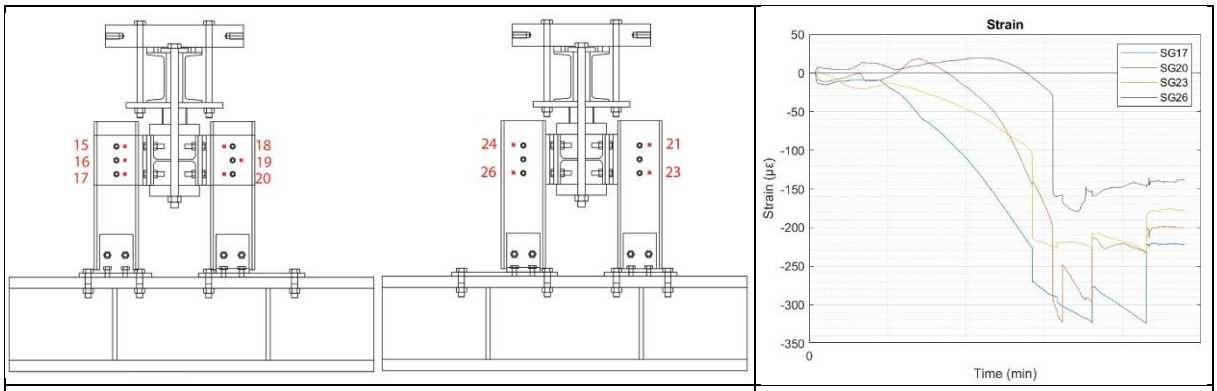

(a) (b)

Figure 177. Detail 5: (a) strain gauges position; (b) strain gauges results.

2.6.2 Monotonic compression test

In Figure 170 and in Figure 171, the specific instrumentation position and numbering are reported. The instruments acquisitions were recorded at 2 Hz.

In Figure 178, the result in terms of the force-displacement diagram is shown. As can be noticed, also in this case, many peaks characterized the curve. Each peak corresponds to the failure of one or many shear planes that occurred during the test. Indeed, 6 peaks can be observed of 12 shear planes present on the specimen. At the end of the test, all the shear planes failed. In addition, the force design of 180 kN was reached. This is was due to a different assembly procedure that induced higher stiffness of the specimen in compression and consequently lower horizontal deformations were recorded (compare Figure 174 and Figure 180). The specimen configuration without the sandwich panels reduced additional forces on the fusible links that withstood the design force.

These findings are also confirmed by the LVTD and strain gauge measurements, as shown in Figure 179 to Figure 183. The local strain levels did not exceed the actual steel yield limit of 1710 με, highlighting that significant bearing effects were not detected.

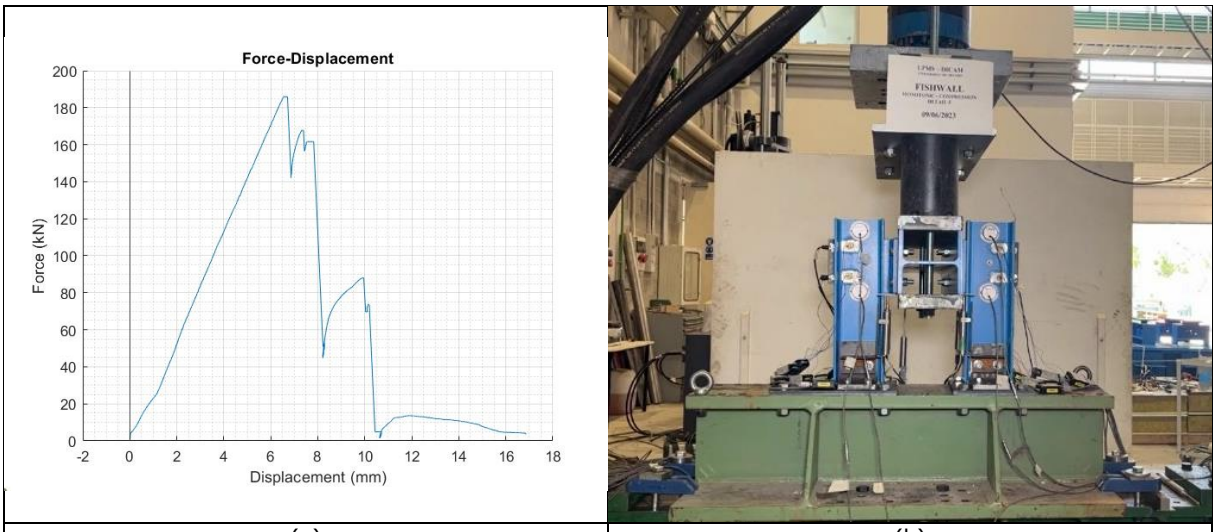

(a) (b)

Figure 178. Detail 5 (a) force-displacement curve of the monotonic compression test and (b) final specimen deformation

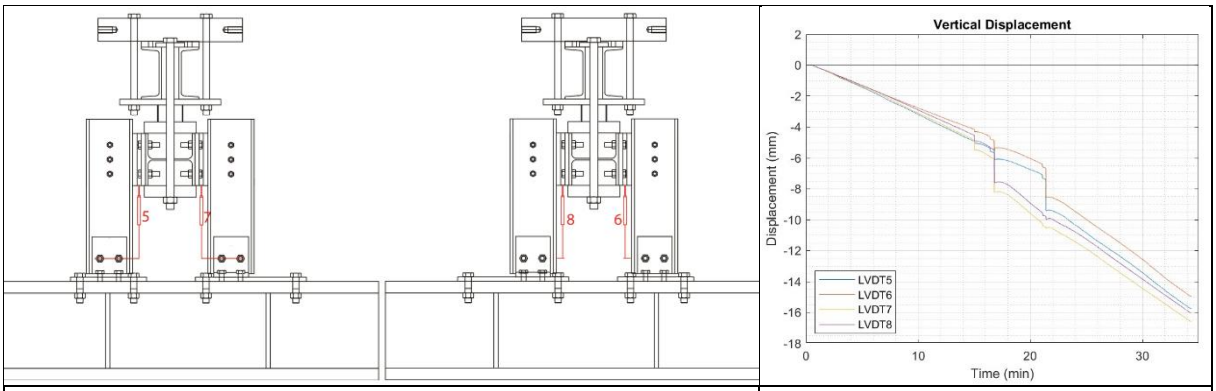

(a) (b)

Figure 179. Detail 5: LVDTs: (a) position;(b) vertical displacement measurements.

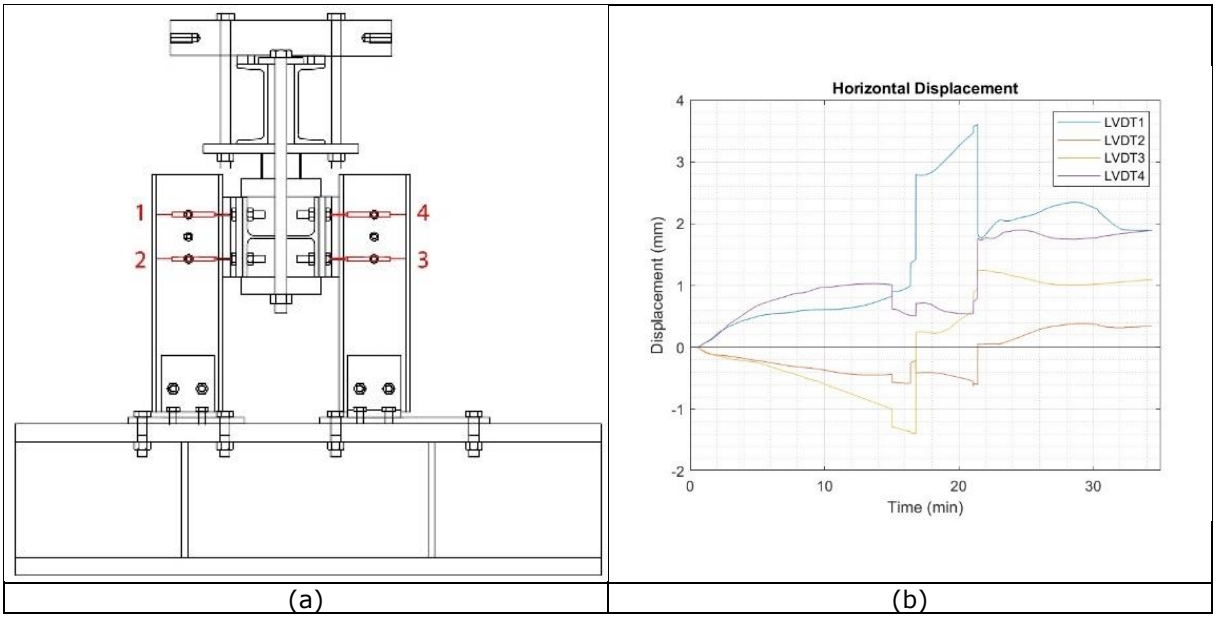

(a) (b)

Figure 180. Detail 5: LVDTs: (a) position;(b) horizontal displacement measurements.

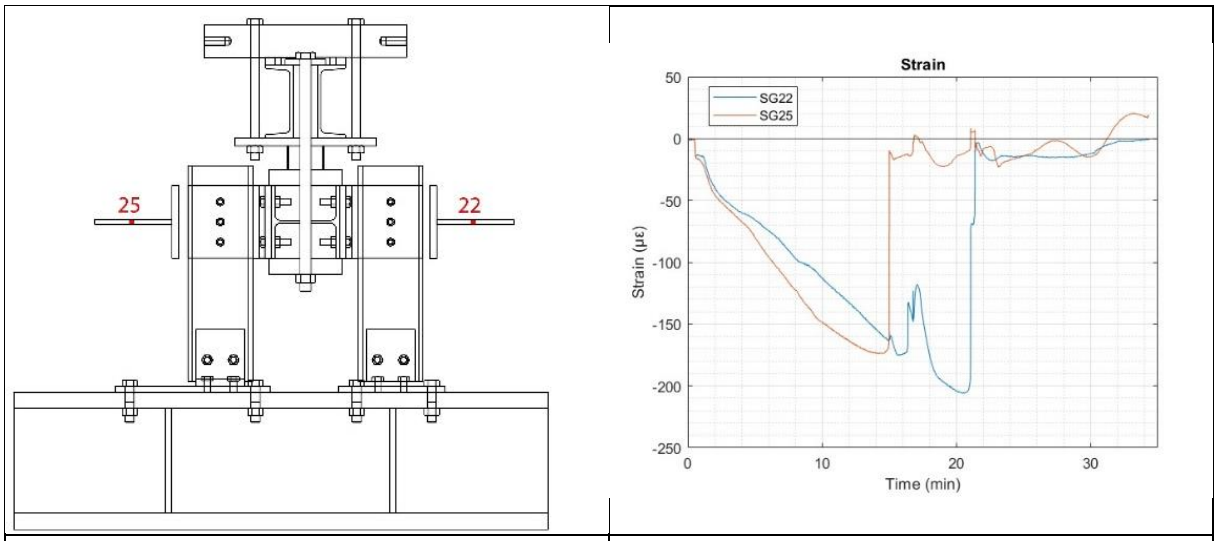

(a) (b)

Figure 181. Detail 5: (a) strain gauges position; (b) strain gauges results.

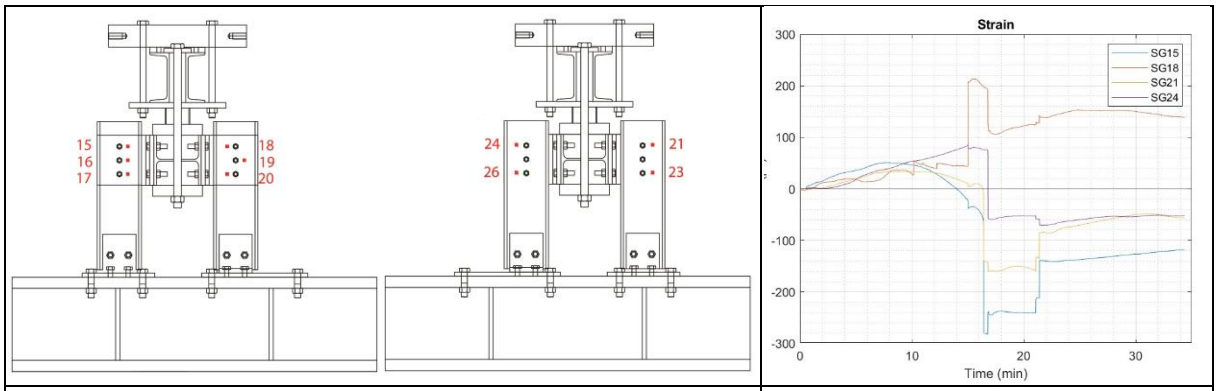

(a) (b)

Figure 182. Detail 5: (a) strain gauges position; (b) strain gauges results.

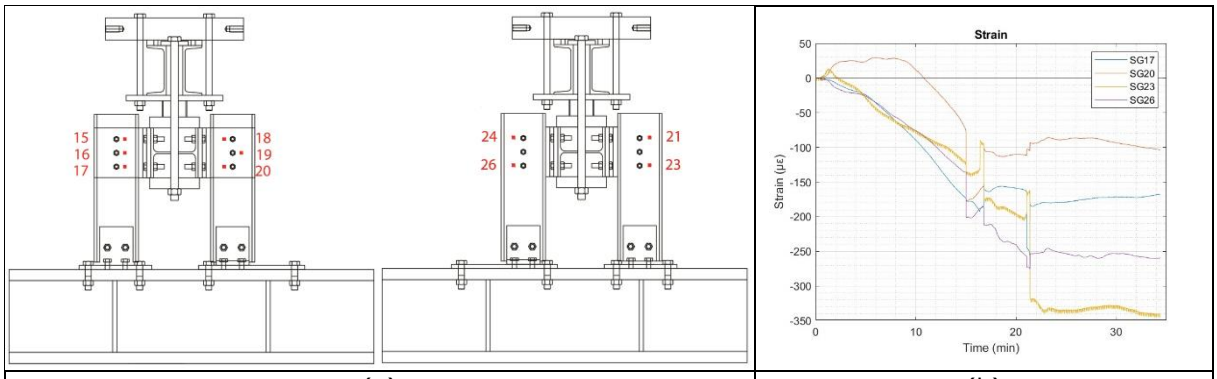

(a) (b)

Figure 183. Detail 5: (a) strain gauges position; (b) strain gauges results.

2.6.3 Cyclic tests

In order to follow the ECCS procedure, as reported in Section 1.3, the two monotonic tests curves were used to define the yield displacement and the displacement history to carry out the cyclic tests.

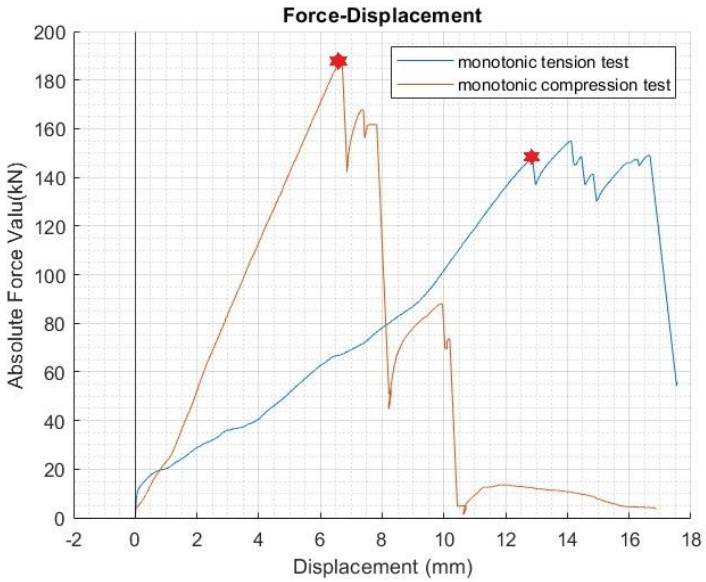

Figure 184. Detail 5 monotonic tests results

Figure 184 reports the comparison, in terms of force-displacement curves, between the monotonic tension and compression tests. The red points represent the yield displacements for the cyclic tests that are reported in Table 21. Two different e_y were chosen to consider the shape of the two curves, that are characterized by different stiffness and strength.

Table 21: Yield displacement from monotonic curves

e_y	12.9 mm
$-e_y$	-6.7 mm

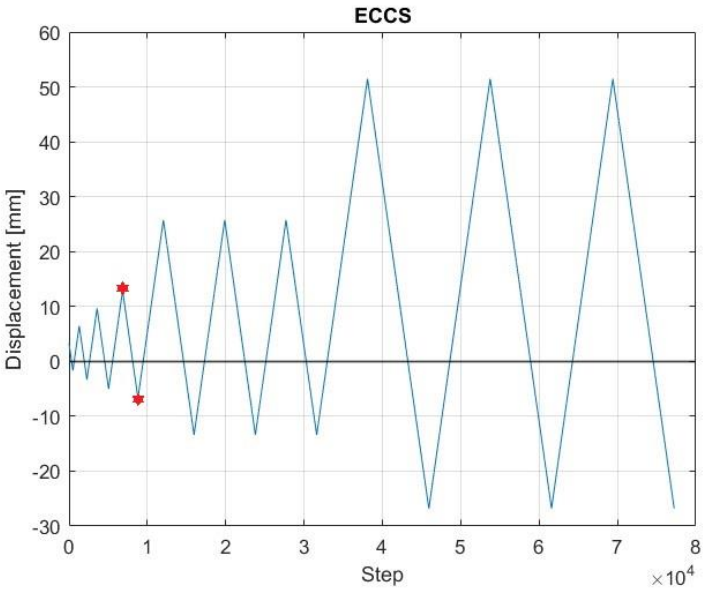

Figure 185. Detail 5 ECCS procedure.

As shown in Figure 185, the displacement history obtained, defined as reported in Section 1.3, is not symmetric. The yield displacements are highlighted in red.
The cyclic tests were conducted in displacement control with a displacement rate of 0.5 mm/min.

2.6.3.1 Cyclic test 1

In Figure 186 and in Figure 187, the specific instrumentation position and numbering are reported. In this case, 14 strain gauges were located on the steel UPN elements to measure the strain close to the aluminium bolts during the test. The instruments acquisitions were recorded at 2 Hz.

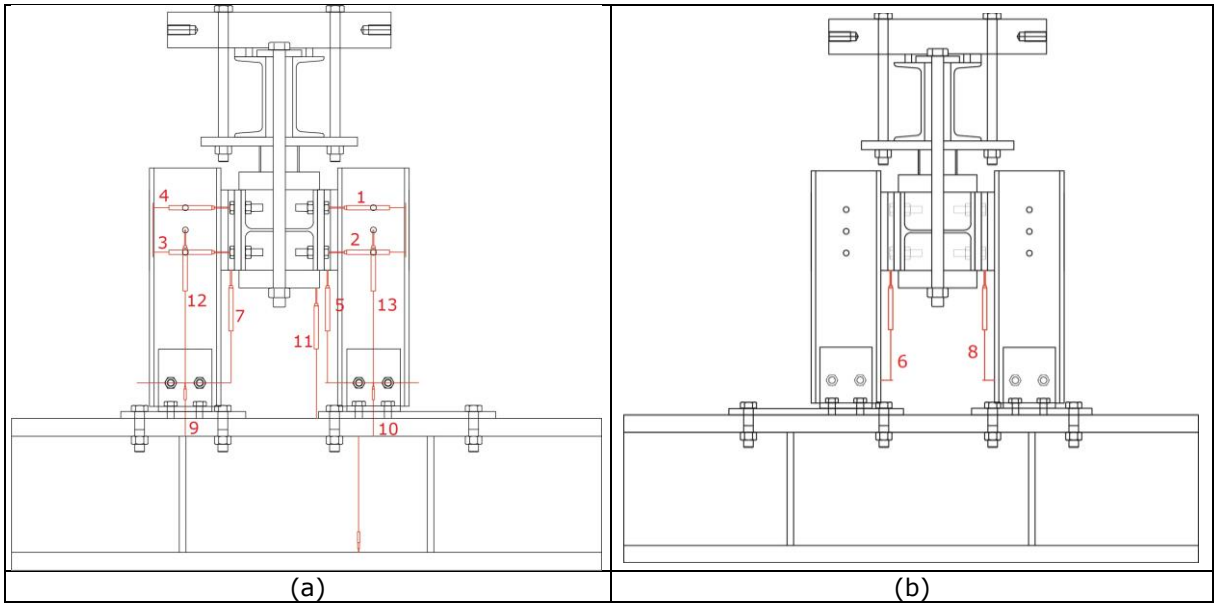

(a) (b)

Figure 186. Detail 5: (a) LVDTs on front side; (b) LVDTs on back side.

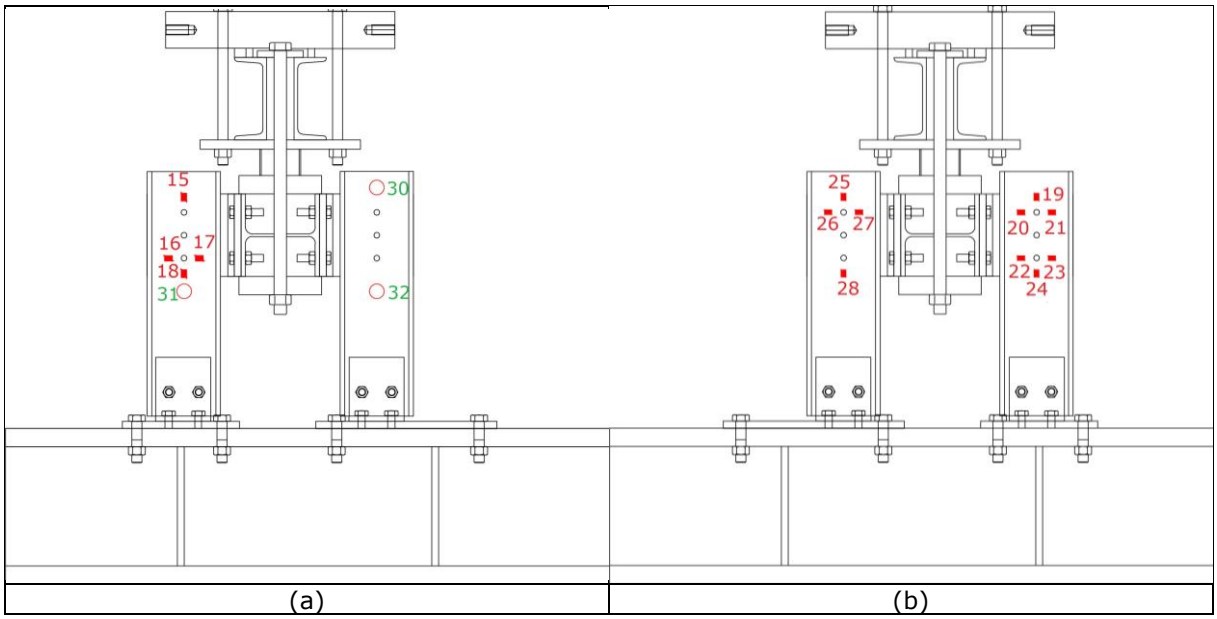

(a) (b)

Figure 187. Detail 5: (a) strain gauges on front side; (b) strain gauges on back side.

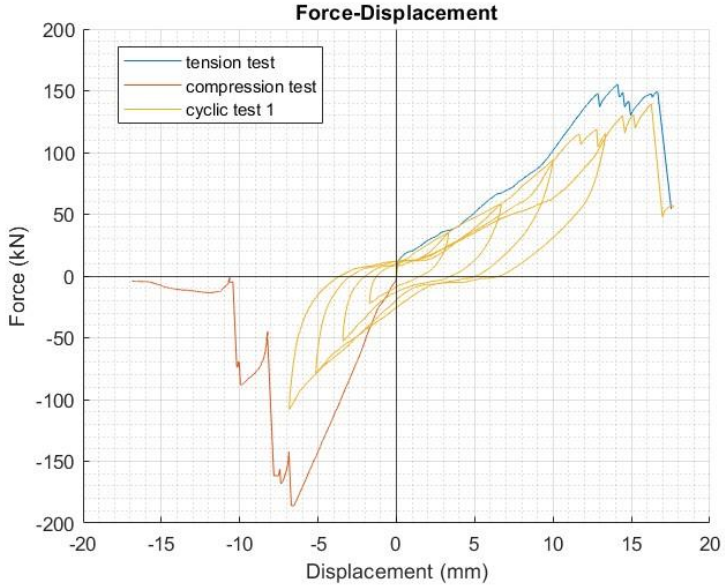

Figure 188. Detail 5 cyclic test 1 results

The results of the first cyclic test on Detail 5, in terms of force-displacement curve, are shown in Figure 188. The failure of the specimen occurred on the reloading at the first cycle to $2e_y$. Besides the brittle nature of the detail, a small hysteretic behaviour can be observed. It is worth noting that also during this test, the design force of 180 kN was not reached because of progressive failure of the bolts in tension, as for the monotonic tension test. The comparison with the monotonic tests highlighted a good agreement with the tension one, while a noticeable difference both in terms of strength and stiffness can be observed on the compression part, which, as previously mentioned, was mainly due to a different procedure adopted in assembling the specimen.
These findings are also confirmed by the LVTD and strain gauge measurements, as shown in Figure 189 to Figure 194. The local strain levels did not exceed the actual steel yield limit of 1710 με, highlighting that significant bearing effects were not detected.

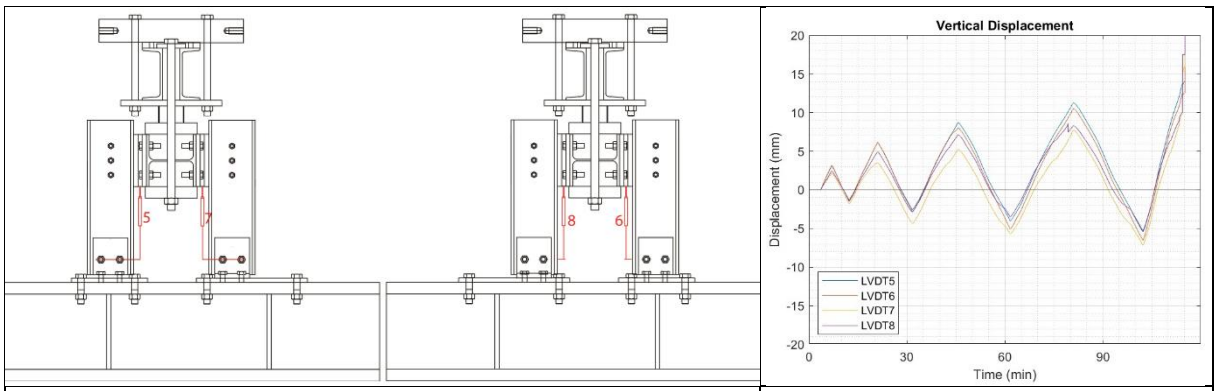

(a) (b)

Figure 189. Detail 5; LVDTs: (a) position;(b) vertical displacement recorded during cyclic test 1.

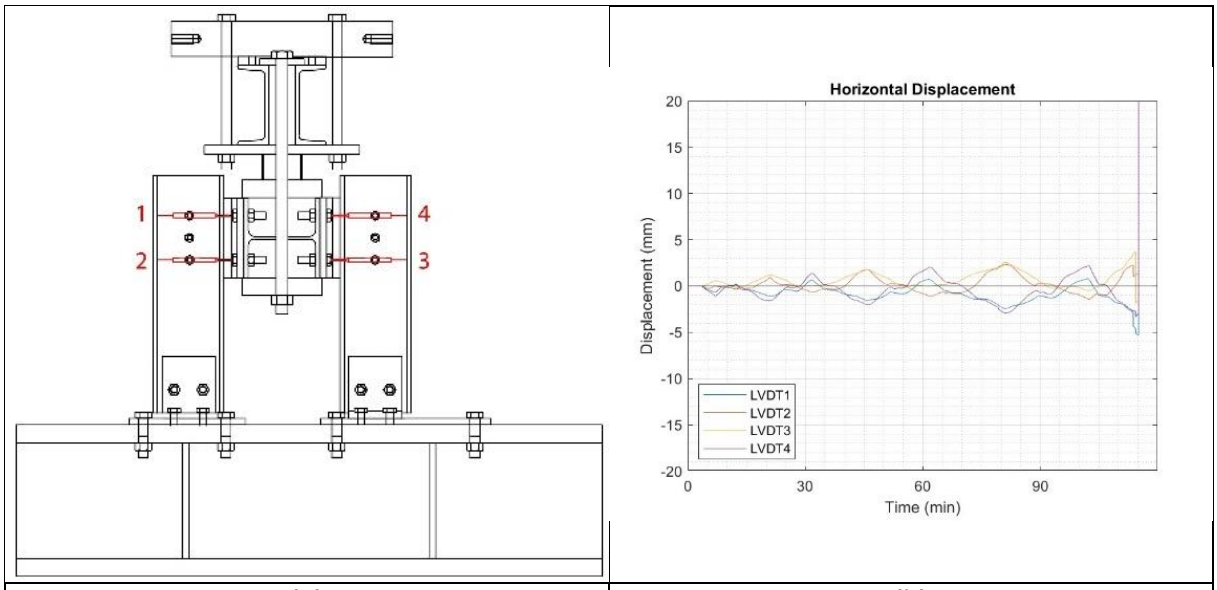

(a) (b)

Figure 190. Detail 5: LVDTs: (a) position;(b) horizontal displacement recorded during cyclic test 1.

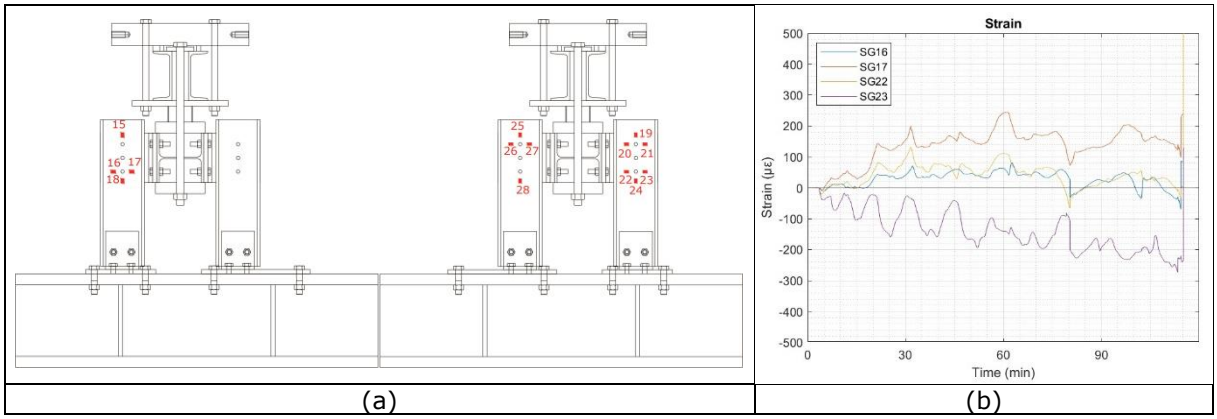

(a) (b)

Figure 191. Detail 5: (a) strain gauges position; (b) strain gauges results.

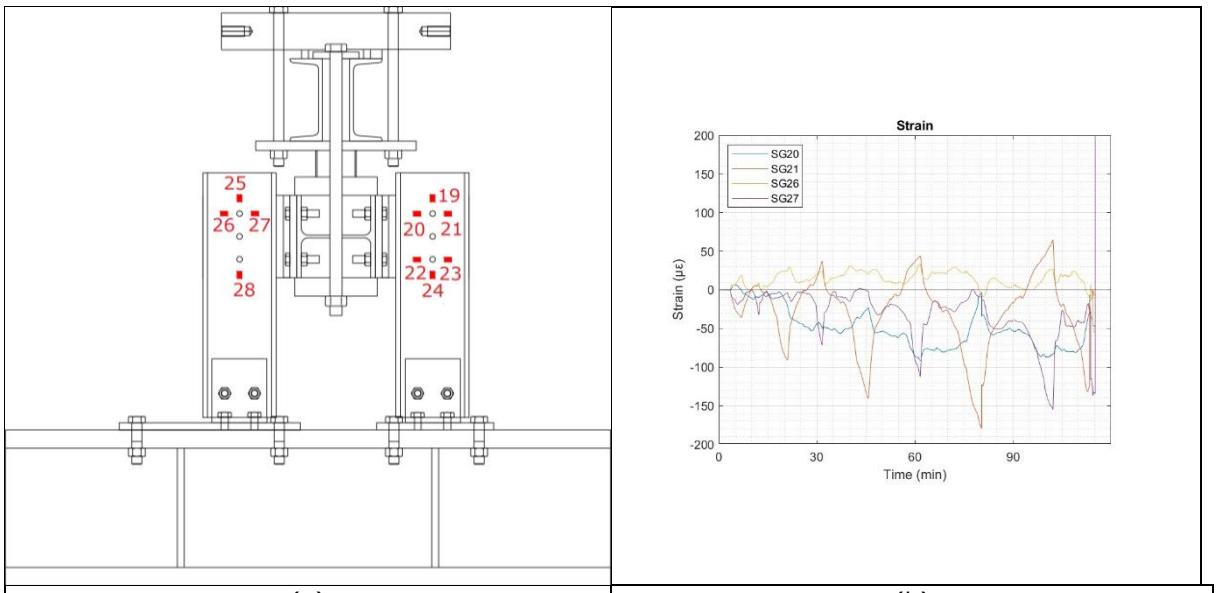

(a) (b)

Figure 192. Detail 5: (a) strain gauges position; (b) strain gauges results.

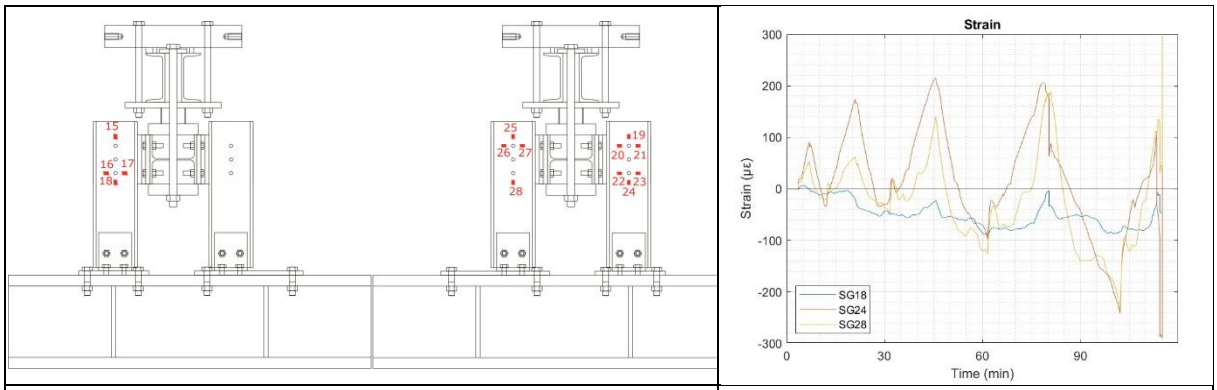

(a) (b)

Figure 193. Detail 5: (a) strain gauges position; (b) strain gauges results.

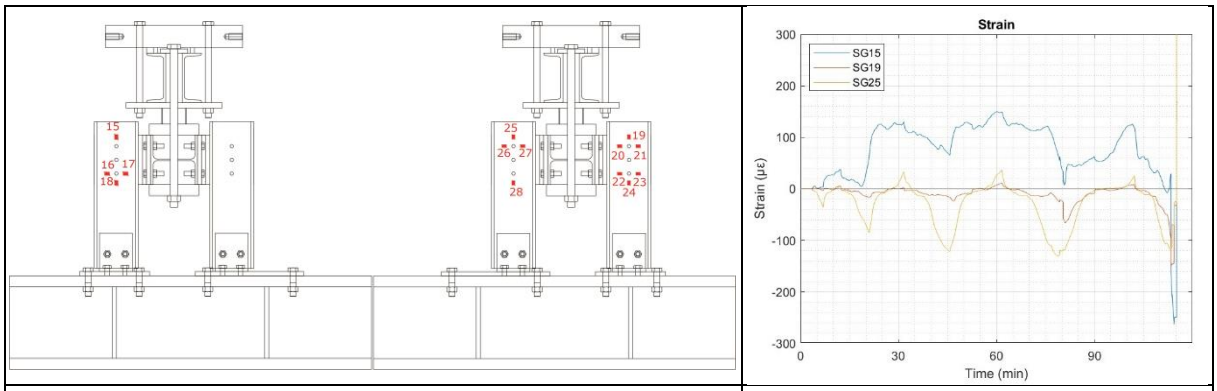

(a) (b)

Figure 194. Detail 5: (a) strain gauges position; (b) strain gauges results.

2.6.3.2 Cyclic test 2

In Figure 186 and in Figure 187, the specific instrumentation position and numbering are reported. The instruments acquisitions were recorded at 2 Hz.

The results of the second cyclic test on Detail 5, in terms of force-displacement curve, are shown in Figure 195. The failure of the specimen occurred on the reloading at the first cycle to $2e_y$. Besides the brittle nature of the detail, a small hysteretic behaviour can be observed. Similarly, with the first cyclic test, also during this test, the design force of 180 kN was not reached. The comparison with the monotonic tests highlighted a good agreement with the tension one, while a relevant difference both in term of strength and stiffness degradation can be observed on the compression part, which was due to a different procedure adopted in assembling the specimen. Good repeatability of the cyclic tests was achieved.

These findings are also confirmed by the LVTD and strain gauge measurements, as shown in Figure 196 to Figure 201. The local strain levels did not exceed the steel yield limit of 1710 με, highlighting that significant bearing effects were not detected.

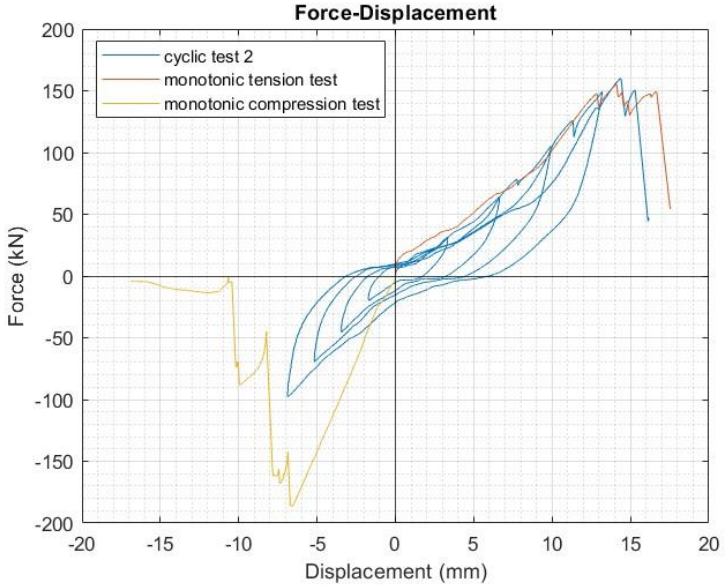

Figure 195. Detail 5 cyclic test 2 results

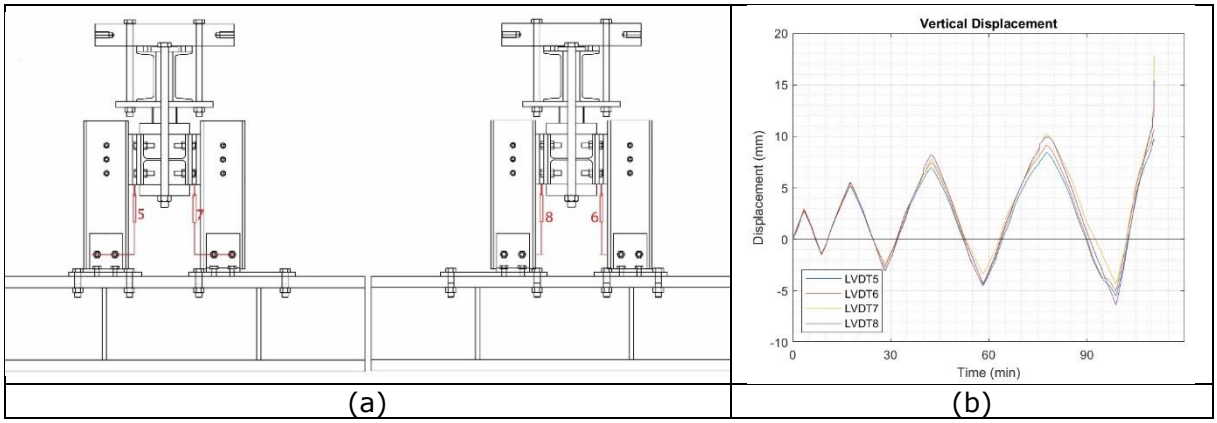

(a) (b)

Figure 196. Detail 5: LVDTs: (a) position;(b) vertical displacement recorded during cyclic test 2.

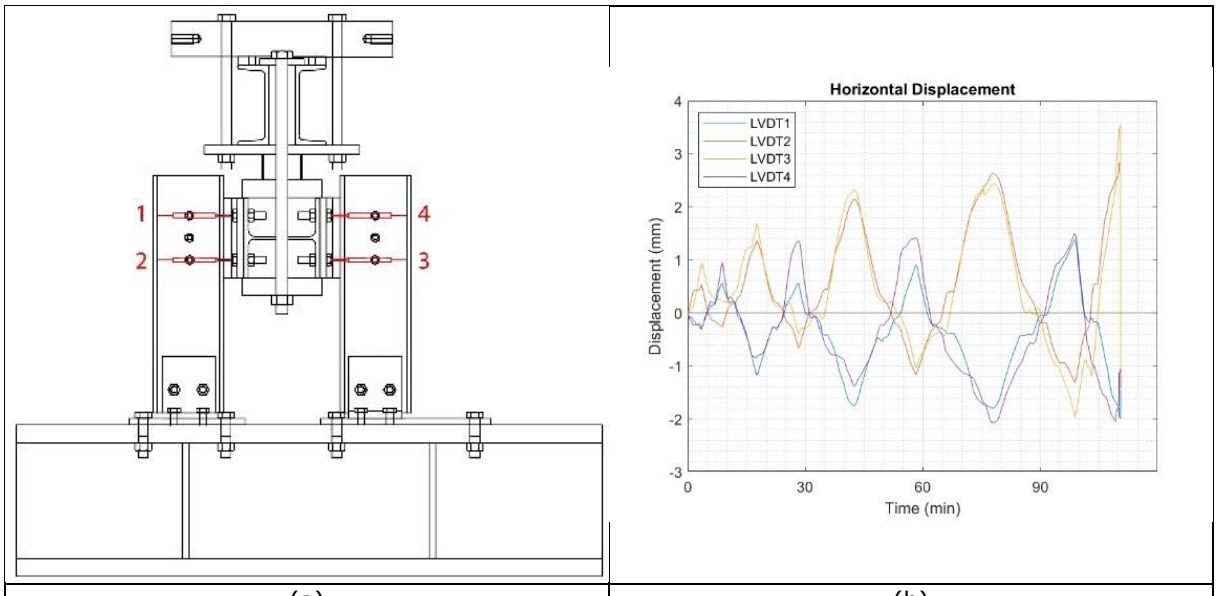

(a) (b)

Figure 197. Detail 5: LVDTs: (a) position;(b) horizontal displacement recorded during cyclic test 2 .

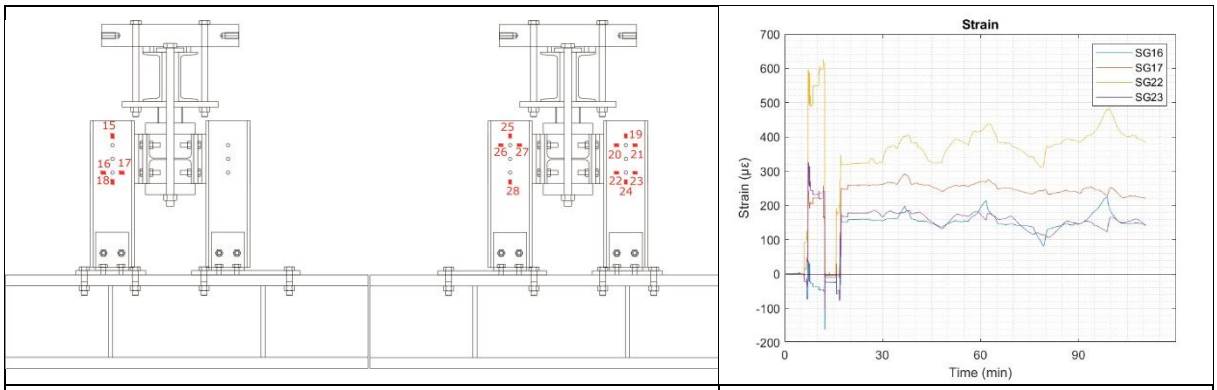

(a) (b)

Figure 198. Detail 5: (a) strain gauges position; (b) strain gauges results.

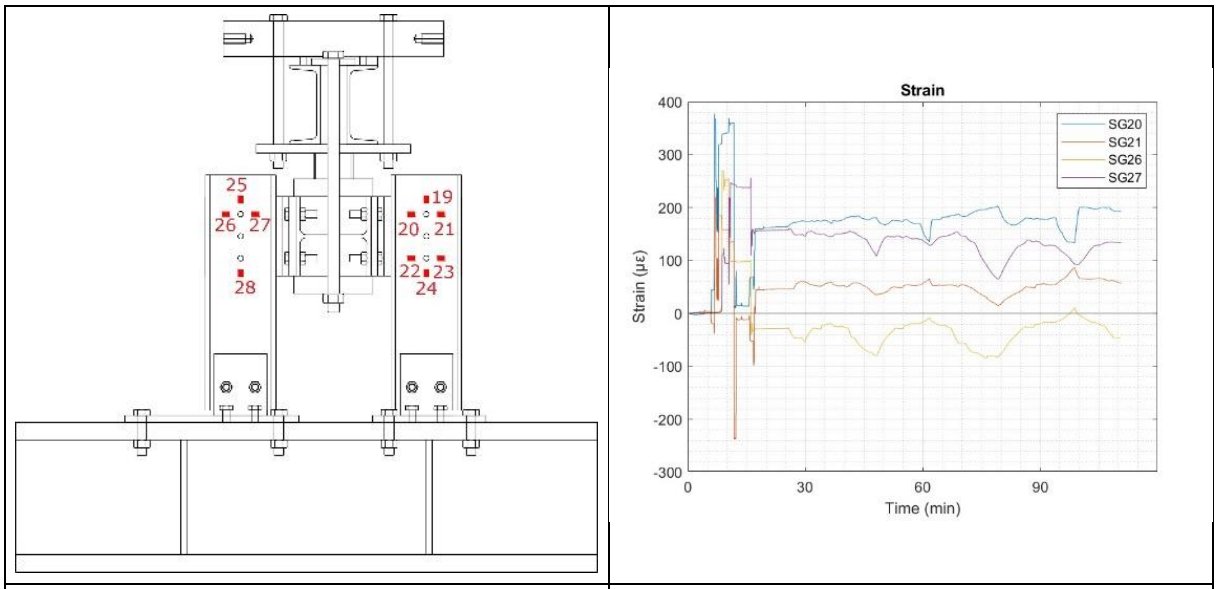

(a) (b)

Figure 199. Detail 5: (a) strain gauges position; (b) strain gauges results.

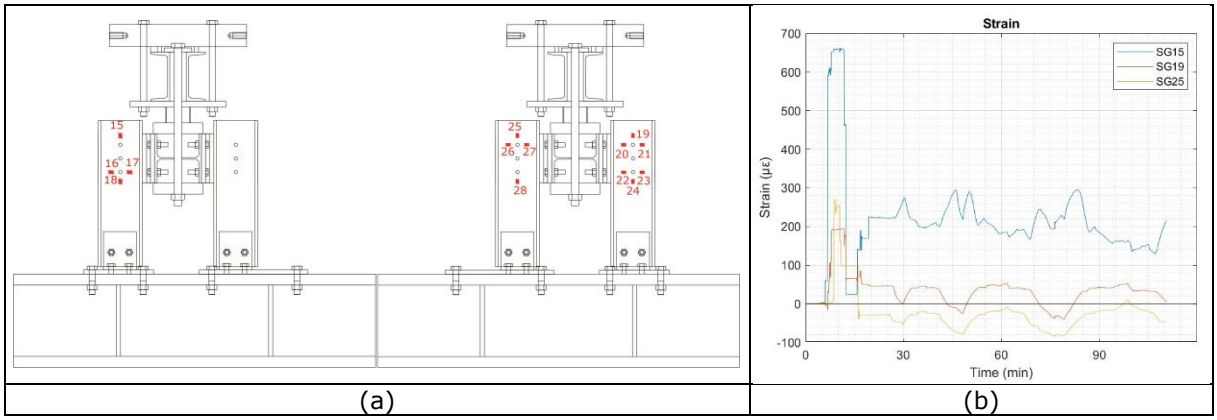

(a) (b)

Figure 200. Detail 5: (a) strain gauges position; (b) strain gauges results.

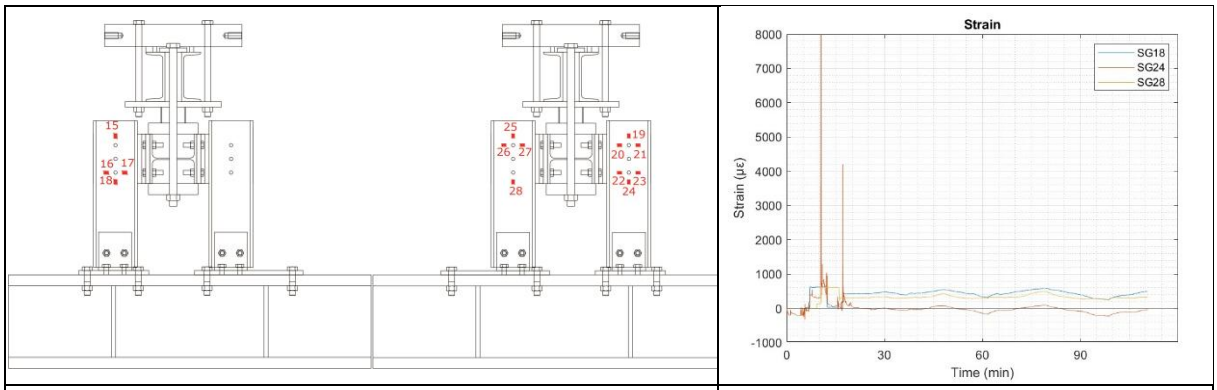

(a) (b)

Figure 201. Detail 5: (a) strain gauges position; (b) strain gauges results.

2.6.4 Summary

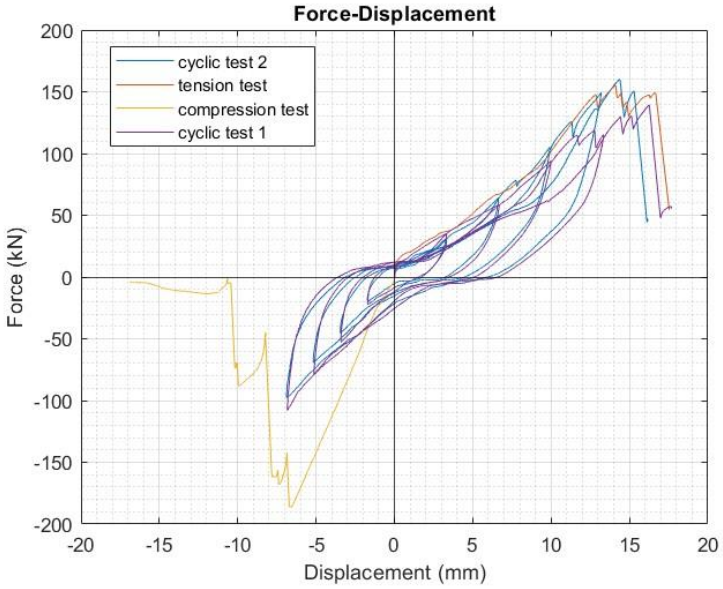

Figure 202. Detail 5 test results comparison

The comparison between the four tests performed on Detail 5 is reported in Figure 202. The cyclic tests are in a good agreement between them, with the same final strength and the same stiffness degradation. The failure occurred due to the progressive failure of the aluminium bolts, that prevented of reaching the design force of 180 kN.

In conclusion, Table 22 summarizes the maximum experimental forces reached by each test at the first failure of an aluminium bolt, in comparison with the design force, in Figure 203 some specimens photos, after the tests, can be observed and in Figure 204 the aluminium bolts after the tests are shown.

Table 22. Failure forces reached during the tests.

Detail 5	Design force	Maximum experimental
Monotonic tension test	180 kN	147.6 kN
Monotonic compression test	180 kN	185.9 kN
Cyclic test 1	180 kN	114.7 kN
Cyclic test 2	180 kN	126.1 kN

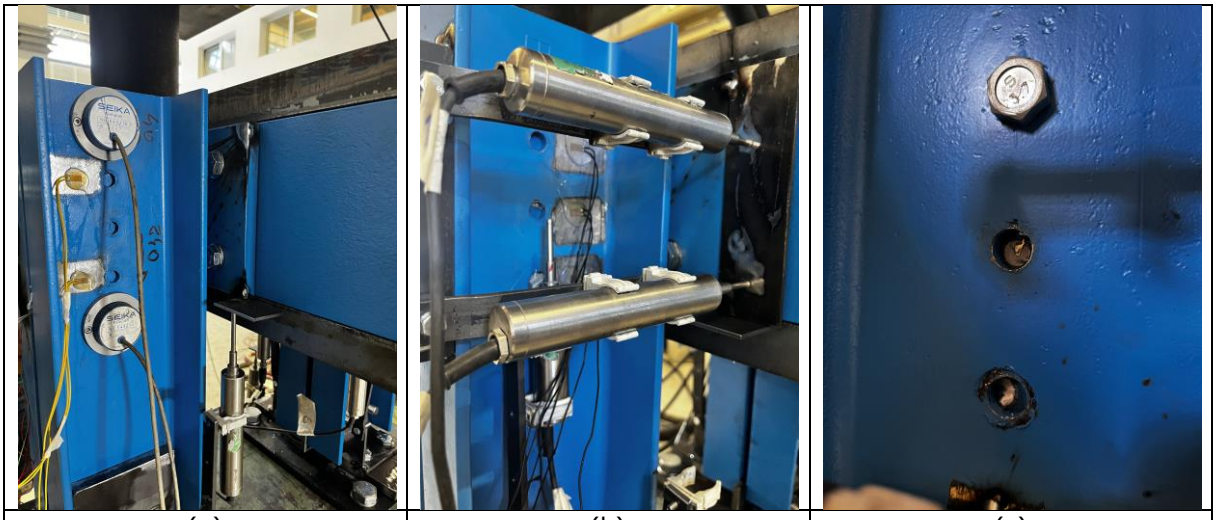

(a) (b) (c)

Figure 203. Detail 5 at failure: (a) frontal view of aluminium bolts under tension force; (b) frontal view of aluminium bolts under compression force; (c) movement between UPN160 elements and T plate elements after cyclic test.

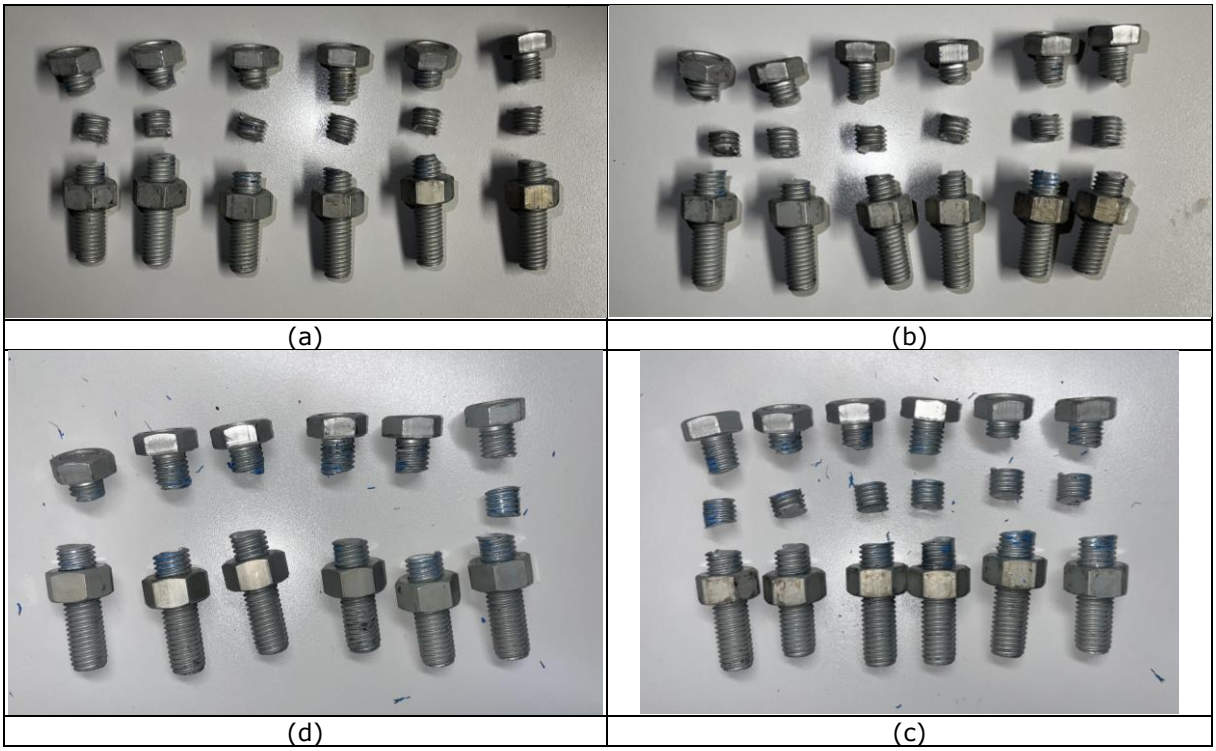

(a) (b)

(d) (c)

Figure 204. Detail 5 aluminium bolts at failure: (a) tension test; (b) compression test; (c) cyclic test 1; (d) cyclic test 2.

2.6.4.1 Comparison between Detail 4 and Detail 5

In order to better characterize the fusible links behaviour, Detail 4 and Detail 5 were developed with the same concept, but different characteristics. In fact, as reported in Figure 205, Detail 4 presented a symmetric specimen with the sandwich panels linked through M20 steel rods, while in Detail 5 the panels were completely removed, and the rods were replaced with M16 steel bolts. Both the details were equipped with 6 M12 aluminium bolts working on two shear planes.

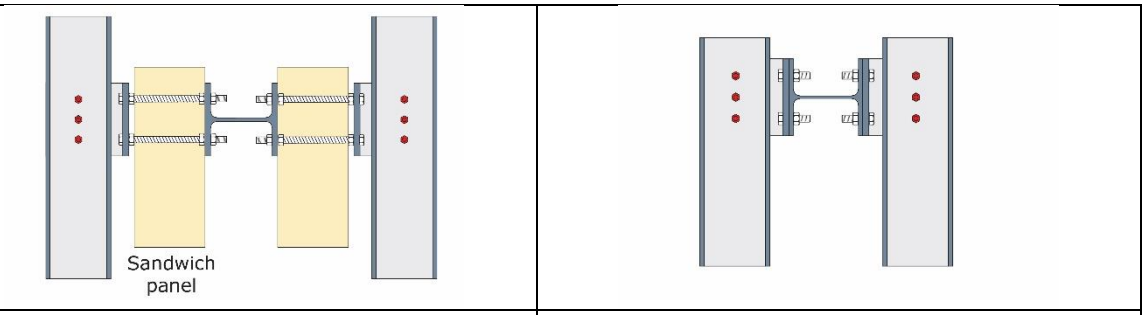

(a) (b)

Figure 205. (a) Detail 4 and (b) Detail 5

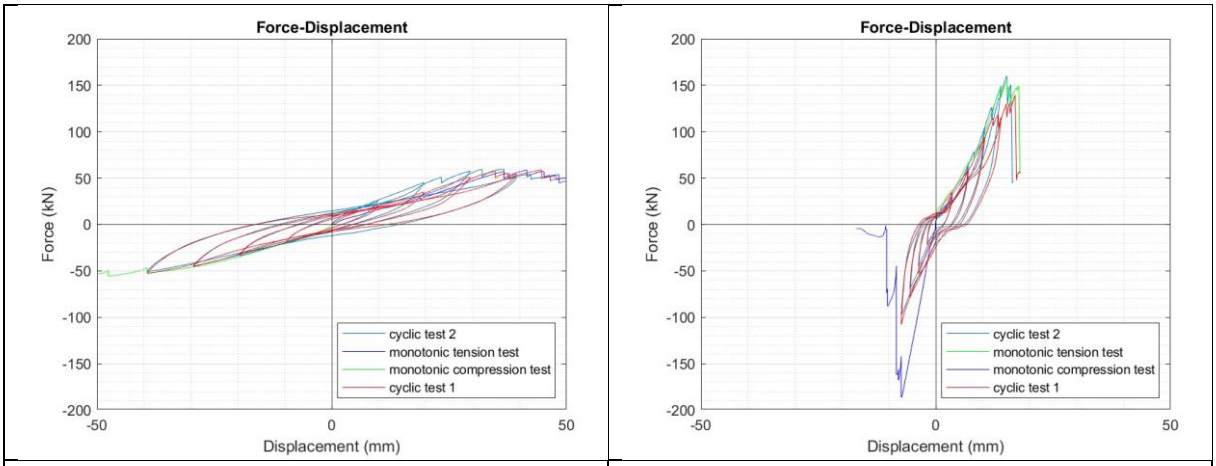

(a) (b)

Figure 206. (a) Detail 4 test results and (b) Detail 5 test results.

The comparison, in terms of force-displacement curves, between Detail 4 and Detail 5 is illustrated in Figure 206. As can be seen, the presence of the steel rods associated to sandwich panels had substantially altered the specimen reaction to the tests. The steel rods have undergone large flexural deformations and the panels rotated significantly during the tests, determining higher global displacements. This also implied additional forces in the fusible links, that did not withstand the design force of 180 kN. On the contrary, Detail 5 did not experience important rotations during the test, but some additional forces were also acting on the aluminium bolts, due to their position and the distance between the force application point. Even in this case the design force was not reached. Imperfections of the specimen may have also contributed to this outcome. In both the details could be observed a similar way of failure, with the progressive fracture of one or many shear planes.

3 CONCLUSIONS

This report described the experimental campaign carried out on six different details designed to withstand design shear forces obtained from preliminary numerical simulations on different case studies. The main objective was to characterize the behaviour of aluminium bolts of two different size, M12 and M16 and in different details, under static and quasi-static cyclic loads. Indeed, to pursue this aim, the ECCS protocol was followed. In this case, considering that all the six details were not symmetric in both directions, the monotonic tests were performed one in tension and one in compression. Moreover, at least two cyclic tests were conducted on each detail. To better characterize the cyclic behaviour of Detail 3.2 affected by higher imperfections, three cyclic tests were performed. When the failure of the aluminium bolts was involved, the collapse was, as expected, brittle. For Detail 1 and 2, in one direction the details worked through contact of the steel elements and an elasto-plastic behaviour was observed.

Detail 1 was conceived to withstand a shear force of 80 kN associated with a low seismicity level. The aluminium bolts were 6 M12. The results, in terms of force-displacement diagrams, highlighted a good agreement between them and all tests reached the design force, and given the mode of failure, the actual expected resistance of half of the bolts. Small hysteretic behaviour was observed. Due to the geometry of the detail, the monotonic compression test was representative of the steel deformation and the aluminium bolt were not affected by the test. Eventually, the cyclic tests fitted the general trend of the test.

Detail 2, very similar to Detail 1, was conceived to withstand a shear force of 180 kN associated with a moderate seismicity level. The aluminium bolts involved were 8 M16. In this case, 6 of them would have been sufficient; however, to have a symmetric detail as much as possible, 2 of them were added. The results, in terms of force-displacement diagrams, highlighted a good agreement between them and all the tests reached the design force. As occurred also for Detail 1, due to the geometry of the detail, the monotonic compression test was representative of the steel deformation and the aluminium bolt were not affected by the test. Eventually, the cyclic tests fitted the general trend of the test. If compared with the Detail 1 the specimens exhibited lower hysteretic energy.

Detail 3.1 and Detail 3.2 were developed with the same design force, and therefore the same geometry and elements, the only difference between them was the aluminium bolt size used. In fact, Detail 3.1 was tested with 3 M16 aluminium bolts working on two shear planes and Detail 3.2 was tested with 6 M12 aluminium bolts working on two shear planes.

The results tests on Detail 3.1, in terms of force-displacement diagrams, highlighted a good agreement between them, indeed all the tests reached the design force. Particularly in the compression phase, a significant pinching phenomenon during the cyclic test was observed due to assembly of the specimen and the cyclic test procedure that starts along the tension branch.

With respect to Detail 3.1, Detail 3.2 exhibited more imperfections caused by a higher number of bolts, e.g. misalignment of the holes. This entailed higher variability in terms of the response among the tests. Some non-negligible difference between the cyclic tests in terms of both force and displacement. Significant pinching effects related to the bolt-hole clearances were observed. In particular, in the monotonic tension test the collapse was determined by progressive failure of some aluminium bolts, and the ultimate load was less than the design force, i.e. 180 kN.

Detail 4 and Detail 5 were conceived from the same reference detail to analyse the effect of the sandwich panels. In Detail 4 the panels were present, whilst in Detail 5 they were not. Both of them were designed to withstand a shear force of 180 kN with 6 M12 aluminium bolts working on two shear planes.

The results of the four tests performed on Detail 4 are in a good agreement, in particular on the compression side, where a correspondence in terms of stiffness and strength degradation can be observed. On the tension part, the trend of the monotonic test and the two cyclic tests is the same, while a stiffer curve can be observed on the second cyclic test. This difference may be caused by a different procedure in assembling the specimen or by an intrinsic imperfection of the elements. The failure mode is the same for each test, where a progressive failure of one or many shear planes occurred. The design force of 180 kN was not reached in any tests. In fact, the detail configuration and the presence of the steel rods and the sandwich panels led to large deformations that induced additional forces on the aluminium bolts, determining their previous collapse. It is worth noting that such large rotations of the sandwich panel are not likely to occur in reality because the wall will be anchored to the ground and its length will be much larger. Nevertheless, the tests provided some

useful information on the interaction between the sandwich panel and the steel rods, whose behaviour was not significantly affected by the panels.

For Detail 5, much lower rotations were observed. Nonetheless, the failure occurred due to the progressive failure of the aluminium bolts, that prevented of reaching the design force of 180 kN. The cyclic tests are in a good agreement between them, with the same final strength and the same stiffness degradation. The absence of the sandwich panels stiffened the specimen. In both cases, the distance between the force application point and the aluminium bolts generated additional forces and the response of the aluminium bolts were consequently affected.

Thus, for details that are expected to be loaded with eccentric forces with respect to the centre of mass of the bolts, careful analysis should be paid, because failure can occur progressively at lower force levels. Moreover, fusible link details with a low number of bolts is preferable (compare for instance Detail 3.1 vs. Detail 3.2), because they imply lower imperfections, e.g. as regards the bolt alignment, and, consequently, a more uniform loading of the fusible links and the detail can achieve higher force levels. Moreover, due to the hole-bolt clearance and an inherent different positioning of the bolts in the hole, a higher number of bolts of lower diameter may increase the force on a single bolt with consequent progressive failure of the bolts. In this respect, the way of assembly the fusible link details may also play a role, as shown in the third cyclic test of the Detail 3.2, but it may be difficult to provide a specific procedure to be realistically applied on site. In low and medium seismicity regions, Detail 1 and Detail 2 represent a good option, because the fusible links are only loaded in one direction, i.e. parallel to the portal frames. Moreover, the detail is loaded consistently with the detail layout in the actual structures, and the magnitude of possible secondary forces owing to geometric eccentricities/imperfections is lower. In both details, failure occurred on one side and the maximum experimental force was consequently about 50-60% of the total expected actual resistance. In fact, due to the presence of inherent imperfections in the test specimens, the simultaneous failure of all bolts is highly improbable. In fact, the observed experimental capacity is close to the expected actual capacity of the aluminium bolt connection. This finding will be also studied in the successive numerical parametric global analyses.

4 REFERENCES

[1] Deliverable D1.4: Design of tests, RFSC project FISHWALL, 2020.

[2] ECCS, Recommended Testing Procedure for Assessing the Behaviour of Structural Steel Elements under Cyclic Loads, ECCS Publication n° 45; ECCS: Bruxelles, 1986.

[3] Deliverable D1.3: Analysis of seismic behavior of single-storey buildings, RFSC project FISHWALL, 2020.

[4] Deliverable D3.1: Material test on aluminium bolts, RFCS project FISHWALL, 2020.

[5] EN 1999-1-1: Design of aluminium structures. Part 1-1: General structural rules, 2007.

APPPENDIX A. DEFORMED SHAPES OF SPECIMENS OBSERVED DURING TESTS

A.1. Detail 1 – Compression test - Screenshots

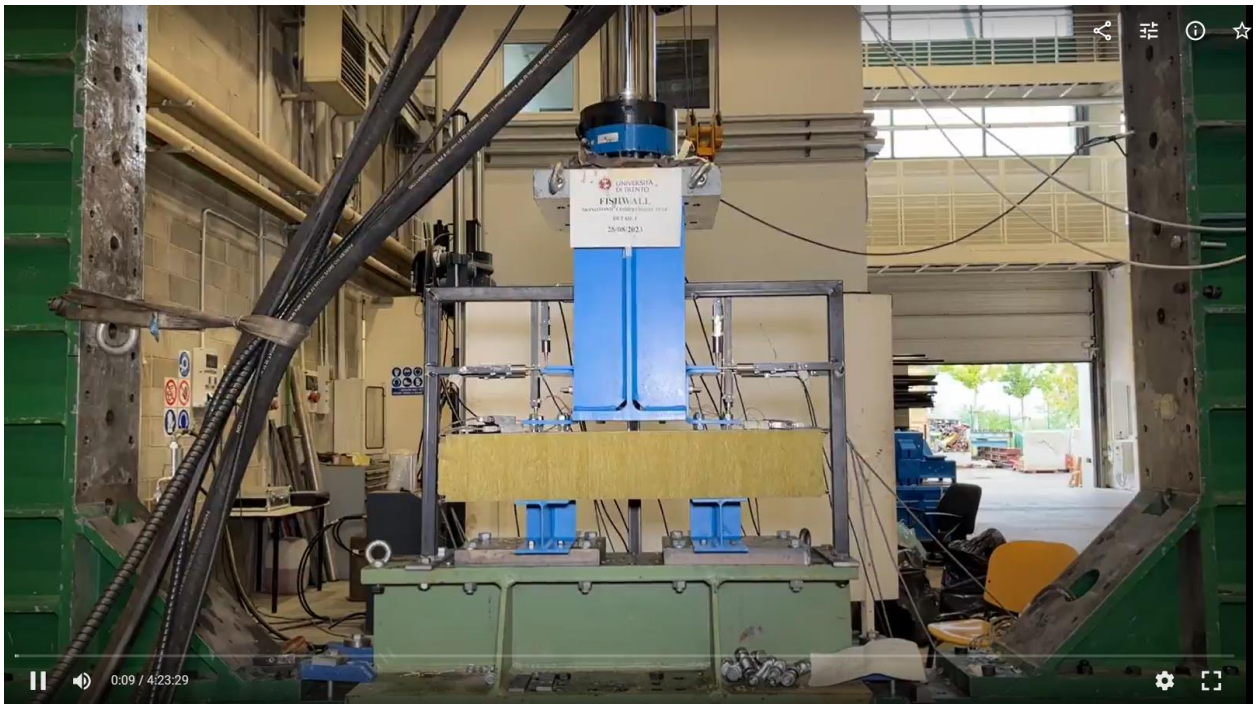

Figure A1. Detail 1 - compression test – beginning of the test.

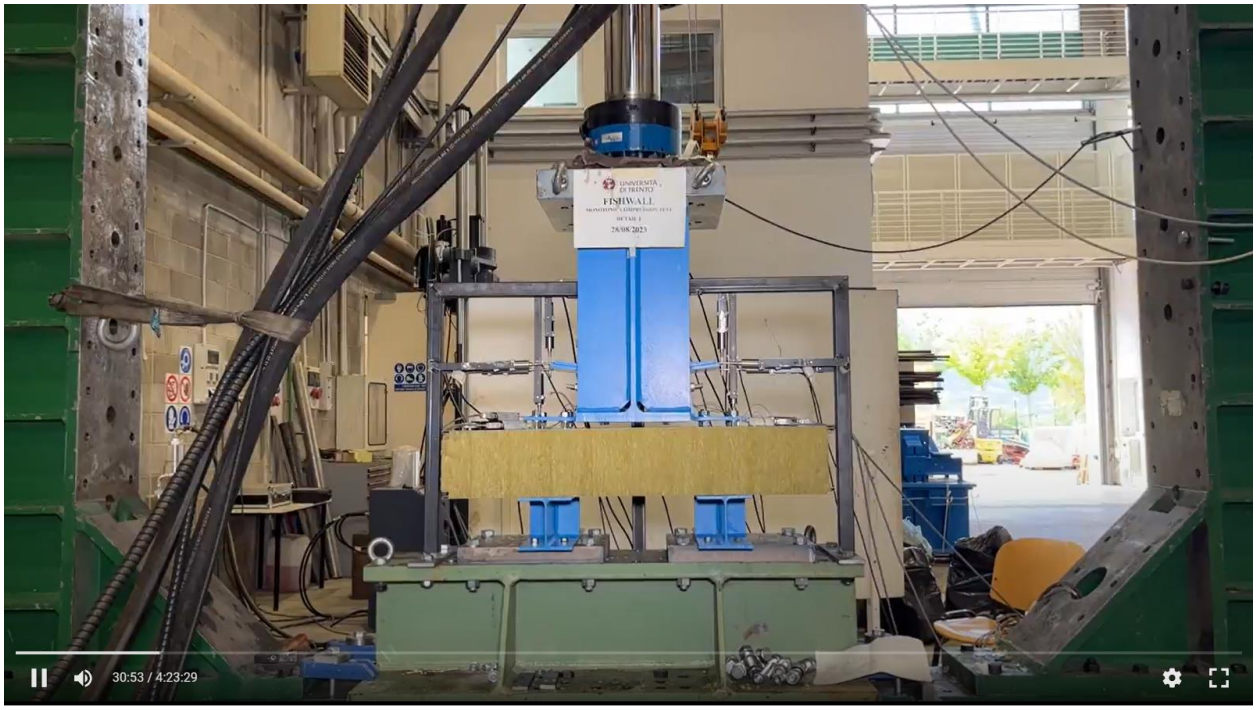

Figure A2. Detail 1 – compression test – deformation at 30 minutes.

Figure A3. Detail 1 - compression test - deformation at 1 hour.

Figure A4. Detail 1 - compression test - deformation at 1.30 hour

Figure A5. Detail 1 - compression test - deformation at 2 hours.

Figure A6. Detail 1 - compression test - deformation at 2.30 hours.

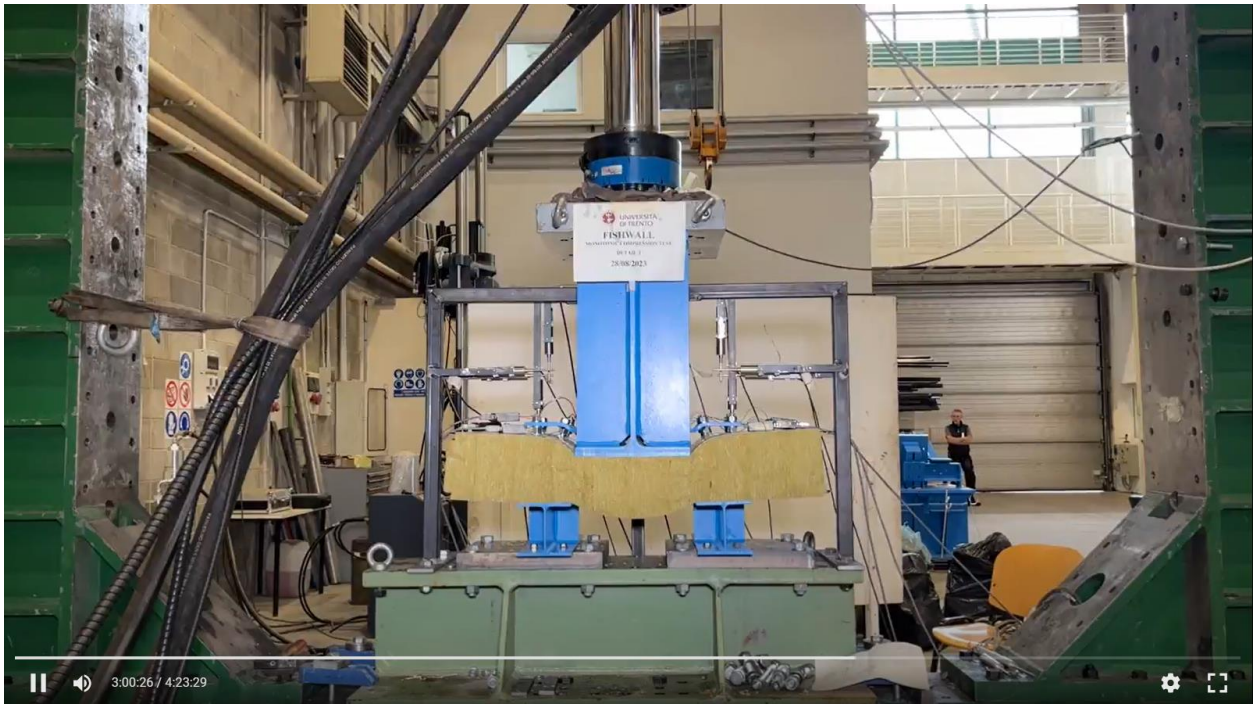

Figure A7. Detail 1 - compression test - deformation at 3 hours.

Figure A8. Detail 1 - compression test - deformation at 3.30 hours.

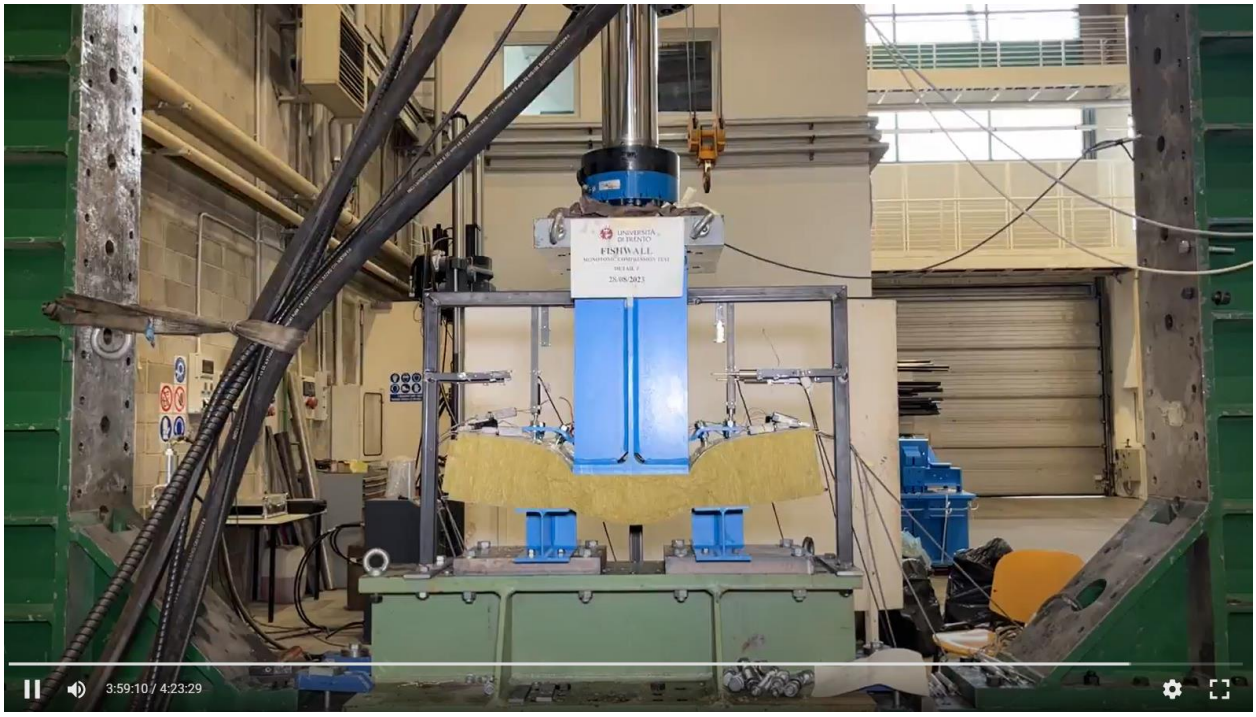

Figure A9. Detail 1 - compression test - deformation at 4 hours.

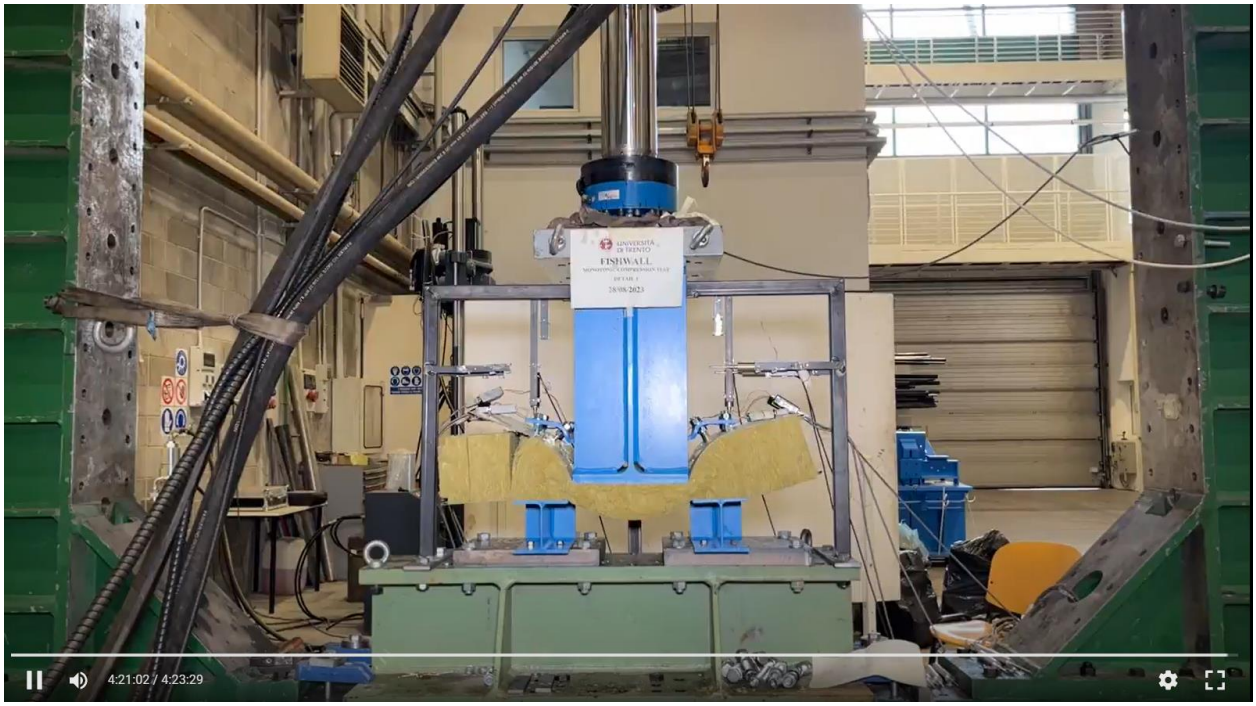

Figure A10. Detail 1 - compression test – deformation at failure

A.2. Detail 1 – Tension test - Screenshots

Figure A11. Detail 1 – tension test – beginning of the test.

Figure A12. Detail 1 - tension test – deformation at 10 minutes.

Figure A13. Detail 1 - tension test – deformation at failure.

A.3. Detail 1 – Cyclic test - Screenshots

Figure A14. Detail 1 - cyclic test – beginning of the test.

Figure A15. Detail 1 - cyclic test – deformation at failure

A.4. Detail 2 – Compression test - Screenshots

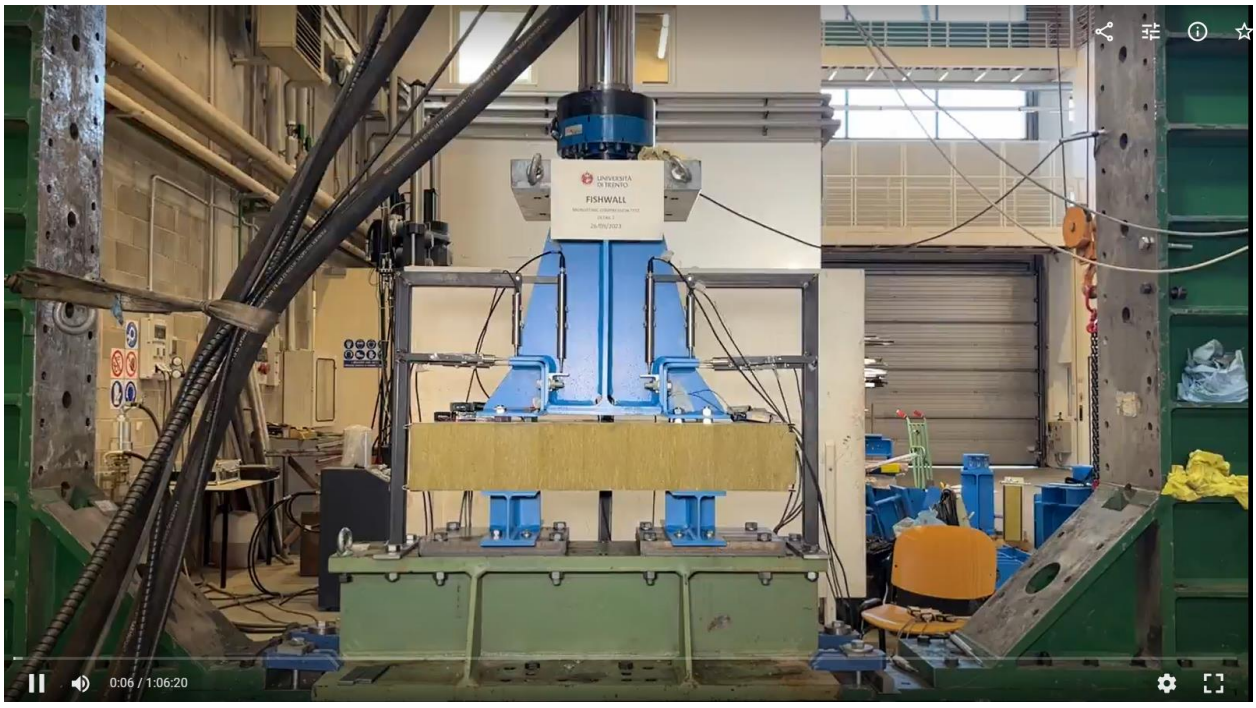

Figure A16. Detail 2 - compression test – beginning of the test.

Figure A17. Detail 2 - compression test – deformation at 20 minutes.

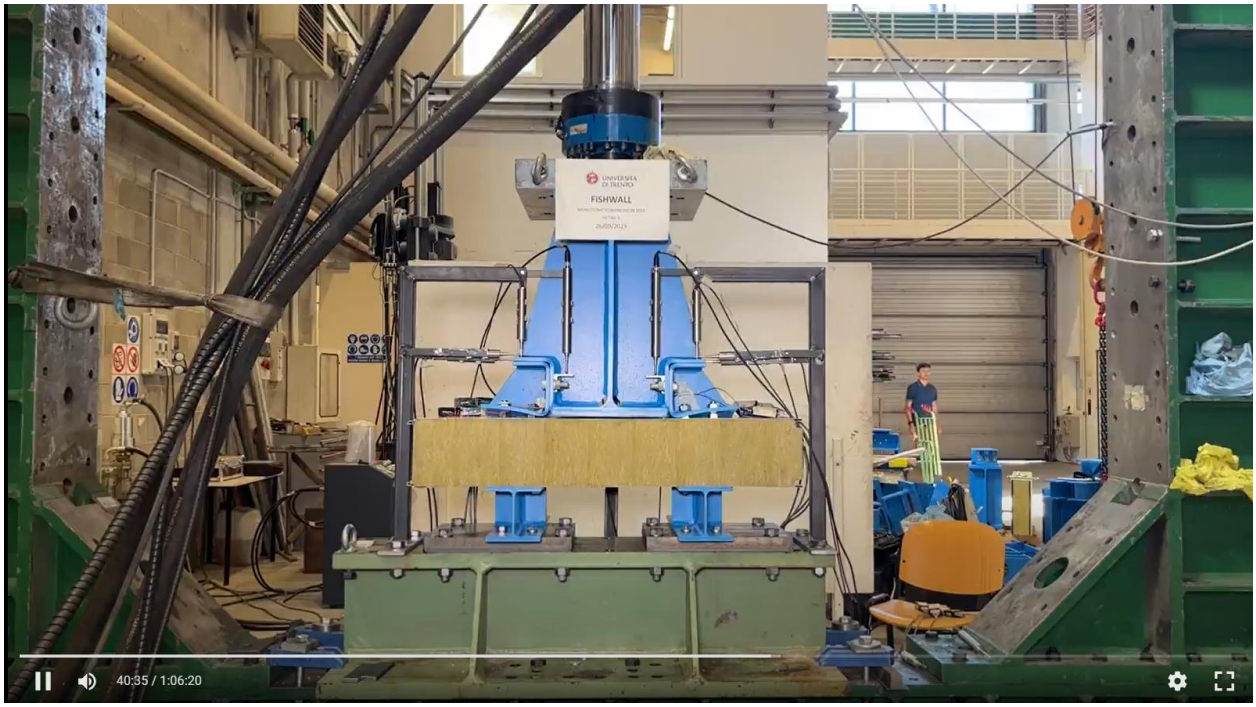

Figure A18. Detail 2 - compression test – deformation at 40 minutes.

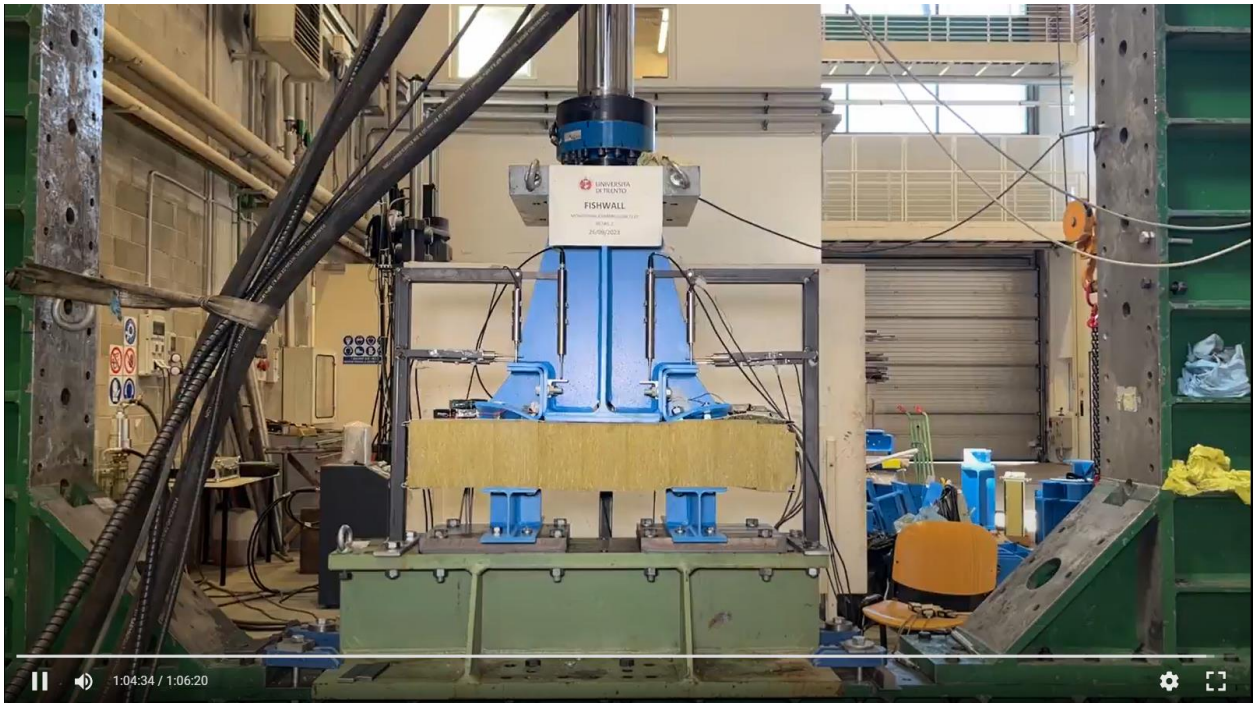

Figure A19. Detail 2 - compression test – deformation at 1 hour.

Figure A20. Detail 2 - compression test – deformation at 1.20 hour.

Figure A21. Detail 2 - compression test - deformation at 1.40 hour.

Figure A22. Detail 2 - compression test – deformation at failure.

A.5. Detail 2 – Tension test – Screenshots

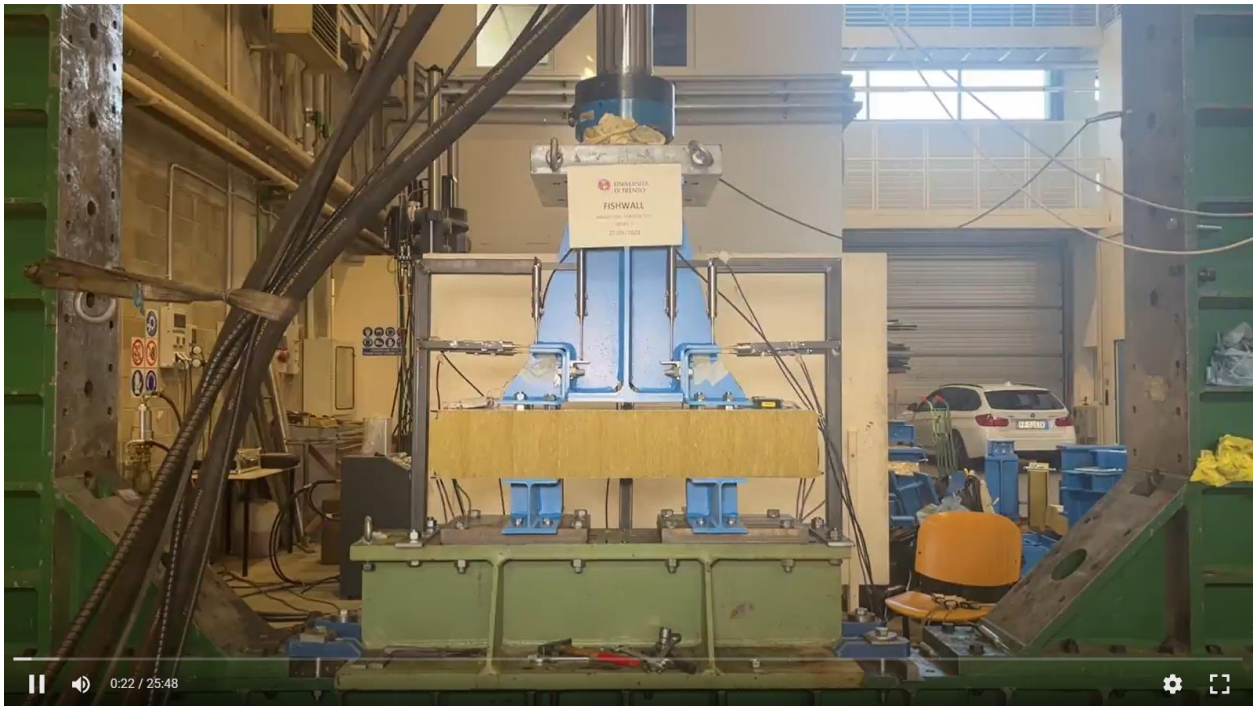

Figure A23. Detail 2 - tension test – beginning of the test.

Figure A24. Detail 2 – tension test – deformation at 12 minutes.

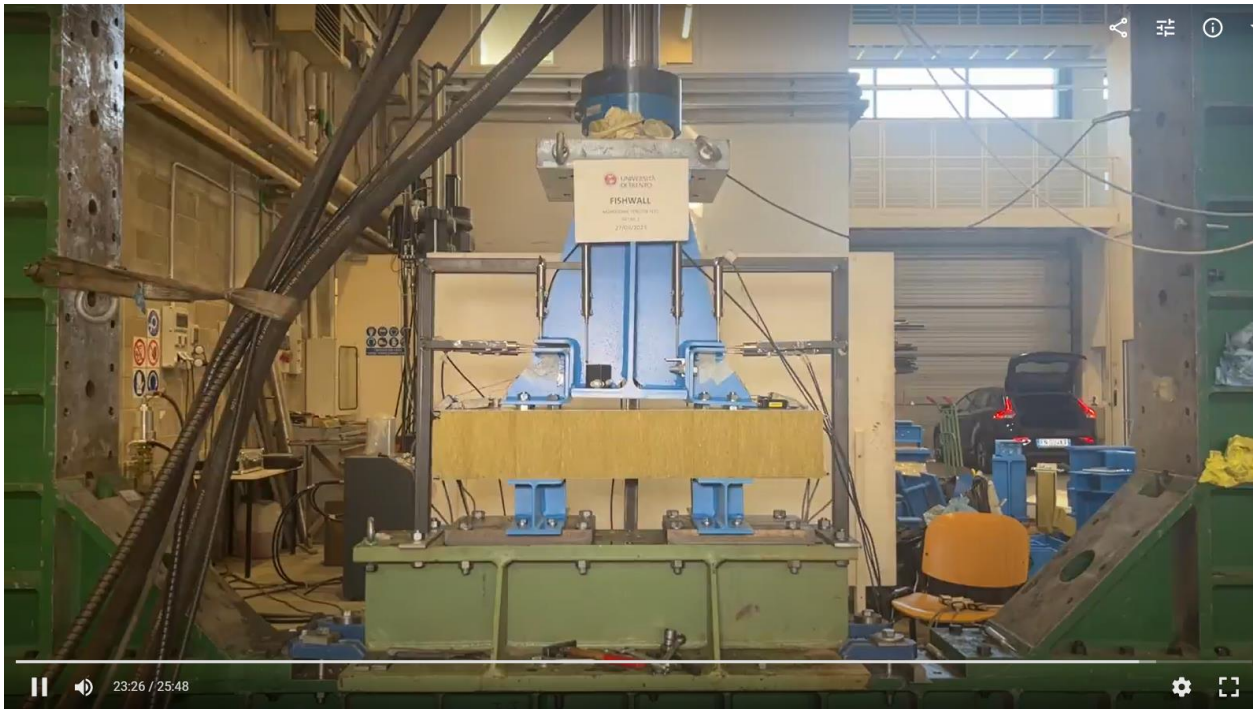

Figure A25. Detail 2 - tension test – deformation at 23 minutes.

Figure A26. Detail 2 - tension test – deformation at failure.

A.6. Detail 2 – Cyclic test - Screenshots

Figure A27. Detail 2 – cyclic test – beginning of the test.

Figure A28. Detail 2 - cyclic test – deformation at failure.

A.7. Detail 3.1 – Compression test - Screenshots

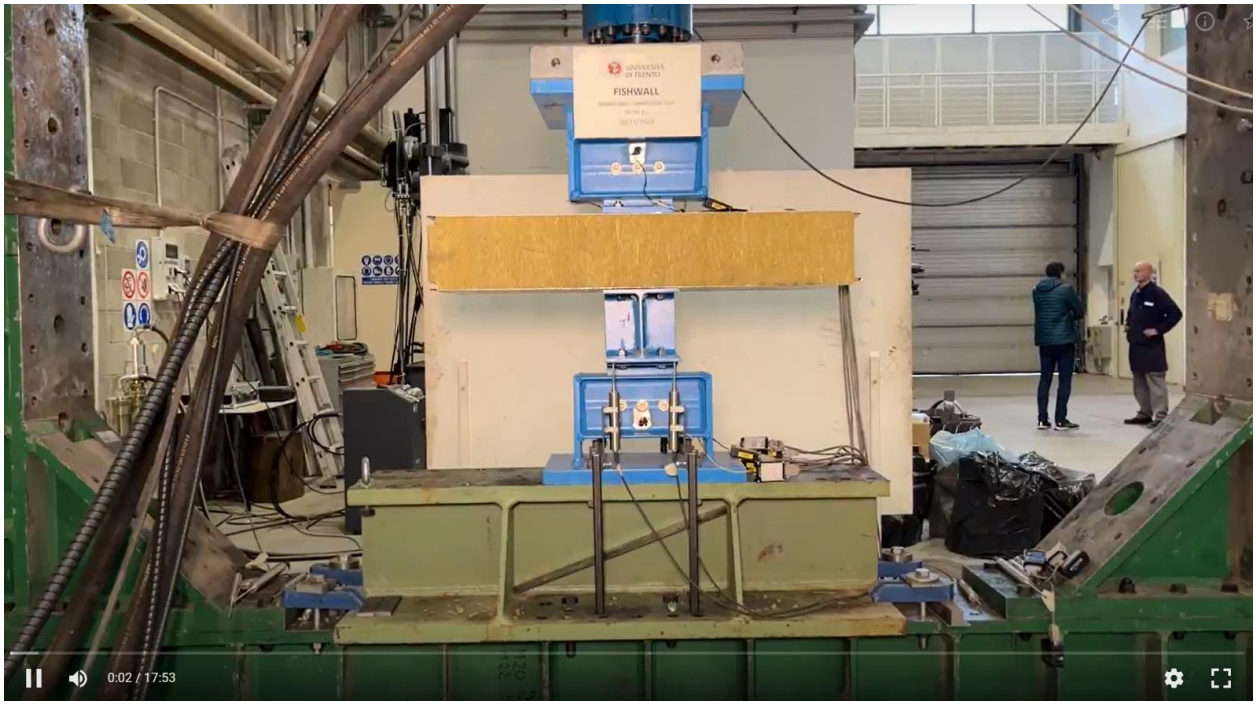

Figure A29. Detail 3.1 - compression test – beginning of the test.

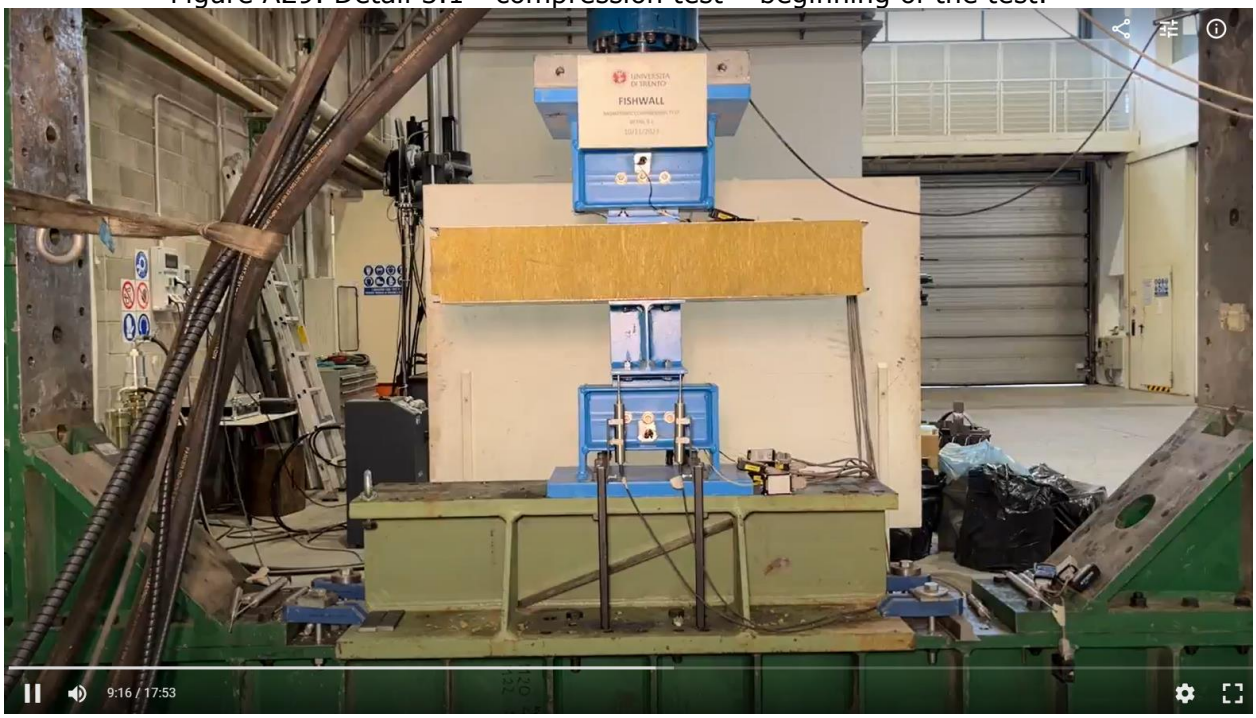

Figure A30. Detail 3.1 - compression test – deformation at 10 minutes.

Figure A31. Detail 3.1 - compression test – deformation at failure.

A.8. Detail 3.1 – Tension test - Screenshots

Figure A32. Detail 3.1 - tension test – beginning of the test.

Figure A33. Detail 3.1 - tension test – deformation at 13 minutes.

Figure A34. Detail 3.1 - tension test – deformation at failure.

A.9. Detail 3.2 – Compression test - Screenshots

Figure A35. Detail 3.2 - compression test – beginning of the test.

Figure A36. Detail 3.2 – compression test – deformation at 15 minutes.

Figure A37. Detail 3.2 - compression test – deformation at failure.

A.10. Detail 3.2 – tension test - Screenshots

Figure A38. Detail 3.2 - tension test – beginning of the test.

Figure A39. Detail 3.2 - tension test – deformation at 10 minutes.

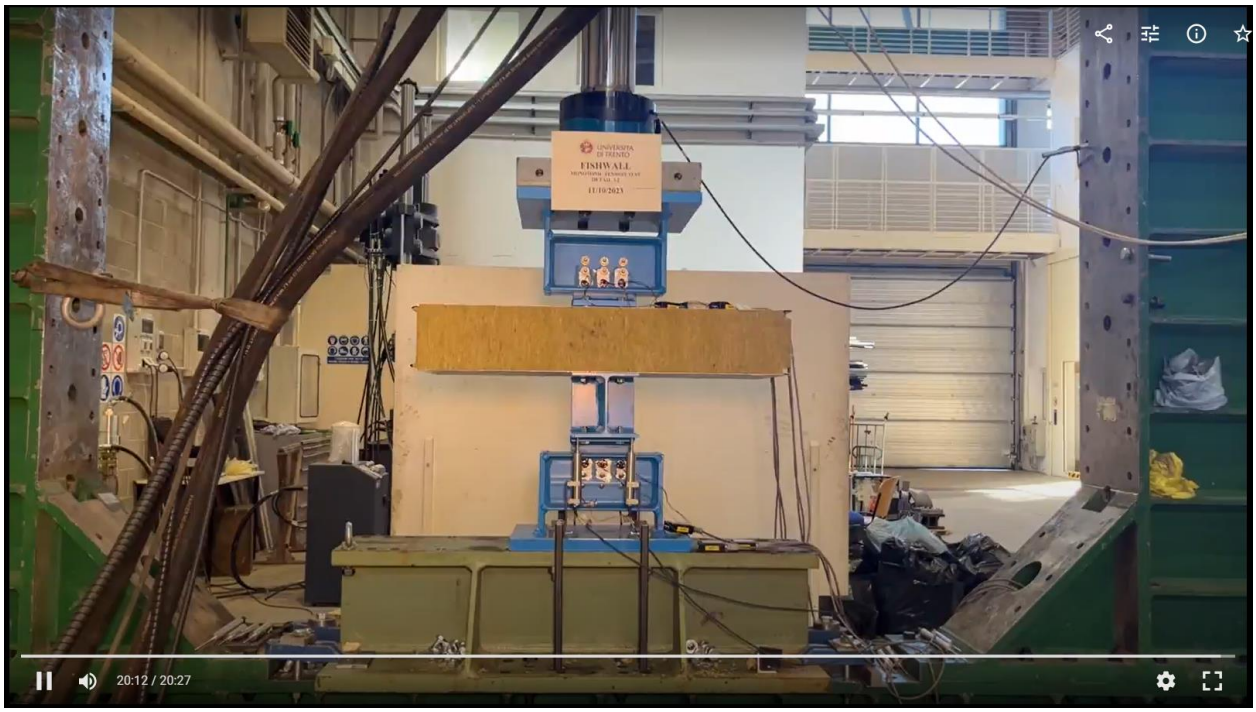

Figure A40. Detail 3.2 - tension test – deformation at failure

A.11.Detail 3.2 – Cyclic test - Screenshots

Figure A41. Detail 3.2 - cyclic test – beginning of the test.

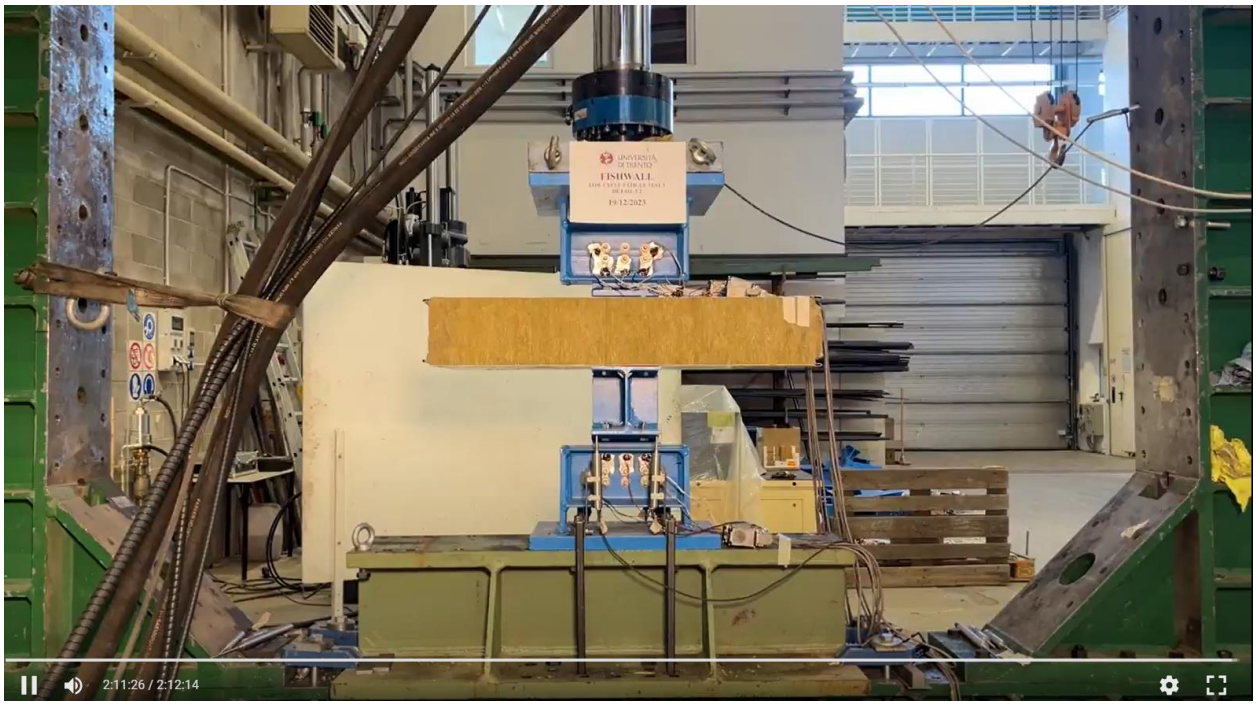

Figure A42. Detail 3.2 - cyclic test – deformation at failure.

A.12.Detail 4 – Compression test - Screenshots

Figure A43. Detail 4 - compression test – beginning of the test.

Figure A44. Detail 4 - compression test – deformation at 30 minutes.

Figure A45. Detail 4 - compression test - deformation at 1 hour.

Figure A46. Detail 4 - compression test - deformation at 1.30 hour.

Figure A47. Detail 4 - compression test - deformation at 2 hours

Figure A48. Detail 4 - compression test - deformation at 2.30 hours

Figure A49. Detail 4 - compression test – deformation at failure

A.13.Detail 4 – Tension test - Screenshots

Figure A50. Detail 4 – tension test – beginning of the test-

Figure A51. Detail 4 - tension test – deformation at 30 minutes.

Figure A52. Detail 4 - tension test - deformation at 1 hour.

Figure A53. Detail 4 - tension test – deformation at 1.30 hour

Figure A54. Detail 4 - tension test - deformation at 2 hours.

Figure A55. Detail 4 - tension test -deformation at 2.30 hours

Figure A56. Detail 4 - tension test - deformation at 3 hours.

Figure A57. Detail 4 - tension test – deformation at failure.

A.14.Detail 4 – Cyclic test - Screenshots

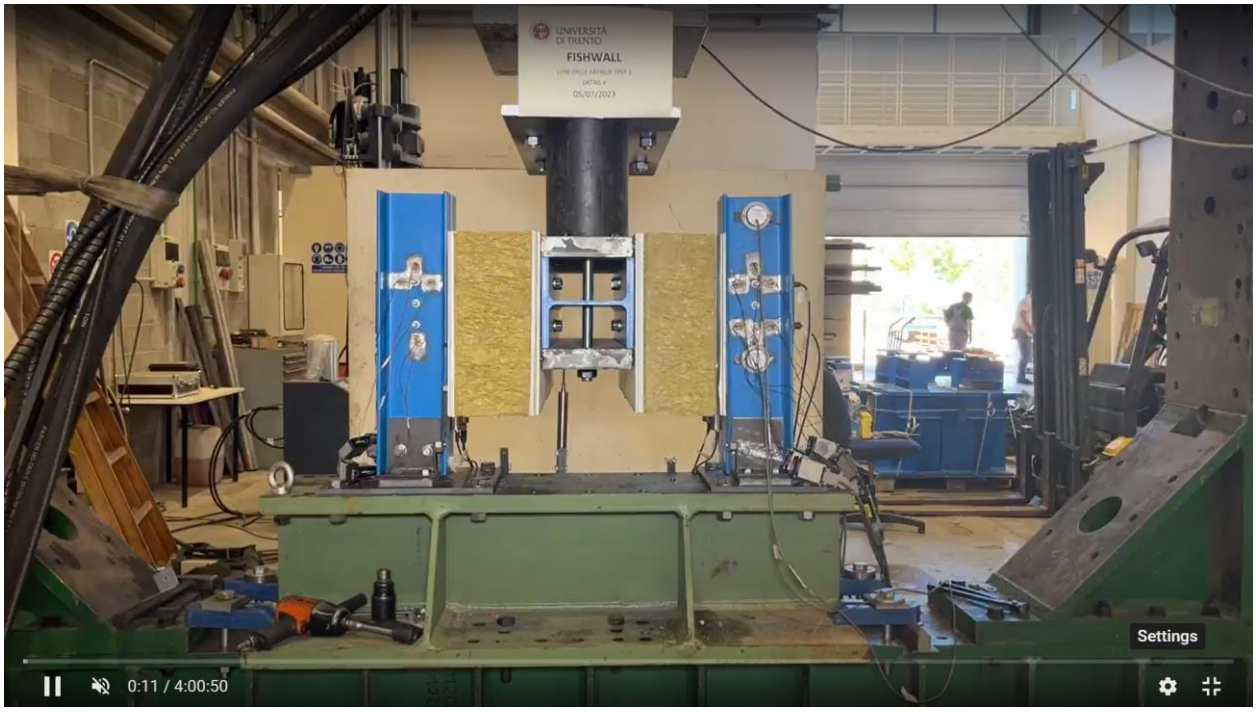

Figure A58. Detail 4 - cyclic test – beginning of the test.

Figure A59. Detail 4 - cyclic test – deformation at $+e_y/4$

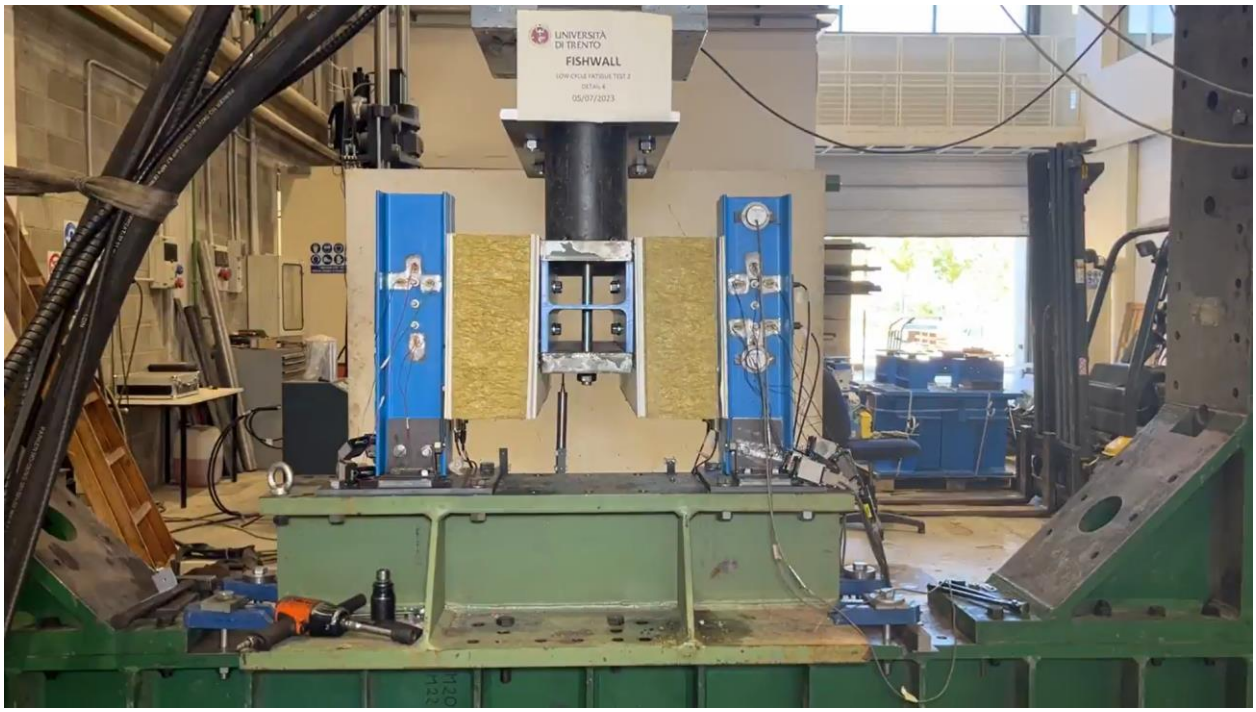

Figure A60. Detail 4 - cyclic test – deformation at $-e_y/4$

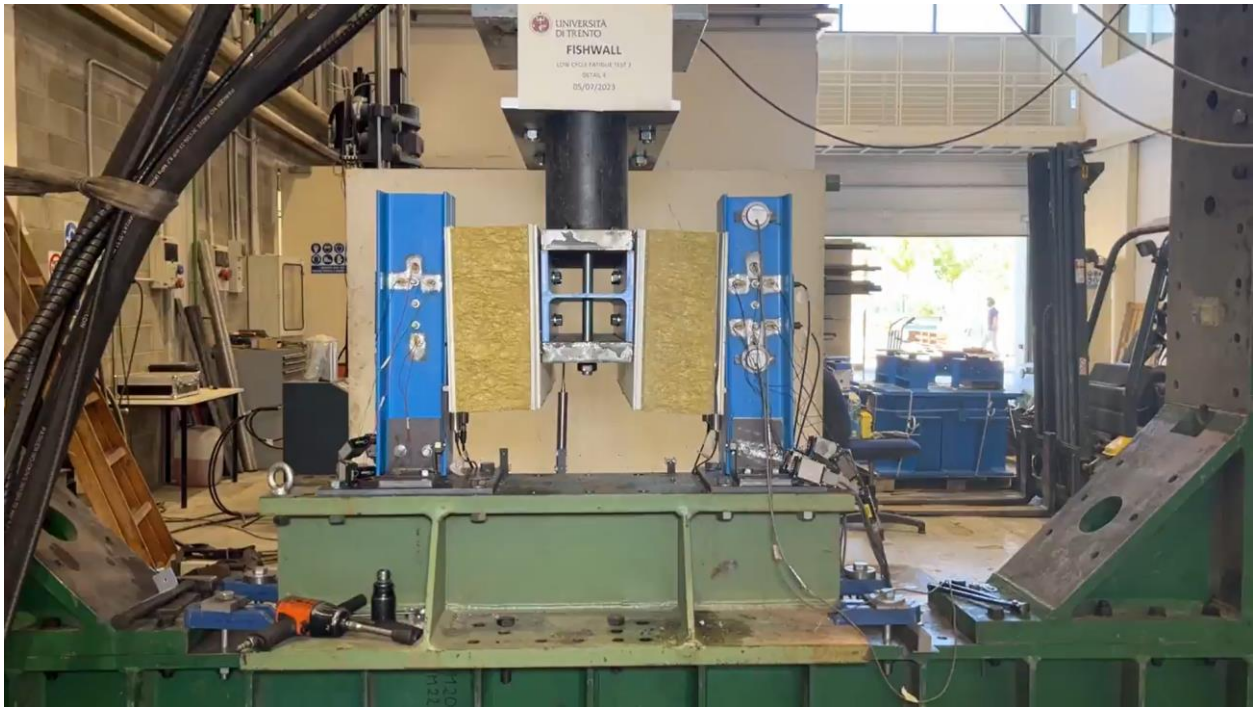

Figure A61. Detail 4 - cyclic test – deformation at $+e_y/3$

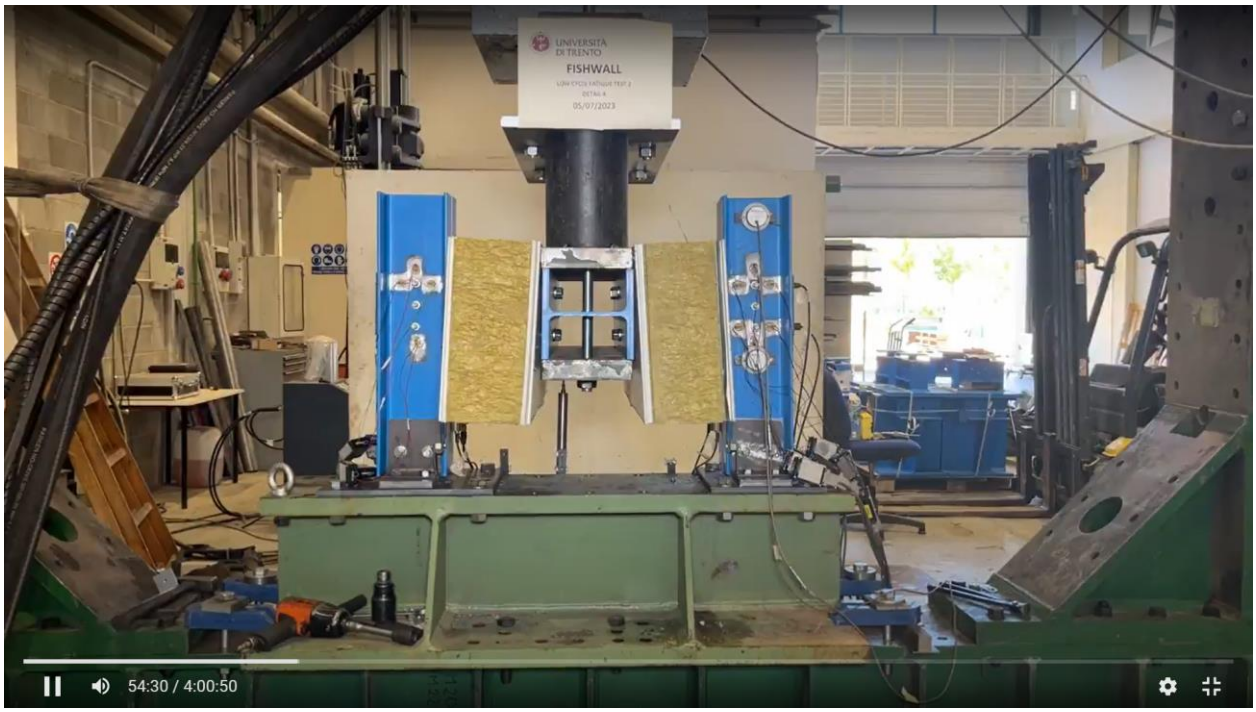

Figure A62. Detail 4 - cyclic test – deformation at $-e_y/3$

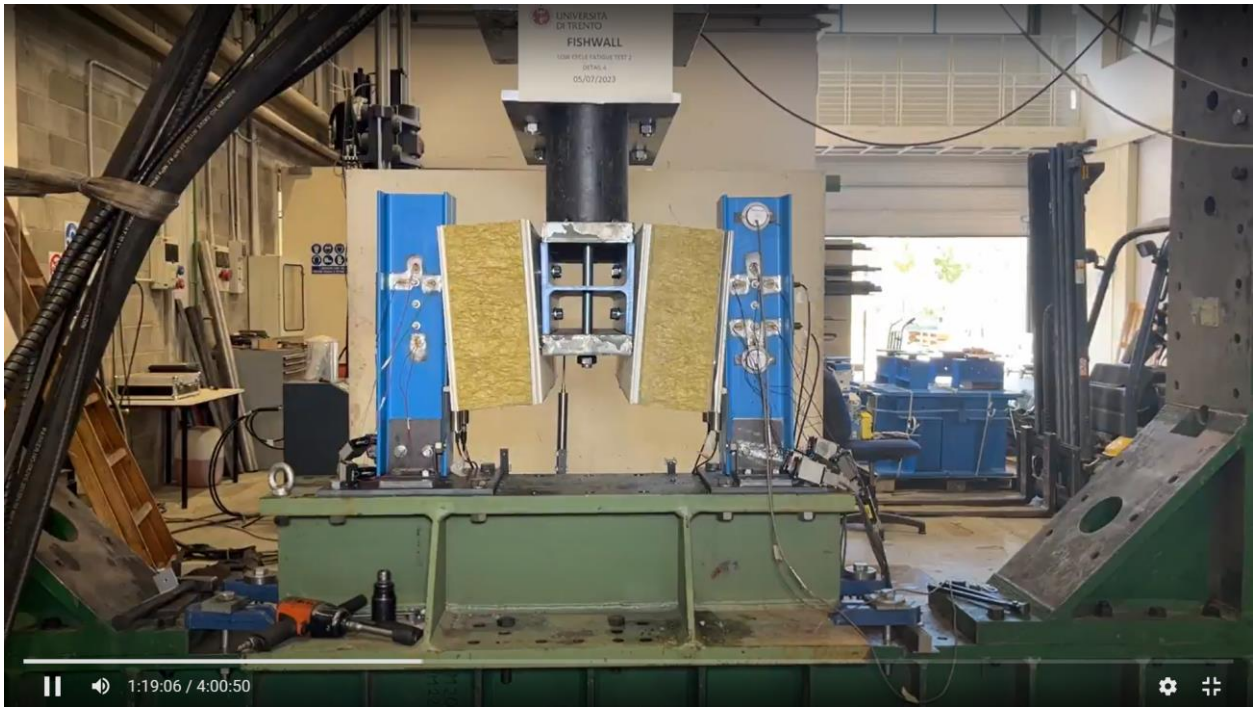

Figure A63. Detail 4 - cyclic test – deformation at $+e_y/2$

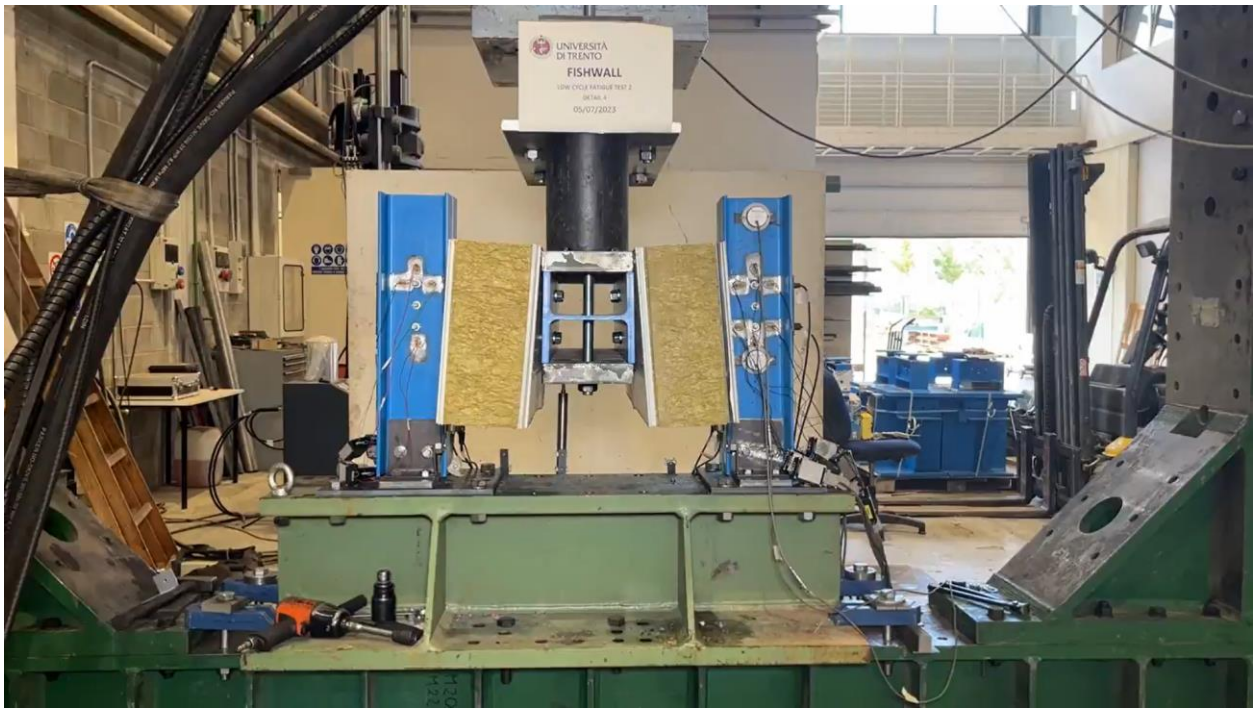

Figure A64. Detail 4 - cyclic test – deformation at $-e_y/2$

Figure A65. Detail 4 - cyclic test – deformation at e_y

Figure A66. Detail 4 - cyclic test – deformation at $-e_y$

Figure A67. Detail 4 - cyclic test – deformation to $+2e_y$

Figure A68. Detail 4 - cyclic test – deformation to $+2e_y$

Figure A69. Detail 4 - cyclic test – deformation to $+2e_y$

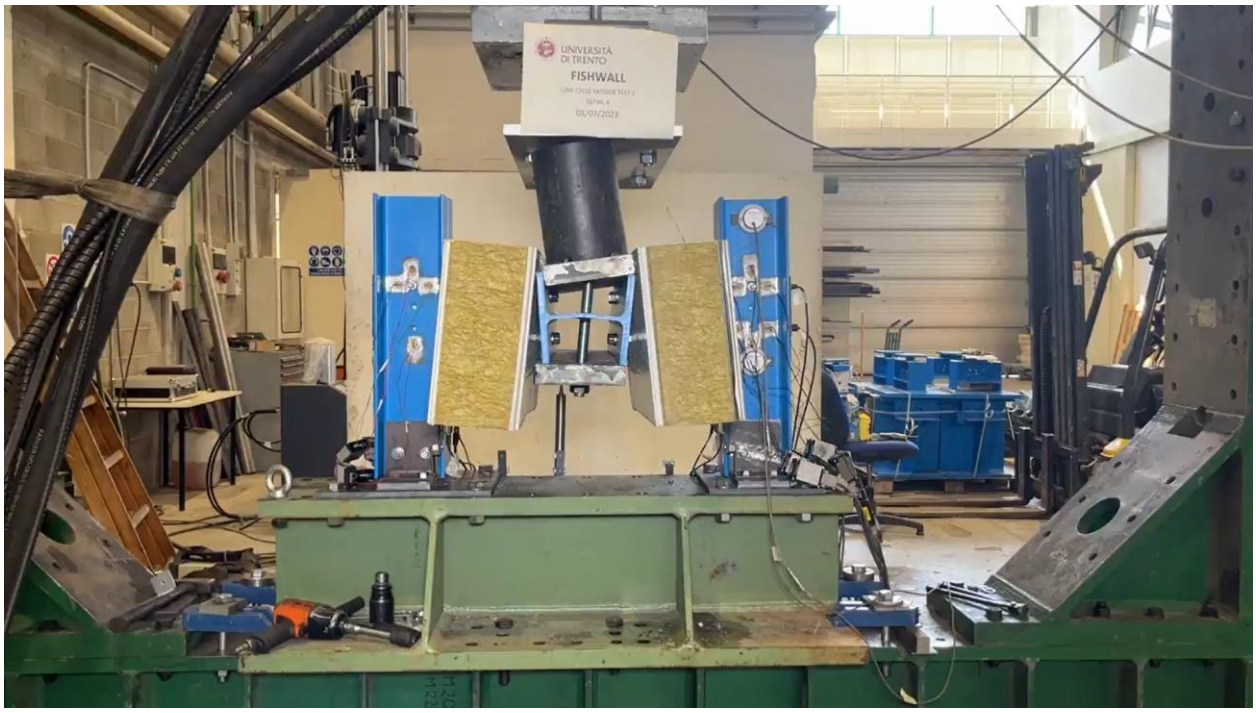

Figure A70. Detail 4 - cyclic test – deformation at failure

A.15.Detail 5 – Compression test - Screenshots

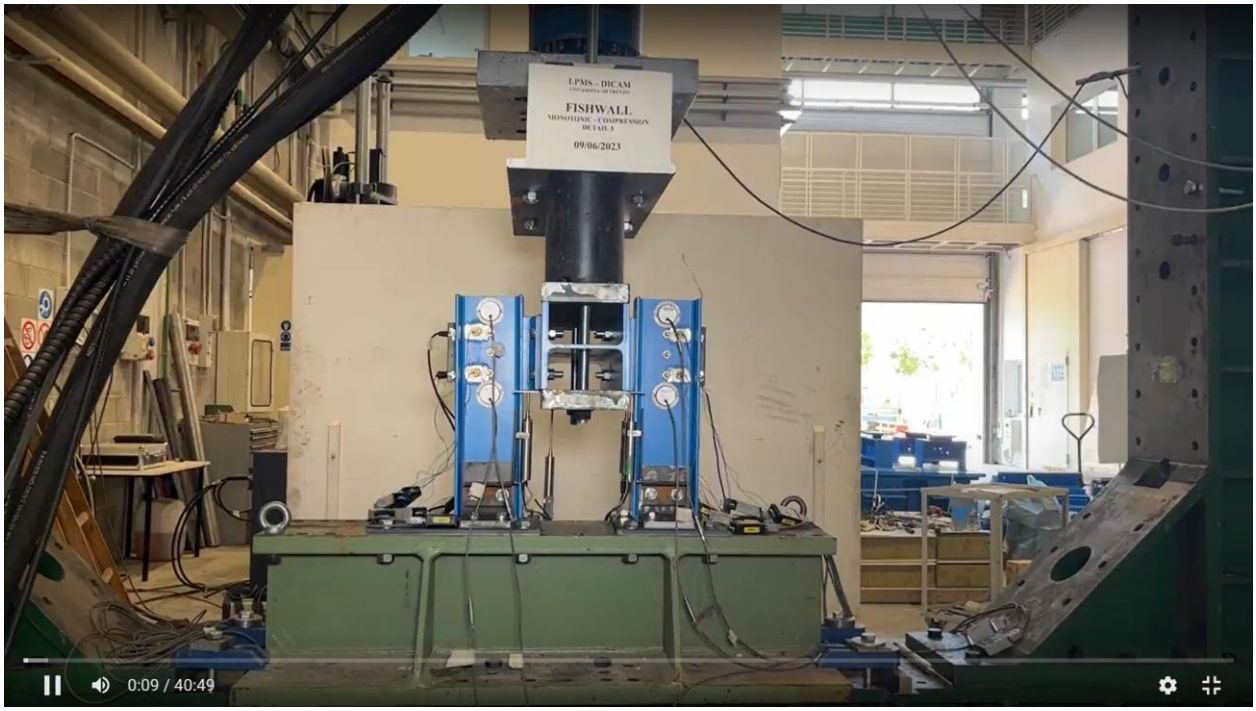

Figure A71. Detail 5 - compression test – beginning of the test.

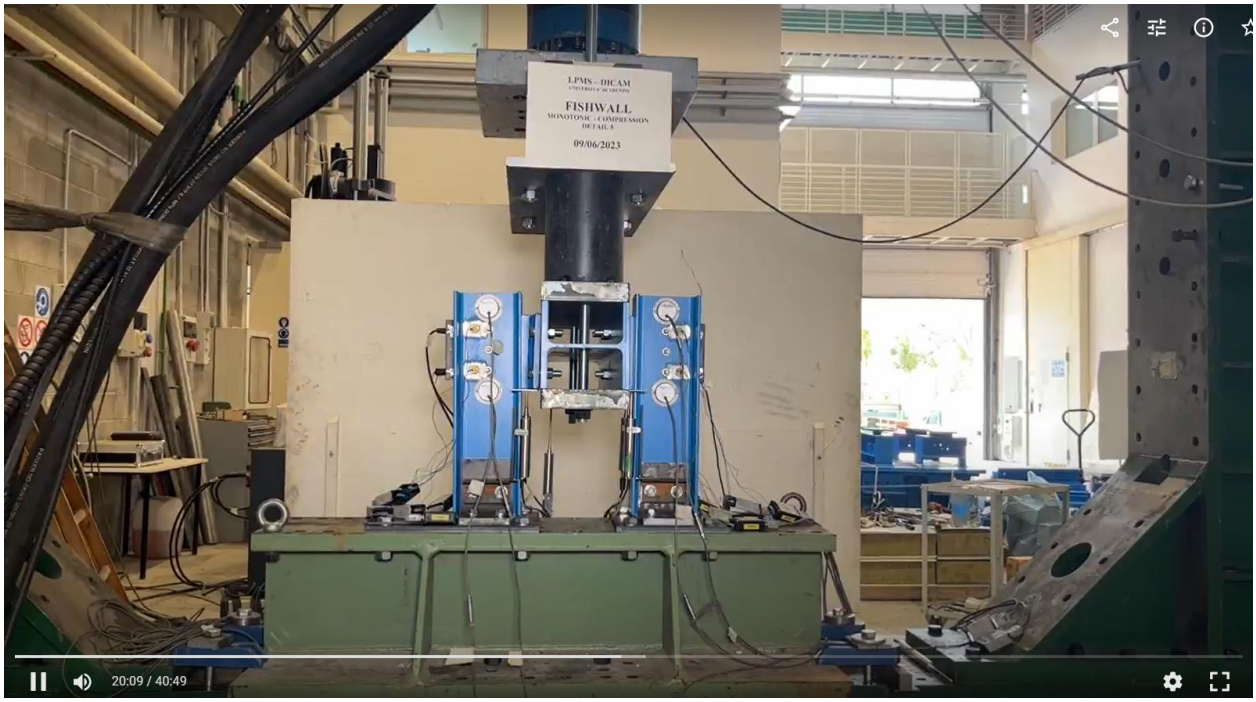

Figure A72. Detail 5 - compression test – deformation at 20 minutes.

Figure A73. Detail 5 - compression test – deformation at failure.

A.16. Detail 5 – Tension test - Screenshots

Figure A74. Detail 5 - tension test – beginning of the test.

Figure A75. Detail 5 - tension test – deformation at 20 minutes.

Figure A76. Detail 5 – tension test - deformation at 40 minutes.

Figure A77. Detail 5 - tension test – deformation at failure.

A.17.Detail 5 – Cyclic test - Screenshots

Figure A78. Detail 5 - cyclic test – beginning of the test.

Figure A79. Detail 5 - cyclic test – deformation at failure.